NUMERICAL MODELLING OF TSUNAMI PROPAGATION IN THE SOUTH EAST ARABIAN SEA (SEAS) AND INUNDATION ALONG THE KERALA COAST

THESIS SUBMITTED TO

THE COCHIN UNIVERSITY OF SCIENCE AND TECHNOLOGY

IN PARTIAL FULFILLMENT OF THE REQUIREMENTS

FOR THE AWARD OF THE DEGREE OF

DOCTOR OF PHILOSOPHY IN PHYSICAL OCEANOGRAPHY

UNDER THE FACULTY OF MARINE SCIENCES

by

PRAVEEN S. S.

CENTRE FOR EARTH SCIENCE STUDIES
THIRUVANANTHAPURAM

MAY 2012

DECLARATION

I hereby declare that the thesis entitled ***"Numerical Modelling of Tsunami Propagation in the South East Arabian Sea (SEAS) and Inundation along the Kerala Coast"*** is an authentic record of research work carried out by me under the supervision and guidance of Dr. N. P. Kurian, Director, Centre for Earth Science Studies, Thiruvananthapuram, in partial fulfillment of the requirements for the award of Ph.D. Degree of Cochin University of Science & Technology. I affirm that this work is not a replicated version of any earlier works and that no part thereof has been presented for the award of any other degree in any University.

Thiruvananthapuram
25 May, 2012

Praveen S. S.
(Reg. No. 3514)
Centre for Earth Science Studies
Thiruvananthapuram - 695 031

CERTIFICATE

This is to certify that this thesis entitled ***"Numerical Modelling of Tsunami Propagation in the South East Arabian Sea (SEAS) and Inundation along the Kerala Coast"*** is an authentic record of the research work carried out by Mr. Praveen. S. S. (Reg. No. 3514), under my supervision and guidance, at the Centre for Earth Science Studies, Thiruvananthapuram, in partial fulfillment of the requirements for the Ph.D. Degree of Cochin University of Science and Technology under the Faculty of Marine Sciences and no part thereof has been presented for the award of any degree in any University.

Thiruvananthapuram — Dr. N. P. Kurian

25 May, 2012 — (Research Guide)

THANK GOD

The benevolent grace of GOD ALMIGHTY that keep me and my research work going

Memories of my Beloved Mother Late ***A. Sathee Devi****, who inculcated a passion of education in me, is my Strength*

A very special dedication to

My Loving Father and Brother

Remembering the immortal souls who lost their lives during the Sumatra Tsunami of December 26, 2004

ACKNOWLEDGEMENTS

"When heart is full, words are less"

This thesis is entirely dedicated and devoted to my mentor, tutor, supervising guide Dr. N. P. Kurian for paving a new window of research and for inducing in me a spirit of research through his constant motivation and encouragement. I consider myself to be fortunate in having him as the guide. The thesis would not have taken this shape but for his constant support and encouragement. I deeply acknowledge his great guidance, fruitful discussions and the effort he has taken in the correction of this thesis amidst his busy schedule.

I am greatly indebted to Dr. Tad. S. Murty, Adjunct Professor, University of Ottawa, Canada for his valuable advice, fruitful discussions and great support.

I owe a lot to Dr. T. S. Shahul Hameed, Scientist-F, for sparing his invaluable time for useful discussions and the unstinted support extended at crucial junctures for the timely completion of this work.

I express my deep sense of gratitude to Dr. K. V. Thomas, Head, Marine Sciences Division, Centre for Earth Science Studies, for the constant encouragement and valuable guidance extended for the research work.

I sincerely acknowledge, the support and encouragement received from Dr. T. N. Prakash, Scientis-F, Marine Sciences Division, Centre for Earth Science Studies.

I am thankful to Dr. M. Baba, former Director, CESS, for the constant encouragement provided to me during the launch of my work.

Special thanks are due to Dr. D. Padmalal, Scientist, Environmental Science Division (ESD), CESS for the constant encouragement and expression of approval and commendation. I am sincerely thankful to Dr. K. Maya, Scientist, ESD for the constant motivation extended for the research work.

Dr. A. N. Balchand, Dept. of Physical Oceanography, Cochin University of Science and Technology (CUSAT) as a member of Research Committee and Doctoral Committee has taken great effort in evaluating the progress and providing valuable advices on several

occasions. I greatly acknowledge the support of Dr. R. Sajeev, Head, Department of Physical oceanography, CUSAT for providing valuable advices.

I am thankful to the Ministry of Earth Sciences (MoES) (previously Department of Ocean Development) for the financial support extended to me as Junior Research Fellow and Senior Research Fellow in the National Project on Tsunami Inundation Modelling funded by them and co-ordinated by ICMAM PD, Chennai. I am also thankful to Dr. M. V. Ramana Murthy, Dr. R. S. Kankara and other Scientists of ICMAM PD for the support extended. I thank Prof. A. D. Rao, IIT Delhi for very useful discussions.

I thankfully acknowledge the support I got from my dearest friend Kalarani Pakkat, Geologist, Geological Survey of India, Chennai throughout the course of my research.

I will not be pardoned if I forget to mention the name of my junior colleague, Shafeer K. B. who enacted the role of a modelling Guru and helped me in various crisis situations during my work.

I express my sincere gratitude to all the Scientists and Technical Officers of Marine Sciences Division. Mrs. Gopika R. Nair deserves special mention for the support rendered towards my research work.

Special thanks are also due to Mr. Tiju I. Varghese for the care he has taken about me at CESS. Moreover Tiju Baiyya has also taken immense care in the scrutiny of my thesis. I profusely thank the sincere efforts taken by my friend Mr. Prasad R., Senior Research Fellow, Marine Sciences Divison in the final stages of my work. Mr. Sreejith C., Assistant Professor, MES College, Ponnani was a reliable source for me to clarify all my doubts during the course of my research. I deeply acknowledge the support, guidance and the oceanographic education provided to me by Dr. V.R. Shamji. I also thank Mr. E. K. Sarathraj, Junior Research Fellow, Marine Sciences Divison for providing effective contributions to my work. Mr. Siju Thankappan Project Fellow, HVRA Cell of Kerala State Disaster Management Authority is thanked for his support. I thank Krishnapriya N. and Ajayakumar for the extended support.

I acknowledge the administrative support extended by Mr. P. Sudeep, Registrar, Mr. A. Gopinathan, Asst. Registrar (Retd.), Mrs. P.C. Rasi, Mrs. Anju and all staff members of

the Administrative and Accounts sections of CESS. I also thank the Librarian and other staff of the library for extending the Library facilities

I thank the officials of Earth Science Forum of CESS and members of Research Committee for their sincere feedbacks during my presentations. I thank all the members of Marine Sciences Division and Centre for Earth Science Studies for the support extended throughout my research work.

The associations and lighter moments shared with Sreekanth K., Madhu Vasudev, Sandeep K. K., Alfred Johny, Lijo Varghese, Vishnu Thilakan, Arun J. John, Noujas, Vimal K .C. and Anoopa has helped to ease my stress and pressure.

I thank the members of fourth estate, especially Mrs. Reema Narendaran of The New Indian Express and Mr. Sreenivas of Deccan Chronicle for giving moral support through wide coverage of my work.

I express my profound gratitude to my father Adv. P. K. Sankarankutty Nair (Former Deputy Director of Employment) and my brother Prabodh S. S. for the unstinted support, understanding and acceptance.

The two girls in my life Reshmi Praveen (Wife), (Assistant Manager, Syndicate Bank) and Niharika Nair (Daughter) require special mention. Reshmi was very considerate to me and allowed me to concentrate on my work without being saddled by the house hold affairs.

A very special mention is required on my father-in-law G. Karthikeyan (Former Branch Manager, Syndicate Bank) and mother-in-law L. Anithakumari (Teacher, Sisuvihar L P S) for the utmost care they have taken in completing my research.

I am quite sure that the immortal souls of my grand parents (Late P. Sivaramapillai-Amminikutty Amma Teacher, Late Koonkoli Parameswaran Nair (Kuttan Pillai Sir) - K. Madhavi Amma) would be happy on the proud moment of me completing this work.

Praveen S. S.

LIST OF FIGURES

LIST OF TABLES

TABLE OF CONTENTS

CHAPTER 1

INTRODUCTION

Tsunamis are water waves generated by a sudden vertical displacement of the water surface. They are waves generated in the ocean by the disturbance associated with seismic activity, under sea volcanic eruptions, submarine landslides, nuclear explosion or meteorite impacts with the ocean. These waves are generated in the ocean and travel into coastal bays, gulfs, estuaries and rivers. These waves travel as gravity waves with a velocity dependent on water depth. The term tsunami is Japanese and means harbour (tsu) and wave (nami). It has been named so because such waves often develop resonant phenomena in harbours after offshore earthquakes.

1.1 GENERATION OF TSUNAMI

Usually tsunamis are generated by a sudden uplift or drop of a large area of the ocean floor caused by a large earthquake, a landfall into a body of water or movement of material at the bottom of the ocean floor by landslides, by several volcanic processes such as crater collapse underwater, mass flow into the water, explosions etc. The water once displaced up or down will seek to move perhaps as far as the opposite side of the ocean. Usually tsunamis are generated by undersea earthquakes. A catalogue of tsunamis in the Indian Ocean and global scenario points that majority of tsunamis are generated by earthquakes. The movement of tectonic plates plays a pertinent role in the generation of earthquakes.

1.1.1 Tectonic Plates

The tectonic plates are a series of plates which cover the entire surface of planet Earth. They can have a depth of up to an estimated 100 km, and are comprised of the entire planet’s crust, most of the moho, and a tiny piece of the upper mantle. This collective area of rocky planets is generally called the 'lithosphere'. The term 'tectonic plates' has been historically used by scientists to describe the movement of the lithosphere, however, nowadays the term 'tectonic plates' is most widely-used for describing the physical plates themselves, rather than their movement. There are 15 major tectonic plates which cover the majority of planet Earth's landmass, and oceanic surface (Fig. 1.1). They all move

gradually about 21 - 75 mm per year (*Pararas Carayannis 2006b*). There are 8 primary plates on the planet (or 7 if the Indo-Australian Plate is counted as a single plate), and they comprise of the majority of the continents' landmass, along with most of the surface area of the world's oceans. The secondary plates are smaller in size than the primary plates, and they do not cover any substantial landmass, apart from the Arabian Plate. There are a further group of smaller plates, often called tertiary plates, which are the disappearing remains of much larger ancient plates that are now on the edges of our major plates, plus some micro-plates, many of whom will be widely considered as a part of a primary or secondary plate on maps and in scientific literatures.

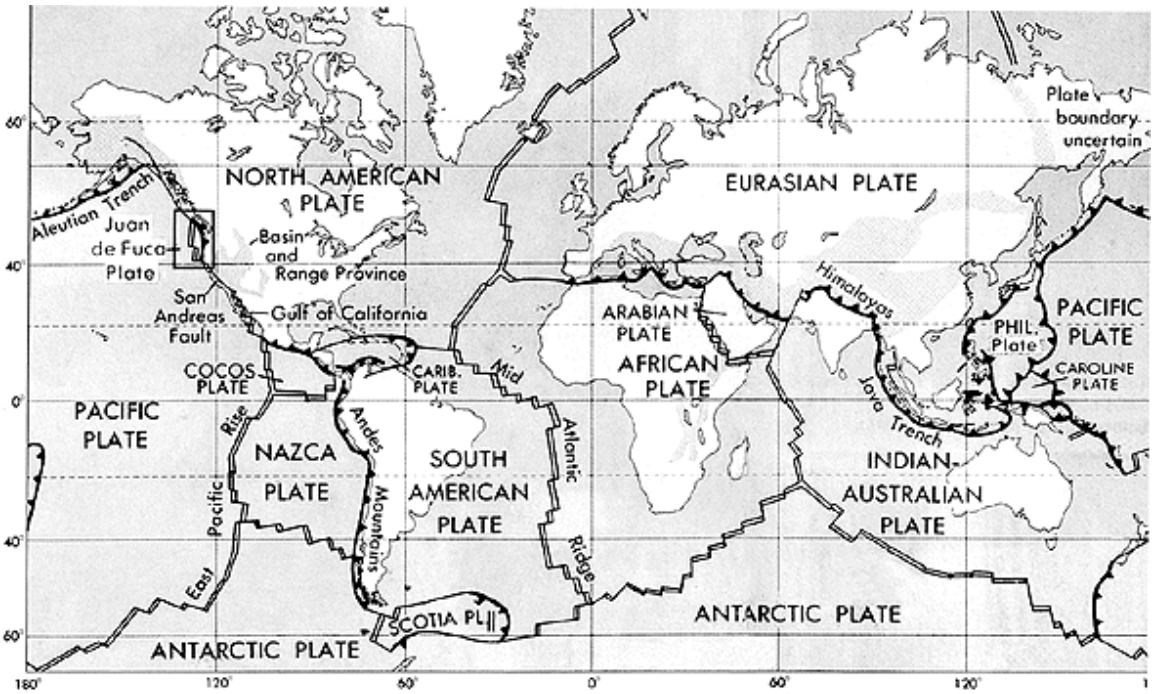

Fig. 1.1 The different primary and secondary plates

The primary plates are:

- African Plate
- Antarctican Plate
- Australian Plate
- Eurasian Plate
- Indian Plate
- North American Plate
- Pacific Plate

- South American Plate

The secondary plates are:

- Arabian Plate
- Caribbean Plate
- Cocos Plate
- Juan de Fuca Plate
- Nazca Plate
- Philippine Sea Plate
- Scotia Plate

The three different type of plate boundaries are

1) Convergent plate boundary

2) Divergent plate boundary

3) Transform plate boundary

1.1.2 Convergent Plate Boundary

Places where plates crash or crunch together are called convergent boundaries (Fig. 1.2). Plates only move a few centimeters each year, so collisions are very slow and last millions of years. Even though plate collisions take a long time, several interesting things happen.

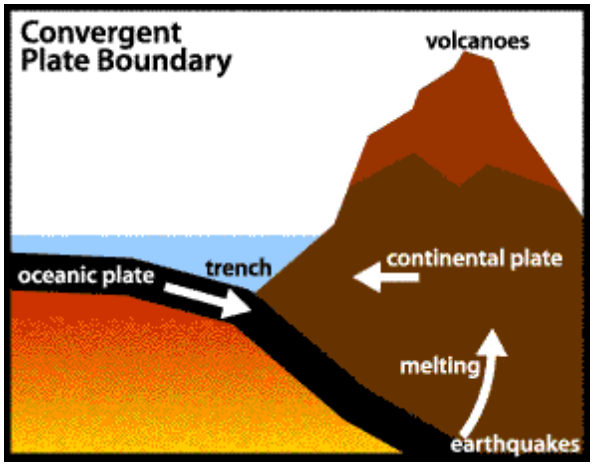

Fig. 1.2 Convergent plate boundary

1.1.3 Divergent Plate Boundary

Divergent plate boundaries are areas under tension where lithospheric plates are pushed apart by magma upwelling from the mantle (Fig. 1.3). Lithospheric plates are regions of earth's crust and upper mantle that are fractured into plates that move across a deeper plasticine mantle. At divergent boundaries, lithospheric plates move apart and crust is created.

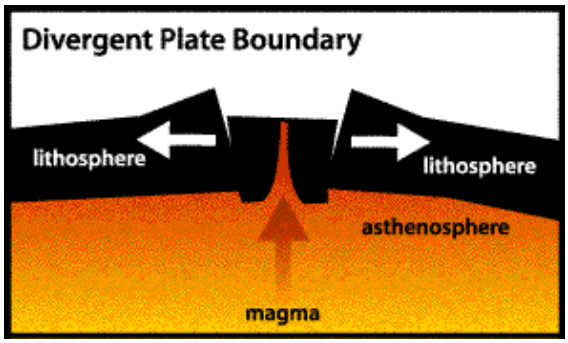

Fig. 1.3 Divergent plate boundary

1.1.4 Transform Plate Boundary

Transform plate boundaries are locations where two plates slide past one another (Fig. 1.4). The fracture zone that forms a transform plate boundary is known as a transform fault. Most transform faults are found in the ocean basin and connect offsets in the mid-ocean ridges. A smaller number connect mid-ocean ridges and subduction zones. Transform faults can be distinguished from the typical strike-slip faults because the sense of movement is in the opposite direction.

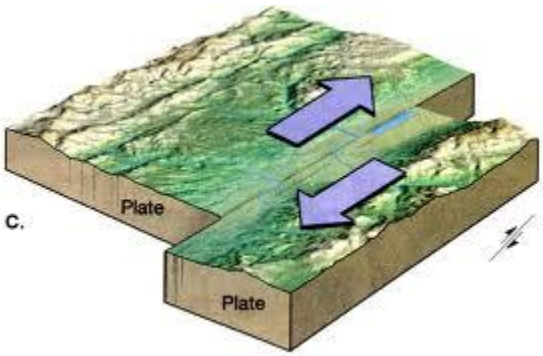

Fig. 1.4 Transform plate boundary

1.2 PROPAGATION OF TSUNAMI

Tsunamis are different from wind waves, which are frequently observed at the coast. They are characterized as shallow water waves, with long periods and wavelengths. A wind wave usually has a period of about 10 s, and a wavelength of 150 m whereas tsunamis actually have a wavelength in excess of 100 km in the deep sea (outside the continental shelf) and period of the order of one hour. A wave becomes a shallow water wave when the ratio between the water depth (d) and its wavelength (L) gets very small, ie,

$$d/L < 0.05$$

Since ocean depth is relatively small when compared to the tsunami wavelength a tsunami wave is in general a shallow water wave. The propagation speed of tsunami thus depends only on depth and is given by

$$c = \sqrt{gd}$$

where $g = 9.8\ m/s^2$ is the acceleration due to gravity

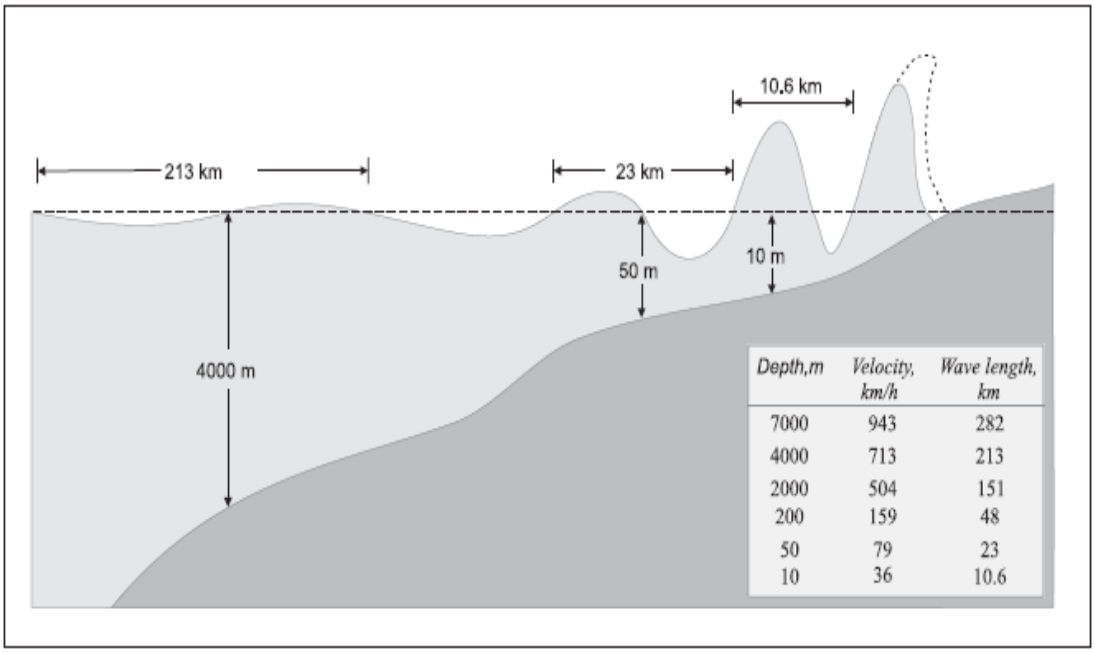

Depth,m	Velocity, km/h	Wave length, km
7000	943	282
4000	713	213
2000	504	151
200	159	48
50	79	23
10	36	10.6

Fig. 1.5 Tsunami wave transformation in the shallow water

Tsunamis not only propagate at high speeds, but they can also travel great transoceanic distances with limited energy loss. As tsunami leaves the deep water of the ocean and travels into shallow water near the coast it gradually transforms (Fig 1.5 and 1.6). As the speed of tsunami is related to the water depths, the speed of tsunami slows down as the water depth decreases. On the other hand the energy flux of tsunami remains almost constant. Tsunami's energy is dependent on both its wave speed and wave height. Subsequently the speed of tsunami diminishes as it travels into shallow water due to shoaling effect; a tsunami imperceptible at the sea may grow to several meters in height near the coast. At the coast a tsunami may behave as a rising or falling tide, a series of breaking waves or even a bore. In the deep ocean an unnoticed tsunami waves can travel at the speed of a commercial jet plane over 900 km/hour. They can propagate from one side of the ocean to the other in less than a day. Oceanographers can predict the arrival time of tsunamis at various locations by knowing the source characteristics of the earthquake that generated the tsunami and the ocean bathymetry.

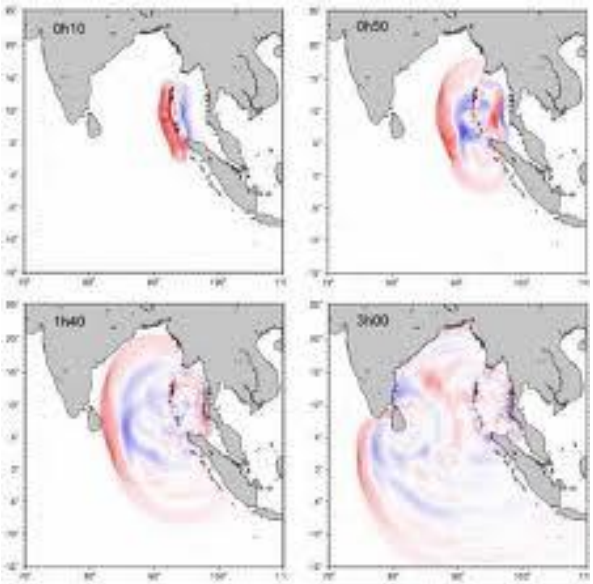

Fig. 1.6 Different stages of propagation of the Sumatra 2004 tsunami

A tsunami wave on approaching the shore slows down and grows to greater heights. Just like other water waves tsunamis begin to lose energy as they reach nearshore, where part of the wave energy can be reflected offshore. The wave energy of the shoreward propagating wave is dissipated through bottom friction and turbulence. Even with all

these losses tsunami still reach the coast with tremendous amounts of energy. Tsunamis still posses the energy to travel thousands of kilometers and still can demonstrate devastating effects on the land. Tsunamis have greater erosional potential, to strip beaches of sand that may have taken years to accumulate and undermining trees and other coastal vegetation. They are also capable of inundating or flooding hundreds of meters of inland past the typical high water level. The fast moving water associated with the inundating tsunami can crush home and other coastal structures.

1.3 TSUNAMI RUN-UP AND INUNDATION

During the tsunami, maximum vertical height up to which the water is observed with reference to sea level is referred to as run-up. The maximum horizontal distance that is reached by a tsunami is referred to as inundation (Fig. 1.7).

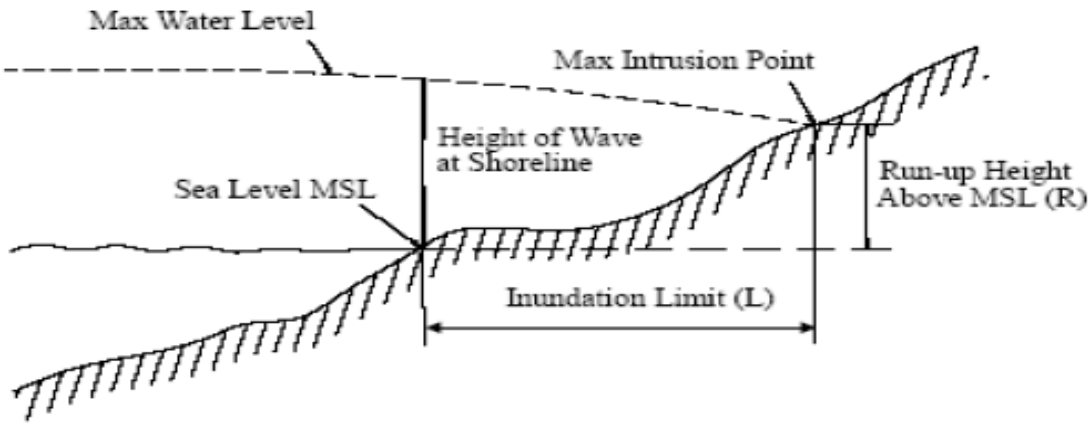

Fig. 1.7 Schematic diagram showing the run-up height and inundation of a tsunami

Run-up is usually expressed in meters above normal tide or Mean Sea Level. Run-ups from the same tsunami can be variable along the coast because of the influence of the offshore bathymetry and geomorphology (shape) of the coastline. In one coastal area destructive waves can be large and violent with large damaging activity, while in another area it can, without being violent, cause extensive flooding with rise in water level to a few meters. The inundation of the area can be up to 2 km and in exceptional cases up to 5 km at locations where estuaries have matching depth profile. While retreating, the waves with considerable velocity tend to carry loose objects and people out to sea. The extent of damage depends on the run-up, velocity of the water, local topography and land use (say settlement, agriculture, forestry etc.).

1.4 TSUNAMI PREDICTION

To forecast tsunamis and determine terminal run-up and destructiveness, one must be able to evaluate the parameters of the tsunami source mechanism in real time, often from inadequate data. Tsunami source mechanism analysis is difficult given the time constraints of a warning situation. Despite the great speed, tsunami waves travel much slower than the seismic waves. Hence earthquake information is often available hours before the tsunamis are able to travel across the ocean. It will suffice to say that forecasting the run-up and potential destructiveness of a tsunami at a distant shore will depend greatly on determining the seismic parameters of the source location such as magnitude of the earthquake, its depth, its orientation, the length of the fault line, the size of the crustal displacements, and depth of the water. Refraction and diffraction processes will affect the energy and height of the tsunami waves as they travel across the ocean. These effects must also be determined. Finally, terminal height, run-up, and inundation of the tsunami at a point of impact will depend upon the energy focusing effect, the travel path of the waves and the coastal configuration.

1.5 TSUNAMI MITIGATION

Earthquakes generating tsunamis have occurred in the past, are occurring now and will continue to occur. To mitigate this hazard, efforts in three directions are needed. On one hand, work has to be done in terms of developing a tsunami early warning system based on online monitoring of causative earthquakes with all its parameters and tsunami generation, propagation and inundation modelling. On the other hand, tsunami hazard maps have to be prepared showing the possible inundation areas in case of a tsunami attack. Lastly, educating people and disseminating information about the impending disaster to the people likely to be affected is another important aspect which should be looked into from the mitigation point of view.

1.6 TSUNAMI EARLY WARNING SYSTEM (TEWS)

Modern technology is capable of offering advance warnings of tsunami events in many areas, giving people the chance to escape to higher ground. The best way to avoid such calamities is by better preparation for any such events in advance. In case of the recent Sumatra earthquake and subsequent tsunami, there was a lag of about 3 hours between the

earthquake and the tsunami reaching the coasts of Indian main land. Unlike the direct damage due to earthquake, where the waves travel much faster and there is hardly any scope for warning, tsunamis may take hours to reach coasts and therefore offer sufficient time for issuing a warning if any such system is in place.

Currently, there are several tsunami warning centers in the world. Many nations like Japan, Australia, Indonesia, Thailand, Europe, Canada and India have come up with their warning centres of tsunami. Subsequently after the tsunami of December 26, 2004 the Ministry of Earth Sciences (MoES) under Government of India established a National Tsunami Early Warning System (NTEWS) in October 2007 at Indian National Centre for Ocean Information Services (INCOIS) in Hyderabad. The oldest of these warning centres is the Pacific Tsunami Warning Centre (PTWC) established in 1946, located at Ewa Beach near Honolulu, Hawaii and the West Coast/Alaska Tsunami Warning Centre (WC/ATWC), established in 1967, located in Palmer, Alaska. Whenever a strong Pacific basin earthquake is detected, scientists at the PTWC locate the earthquake and estimate its magnitude. If the earthquake is located beneath the sea floor and has a surface magnitude of 7.0 or larger, tsunami warnings, watches and information bulletins are issued. Warnings are issued for the communities which are within a three hour travel time from epicenter. A warning means that a damaging tsunami may be on its way. The interpretation of a warning, however, may vary from state to state, and decisions in evacuation of the coastal areas among other things are taken by local authorities. All communities within 3 to 6 hours travel time from the epicenter are put into a tsunami watch situation. A watch means that an earthquake that has a potential to create a tsunami has occurred and local bodies should be on the alert for further information. Tsunami information bulletin is issued to the communities farther than 6 hours travel time from the epicenter. This also works as an alert for the local authorities; however, tsunami information bulletin is also issued when there is no tsunami threat posed by a particular earthquake.

Recently, there have been efforts to detect the tsunamis as they travel through the ocean. As tsunamis may take a few hours to reach the coasts, if they are detected near the source, this time lag can be used to warn the people of a tsunami heading towards them. One such system is the “Deep Ocean Assessment and Reporting of Tsunamis” (DART) (Fig. 1.8), operated by the National Oceanic and Atmospheric Administration (NOAA) of the

United States as part of the U.S. National Tsunami Hazard Mitigation Programme. DART systems consist of an anchored seafloor bottom pressure recorder (BPR) and a companion moored surface buoy for real-time communications. The BPR can detect tsunamis with heights as small as 1 cm in water depths of 6,000 m. An acoustic link transmits data from the BPR on the seafloor to the surface buoy. The data are then relayed via a Geostationary Satellite Server (GOES) to ground stations, which demodulate the signals for immediate dissemination to NOAA's Tsunami Warning Centers. Currently six such buoys are operating in the Pacific Ocean.

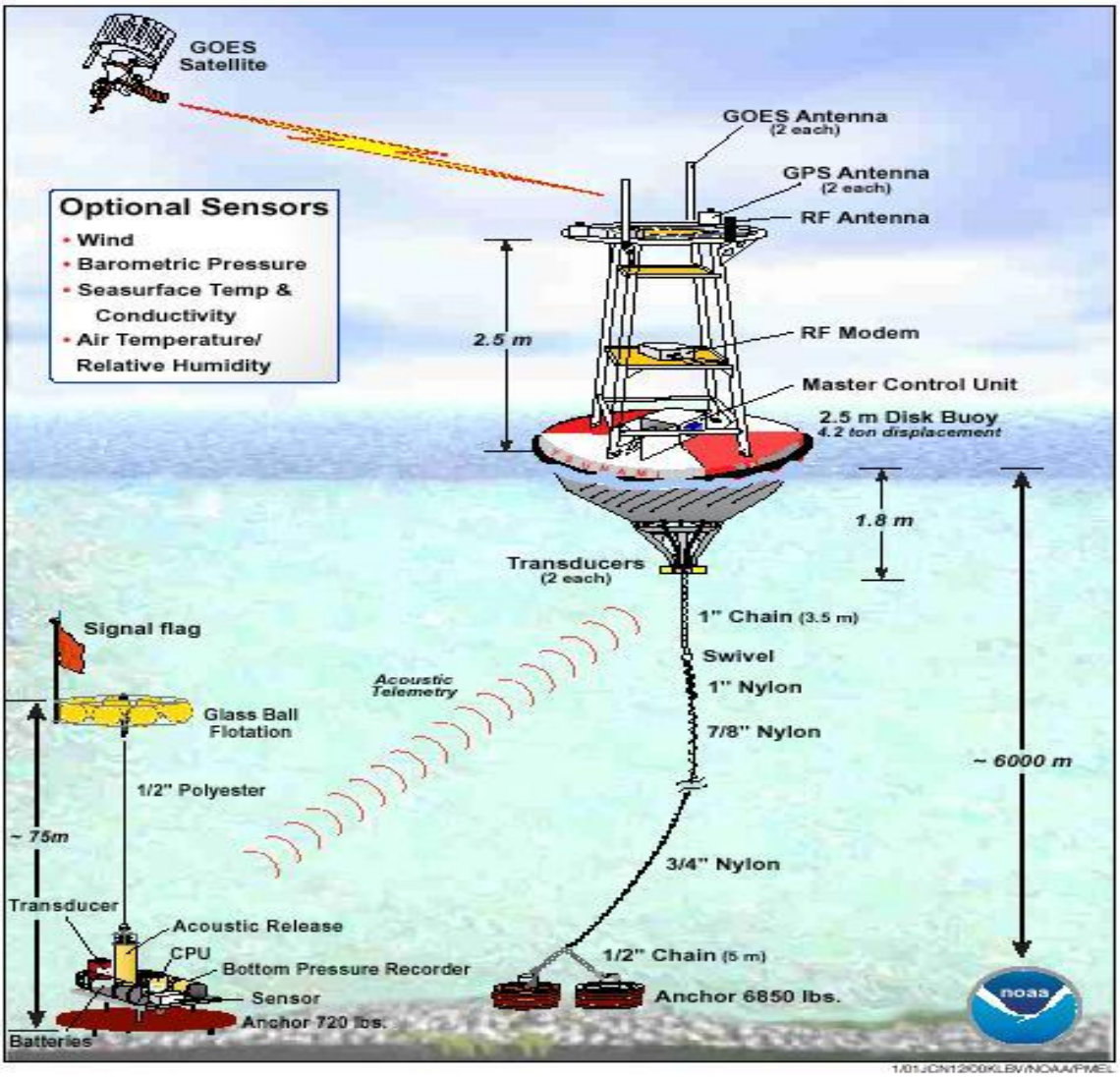

Fig. 1.8 Deep Ocean Assessment and Reporting of Tsunamis
(Source: http://nctr.pmel.noaa.gov/Dart/dart_ms1.html)

The other techniques that can be used for real-time detection of a tsunami may involve sensitive radar altimeters aboard satellites, which can detect subtle rises in the sea or measurement of the rise of water surface through GPS sensors aboard ships or buoys.

However, a warning system may never be quick enough to alert those living near the earthquake source (for example, Andaman and Nicobar Islands in case of Sumatra earthquake). In such situations, the earthquake shocks themselves work as a warning. The earthquake waves reach before tsunamis and can warn the inhabitants of a potential tsunami. Pacific warning centre in USA follows similar practice in Hawaii Islands. In Hawaii, which is targeted by tsunamis from all directions, the maps of safe zones are printed in each island's telephone book. Thus, apart from the development of a unified tsunami warning system, the need of the hour is to train people to understand the hazard of tsunami, and the ways to minimize its devastating effects. People living along the coastlines need to be educated about some simple facts about tsunamis, which can prove very helpful in preventing large number of casualties and damages. Some of these are:

- A tsunami may consist of several waves with an interval of up to an hour. Therefore, one should stay away until all of them have passed
- An earthquake near the coast is very likely to produce a tsunami and therefore, one should take such an earthquake as a warning of a potential tsunami and should move away from the coasts immediately
- Tsunamis are preceded by a noticeable rise or fall in water level, and this may also be considered as a subtle warning of a tsunami on its way
- One should never go down to the beach to watch a tsunami, especially to the near shore zone exposed during initial withdrawal as by the time one sees a wave coming it may be too late to escape

1.7 INDIAN TSUNAMI EARLY WARNING SYSTEM

Recognizing the imperative to put in place an Early Warning System for mitigation of oceanogenic disasters that cause severe threat to nearly 400 million of our population that live in the coastal belt, the Ministry of Earth Sciences (MoES) has established the National Tsunami Early Warning System in October 2007.

The Warning System has been established by MoES as the nodal ministry in collaboration with Department of Science and Technology (DST), Department of Space (DOS) and the Council of Scientific and Industrial Research (CSIR). The National Tsunami Early Warning Centre has been set up at Indian National Center for Ocean Information Services (INCOIS), Hyderabad with all the necessary computational and communication infrastructure that enables reception of real-time data from the network of national and international seismic stations, tide gauges and bottom pressure recorders (BPRs). Earthquake parameters are computed in less than 15 minutes of occurrence. A database of pre-run scenarios for travel times and run-up height is being created using TUNAMI N2 model. At the time of event, the closest scenario is picked from the database for generating advisories. Water level data enables confirmation or cancellation of a tsunami. Tsunami bulletins are then generated based on decision support rules and disseminated to the concerned authorities for action, following a standard operating procedure. The criteria for generation of advisories (warning/alert/watch) are based on the tsunamigenic potential of an earthquake, travel time (i.e. time taken by the tsunami wave to reach the particular coast) and likely inundation. The performance of the system was tested for the earthquake of magnitude 8.4 off Java coast on 12th September 2007. The system performed as designed. It was possible to generate advisories in time for the administration and unnecessary evacuation was avoided.

The Indian coast has recorded few tsunamis in the past. However, in spite of infrequent occurrence of tsunamis (about 6 events reported in the 20th century) in the Indian Ocean, they could occur at any time and could be very devastating. The latest Indian Ocean Tsunami (26th December 2004) has been one of the strongest in the world and the deadliest of all time by an order of magnitude. The east and west coasts of India and the island regions are likely to be affected by tsunamis generated mainly due to earthquakes in the subduction zones in the Indian Ocean. Hence there was a need for developing Tsunami Warning System.

1.7.1 Components of Indian Tsunami Warning System

The following are the major components of the Indian Tsunami Warning System.

1.7.1.1 Seismic stations

A Network of land-based seismic stations for earthquake detection and estimation of focal parameters in the Andaman-Sumatra and Makran tsunamigenic zones is a prime requirement of the warning centre. INCOIS is receiving real-time seismic data from international seismic networks as well as from India Meteorological Department (IMD) and has been detecting all earthquake events occurring in the Indian Ocean in less than 15 minutes of their occurrence. Necessary softwares have been installed for real-time data reception, archiving, processing and auto-location of earthquakes as well as for alert generation and automatic notification.

1.7.1.2 Tide Gauges and Bottom Pressure Recorders (BPRs)

In order to confirm whether the earthquake has actually triggered a tsunami, it is essential to measure the change in water level as near to the fault zone as possible with high accuracy. Bottom Pressure Recorders (BPRs) are used to detect the propagation of tsunami waves in open ocean and consequent sea level changes. The National Institute of Ocean Technology (NIOT) has installed 4 BPRs in the Bay of Bengal and the 2 BPRs in Arabian Sea. These BPRs can detect changes of 1.0 cm at water depths up to 6 km. A network of tide gauges along the coast helps to monitor progress of tsunami as well as validation of the model scenarios. The NIOT and Survey of India (SOI) have installed 30 tide gauges to monitor the sea level. Near-real time data is being received from national and international centers. Necessary software for real-time reception, display and archiving of tide gauge data has been developed.

1.7.1.3 Tsunami inundations models

The TUNAMI N2 model basically takes the seismic deformation as input to predict the run-up heights and inundation levels at coastal regions for a given tsunamigenic earthquake (Imamura, 2006). The seismic deformation for an earthquake has been computed using Smylie and Mansinha (1971) formulation using the earthquake parameters like location, focal depth, strike, dip and rake angles, length, width and slip of the fault plane. At the time of earthquake, only location, magnitude and focal depth are available immediately. For operational quantitative tsunami forecast, there needs to be a method to quickly estimate the travel times and run-up based on the above available

parameters. For this purpose, all the other input parameters such as length, width and slip are calculated from the magnitude using global relations (Papazachos et al., 2004).

1.7.1.4 High resolution data base on bathymetry and coastal topography

Generating and updating a high resolution database on bathymetry, coastal topography, coastal land use, coastal vulnerability as well as preparing historic data base on tsunami and storm surge inundation are vital. The accuracy of model predictions is directly related to the quality of the data used to create the bathymetry and topography of the model area. Coastal bathymetry is the prime determinant of the height of the tsunami wave or storm surge as it approaches the coast. High resolution coastal bathymetry is thus the key input for various tsunami and storm surge prediction models. Preliminary surveys have already been conducted to acquire high-resolution bathymetry for a few vulnerable areas of the coastline. Naval Hydrographic Office (NHO) has been providing detailed bathymetry data. Topography of the entire coastline of the country is required at 1:25,000 scale with contours at intervals of 0.5 m up to 20 m contour interval. The National Remote Sensing Agency (NRSA) has been mapping the topography of about 15,000 sq. km area with airborne LIDAR & Digital Camera data in conjunction with GPS control survey using photogrammetric techniques. 3000 sq. km area has already been mapped. These products have been used to prepare coastal vulnerability maps.

1.7.1.5 A fully operational warning centre

A dedicated Tsunami Warning Centre comprising of necessary computational, communication and technical support infrastructure as well as a robust application software that facilitates data reception, display, analysis, modelling, and decision support system for generation of tsunami advisories following a standard operating procedure has been established. The warning centre continuously monitors seismic activity in the two tsunamigenic source regions and sea level through the network of national and international seismic stations as well as tide gauges and bottom pressure recorders (BPRs). The monitoring of water level enables confirmation or cancellation of a tsunami. A custom-built software application generates alarms/alerts whenever a pre-set threshold is crossed. Tsunami bulletins are then generated based on pre-set decision support rules and disseminated to the concerned authorities for action, following a Standard Operating Procedure (SOP).

1.8 BACKGROUND OF THE PRESENT INVESTIGATION

Tsunami was not known in India till 2004, other than as a formidable process elsewhere. If at all tsunamis have occurred in India back in history, the frequency might have been small. Tsunami is one of the most devastating natural coastal disasters. Most of the tsunamis are generated by submarine earthquakes occurring in subduction zones. Tsunamis can also be triggered by volcanic eruptions and large landslides. Although the skill for predicting earthquake is still in its infancy, tsunami warning is possible if the tsunami can be detected in the open ocean. Tsunami warning system has been operational in the Pacific Ocean for several decades and has proven its effectiveness and trustworthiness. If a similar early warning system had been available in the Indian Ocean in 2004, the devastation due to the 2004 Indian Ocean tsunami would have been much less.

As already described in the previous section, the establishment of a Tsunami Warning System in the Indian Ocean was the immediate task undertaken by the Government of India in the aftermath of the 2004 Tsunami. As already seen, one important component of the Tsunami Warning System is the numerical model for prediction of tsunami inundation in the event of a tsunami. This can be accomplished by the set up of tsunami inundation models and by preparing inundation maps for vulnerable locations of the coasts for different scenarios of earthquakes. These models have to be set up for each coast and calibrated using past tsunami field data. The set up of these models enables us to analyse the generation, propagation and inundation characteristics of tsunami and identify the different physical processes involved. It also helps us in simulating future scenarios which ultimately will pave way for planning of mitigation measures.

In the light of the above, the set up of a tsunami inundation model, and an investigation on the tsunami propagation in the South East Arabian Sea (SEAS) and the scenarios of inundation characteristics along the Kerala and Lakshadweep coasts was felt very important and hence the present investigation was taken up.

1.9 OBJECTIVES OF THIS INVESTIGATION

The investigation which was the first of its kind for the SEAS was launched with the following objectives:

- Set up and calibration of Tsunami inundation model for the Kerala coast
- Study of tsunami propagation characteristics in the South East Arabian Sea (SEAS)
- Study of tsunami vulnerability along the Kerala coast for different sources
- Tsunami vulnerability analysis for selected islands of Lakshadweep
- Study of resonance in selected harbours during tsunami propagation.
- Assessment of scenarios of tsunami inundation in the context of sea level rise in the climate change scenario

This thesis embodies the results of the studies carried out in realising the above objectives.

1.10 STRUCTURE OF THE THESIS

The Thesis comprises of eight chapters. Chapter 1 gives an introduction to the present investigation. The basics of tsunami generation, propagation, inundation and run-up are discussed. The chapter also explains the working of tsunami early warning system with special reference to the functioning of Indian Tsunami Early Warning System and its components. The background of the present study, the objectives of the study and the structure of the thesis are enunciated.

The extensive literature review carried out for this work which includes literature review about the numerical modelling of tsunami inundation, field investigations carried out in the aftermath of December 2004 tsunami and a catalogue of the previously occurred tsunamis in the global and Indian scenario are presented in the Chapter 2.

The Chapter 3 describes the numerical models used globally for tsunami inundation modelling with special reference to TUNAMI N2 model used in this investigation. The model equations, structure of the model, model grids and the various input parameters of TUNAMI N2 are described.

The Chapter 4 presents the data and methodology used in this work. The whole process associated with the collection and collation of data, its processing, extraction of necessary input parameters, model set up and running, and finally extraction of output is described in this chapter. The calibration of the model is the major highlight of this chapter.

The propagation characteristics of tsunami in the South East Arabian Sea with special reference to Laccadive Maldive Ridge (LMR) and the role played by LMR in the reflection, interference, focussing and defocussing of tsunami energy leading to site specific inundation and run-up are presented in the Chapter 5. Simulations were also carried out excluding the ridge for getting an in-depth idea about the role played by LMR. The results of numerical simulation carried out for understanding the resonance phenomenon in two harbours of south west coast of India are also presented.

The Chapter 6 deals with the run-up and inundation characteristics along the Kerala and Lakshadweep coasts for three different sources viz. Sumatra 2004, Makran 1945 and a hypothetical potentially worst case source from Makran. The results of tsunami vulnerability analysis for the whole Kerala coast and for four selected Islands of Lakshadweep viz. Chetlat, Kavaratti, Kadmat and Androth are presented in this chapter.

There is a growing perception that the sea level is going to increase in the next century. Numerical modelling studies carried out for understanding the scenarios of tsunami inundation arising out of possible rise in sea level are presented in the Chapter 7. The run-up and inundation characteristics for different scenarios of sea level rise are analysed for three representative sectors of the Kerala coast.

The thesis ends with the Chapter 8 presenting the summary and conclusions of the work and the recommendations for future work.

CHAPTER 2

LITERATURE REVIEW

2.0 INTRODUCTION

The havoc brought by the 2004 Sumatra tsunami was an eye opener for all the entire countries in the Indian Ocean region to take up research and development activities and mitigation measures with regard to tsunami. Subsequently research on different aspects of tsunami picked up momentum. A good number of publications are right now available covering various aspects of the tsunami. This chapter presents a review of literature survey carried out on various aspects related to the present investigation, such as historical tsunami, field data on tsunami vulnerability, numerical modelling of tsunami inundation, etc.

2.1 HISTORICAL TSUNAMI

A review about historical tsunamis in the global scenario and Indian vicinity are presented below.

2.1.1 Historical Tsunami in the Global Scenario

The tsunami generated by the December 2004 Sumatra earthquake is probably the worst globally in the total recorded history of tsunamis. It devastated several countries. The toll was very heavy in Indonesia, Sri Lanka, India and Thailand. Prior to 2004 also several tsunamis devasted different coasts of the globe. The Pacific Ocean is a place for frequent tsunamis since it is a zone of several convergent tectonic plate boundaries. In Atlantic Ocean the plate boundaries being divergent tsunamigenic earthquakes are infrequent. Table 2.1 compiled from the information available at the website of www.georgepc.com lists out the major global tsunamis from time immemorial.

2.1.2 Historical Tsunamis in the Indian Peninsula

Unlike the Pacific Ocean, tsunamis are not common in the Indian Ocean. Pacific Ocean reports at an average of about eight tsunamis per year, whereas Indian Ocean has one in three years or so (Rastogi and Jaiswal, 2006). Out of the total 90 plus tsunamis that is

Table 2.1 Historical tsunamis in the Global scenario
(Source: www.drgeorgepc.com, Last Accessed on 21 May 2012)

SL. No.	Date	Location	Earthquake Magnitude (M_w)	Max. Tsunami Run-up (m)
1	1650 B.C (+/- 50 yrs)	Volcanic eruption at Santorin during Bronze age	NA	NA
2	325 B.C.	Earthquake in Makran coast in North Arabian Sea	8.0	2
3	November 1, 1755	West South West (WSW) of Cape St. Vincent Atlantic Ocean	9.0	20
4	September 20, 1771	Ryukyu Islands	7.7	5
5	December 1812	Sant Barbara, Southern California	NA	10.5
6	August 26, 27 1883	Krakatau volcanic eruption	NA	22-30
7	1833	Central Sumatra	8.7	No tsunami
8	1945	Makran coast in Northern Arabian Sea.	8.0	10-15
9	May 22, 1960	South Central Chile	9.5	2.2
10	March 27, 28, 1964	Alaska- Hawaiian Islands	8.0	6.3
11	October 17, 1966	East of Peru Trench axis	7..5	1.6
12	November 29, 1975	South Coast of Hawaii	7.2	3.5
13	August 16, 1976	Cotabato	7.2	4.5
14	Aug 19, 1977	Lesser Sunda Islands (Indonesia)	7.7	6
15	December 12, 1979	Columbia	7.9	5
16	September 19, 1985	West Coast of Mexico	8.1	3
17	November 12, 1999	North West Turkey	7.2	NA
18	November 26, 1999	South West Pacific	7.3	2-3
19	May 3,1999	North East of Nukualofa	7,9	0.60
20	January 13, 2001	Elssalvador	7.9	NA
21	January 25, 2001	North East town-Bachau, Gujarat	7.9	NA
22	February 28, 2001	Seattle-Taloma area	6.8	NA

23	June 23, 2001	Southern Peru	8.1	4-5
24	January 2, 2002	West port vila	6.3	0.8
25	December 26, 2004	West coast of Northern Sumatra	9.3	20
26	March 28, 2005	Western Sumatra	8.7	0.30
27	January 8, 2006	Southern Greece	7.9	NA
28	July 17, 2006	North East of Christmas Island, Jakartha	7.7	5
29	October 15, 2005	North West coast of Hawaii	6.7	0.20
30	November 15, 2006	Kuril Islands, Russia	8.3	0.40
31	Jan 13, 2007	Near the Kuril Islands	8.1	NA
32	April 1, 2007	North West Honiara Soloman Islands	8.1	NA
33	August 15, 2007	North West of Chinja-Alta Peru	8.1	10.0
34	September 12, 2007	South Coast of Sumatra	8.4	0.90
35	September 29, 2009	Samoan Islands	8.3	3.14
36	March 11, 2011	Japan	9.0	39.0
NA - Information not available				

reported so far for the Indian Ocean 70 are from Sunda. Though rare, tsunamis have hit India earlier. The tsunamis in the Indian region and vicinity as reported by Rastogi and Jaiswal (2006) are listed in the Table 2.2.

The oldest record of tsunami is available from November 326 BC earthquake near the Indus delta/Kutch region that set off massive tsunami waves in the Arabian Sea. Alexander the Great was returning to Greece after his conquest and wanted to go back by a sea route. But a tsunami due to an earthquake of large magnitude destroyed the mighty Macedonian fleet (Lisitzin, 1974). Poompuhar is a town in the southern part of India in the state of Tamil Nadu. It was a flourishing ancient town known as Kaveripattinam that was washed away in what is now recognized as an ancient tsunami in around 500 AD. This time matches with the Krakatau explosion.

There is a mention in the scriptures about a tsunami effect that destroyed a Budhist monastery in 900AD at Nagapattinam as reported by Rastogi and Jaiswal (2006) and subsequently they quote: "According to literature available in the library of Thondaiman kingdom in Puduckottai, Tamilnadu, it was during the reign of Raja Raja Chola that waves had washed away the monastery and several temples and killed hundreds of people. There is evidence of this in Kalki Krishnamurthy's book "Ponniyin Selvan- the Pinnacle of Sacrifice". In the chapter "The Sea Rises", the author explains how the sea had risen very high and the black mountain of water moved forward. The sea inundated warehouses and sheds and began to flow into the streets. Ships and boats seemed suspended in mid-air, precariously poised on the water peaks. The book also describes "how an elephant was swallowed by the gushing water of tsunami".

Murty et al. (1999) reported that a tsunami had occurred in the North Indian Ocean which originated in the Iranian coast from a local earthquake between 1st April and 9th May 1008. The details regarding an earthquake which occurred in 1524 off the coast of Dabhol, Maharashtra was reported by Bendick and Bilham (1999). The earthquake led to a large tsunami which resulted in a huge alarm to the Portuguese fleet that was assembled in the area. An earthquake in the Bangladesh-Myanmar border region generated a tsunami on 2nd April 1762 which resulted in inundating more than 160 km length of Arakan coast (Mathur, 1998). The epicenter was 257 km SE of Dhaka, Bangladesh. Water levels in the Hoogly River in Kolkata rose to around 2 m. Causalities were also reported at Dhaka where hundreds of boats capsized and several people were drowned. A severe earthquake in Kutch of magnitude 7.8 (Macmurdo, 1821) led to large inundation in the town of Sindri on 16th June 1819. The earthquake and tsunami was followed by large changes in the elevation of land. Mihir Guha, Former Director General of Indian Meteorological Department reported that a tsunami struck Sunderbans in May 1874 (Rastogi and Jaiswal, 2006). An earthquake in the Bhola district gave rise to tsunami and created havoc in vast areas of Sunderbans, 24 Paraganas, Midnapore, Barishal Khulna and Bhola. Twenty three years later on 11th November 1842 an earthquake near the northern end of Bay of Bengal caused a tsunami by which waters of the distributaries of the Ganges Delta were flooded leading to large destruction. Nelson (1846) reported about a tsunami on 19th June 1845 in Kutch as: "The sea rolled up the Koree (Kori creek, 23.6° N, 68.37° E) mouth of the Indus overflowing the country as far westward as the Goongra river, northward to the vicinity of Veyre, and eastward to the Sindree Lake". On 31st October 1847 the small

Table 2.2 Historical tsunamis in the Indian coast
(Source: Rastogi and Jaiswal 2006)

Sl. No.	Date	Location	Lon (Deg)	Lat (Deg)	Eq. Mag. (M_w)
1	326 BC	Indus Delta/Kutch region	NA	NA	NA
2	About 500 AD	Poompuhar, Tamil Nadu	79.52	11.12	NA
3	900 AD	Nagapattinam, Tamil Nadu	79.53	10.46	NA
4	1008	Iranian coast	60.00	25	NA
5	12.04.1762	Bay of Bengal (Bangladesh)	92.0	22	NA
6	16.06.1819	Kutch	26.60	71.9	7.8
7	11.11.1842	Northern Bay of Bengal	90.00	21.5	NA
8	19.06.1845	Kutch	23.60	68.37	NA
9	31.10.1847	Little Nicobar Island	93.66	7.333	7.5-7.9
10	19.08.1868	Andaman Islands	92.73	11.67	NA
11	1874	Sunderbans (Bangladesh)	89.00	22	NA
12	31.12.1881	West of Car Nicobar	92.43	8.52	7.9
13	January 1882	Sri Lanka	81.14	8.34	NA
14	27.08.1883	Krakatau (Volcanic Eruption)	105.25	-6.06	NA
15	1884	West of Bay of Bengal	NA	NA	NA
16	31.05.1935	Andaman-Nicobar	NA	NA	7.5
17	25.11.1935	Andaman-Nicobar	94.00	5.5	6.5
18	26.06.1941	Andaman Islands	92.50	12.1	7.7
19	27.11.1945	Makran coast	63.50	25.2	8.0
20	30.11.1983	Chagos ridge	72.11	-6.85	7.7
21	26.12.2004	Off west coast of Sumatra and Andaman-Nicobar	95.94	3.307	9.3
NA = Not Available					

Island of Kondul (7° 13’ N, 93° 42’ E) near Little Nicobar was inundated by an earthquake of magnitude greater than 7.5 as reported by Heck (1947), Berninghausen (1966) and Bilham et al. (2005).

A tsunami was generated by an earthquake of magnitude M_w 7.9 that occurred at Car Nicobar Island on 31st December 1881 in the Bay of Bengal. Eventhough the run-up of this tsunami was not so large the impact was visible at Andman & Nicobar Islands and east coast of India. A run-up of 1m was observed at Port Blair on South Andaman Island (Berninghausen, 1966) whereas in the Nicobar Islands, the run-up was less than 0.75 m. At Nagapattinam where the tsunami first arrived on the east coast of India the run-up was around 1.2 m. Amplitudes of less than 0.3 m were recorded later in the day by tidal gauges at Dublat at the mouth of the Hoogly river at 13:00 LT and then in Diamond Harbour at 15:10 LT (Ortiz and Bilham, 2003). The east coast of Sri Lanka was also not spared from this tsunami as waves were also observed at Batticaloa and Trincomalee (Berninghausen, 1966). Ortiz and Bilham, (2003) reported that no tsunami was visible in Myanmar during this event. The Andaman earthquake on 26th June1941 with a moment magnitude M_w 7.7 (Bilham et al., 2005) had triggered a tsunami in the Bay of Bengal. Run-up of the order of 0.75 -1.25 m was reported along the east coast of India. At that time no tide gauge was in operation. The deadliest tsunami prior to 2004 in South Asia was in November 1945 (Rastogi and Jaiswal, 2006). This tsunami originated off the Makran coast of Pakistan in the Arabian Sea and caused deaths as far as Mumbai. More than 4000 people were killed on the Makran coast by both the earthquake and the tsunami. The tsunami reached a height of 12-15 m in some parts of Makran and caused great damage to the entire coastal region. The tsunami had a run-up of 11.0-11.5 m in Kutch, Gujarat (Pendse, 1945). It was recorded in Bombay Harbour, Versova (Andheri), Haji Ali (Mahalaxmi), Juhu (Ville Parle) and Danda (Khar). The run-up of tsunami in Mumbai was 2 m.

2.2 FIELD OBSERVATIONS ON RUN-UP AND INUNDATION

Hettiarachchi and Samarawickrama (2005) carried out post-tsunami survey for the 2004 Sumatra tsunami along the Sri Lankan coast and from the analysis of data found that, among the series of tsunami waves, the second set of waves were the largest along the coastline of Sri Lanka. The eastern portion of Sri Lanka witnessed huge run-up while comparing with that of other sectors. The observed run-ups in the eastern portion were in the range of 5-15 m. The western region recorded considerably less run-up in the range of 2-10 m. The run-up was in the range of 3-4 m at the northern sector and 7-9 m in the southern sector of Sri Lanka.

Borrero (2005) carried out a field survey of 2004 Sumatra earthquake and tsunami effects in the region around Banda Aceh in northern Sumatra. The highest run-up and wave height traces were observed to the southwest of Banda Aceh, on the open west coast near the town of Lhoknga. The authors reported that run-up heights even exceeded 30 m at Banda Aceh. At the other locations on the east coast like Idi and Panteraja the run-up heights were 2.5 m and 5 m respectively whereas 6 m run-up was observed at Kreung Raya 45 km east of Banda Aceh. The run-up was around 8 km at Kreung Raya and Banda Aceh. The authors found that the leading edge of the tsunami propagated at around 2 m/sec and then got increased to 10-15 m/sec by analysing the video and still images. The video and images were analysed in three sections, 1) pre-tsunami 2) during the event of tsunami and 3) post-tsunami. The observed run-up at other locations are 20.1 m at Breuh Island and 10.7 m at Deudap Island.

Papadopoulos et al. (2006) conducted post tsunami field surveys and measurements in Sri Lanka and Maldives about two weeks after the catastrophic Indian Ocean tsunami of 26 December 2004. Their measurements indicated maximum water levels ranging from 3-11 m along the southwest, south and east coastal zones of Sri Lanka. The highest observed run-up were 10 m and 11 m in the south of the island namely Galle and Hambantota. A maximum inundation of around 2 km was observed in Hambantota. But in Maldives, the maximum water level was only around 3 m in Laamu Atoll. In Thailand eyewitnesses reported that the strong wave arrival occurred between 02:55 and 03:10 Hrs. at locations like Patong beach, west side of Phucket Island, in the Boat Lagoon Port, east side of Puchet, and in Maya Bay, Phi-Phi Islands. From the observed and collected information the authors clearly indicated that tsunami propagated as a leading crest wave to the west side, e.g. in Sri Lanka and Maldives, and as a leading trough wave to the east, e.g. in Thailand.

Koh et al. (2009) compiled the post tsunami data from surveys conducted twice in 2005 along tsunami-impacted beaches in Peninsular Malaysia. The authors reported that surveyed tsunami run-up heights along the beaches in Penang varied between 2.3 m and 4.0 m, while run-up in Langkawi were in between 2.2 m and 3.7 m. For the state of Kedah excluding Langkawi the run-up heights were observed to vary between 0.38 m and 3.8 m exhibiting significant scattering. Miami Beach showed a run-up of 4.5 m which was the maximum followed by run-up heights of 3.46 m, 3.75 m and 3.66 m at Teluk

Bayu, Pantayi Chenang and Pantayi Tengah respectively. A minimum run-up of 0.39 m was observed at Tanjung Dawai. There was no significant inundation except for a 190 m inundation at Tanjung Tokong. The variations in run-up were attributed to the local features such as bathymetry, land curvature and sea–land nonlinear interactions.

Ramana Murthy et al. (2011) carried out post-tsunami survey for the 2004 December 26 Sumatra tsunami along the Cuddalore coast using RTKGPS. The authors reported that the maximum inundation was about 2 km from the shore in the low lying areas. They also reported about the destruction that happened to the landforms. The authors pointed out that landform such as sand dunes have acted as a barrier in the inundation of tsunami water and it mainly contributed towards the variation of tsunami inundation from place to place in Cuddalore. The survey highlighted Pachaiyankuppam as the highest inundated location with an inundation of 930 m and Trichopuram as the least inundated location with 343 m. The inundation in other locations were as follows: Kudikadu-906 m, Thiyagavalli-729 m, Aryagoshti-664 m, Kayalpattu-573 m, Andarmullipalam-514 m, Periyapattu-391 m, Silambimangalam-366 m and Villanallu-416 m.

Ranga Rao et al. (2011) reported about the field observations of 2004 Sumatra tsunami along the South Andhra Coast. The authors reported that the 2004 Sumatra tsunami caused considerable damages along the south Andhra coast, especially along the Krishnapatnam, Kaveli and Ongole coasts. The field observations showed Krishnapatnam and Kaveli as the most affected with a run-up value of 1.9 m and inundation in the range of 200-1350 m. The authors observed that the inundation was limited to the range of 200-400 m in places of straight coasts whereas inundation extended further inland in the range of 600-1350 m in coastal sectors characterized by creeks, inlets and river mouths. The inundation of the other locations are mentioned in the Table 2.3.

Ramana Murthy et al. (2012) mapped the field observations of about eight villages in the coastal Nagapattinam Taluk. The authors reported that the Nagapattinam beach was totally eroded in the 2004 Sumatra tsunami claiming about 30 lives (Table 2.4). Moreover tsunami caused heavy damage to the wharfs and structures at Nagapattinam Portland. The damage was attributed to the prevailing topography of the area which is compounded by

Table 2.3 Observed inundation of tsunami along the South Andhra coast due to 2004 Sumatra tsunami (Source: Ranga Rao et al., 2011)

Sl. No.	Location	Run-up (m)
1	Chinnapallipalem	1.8
2	Patapattapalem	1.6
3	Kattapalem	1.6
4	Krishnapatnam	1.5
5	Tammanapatnam	1.6
6	Momidi	1.5
7	Kottapatnam	1.5
8	Tummalapenta North	1.9
9	Kotasatram	1.9
10	Peda Ramudi palem	1.8
11	Tummalapenta south	1.7
12	Nadimpalla	1.7
13	Lakshmipuram	1.7
14	Kota Bangaru palem	1.8
15	Chellammagorlpalem	1.5
16	North Manneru	1.7
17	Alagayapalem	1.7
18	Pattu palem	1.2
19	Ramya patnam	1.3
20	Kurlapalem	1.3
21	Chennayam Palem	1.7

Table 2.4 Observed inundation of tsunami along the Nagapattinam coast (Source: Ramana Murthy et al., 2012)

Sl. No.	Location	Run-up (m)	Inundation (m)
1	Pattanachcheri	3.62	958
2	Nagoore	3.60	976
3	Nambiyarkuppam	3.80	772
4	Nagapattinam Beach	3.70	1468
5	Akkara pettai	2.0	2822
6	Kallaru	2.0	1057
7	Therkku Poyyur	5.70	804
8	Velan Kanni	4.46	853

the combination of features like narrow beach, shallowness of the continental shelf and flat backshore.

Usha et al. (2012) documented the field observations on 2004 Sumatra tsunami in the city of Chennai. They reported a maximum inundation of 575 m at Chepauk and a minimum inundation of 115 m at Kasimedu. The other regions like Royapuram, Ayodhya Kupam, RK Road, Thideer Nagar, Sreenivasapuramkuppam and Ururkuppam showed an inundation of about 320 m, 360 m, 295 m, 200 m, 340 m and 160 m respectively.

Jayakumar et al. (2005) carried out post tsunami survey along the Tamil Nadu coast. For that a total of 23 locations were surveyed. Based on the field observations they observed that the southern region of Tamil Nadu coast is highly vulnerable to a tsunami attack while compared with the northern coast and attributed it to the flat topography in this sector. Moreover they pointed out that inundation was so high in places where the hinterland is unprotected by coastal dunes. Besides inundation was also high at places having slight openings in dune. They mentioned that places like Periyakalpet, Mahabalipuram and Sadavangapattinam were noted for higher run-ups.

Ramana Murthy et al. (2005) carried out post-tsunami survey for the estimation of inundation in Andaman and Nicobar Islands and parts of Tamil Nadu coast for the 2004 Sumatra tsunami. From the survey the authors found Malacca as the region of highest run-up. The observed run-up at this location was 7 m, whereas Diglipur and Rangat showed the least run-up. The least run-up was about 1.5 m. The other sectors like South Andaman, Little Andaman and Great Nicobar showed maximum run-up of 4.5 m, 5.0 m and 6.0 m respectively. The authors also evaluated relationship between inundation and beach slope for having a proper understanding of vulnerability. The authors pointed that an inundation of 1000 m and 1200 m had occurred in Malacca of Carnicobar and Hut Bay of Little Andaman with slopes of 1 in 167 and 1 in 325 m respectively. The inundation was only 130 m at Chidyatopu in south Andaman where the slope was in the range of 1 in 32.

Subramaniyan et al. (2006) reported the field observations of tsunami along the coast of Tamil Nadu and reported that the districts Kancheepuram, Villupuram, Cuddalore, Nagapattinam and Kanyakumari were the worst affected regions in the state of Tamil Nadu (Table 2.5). The sectors south of Nagapattinam till Kanyakumari was partially affected. The Thiruvaloor district in the north was also partially affected.

Table 2.5 Observed run-up and inundation due to 2004 Sumatra tsunami at different locations of Tamil Nadu coast (Source: Subramaniyan et al., 2005)

Sl. No.	Location	Run-up (m)	Inundation (m)
1	Kattupalli (Thiruvaloor District)	2.5	600
2	Kadalur (Kancheepuram District)	4.7	778
3	Mamallapuram (Kancheepuram District)	6.0	638
4	Kunnimedu (Villupuram District)	NA	380
5	Parangipettai (Cuddalore District)	2.9	1680
6	Akkaravattam (Nagapattinam District)	1.55	2090
7	Melamanakudi (Kanyakumari District)	5-6	1500
8	Kolachel (Kanyakumari District)	5-6	1500

2.3 FIELD OBSERVATION OF TSUNAMI INUNDATION AND RUN-UP ALONG THE KERALA COAST

Extensive data are available on the Sumatra 2004 tsunami inundation characteristics along the Kerala coast from the studies by Kurian et al. (2005), Prakash et al. (2005), Prakash et al. (2006), Kurian et al. (2006), Kurian et al. (2006 a-c), Baba et al. (2006) and Kurian et al. (2007). According to Kurian et al. (2006) the observed run-up along the Kerala coast showed wide variations along the coast (Fig. 2.1). In the Pozhiyur to Vizhinjam (southernmost) sector, the run-up level was only up to 1.5 m, whereas in the Vizhinjam-Varkala sector, it was 2-2.5 m. In the southern sectors of the Quilon district, the run-up was up to 3 m. The run-up increased further in the northern sectors of Quilon district. In the Cheriyazheekkal area, run-up up to 4.5 m was reported. In Azheekkal and up to Kayamkulam inlet, severity of attack of the tsunami was further intensified, with the highest run-up of up to 5 m. In the sector immediately to the north of Kayamkulam inlet also, the tsunami onslaught was severe with run-up level up to 5.0 m. Further north, in the Arattuppuzha region and up to Thottappally, the run-up level got reduced to 3.5 m. From Thottapally onwards, there was further decrease till south of Anthakarnazhi inlet.

In the zone around Anthakaranazhi inlet, there was an increase in the run-up level reaching up to 3.5 m. Further north, in the Chellanum-Puthuvype region around Cochin, run-up level decreased to 3 m. However, in the Edavanakkad region, the run-up level increased drastically and went upto 4.5 m. There was reduction in the run-up level further

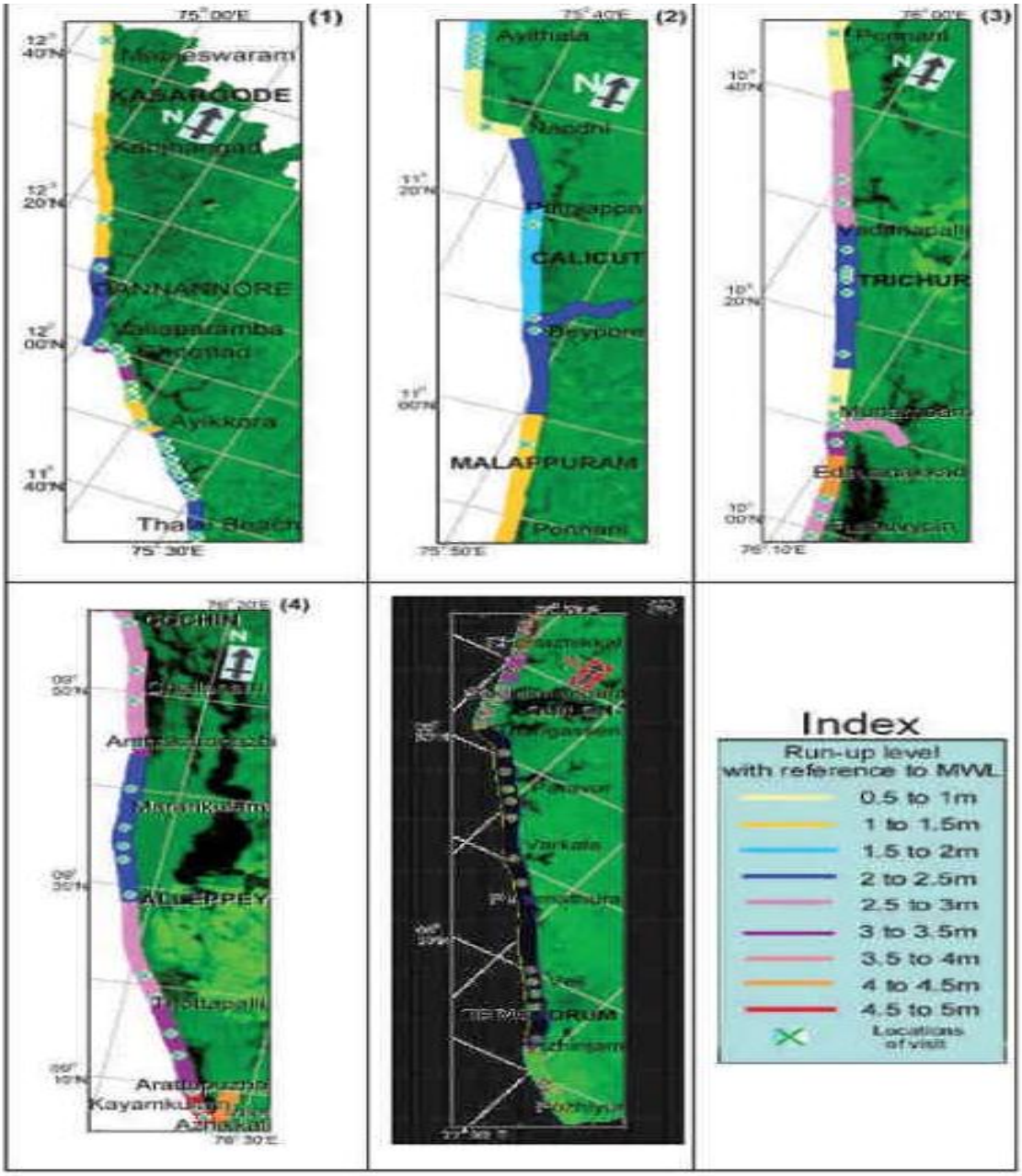

Fig. 2.1 The observed run-up level along the Kerala coast during the 2004 Sumatra tsunami (Source: Kurian et al. 2006 b)

north, with a drastic reduction in the zone immediately north of the Munambam inlet. However, in the sector further north, the level increased showing up to 3 m around Vadanapally. There was again a drastic decrease in the sector south of the Ponnani inlet. An increase in the level was found north of Ponnani inlet and run-up level up to 2.5 m was found in Beypore inlet, south of Calicut. In the northern parts of Kerala coast comprising of the Calicut, Cannannore and Kasargod districts, the run-up levels were generally low in the range 1.0 to 2.5 m. However, a short sector around Choottad was

notable for a high run-up level of 3-3.5 m, which was not reported anywhere in the northern Kerala.

The extent of horizontal inundation along the Kerala coast has been presented by Kurian et al. (2006 c). In the Trivandrum-Quilon sector of southern Kerala, where the run-up was of medium value, the inundation was very less with values less than 50 m. The relatively lower inundation here not extending beyond the berm for most part of this sector is due to the higher elevation of the backshore. However, further north, in the northern sectors of Quilon district, the inundation increases commensurate with the higher run-up and lower backshore terrain level. The highest inundation of 2350 m along the Kerala coast was observed in the sectors adjoining the Kayamkulam inlet where the highest run-up also was observed. Further north, the inundation decreased, but it was not as low as in the Trivandrum-Quilon sector, in spite of the lower run-up values; in a couple of locations inundation of 1000 m or more were also observed.

The arrival times of Sumatra 2004 tsunami along the Kerala coast has been studied by Baba et al. (2006). In the Trivandrum-Quilon sector of southern Kerala, three waves were reported in most of the locations while a fourth wave also was reported in a couple of cases. However, further north in the Alleppey-Cochin sector only two waves were reported though at Anthakaranazhi the third wave also was reported in the late afternoon. In the northern Kerala the third wave was observed in most of the locations. It is significant that the second and third waves correspond to either late evening of 26th or early morning of 27th December. It is also evident that the first few direct waves from the tsunami did not arrive at all the locations with significant amplitudes, to be noticed by eye witnesses.

2.4 NUMERICAL MODELLING STUDIES ON TSUNAMI RUN-UP AND INUNDATION

Titov and Synolakis (1995,1996) and Titiov and Gonzalez (1997) describes the MOST (the short form of Method of Splitting Tsunami) model, a model developed at the Pacific Marine Environmental Laboratory (PMEL) of National Oceanic and Atmospheric Administration (NOAA) in Seattle, USA. The model was aimed at simulating all the three stages of tsunami, namely generation, propagation and inundation/run-up. The elastic deformation theory of Gusiakov (1978) and Okada (1985) was used for the initial tsunami

generation. It assumes an incompressible liquid layer on an underlying elastic half space to characterize the ocean and the earth's crust. For that an elastic fault plane model is used which contains a formula for static seafloor displacement to compute the initial conditions which in turn will be used for further simulations of tsunami propagation and coastal inundation. Murty (1984) reported that in this model the earth's curvature is also taken into account since tsunami propagate large transoceanic distances and hence the momentum and continuity equations are written in spherical polar co-ordinates. Coriolis force and dispersion are the other two parameters used in this modelling. MOST model makes use of non-linear shallow water equations in spherical polar co-ordinates and uses numerical dispersion. The equations are solved using splitting method.

Agarwal et al. (2005) mentioned about the Tidal Ocean Atmosphere Surge and Tsunami simulations (TOAST) model. They reported that this model is actually a combination of different models developed under Advance Ocean State Forecast activity at MOG/SAC. The model was particularly intended for the simulation of ocean general circulation, prediction of tides and storm surges coupled with a cyclone prediction model. This circulation model has separate barotropic and baroclinic modes of energy propagation. The model uses flexible grids which allow the smooth simulation of coastal inundation due to storm surges. Agarwal et al. (2005) calibrated this model for the 2004 Sumatra tsunami using elastic plate movement model for initial tsunami generation. They also validated the results of modelling with Jason altimeter pass in the central Bay of Bengal at 0256 UTC and the results were found to be promising.

Babeyko and Sobolev (2005) developed a non-linear shallow water model in spherical co-ordinates with coriolis and bottom friction term included. It is an explicit finite difference model with a grid size of 2 min for the coarser model and 30 arc seconds for a finite grid model. The time steps for these two models are 2 s and 1 s respectively. The authors carried out simulation for minimum six hours and remarked that the model results degrade in the nearshore region and so an effective fine tuning of the model is necessary.

Annunziato and Best (2005) developed a simple model for computing the travel times of the tsunami under the shallow water approximation. The model was developed for predicting travel times quickly contributing to the effective functioning of early warning systems of tsunami. The main shortcoming of this model is that physical oceanographic processes like diffraction, refraction are not included.

Kowalik et al. (2005a, b) applied a global tsunami model (GTM) to the Indian, Atlantic and Pacific Oceans. The model domain covered the entire World Ocean extending from 80° S to 69° N. The model spatial resolution was 1 min and its domain included approximately 200 million grid points. In order to carry out this simulation, a parallel version of the model code was developed and run on a supercomputer. The model for the Indian Ocean Tsunami showed that the tsunami encompassed the entire World Ocean. Post Indian Ocean tsunami analysis depicted numerous reflections and quite long ringing of the tsunami oscillations in the coastal regions suggesting local resonance and local trapping of tsunami energy. Computed distributions of the maximum amplitude compare well with observations by Merrifield et al. (2005) and by Rabinovich and Thomson (2007). The observed and computed temporal variation of the tsunami at gauge stations in the Indian Ocean displayed quite similar amplitude and variability. Although the model resolution is about 2 km it still needs to be improved for proper run-up calculations. The comparison against satellite data shows that improvements in the source function are needed. As the source function is one of the major building blocks of the tsunami model and, as some new insight on the source function pattern and tsunami generation has been suggested by Lay et al. (2005) and Hirata et al. (2005), it is important to improve the GTM using this new information

Numerical modelling of the tsunami in the Indian Ocean was done by Baird and Associates (Ottawa, Canada) using Danish Hydraulic Institute's MIKE-21 Hydrodynamic flow module (Chittibabu and Murty, 2006). It is a 2D shallow water model for free surface flows. The hydrodynamic module used here was the flow model and was used to simulate water level variations and flows driven by wind, tide and other forcings. The model included the bottom shear stress, wind shear stress, barometric pressure gradients, coriolis force, dispersion sources and sinks, evaporation, flooding and drying. A preliminary simulation of Indian Ocean Tsunami was carried out using a rectangular grid (with 15 km resolution) covering entire Indian Ocean. Three fine grids (with resolution of 5, 1 and 500 m) were nested within the main grid to resolve the tsunami propagation around Southern India, Sri Lanka and Indonesia coasts. ETOPO 2 ocean bathymetry as well as hydrographic charts was used for the grid generation. Initial sea surface elevation was based on the data provided by USGS. The shortcoming with this model is that an additional module must be incorporated into this model for near shore computations such

as run-up and inundation. The default model computes and simulates tsunami propagation and amplitudes up to a certain depth as per the selected model domain.

DELFT Hydraulics has carried out numerical experiments to better understand the dynamics of tsunami generation, propagation and flooding and to support the restoration efforts of habitats [coral reef, mangroves, wetlands and coastal structures] (Chittibabu and Murty, 2006). This forms an essential part of the risk and safety assessment for the disaster stricken area and the development of future flood hazard maps. The basis of such a risk assessment is a modelling framework that is relatively accurate, robust and computationally efficient. The propagation of a tsunami wave can be coupled directly with DELFT-3D hydrodynamic model, which in turn is coupled to an inundation model. Real time observations enhance the accuracy of the system through data assimilation. There are two versions - a three dimensional (3D) and a two dimensional (2D). These models are mainly applied for simulation of tides and storm surges. In the 3D version, the vertical grid follows sigma coordinates and in the 2D version, a curvilinear boundary fitted grid is used. The DELFT-3D model solves the non-linear shallow water equations.

Watts et al. (2003) compared the available tsunami propagation and inundation models, and reported that three types of tsunami propagation and inundation models are commonly used. They are nonlinear shallow water wave models, Boussinesq long wave models and complete fluid dynamic models. They compared the performance of different kinds of models and suggested that the range of accurate non linear shallow water wave simulations are more restricted. The authors also pointed out the shortcoming arising due to the lack of an in-depth analysis of different models for understanding the credibility of each.

Yalciner et al. (2005) studied the generation, propagation and coastal amplification of 26th December 2004 Sumatra tsunami waves using TUNAMI N2 model. For that they conducted the post-tsunami field survey during January 21-31, 2005 at North Coast of Sumatra Island at Medan, Meulaboh cities and Simeulue Island. They documented the survey data on run-up, inundation, arrival time and damages due to tsunami together with inundation data. These results were also compared with simulation results. Reasonable agreement between survey and simulation results were obtained except for the amplitude of the tsunami waves near Meulaboh and Banda Aceh coasts (northwest of Sumatra Island).

Sharma et al. (2005) carried out the numerical simulation of tsunami due to 1945 Makran earthquake. The algorithm of Okada (1985) was used for modelling the tsunami generation. Since the source data was not available, they used the source model based on three conditions viz., a) historical perspective b) a hypothetical rise in the crustal deformation and c) Sumatra-similar earthquake data. The maximum positive amplitude (+10.7 m) and maximum negative amplitude (-6.6 m) at tsunami source predicted by their simulation agree well with the reported values of the amplitude. TUNAMI N2 code has been used for modelling the tsunami propagation. For this work, sources of bathymetry were used from the ETOPO 2 data, available from the National Geophysical Data Centre. The computation domain for the study was 4 min grid (11° N - 27° N) latitude and (56° E - 78° E) longitude. The model predicted the historically observed wave heights (1.5-2 m in Mumbai, 9-11 m in Kutch and 12 m in near Makran coast). They concluded that the numerical analysis technique can be used effectively to simulate the generation, propagation and run-up of tsunami events.

Muraleedharan et al. (2006) developed a predictive model for tsunami beach run-up heights based on work-energy theorem and validated it for various tsunami events including the 26th December 2004 Indian Ocean tsunami along the coasts of the Indian Ocean countries. The predicted tsunami heights compared reasonably well with observed beach run-up and inundation.

Kervella et al. (2007) compared different linear and non-linear models and proved that there was good agreement between these two models on plotting the wave profile characteristics. The authors indicated that frequency dispersion is a shortcoming of non-linear shallow water models while modelling the moving bottom.

Somporn and Wattana (2007) proposed a new mathematical model for tsunami generation and propagation in real-time simulation and visualization. The model is called SiTProS (Siam Tsunami Propagation Simulator). They have deduced the shallow water wave equation, nonlinear wave equation and the continuity equation that must be satisfied when a wave encounters a discontinuity in the sea depth by selecting a computation grid from the ETOPO 2. The SiTProS can run for any given regional or global grid with a prescribed topographic dataset as ETOPO2. The finite difference method was used to solve the equations. The SiTProS effectively simulated and animated tsunami generation

and propagation of the 26th December 2004 Sumatra tsunami for Asia, Europe, Arab (Iran-Kenya), Africa and Andaman.

Ilayaraja et al. (2008) carried out the numerical simulation of the 26th December 2004 for the Andaman and Nicobar Islands. They have used the FUNWAVE code to compute reliable tsunami propagation and inundation models. Their simulation approach was based on a fully nonlinear Boussinesq tsunami propagation model and included an accurate computational domain and a robust co-seismic source. The result of simulation was validated through available observations, i.e. a tide gauge record at Port Blair and run-up surveys (Ramana Murthy et al. 2005). As a result a full picture of the tsunami impact was provided over the entire coastal zone of Andaman and Nicobar Islands.

Ioualalen et al. (2010) carried out numerical simulation of the 26 December 2004 Sumatra tsunami for the south eastern coast of India by constructing a robust computation based on a well constrained co-seismic tsunami triggering source model (Chileah et al., 2007), accurate computational domain and a reliable fully nonlinear Boussinesq model. The authors used the FUNWAVE tsunami propagation and run-up model which is fully nonlinear and dispersive for model computations. The result obtained from the simulation was validated through available run-up observations (Jayakumar et al., 2005 and Yeh et al., 2007). A full picture of the tsunami impact was provided over the entire Tamil Nadu coastal zone by the model. The role of different processes like shoaling, wave refraction, amplification and focusing of waves in the coastal vulnerability were also elucidated.

Praveen et al. (2011) carried out the numerical modelling of tsunami inundation along the Kerala coast for the 2004 Sumatra earthquake using TUNAMI N2 model. The Neendakara-Trikkunnapuzha stretch of Kerala coast was chosen for the study. The fault parameter of the 2004 Andaman-Sumatra earthquake was taken from Chlieh et al. (2007). The data for grid D was provided from the high-resolution bathymetric and topographic data available with Centre for Earth Science Studies (CESS). The data for the outer coarse grids were taken from sources such as General Bathymetry Chart of Oceans (GEBCO), Coastal Map (CMAP), and Shuttle Radar Topographic Method (SRTM). From their model results it was observed that the model produces reasonably good comparison with the field data with an average error estimate of 9.22 %.

Arjun et al. (2011) carried out the numerical simulation of the 1945 Makran tsunami on the southwest coast and Lakshadweep Islands of India using TUNAMI N2 model. Validation of the model was done using the tide gauge data available for Apollo Bunder, Mumbai. Their simulations showed that the run-up due to the 1945 Makran tsunami along the southwest coast of India and Lakshadweep Islands was much less than that of the 2004 Sumatra tsunami as documented by Kurian et al. (2006).

Ranga Rao et al. (2011) carried out numerical modelling for the evaluation of tsunami hazard along the South Andhra coast. The TUNAMI N2 model was used for the computation for three sources which include a potentially worst case from Car Nicobar. The run-up levels were found to be extremely high for the worst case scenario from Car Nicobar. The results of modeling indicated that Krishnapattanam, Kavali and Ongole of the Andhra coast are highly vulnerable to a tsunami from Car Nicobar. The simulation results underlined the role played by the 420 km long Buckingham canal running parallel to the coast in reducing the inundation extent.

Murty et al. (2005) studied the leakage of the 2004 Indian Ocean Tsunami and asserted that the tsunami propagated not only through the Indian Ocean but also into the Pacific and Atlantic Ocean. The leakage of tsunami energy from the Indian Ocean produced maximum tsunami amplitudes of 0.65 m on the pacific coast of South America and maximum amplitude of 0.3 m on the coast of Nova Scotia in the Atlantic Ocean. The authors adapted a simple analytic model for this study and proved that tsunami flux from the Indian Ocean into the Pacific Ocean was greater than the flux into the Atlantic Ocean, which they attributed partly to the directivity of tsunami energy. It was also attributed to the fact that distance from the epicentre to the Atlantic gap was much greater than the travel distance from the epicentre to the pacific gap.

Narayana et al. (2005) reported about tsunamigenic earthquakes, and how it contributed to a tsunami. They quantitatively explained the features of tsunami and the specific characteristics both in offshore and onshore. They also reported about the role played by Coriolis force in steering the tsunami towards the right side of the travel direction in the northern hemisphere. The paper portrayed the pre-tsunami scenario and post-tsunami scenario in the Kerala coast as far as beach morphology is concerned.

Murty et al. (2006 b) dealt with the non-generation of transoceanic tsunamis in the Atlantic Ocean. Many scientific facts were attributed to that. The fault zones in the Atlantic Ocean are smaller than those in the Pacific and Indian Oceans. Besides the number of convergent zones are less in the Atlantic Ocean which is of major importance in the generation of a tsunamigenic earthquake. The authors concluded that there are usually no tsunamis travelling across the Atlantic Ocean eventhough there are occurrences of tsunamis in the relatively shallow waters at the margins of this ocean.

Gupta (2005) dealt with the large tsunamis around the globe and on the coastlines of India. He identified the critical areas which could possibly generate tsunamigenic earthquakes along the coastline of India. According to him the areas that could possibly generate tsunamigenic earthquakes are the extension of Java-Sumatra earthquake belt into the Andaman and Nicobar and some areas in the Arabian Sea. He divided the globally occurring earthquakes into three regional zones: a) more than 75 % of the earthquake energy is released in the circum Pacific belt, b) about 20 % in Alpine-Himalayan belt and c) the remaining 5 % through the mid oceanic ridges and other stable continental region earthquakes.

Rastogi and Jaiswal (2006) presented a catalogue of about ninety tsunamis in the Indian Ocean from 326 BC to 2005 AD, with Sunda Arc as the most active region. The source zones of the remaining tsunamis are Andaman - Nicobar Islands, Burma-Bangladesh region in the eastern side, and Makran accretion zone and Kutch-Saurashtra region in the west. They reported that eighty percent of tsunamis in the Indian Ocean are from Sunda Arc region, where on an average one tsunami is generated in three years.

Rasheed et al. (2006) studied the variation in run-up observed along the south west coast of India and attributed it to the topography of the coastline, nearshore bathymetry, beach slope, coastal orientation and the direction of the incoming wave. The low-lying coastal areas with narrow strip of land between the sea and backwater at Cheriyazheekal, Valiyazheekal and Edavanakkadu, amplified the effect of waves and caused severe damages and loss of life, whereas the wider beach at Puthu Vype reduced the impact / damage of tsunami on life and property.

Varma and Sakheer (2007) studied the refraction of the December 2004 tsunami waves. They concluded that convergence was the main cause behind the greater destruction at

Kolachel and Kollam. They pointed out that bottom topography is one of the prominent factors which determine the intensity of tsunami waves.

Bapat (2007) reported that the west coast of India is vulnerable to tsunami attack. The paper also pointed to the existence of a few more tsunamigenic locations in the Arabian Sea such as Makran coast, Persian Gulf, Aden Gulf, Socotra Island and Galapagos Island. He opined that by clubbing the advanced computer modelling techniques with earthquake fault parameters, measurements by ocean bottom seismometers and satellite, installations of tide gauges, it is possible to develop a suitable tsunami disaster management plan.

Borah et al. (2007) studied the tsunami risk assessment for Galle city in South-Western Sri Lanka, one of the major tsunami affected areas in Sri Lanka, incorporating tsunami hazard, population and land use vulnerability information. The numerical simulation of tsunami inundation was carried out using TUNAMI N2 model. The risk analysis shows 2 % of the study area falls in high risk zone while 37.3 % falls in medium and the rest 60.7 % falls in low hazard zone. The inundation modelling used for tsunami hazard assessment incorporated high resolution nearshore bathymetry and Digital Elevation Model (DEM) to model the 26th December 2004 tsunami inundation event. However, the validations of the model results with post-tsunami field survey data on inundation showed that 72.5 % matched with the ground observations. The inaccuracy in prediction can be attributed to uncertainty involved in the estimation of earthquake source parameters, modelling of far field tsunami and accuracy of DEM.

Jaiswal et al. (2008) made an attempt for a numerical simulation of the Arabian Sea tsunami generated due to 1945 Makran earthquake and its effect on western parts of Gujarat (India) using TUNAMI N2 model. For the modelling of tsunamis, open source bathymetry and topography data viz. General Bathymetric Chart of the Oceans (GEBCO), Shuttle Radar Topographic Mission (SRTM), Coastal Map (C-Map), Naval Hydrographic Office (NHO chart), and RTKGPS (Real Time Kinematic Global Positioning System) data for coastal and nearshore regions were used. The fault parameters of the earthquake were taken from Mohan and Krishnamurthy (2007). The model has successfully simulated the propagation of tsunami event of November 1945. The model results are qualitatively consistent with the reported damage and the model gives maximum amplitude along the creeks at the coast of Gujarat.

Heidarzadeh et al. (2008) studied the tsunami hazard in the Makran Subduction Zone (MSZ), off the southern coasts of Iran and Pakistan, by numerical modelling of historical tsunami in this region. Their research resulted in the recognition of five events including four events of seismic origin, and one of volcanic. The algorithm of Mansinha and Smylie (1971) was used to calculate the sea floor deformation. This algorithm is based on the input seismic parameters that include the strike, dip, and slip angles, the amount of slip, the dimensions of the rupture area, and the earthquake depth. The numerical model TUNAMI N2 was used for simulation and propagation and coastal amplification of tsunami waves in the coastal zone of Pasni, Raan of Kutch, Gulf of Kutch, and Mumbai. The numerical modelling revealed that a larger earthquake and tsunami in the MSZ was capable of producing considerable run-up in the field. They concluded that there was a high risk for tsunami generation from submarine landslides and volcanic sources in the MSZ. The simulated run-up height at Pasni is in agreement with the observed run-up during the 1945 event reported by Page et al. (1979) and Ambraseys and Melville (1982). However, it is smaller than the run-up of about 12-15 m reported by Pendse (1946), Berninghausen (1966), and Snead (1966). The authors also identified a seismic gap area in western Makran off the southern coast of Iran.

Heidarzadeh et al. (2008) evaluated the tsunami hazard in the northwestern Indian Ocean and found that the maximum regional earthquake magnitude in the MSZ is 8.3 with a return period of 1000 years. The maximum expected run-up for a tsunami is 9.6 m along the southern coasts of Iran and Pakistan. The vulnerability analysis for the other regions indicate 3-7 m run-up in the northern coast of Oman, 1 - 5 m along the southern coast of Oman and 1.0 - 4 .4 m along the eastern coasts of Makran. The authors urged the need for developing a tsunami warning system in the northwestern Indian Ocean for hazard preparedness for a tsunami propagating from Makran.

Usha et al. (2009) studied the vulnerability of the Car Nicobar coast to tsunami hazard using TUNAMI N2 numerical model for various past earthquake scenarios. The elevation data sets have been collected using Airborne Laser Terrain Mapper (ALTM) for a distance of 2 km from the coast all around the island. For higher altitudes inland, 1:25000 toposheet was used to derive the elevation data. On the sea side, bathymetry data was obtained from C-Map and NHO charts. GEBCO data was used for the deep sea regions. The island was found to be most vulnerable along the eastern and the southern side

compared to the western side. The persistence of high water level around the island for many days after the tsunami was attributed to the high length of the pendulum day in the Andaman and Nicobar Islands which varies from 100-231 hours

Heidarzadeh et al. (2009) carried out a preliminary estimation of the tsunami hazards associated with the MSZ which has produced some tsunamis in the past at the northwestern Indian Ocean. Numerical modelling was carried out for this which was further verified using historical observations of the 1945 Makran tsunami. They concluded that

a) The energy of tsunami in the MSZ propagates in the north-south direction
b) The main focus will be on the southern coasts of Iran and Pakistan coupled with northern coast of Oman and eastern coast of UAE with maximum run-ups in the range of 5-7 m.
c) The most populous cities Karachi and Muscat will experience high wave amplification and due to the effect of directivity minor effects of tsunami will persist in the Omani and Emirian coasts.

Heidarzadeh and Kijko (2010) carried out a probabilistic tsunami hazard assessment for the MSZ at the northwestern Indian Ocean. The authors estimated the probabilistic percentage as 17.5 for a tsunami exceeding 5 m over a 50 year period and 45 for moderate tsunamis from Makran. The authors stressed the need for fine tuning of probabilistic assessment leading towards the development of a regional tsunami warning system in the Makran zone.

Divyalakshmi et al. (2011) studied the modification of a tsunami wave by submarine canyon using a case study of multiple canyons at Palar in the southeast coast of India. The interactions of submarine canyons on tsunami wave were tested using the TUNAMI N2 numerical model for various configurations viz. a) without canyon b) single canyon and c) double canyons. The results of numerical modelling showed that submarine canyons contributed significantly in the modification of tsunami wave height while approaching the coast. The study indicated that the presence of submarine canyons would help in reduction of tsunami wave height upto 44 %. It was concluded that in the event of a tsunami the canyons act as a blockade to decelerate the wave height.

Swaroopa et al. (2011) simulated the tsunami propagation and inundation due to tsunamigenic earthquake in the Sumatra-Andaman subduction zone and its impact at Vishakapatnam. The paper presents the simulated results of two scenarios of inundation arising out of tsunamigenic earthquakes viz., 2004 Sumatra earthquake and a possible great earthquake in the Andaman region. It was found that the inundation of the Andaman earthquake is much more than the 2004 Sumatra EQ. The tsunami from the Andaman source reached Vishakapatnam in 1.5 hours which is about 38 minutes earlier than Sumatra. This was explained in terms of the proximity of the source and the directivity of the waves.

Ramanamurty et al. (2011) carried out numerical modelling studies for assessing the tsunami vulnerability of Cuddalore district in Tamil Nadu which was one of the worst affected coastal areas in Indian mainland. It was found that the inundation extent was very high in the northern part of Cuddalore while the run-up height was high in the southern part. The high inundation in the northern part of Cuddalore was mainly due to the presence of rivers like Gaddillum, Ponniyar and Uppanar flowing through this area. The high beach ridges and the bio-shielding effect of the green belt in the southern Cuddalore were the reason for high run-up and low inundation in this region. The modelling results matched closely with the field observation.

Rajakumari and Subramanian (2011) studied the behaviour of tsunami waves along the coasts of Kancheepuram and Villupuram districts in Tamil Nadu, India. The authors used TUNAMI N2 model to predict inundation for the earthquakes of Carnicobar 1881, Sumatra 2004 and a worst case scenario. The results showed that more inundation was visible in coastal area with a gentle slope, whereas inundation was less in the areas of varying slope habited by sand dunes and coastal vegetation. The worst case scenario predicted extreme vulnerability along the coasts of Kancheepuram and Villupuram.

Usha et al. (2012) carried out a tsunami vulnerability assessment for the city of Chennai, east coast of India. The authors devised a method using a combination of spatial tools such as remote sensing, GIS, GPS based field data along with numerical modeling using TUNAMI N2 model to generate the large scale vulnerability map for Chennai. The results of the model were validated using the post-tsunami field data. Large scale maps in 1:5000 scales which could be used for tsunami mitigation efforts were prepared by overlaying

thematic maps on the extent of inundation due to various scenarios, land use, elevation, infrastructure, HTL and coastal regulation buffer zones.

2.5 SUMMARY

This chapter presents a review of literature carried out on various aspects related to the present investigation, such as historical tsunami, field data on tsunami vulnerability, numerical modelling of tsunami inundation, etc. In the global scenario, records of tsunami are available since 1650 BC. The Pacific Ocean is a place for frequent tsunamis since it is a zone of several convergent tectonic plate boundaries. In Atlantic Ocean the plate boundaries being divergent tsunamigenic earthquakes are infrequent. Unlike the Pacific Ocean, tsunamis are not common in the Indian Ocean. Pacific Ocean reports at an average of about eight tsunamis per year, whereas Indian Ocean has one in three years or so. Out of the total 90 plus tsunamis that is reported so far for the Indian Ocean 70 are from Sunda. Though rare, tsunamis have hit India earlier. Literature on run-up and inundation characteristics of some of the historic tsunamis is available. Being very recent, post-tsunami field survey data corresponding to the 2004 Sumatra tsunami is available for most of the Indian Ocean rim countries which were affected by the tsunami. The tsunami run-up and inundation characteristics along the Kerala coast pertaining to the 2004 Sumatra tsunami are well documented. There are several tsunami inundation models reported in the literature; all these models mainly deal with tsunami generation, propagation and coastal inundation aspects. TUNAMI N2 and MOST are the most widely used tsunami inundation models

CHAPTER 3

MODEL USED

3.0 INTRODUCTION

Numerical modelling has emerged as an effective tool in the area of research and development for analyzing physical systems and understanding the various physical phenomena involved in the functioning of the system. Numerical Modelling is an excellent method for analyzing the past events and predicting the future ones. Numerical Modelling is the only way to determine the potential run-ups for different scenarios of tsunami generation since data regarding historical tsunamis are sparse. Models can be set up with potentially worst case scenarios as well as less impact sources for having a proper understanding about the rate of vulnerability. The information thus forms the basis for generating tsunami vulnerability maps and planning mitigation measures. Such models usually solve similar equations but often employ different numerical techniques and are applied to different segments of propagation of the tsunami divided into its generation, propagation and run-up. The models have used finite difference, finite element and boundary integral methods to solve linear long wave equations for generating tsunami simulations. One of the essential components of a tsunami warning system is the prediction of inundation and run-up along a coastline which can only be accomplished through the process of numerical modeling. Since it is practically impossible to run computer models in real time at the time of a tsunami a pragmatic approach is adapted in which models will be initiated for a coastline encapsulating all possible permutations and combinations of tsunamigenic earthquake from various sources, and the results of these pre-run scenarios will be converted to vulnerability maps as well as a buffer database for future reference. In the event of a tsunami warning the closest match from several pre-run scenarios will be taken and information disseminated to the general public. Subsequently mitigation can be accelerated by referring to such maps already available with state / district level disaster management centres.

3.1 MOST WIDELY USED MODELS

Several models are available for tsunami inundation modelling. Basically all these models mainly deal with tsunami generation, propagation and coastal inundation aspects. Some

important global tsunami models are:

1) MOST Model
2) TOAST Model
3) Delft Model
4) Italy Model
5) ECJRC Model
6) ADCIRC
7) COULWAVE
8) TUNAMI N2

As seen from the literature review, the MOST and TUNAMI N2 are the two globally used models. Before going ahead with the details of the model used for the present study, it is intended to give a brief overview of both the models which will enable a comparison of these two widely used models.

3.1.1 MOST Model

MOST model is the short form of “Method of Splitting Tsunami”, a model developed at the Pacific Marine Environmental Laboratory (PMEL) of National Oceanic and Atmospheric Administration (NOAA) in Seattle, USA. Details of the model are described by Titov and Synolakis (1995, 1996) and Titov and Gonzalez (1997). This model generates all the three stages of tsunami, namely generation, propagation and run-up. The initial tsunami generation is based on the elastic deformation theory (Gusiakov, 1978; Okada, 1985). It assumes an incompressible liquid layer on an underlying elastic half space to characterize the ocean and the earth's crust. For that an elastic fault plane model is used which contains a formula for static seafloor displacement to compute the initial conditions which in turn will be used for further simulations of tsunami propagation and coastal inundation. In this model the earth's curvature is also taken into account since tsunami propagates large transoceanic distances and hence the momentum and continuity equations are written in spherical polar co-ordinates (Murty, 1984). Coriolis force and dispersion are the other two parameters used in this modelling. So MOST model makes use of non-linear shallow water equations in spherical polar co-ordinates and uses numerical dispersion. The equations are solved using splitting method.

3.1.2 TUNAMI N2 Model

The TUNAMI N2 model was originally authored by Professors Nobuo Shuto and Fumihiko Imamura of the Disaster Control Research Centre in Tohoku University (Japan) through the Tsunami Inundation Modelling Exchange (TIME) program (Goto et al., 1997; Yalciner et al., 2004). TUNAMI N2 is an acronym of "Tohoku University's Numerical Analysis Model for Investigation of Near-field tsunamis, No.2". TUNAMI N2 is one of the key tools for developing studies for propagation and coastal amplification of tsunami in relation to different initial conditions (Yalciner et al., 2002). It solves the linear form of the long-wave equations in spherical coordinates in the largest domain (the deep sea), and nonlinear shallow-water equations in Cartesian coordinates in smaller domains with finer grids for basins of irregular shape and topography. The equations are solved using the leap-frog scheme of finite differences (Yalciner et al., 2004).

3.1.3 Reasons for Selecting TUNAMI N2

Numerical simulations of tsunami impact require three components: (1) a source, reflecting the known geology and seismology of the event; (2) ocean bathymetry and coastal topography, and (3) a tsunami propagation and run-up model, representing the relevant physics. As mentioned, several different global models are available for tsunami inundation modeling and from that reviews of various literature carried out under this investigation unravel the fact that only two models viz. TUNAMI N2 and MOST are capable of modelling the entire range of tsunami wave propagation starting from its source till its inundation of the coast. The common feature of both TUNAMI N2 and MOST is the use of finite-difference (FD) algorithms to solve the Non-linear Shallow Water (NSW) equations. TUNAMI N2 and MOST differ in two ways. MOST uses a variable computational grid, no friction factors, and its run-up prediction is based on the elevation of the last wet grid point the wave encounters as it propagates up on the beach whereas TUNAMI N2 uses a fixed computational grid, involves a friction factor and, lets the wave advance past the initial shoreline. Moreover its maximum run-up prediction is based on the maximum wave height at the shoreline. Besides that TUNAMI N2 gives more prominence to fine grid data which is of utmost importance while dealing with the run-up and inundation characteristics of the coast. Apart from that TUNAMI N2 is more widely and globally accepted for simulation of tsunami inundation. The Indian Tsunami Warning Centre at Indian National Centre for Ocean Information Services (INCOIS),

Hyderabad is also relying upon this model for providing early warning. Hence, this model was chosen to simulate the tsunami propagation, run-up and inundation along the South East Arabian Sea (SEAS) and Kerala coast under this investigation

3.2 MODEL EQUATIONS

The TUNAMI N2 model has been widely used to study the generation and propagation of tsunami for different parts of the world ocean (Goto et al., 1997; Mercado and Mc. Cann, 1998; Yalciner et al., 2002, 2005 and Zahibo et al.., 2003). It is based on long wave theory i.e. very small ratio of water depth to wavelength, which is the case in very shallow water. The model considers the effect of the bottom friction on the attenuation of long waves as examined by Fujima et al. (2002). It can simulate reflecting boundaries for fixed coastlines and considers free outward passage of the wave at open sea boundaries. The total depth is usually taken as the parameter to be tested for the presence of the wet or dry points (Imamura, 1996). The wet and dry points are identified by setting the average (undisturbed) ocean depth (wet points) as positive and elevations (dry points) as the negative values. Detailed analysis of governing equations, procedure adopted, and the computational techniques involved in TUNAMI N2 model are described by various authors (Kajiura, 1963; Shuto and Goto, 1978; Takeda, 1984; Hibbard and Peregrine, 1979; Aida, 1977; Houston and Butler, 1979; Goto and Shuto, 1983; Uda, 1988; Kajiura, 1970; Mansinha and Smylie, 1971 and Okada, 1985). For the propagation of tsunami in the shallow water, the horizontal eddy turbulence could be negligible compared to the bottom friction except for run-up on the land. The model is only for tsunamis. No wind waves and tides are take into consideration. The still water is given by tides and it is assumed constant during tsunami propagation. The following equations are therefore given as the fundamental equations in the present model (Imamura, 1996).

$$\frac{\partial \eta}{\partial t} + \frac{\partial M}{\partial x} + \frac{\partial N}{\partial y} = 0 \tag{3.1}$$

$$\frac{\partial M}{\partial t} + \frac{\partial}{\partial x}\left(\frac{M^2}{D}\right) + \frac{\partial}{\partial y}\left(\frac{MN}{D}\right) + gD\frac{\partial \eta}{\partial x} + \frac{gn^2}{D^{7/3}} M\sqrt{M^2 + N^2} = 0 \tag{3.2}$$

$$\frac{\partial N}{\partial t} + \frac{\partial}{\partial x}\left(\frac{MN}{D}\right) + \frac{\partial}{\partial y}\left(\frac{N^2}{D}\right) + gD\frac{\partial \eta}{\partial y} + \frac{gn^2}{D^{7/3}} N\sqrt{M^2 + N^2} = 0 \tag{3.3}$$

Where,

$$M = \int_{-h}^{\eta} u dz = u(h+\eta) = uD \tag{3.4}$$

$$N = \int_{-h}^{\eta} v dz = v(h+\eta) = vD \tag{3.5}$$

M and *N* are the discharge fluxes in the *x* and *y* directions, *u* and *v* are the vertically averaged horizontal particle velocities, *t* is the time, *g* is the gravitational acceleration, *h* is still water depth, *η is* the vertical displacement of the water surface above the still water level *(z = 0), D* is the total water depth *(h + η),* and *n* is Manning's roughness coefficient. The bottom frictions in the *x* and *y* directions are expressed as;

$$\frac{\tau_x}{\rho} = \frac{fn^2}{D^{7/3}} M\sqrt{M^2 + N^2} \tag{3.6}$$

$$\frac{\tau_y}{\rho} = \frac{fn^2}{D^{7/3}} N\sqrt{M^2 + N^2} \tag{3.7}$$

where, *f* is the friction coefficient. The nonlinear terms are kept only for the computations performed in the inner and higher resolution grid, namely Grid D.

The above set of equations was solved by finite differences (Goto and Ogawa., 1992). A leap-frog scheme was used, with truncation error of the second order. Stability of the model was checked with Courant, Friedrichs, and Lewy (CFL) criteria. The CFL condition states that the time step must be smaller than the time it takes for a wave to propagate from one grid point to the next. The dry or submerged cells were considered based on the criteria of the total water depth, i.e., D = h + η > 0, the cell is submerged, and D = h + η < 0, the cell is dry. A wave front is thus located between the dry and submerged cells. The discharge flux across the boundary between the two cells is computed if the ground height in the dry cell is lower than the water level in the submerged cell. In other cases, the discharge flux is considered zero.

3.3 MODEL GRIDS

The TUNAMI N2 numerical model uses the nested grids where the code has the option of switching to either a linear or a non-linear mode. The extent of grids was decided based on the region to be modelled and computational time. Nesting is the process of interconnecting all the grids from source to the destination. The model uses four grids A,B, C and D as shown in Figure 3.1. The inner grids D and C were nested first. Consequently, the grids C and B and finally the grids B and A were nested. The spacing of the grids for A, B, C and D was decided based on the Courant, Friedrichs, and Lewy (CFL) condition. The CFL condition states that the time step must be smaller than the time it takes for a wave to propagate from one grid point to the next. The lower left coordinates, the upper right coordinates and the spacing of each grid was assigned individually in the grid line geometry for all the grids. Thus, the boundaries for the grids namely A, B, C and D were fixed. Grid line geometry defines the grid limits and grid density. Grid limits are the minimum and maximum X and Y coordinates for the grid.

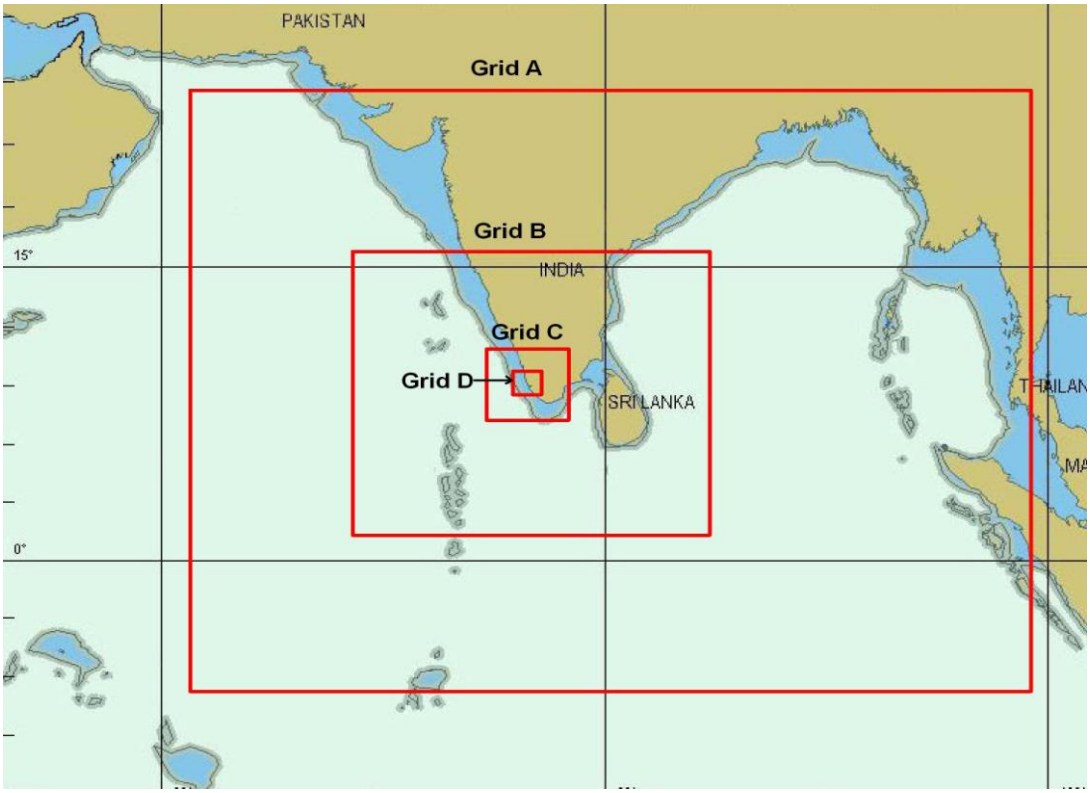

Fig. 3.1 Pattern of grids used for model calibration

Grid density is usually defined by the number of columns and rows in the grid. By defining the grid limits and the spacing value, as the distance in data units between adjacent rows and adjacent columns, the number of rows and columns are automatically determined. The resolution of Grids A, B, C and D are respectively 81” (2430 m), 27” (810 m), 9” (270 m) and 3” (90 m). TUNAMI N2 requires a specific file format for the output grid file which is ASCII (American Standard Code for Information Interchange) grid file format.

3.4 INPUT PARAMETERS

Most of the simulations of tsunami generated by earthquakes make use of the deformation formulae of Mansinha and Smylie (1971) or Okada (1985). For tsunami models, the static vertical tectonic displacement is used to model initial wave heights (Synolakis, 2003). Tsunami models assume that water motion occurs instantaneously. In other words, the initial tsunami wave is assumed to be of the same shape as the seafloor deformation (Synolakis, 2003). In the present study, the algorithm of Mansinha and Smylie (1971) was used to calculate the seafloor deformation. This algorithm is based on the seismic parameters strike, dip, slip, rake, dimensions of the rupture area and the earthquake depth. The initial displacement is generated in the exterior domain (A), and it is interpolated into the higher resolution grids B, C and D (Fig. 3.2).

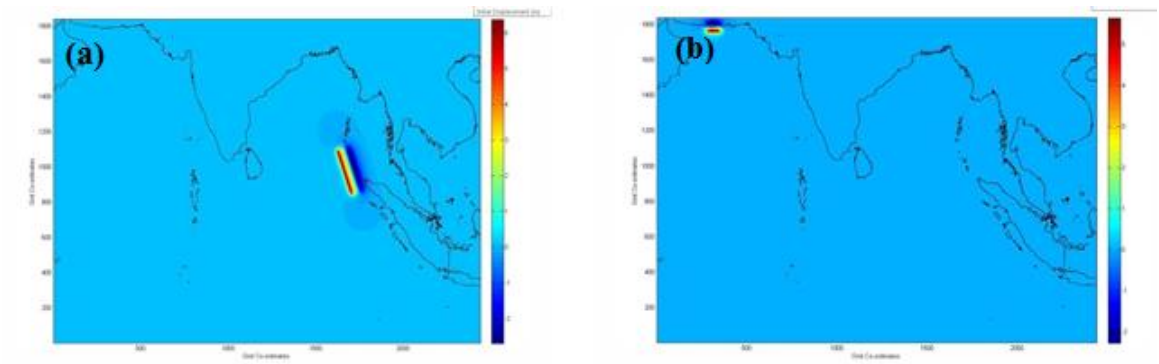

Fig. 3.2 The simulated initial sea surface displacement a) Sumatra 2004 b) Makran 1945

The end result is an initial sea surface profile that extends smoothly from the exterior, lower resolution, domain into the higher resolution domains. This is the sea surface condition at time t = 0 seconds. That is, the hypothesis is that the sea bottom displacement is immediately reflected in a sea surface displacement. TUNAMI N2 program uses the

bathymetry and topography of the area as input data. The bathymetry and topography of the area is usually stored as data files. This file consists of three values; x coordinate, y coordinate and the depth values. However, data files are typically randomly spaced files, and this data must be converted into an evenly spaced grid before using as input file of the program. The gridding method used in the present study is Krigging gridding method. Gridding is the process of using original data points (observations) in an XYZ data file to generate calculated data points on a regularly spaced grid. Interpolation scheme estimates the value of the surface at locations where no original data exists, based on the known data values (observations). This method gives good results for most XYZ data sets. Krigging is one of the most flexible methods and is useful for gridding almost any type of data set. With most data sets, Krigging with a linear variogram is quite effective.

3.5 SUMMARY

The MOST and TUNAMI N2 are the two globally used models that are capable of modelling the entire range of tsunami wave propagation starting from its source till its inundation of the coast. TUNAMI N2 and MOST differ in two ways. MOST uses a variable computational grid, no friction factors, and its run-up prediction is based on the elevation of the last wet grid point the wave encounters as it propagates up on the beach whereas TUNAMI N2 uses a fixed computational grid, involves a friction factor and it lets the wave advance past the initial shoreline and its maximum run-up prediction is based on the maximum wave height at the shoreline. TUNAMI N2 gives more prominence to fine grid data which is of utmost importance while dealing with the run-up and inundation characteristics of the coast. Considering the above, as well as the fact that the Indian Tsunami Warning Centre is also relying upon this model for providing early warning, the TUNAMI N2 model was chosen to simulate the tsunami propagation, run-up and inundation under this investigation. The TUNAMI N2 numerical model uses four nested grids where the code has the option of switching to either a linear or a non-linear mode. In the present study, the algorithm of Mansinha and Smylie (1971) based on the seismic parameters strike, dip, slip, rake, dimensions of the rupture area and the earthquake depth was used to calculate the seafloor deformation. The initial displacement is generated in the exterior domain (A), and it is interpolated into the higher resolution grids B, C and D, providing an initial sea surface profile that extends smoothly from the exterior, lower resolution, domain into the higher resolution domains.

CHAPTER 4

DATA AND METHODOLOGY

4.0 INTRODUCTION

Numerical modelling is an efficient tool for hindcasting the past events and predicting the future ones. The accuracy of the model output is directly linked to the quality of input data. Numerical modelling of tsunami inundation and run-up require fine quality topographic and bathymetric data. Also of equal importance is the accuracy of the seismological data pertaining to the earthquake event that generates the tsunami. The chapter presents the methodology followed which includes the calibration of the model.

4.1 AREA OF STUDY

The area of study is the South East Arabian Sea (SEAS) and the coasts of Kerala and Lakshadweep (Fig. 4.1). The 560 km long Kerala coast has strikingly different geomorphological characteristics. Lateritic cliffs, rocky promonotories, offshore stalks, long beaches, estuaries, lagoons, spits and bars are characteristics of this coast (Soman, 2002). The sand ridges, extensive lagoons and barrier islands are indicative of a dynamic coast with transgression and regression in the geological past. The coastline of Kerala is more or less straight trending in NNW-SSW direction from north till the Thangassery headland near Kollam. The coastline orientation south of Thangassery is in the NW-SE direction. The southern sector of the coast from Poovar up to Thangasseri near Kollam is a high energy coast with steep beach face, coarser sediments and steep inner shelf. The sector from Thangassery further north is characterized by lower energy, finer sediments and gentle inner shelf. This variation in the geomorphological and oceanographic characteristics spatially has resulted in a wide variation in the December 2004 tsunami run-up and inundation characteristics along the coast as seen in Chapter 2.

Numerical Modelling was carried out for the 560 km coastal stretch of the Kerala coast starting from Pozhiyur in the south of Thiruvananthapuram district to Talappadi in the north of Kasargod district, divided into 21 different sectors with each sector roughly around 25-35 km following the model grid logistics. Numerical modelling was carried out for four selected Islands of Lakshadweep viz. Androth, Chetlat, Kadamat and Kavaratti.

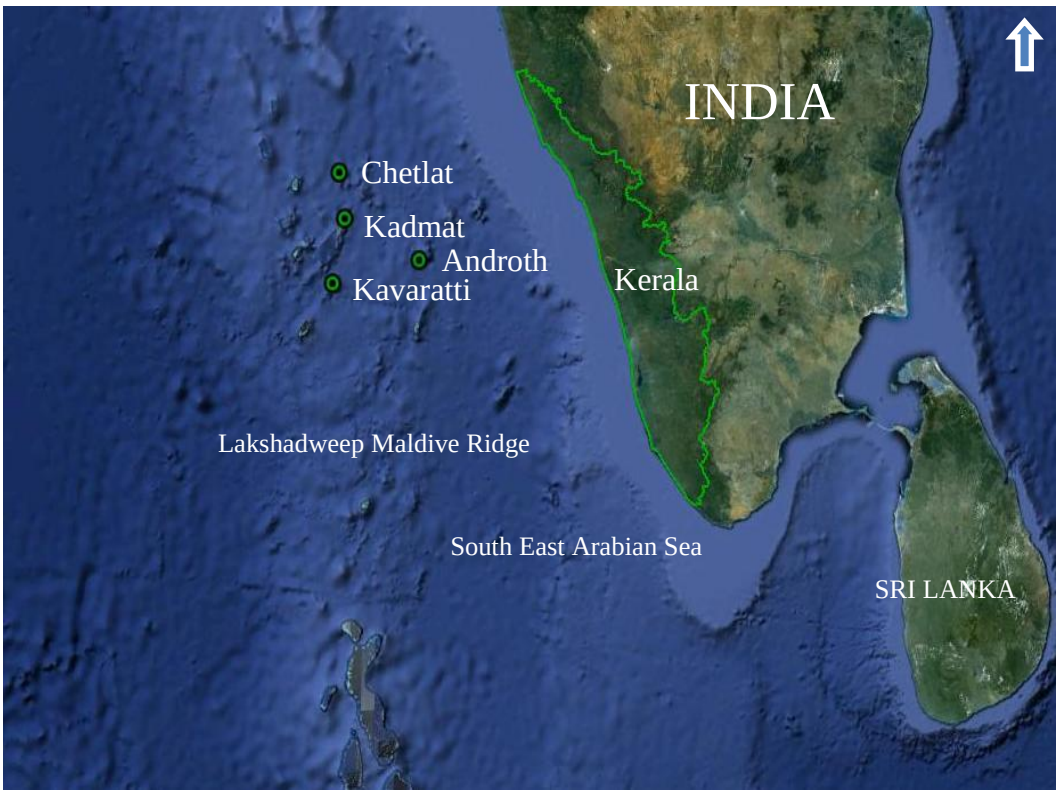

Fig. 4.1 South East Arabian Sea (SEAS), Kerala coast and Lakshadweep Islands

Kavaratti, the capital island has a land area of 3.63 sq. km extending in the NNE-SSW direction. At the northern end the lagoon is shallow and coral growth is maximum. The southern part of the island has a narrow area popularly called Chicken Neck. Kavaratti is the most centrally located island in this archipelago. Androth is a unique island of the Lakshadweep group of islands which has an E-W orientation and has no lagoon. The island occupies the whole interior of the atoll except at the north east extremity where the reef flat is exposed at low tide. The corals have been blasted extensively and a breakwater has been constructed here recently. Androth is also having the largest land area viz. 4.8 sq. km. Chetlat has an area of 1.14 sq. km and is one of the northern most islands. The lagoon is very large and very perfect. Shores are well protected. This island is well connected to the main land and vessels usually sail directly to Mangalore. The island of the Kadamt with land area of 3.12 sq. km is the longest island and has very white and striking beaches. The eastern side of the reef is exposed at low tide and forms a level platform stretching from the beach. A high ridge of sand runs down the western side of the island.

4.2 PREPARATION OF TOPOGRAPHIC GRID

As already stated, the accuracy of topographic/bathymetric grid used is one of the important factors deciding the accuracy of the simulations using the model. Fine scale topographic data is not available for the Kerala**.** Hence the preparation of fine scale topographic grid was taken up as a priority work. This work involved three stages : i) pre-field laboratory work, ii) field survey and iii) post field laboratory work for processing of field survey data. The work involved under each of the above stages is described in the following sections.

4.2.1 Pre-field Laboratory Work

Pre-field laboratory work consisted of the following important tasks:

4.2.1.1 Preparation of base maps

The topographic sheets of 1:25,000 scales pertaining to the study area were taken. Base maps were prepared by tracing all the features, present on the topographic sheets, on a tracing paper. These base maps were then scanned and converted into soft copies/digital formats for further work. Also the satellite images pertaining to the study area were taken from the IRS-P4/P6 satellite sensor with a spatial resolution of 5.8 m.

4.2.1.2 Preparation of grids in base map

The coastal stretch was divided into different sectors with each sector taking roughly around 25-35 km in NNW-SSW direction. The width of the coastal sector was restricted to 4 km since literature reviews underscores the fact that it is the maximum width of coast that could be inundated by any tsunami. In order to fix up the boundary and to carry out the field survey along the study area grids of size 1 x 1 km were drawn on the base maps. These grids were drawn perpendicular to shoreline up to a maximum limit of 4 km. Around 100 (i.e. 25 x 4) such grids were drawn on each base map.

4.2.1.3 Identification of different Ground Control Points (GCPs)

Ground control points (GCPs) are reference points, at which the longitude, latitude and elevation measurements have to be carried out using DGPS (Differential Global

Positioning System). After drawing the grids on base map the study area was examined in detail and different ground control points were identified based on their location, purpose, characteristics etc. They were then marked on the base maps prior to the survey. This work was carried out so as to access the ground control points easily during the field survey of the study area. The ground control points were further used for the rectification of base maps.

4.2.2 Field Survey along the Study Area

The main objective of this work was to map the elevation of the study area and measure coordinates of the GCPs, besides mapping the infrastructure and public places in the area of study. The following surveying instruments were used for the field survey:

- Dumpy Level
- Differential Global Positioning System (DGPS) and
- Hand held GPS

4.2.2.1 Dumpy Level survey

The 25 km long and 4 km wide study area was very difficult to be surveyed using Dumpy Level alone because, of, obstructions like trees, plants, buildings etc. Apart from that, this is a tedious and time consuming work. Therefore, the dumpy level survey was restricted to the zone from still water level up to a maximum of 1 km towards the land. The measurements were made along shore-normal transects at 100-200 m interval along the coast. Similarly, the survey was also conducted in the banks of backwaters wherever they were present.

4.2.2.2 Differential Global Positioning System (DGPS) survey

The Differential Global Positioning System (DGPS) survey was carried out using Leica GPS 500 to measure the longitude, latitude and ellipsoidal height of selected Ground Control Points (GCPs). Ellipsoidal height is the vertical distance of a point above or below the ellipsoid. For the DGPS survey the first task involved was fixing up of Primary Reference Point (PRP) and several Secondary Reference Points (SRP) along the coast.

PRPs were fixed at selected locations along the coastline by operating the DGPS continuously for 72 hours. Subsequently several SRPs were fixed along the north and south of the PRP. SRPs were fixed at regular intervals of roughly 5-6 km for better accuracy of data collection. The SRP points were operated continuously for 24 hours in order to arrive at steady values. These SRPs were used as base stations for the entire DGPS survey pertaining to different coastal sectors along the Kerala coast in the entire modelling domain. The survey was conducted in the quick static mode of the DGPS. One GPS was kept as the RP base/reference and the other one at the selected GCP (Ground Control Point) as rover. The longitude, latitude and the ellipsoidal height were recorded. Keeping one GPS as the base, the rover GPS was moved along all the selected GCPs and the readings were recorded. A base station was used to a maximum of 12 km vicinity for continuous monitoring of GCP. In addition to the GCPs the GPS measurements were taken landwards up to 4 km at intervals of 0.5-1.0 km along each transect to estimate the elevation. Moreover the GPS readings were taken on all the first berms, for which dumpy readings were already taken, in order to convert the ellipsoidal heights into elevations with respect to mean water level. Photographs of field survey for DGPS measurements are given in fig. 4.2.

Fig. 4.2 Field survey in progress a) DGPS base station b) DGPS rover station

4.2.3 Post-Field Laboratory Work

Post-field laboratory work consisted of the following important tasks.

4.2.3.1 Processing of measured GPS points using Ski-Pro and conversion to shapefile

After the successful completion of field survey along the study area, the data which was stored in DGPS during the field survey was processed using SKI-Pro 1.1 Software. SKI-Pro (Static Kinematic-Professional) software is the Leica multi-baseline post-processing software provided with the Leica GPS System 500. To accomplish the data processing, firstly the data was downloaded from the GPS memory card to the computer. The raw data was then imported in the Ski-Pro software and the base point was assigned as reference and the rover points as rover. Before commencement of the data processing, the processing parameter i.e. cut off angle was set to 15°. Cut-off angle is the minimum elevation angle below which no more satellites are tracked by the GPS sensor. The cut off angle is inversely proportional to the number of satellites. In other words, if the cut off angle is less then the number of satellites tracked will be more and vice versa. For Leica GPS 500, 15° is the recommended value which tracks a maximum of 24 satellites in dual frequency during the survey.

Finally, the data processing was carried out and the processed longitude, latitude and the ellipsoidal height of each rover was obtained. The processed data was converted into a shapefile using ArcView GIS 3.2 Software. A shapefile is a homogeneous collection of features that can have either point, multipoint, polyline or polygon shapes. In other words, shapefile is a vector data storage format for storing the location, shape and attributes of geographic features. A shapefile is stored in a set of related files and contains one feature class.

4.2.3.2 Georeferencing of satellite images

The georeferencing of base maps was first carried out. Geo-referencing is the process of describing the correct location and shape of features, typically by assigning coordinates from a known reference system, such as longitude/latitude, Universal Transverse Mercator (UTM), or State Plane. This task was carried out using ArcView GIS software.

After georeferencing the base maps, the georeferencing of satellite images pertaining to the study area was carried out. For georeferencing one satellite image, around 20 GCPs spanning all around from the base map were taken and, the satellite image georeferenced. In this way all the satellite images pertaining to the entire Kerala coast were georeferenced.

4.2.3.3 Incorporation of current shoreline from rectified satellite imagery

Since the topographic sheets used for the base map preparation pertain to 1984 and there is a possibility for shoreline change over a period of time due to erosion/accretion the current shoreline had to be incorporated. Incorporation of current shoreline can be done in two ways: Survey using Real Time Kinematic (RTK) mode of DGPS or by digitization from the latest available satellite imagery. The Real Time Kinematics (RTK) survey method is a time consuming work. Since the second method can give the desired accuracy it was adopted for the present study. Towards this the latest available satellite imagery was used. For the southern sectors of Kerala coast only the 2004 imagery was available whereas for the northern sectors 2006 imagery was taken. The satellite imageries were georeferenced with reference to the base map and the shoreline from the satellite images (since it is the latest updated one available) were incorporated as the shoreline after digitization.

4.2.3.4 Applying tidal correction to Dumpy Level data

Since dumpy level measurements were carried out with reference to water level during different phases of tidal level, tidal level corrections had to be applied to reduce the elevation to mean water level. This was accomplished by using predicted tidal data for the nearest or adjacent areas using C-Map, a part of Mike 21 suit of models. The mean water level for the month was calculated from the predicted tidal data and then each measurement was reduced to the mean water level by applying appropriate corrections for the level difference.

4.2.3.5 Calculation of elevations from ellipsoidal heights

The ellipsoidal heights from DGPS were reduced to elevations with reference to Mean Water Level (MWL) by calculating the MWL ellipsoidal height. For this the concurrent

measurements made at berm crest using dumpy level and DGPS were used. The ellipsoidal height of a point, taken from DGPS, can be converted into the elevation of a point with respect to MWL by knowing the mean sea level ellipsoidal height. This means that, the ellipsoidal height of a MWL point minus the ellipsoidal height of a point gives the elevation of a point with respect to MWL. The ellipsoidal height of MWL at every 100 m interval along the coast and the ellipsoidal height of each GCP towards the land were available. By using the above data the elevations with respect to the MWL were calculated for the entire study area.

4.2.3.6 Entry of GCP data and creation of shapefile

After calculating the elevations of all the points with respect to the mean water level, a shapefile was created using ArcMap 9.2 Software. The GCPs were then identified and accurately placed on the geocoded satellite images. Finally, the elevation values for all the GCPs were assigned individually. Also, the intermediate elevation values between the successive GCPs were assigned by interpolation to give a general overview of the terrain.

4.2.3.7 Entry of infrastructure data and creation of shapefile

The infrastructures data i.e. the longitude and latitude of all the structures/buildings was created and this data was converted into a shapefile for superimposing it on to the base map for final vulnerability map preparation.

4.2.3.8 Digitization of various attributes present in the map

The shapefiles for various attributes viz, the shoreline, first berm, second berm, kayal bathymetry, kayal banks, elevations along the kayal banks, elevations of GCPs, interpolated elevations between the successive GCPs present on the satellite images, were created in individual shapefiles. All the attributes were digitized separately in accordance with the individual shapefiles using ArcMap 9.2 Software. Also the topographic contours were incorporated.

4.2.3.9 Providing topographic and bathymetric data

After digitization, the topographic and bathymetric data for the coarser grids were provided from the sources such as SRTM (Shuttle Radar Topographic Mission), C-Map

(Coastal Map), NHO (Naval Hydrographic Office) map and GEBCO (General Bathymetric Chart of the Oceans) and the field survey data was provided for the finer grid. The C-Map has fine resolution data when compared to NHO map. To minimize or reduce the ambiguities/errors in this data it was compared with NHO map for rectification before being fed into the model. The bathymetry of Grid A and Grid D (Neendakara-Trikkunnapuzha sector) are given in fig. 4.3.

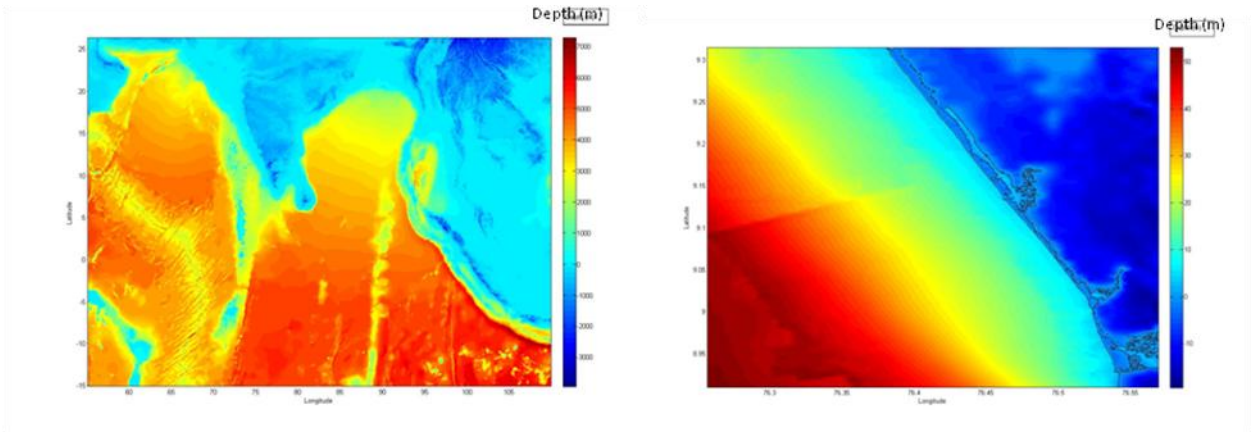

Fig.4.3 Bathymetry of different grids used in modelling a) Grid A b) Grid D (Neendakara-Trikkunnapuzha sector)

4.2.3.10 Merging the topographic and bathymetric data

Merging is combining all the individual data files into a single data file. After providing all the necessary data each individual shapefile was exported as delimited text (*.txt) format using ArcView GIS 3.2. Each text file was subsequently loaded individually and merged in a single text file using MATLAB 6.5 software for further work. Fig. 4.4 shows the merging of datasets for creation of topographic/bathymetric grids.

4.3 TSUNAMIGENIC SOURCES SELECTED FOR THE STUDY

In order to understand the tsunami wave propagation characteristics and assess the hazard proneness of the coastal locations numerical models have to be set up for different tsunamigenic sources. The tsunamigenic sources relevant for the study area are discussed below.

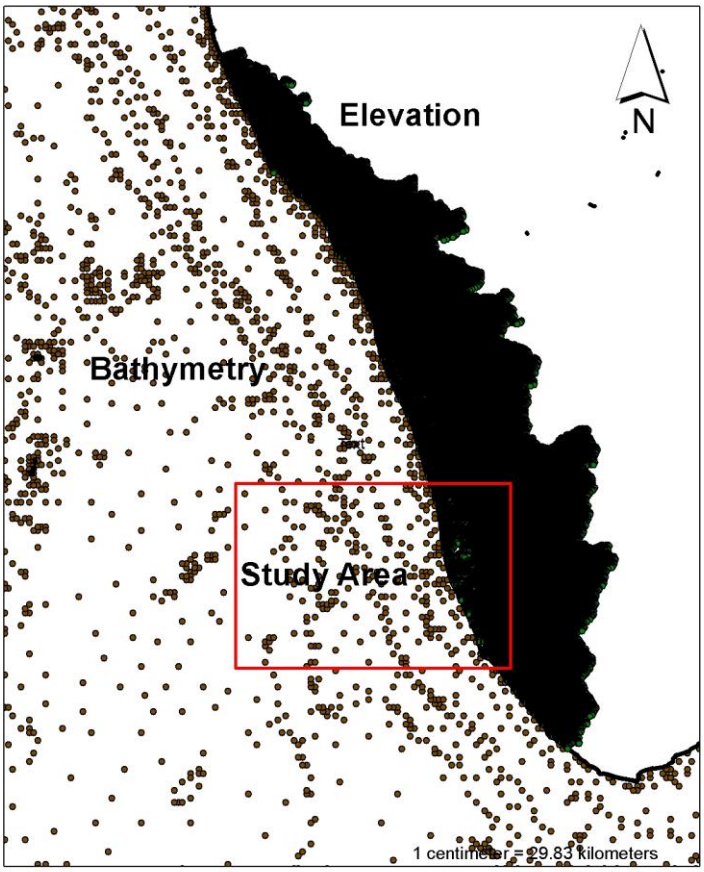

Fig. 4.4 Merging of different datasets for the creation of topographic/bathymetric grids

4.3.1 Sumatra Andaman Subduction Zone (SASZ)

In the 19th and 20th century tsunamis have been much more frequent in the eastern Indian Ocean with a period of 3 years or so (Rastogi and Jaiswal, 2006). The source zones of tsunamis in the eastern Indian Ocean are Sunda Arc, Andaman Nicobar Island and Burma-Bangladesh region among which Sunda Arc is the most active region which has generated about 70 tsunamis. The occurrence of 26 December 2004 earthquake which was followed by a catastrophic tsunami in the Indian Ocean has placed the Sumatra region as one of the most potential earthquake prone and tsunamigenic region in the Indian Ocean (Fig. 4.2). The Sumatra Andaman Subduction Zone accounts for the most disastrous tsunami. The Sunda belt extends northward to Andaman Nicobar Island where

a few tsunami have originated. Further north of this point the Bangladesh Myanmar coast has also produced some well documented tsunamis.

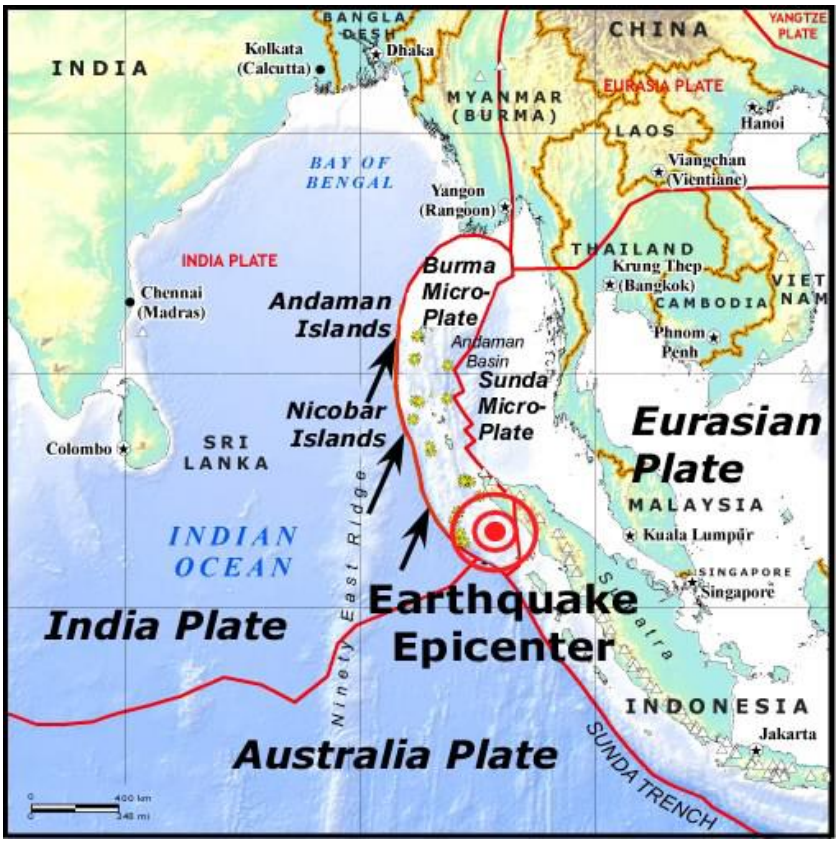

Fig. 4.5 The Sumatra Andaman Subduction Zone (SASZ) where the 2004 tsunami originated (Source: USGS, 2004)

The seismic gap along the subduction zones are possible sites for generation of great earth quakes in future. Along Sunda arc great earthquake of Magnitude 8.5 or greater can repeat every 2 centuries but smaller tsunamigenic earthquakes can repeat every few decades. However, tsunamis from Java region can't affect the countries other than Indonesia.

4.3.2 Makran Subduction Zone (MSZ)

Makran is the source of the second deadliest tsunami in the Indian Ocean with a death toll of about 4000 people (Heidarzadeh et al., 2008). The Makran zone is located off the southern coasts of Iran and Pakistan (Fig. 4.3). The Makran Subduction Zone extends east from Straight of Hormoz in Iran to Karachi in Pakistan with a length of about 900 km. The zone of Makran coast forms the boundary between Arabian and Eurasian plates

(Stoneley, 1974). The major plate boundaries in the Makran region are 1) The Ornach-Nal fault system in the eastern boundary of the Makran, 2) The Zendan-Minab fault system in the western boundary of Makran and 3) The Murray ridge in the south which delineates part of the Arabian-Indian plate boundary.

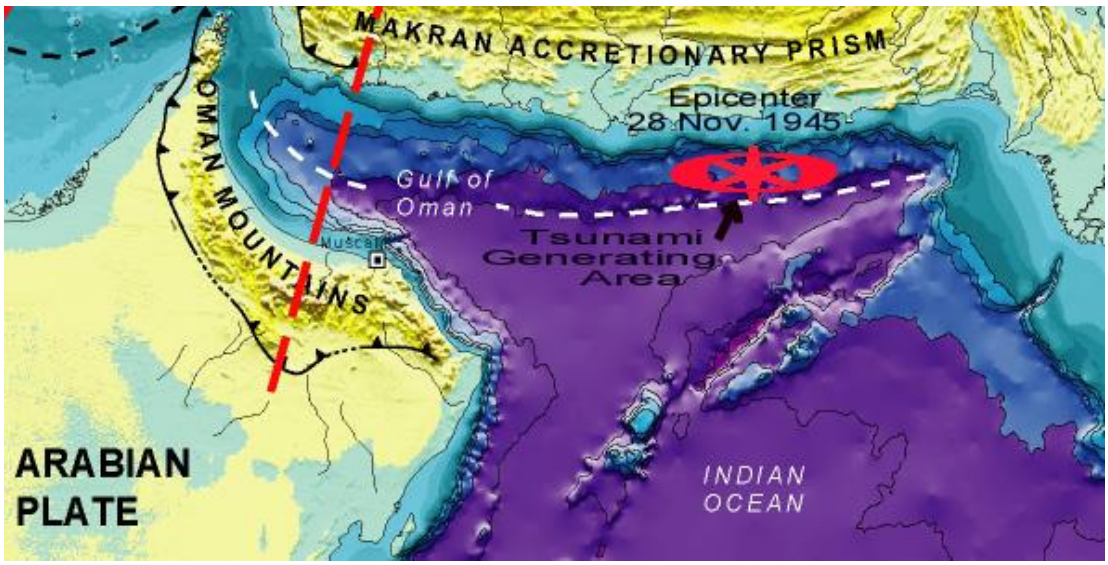

Fig. 4.6 The Makran Subduction Zone (MSZ) where the 1945 tsunami originated (Source: Pararas Carayannis 2006b)

The boundaries of Makran subduction zone are complex tectonic areas. Byrne et al. (1992) reported that the rate of convergence between the two plates in the Makran subduction zone is about 40 mm/year. But recent studies made by Vernant et al. (2004) reveals that the subduction rate at Makran subduction zone is about 19.5 mm/year. While comparing with the convergence rate of world's other subduction zone Makran is a relatively slow moving subduction zone characterized specifically by extremely shallow subduction angle (Kopp et al., 2000). Kopp et al. (2000) also reported that Makran has one of the largest accretionary wedges and is characterized by large sediment thickness of 7 km. Unlike the other subduction zones there is no trench at the location of Makran subduction zone. Schluter et al. (2002) and Wiedicke et al. (2009) reported the presence of active mud volcanoes all along this subduction zone. Rajendran et al. (2008) observed a significant discrepancy between the predicted and the observed arrival time of 1945 Makran tsunami and they attributed this disparity to submarine landslides triggered by earthquake. Page et al. (1979) reported a reoccurrence cycle of 125-250 years for similar event of 1945 whereas Byrne et al. (1992) reported 175 years. After reviewing the seismicity of Makran Jackson and Mckenzie (1984) concluded that nearly all of the earth-

quakes usually occur at a depth of less than 20 km. Byrne et al. (1992) reported that the average depth of the 1945 event was about 25 km. Byrne et al. (1992) reported seven large earthquakes of magnitude greater than seven in the Makran subduction zone in the past five centuries. But none of these events were as large or deadly as the1945 event.

4.3.3 Other Tsunamigenic Sources

Besides Makran, the North West Indian Ocean has four more tsunamigenic zones as reported by Bapat et al. (2007). They are:

1) Persian Gulf area
2) Aden Gulf area
3) Socotra Island region
4) Diego Garcia region

The above mentioned regions have been producing tsunamigenic earthquakes up to magnitude 7.0 as per historical records. Anyhow for the last thirty years these locations are almost seismically silent.

Thus the two potential tsunamigenic locations in the Indian Ocean viz. Andaman-Sumatra and Makran subduction zones were selected for numerical modelling. In addition based on discussions with experts in the field a third Hypothetical Worst Case Scenario (HWCS) of Sumatra-like earthquake in the Makran Subduction Zone was also chosen for the simulations.

4.4 MODEL SETUP

The setup of a model is the preliminary step in the numerical modeling procedure and the setup includes the following procedures.

4.4.1 Inclusion of Source/Fault Parameters or Seismic Parameters

Seismic parameters are contributing factors of an earthquake which in turn gives rise to a tsunami. The identification of seismic/rupture parameters is one of the basic task involved in the tsunami modeling since it determines the rupture intensity, directivity and

amplitudes of tsunami. The seismic parameters in respect of the 1945 Makran and 2004 Sumatra earthquake are given in Table 4.1.

Table 4.1 Seismic parameters in respect of 1945 Makran and 2004 Sumatra earthquakes (Sources: Chileah et al., 2007and Arjun et al., 2011)

Sl. No.	**Source / Parameter**	**1945 Makran**	**2004 Sumatra**
1	Longitude (degrees)	63 E	95.85 E
2	Latitude (degrees)	24.5 N	3.32 N
3	Magnitude (M_w)	8.0	9.3
4	Slip (m)	15	15
5	Fault length (km)	200	680
6	Fault width (km)	100	150
7	Strike (degree)	270	342
8	Dip (degree)	15	15
9	Rake (degree)	90	90
10	Depth (km)	30	20

4.4.2 Fixing Time Step and Propagation Time

Prior to the running of the model we have to fix the propagation time and the time step required for the propagation for capturing the instantaneous events of tsunami propagation and for getting the desired output. The propagation time have to be fixed with reference to the historical events depending upon the source and the time taken by that event to reach the particular study area domain. The propagation time was fixed as 8-10 hours for Sumatra 2004 and 10-12 hours for Makran 1945 scenarios under this investigation.

4.4.3 Selection of Points for In-depth Analysis

Points can be selected in the nearshore area as well as offshore area pertaining to fine grid and coarse grid for specifically evaluating the amplitude variation occurring during the propagation of tsunami. The selected points have to be fed to the program for getting the time series output for the specified points.

4.4.4 Executing/Running the TUNAMI N2 Model

The TUNAMI N2 model, with the Microsoft FORTRAN 4.0 as front end and MATLAB 6.5 as back end, has been used to successfully simulate the tsunami propagation *(See. Figs. 5.1 and 5.2 in sec. 5.2)*, run-up and inundation for the coastal areas selected for the study. The simulations were done for all the three cases namely, the 2004 Sumatra, 1945 Makran and the Hypothetical Worst Case Scenario.

4.4.5 Analysis of Output Files

The output files of TUNAMI N2 program cannot be easily interpreted as given in the output files. In order to get the best results, the output files are needed to be converted into diagrams or graphs so that the interpretation and the comparison of different data can be achieved easily. After running the TUNAMI N2 model successfully, the run-up and the inundation values for the study area has been generated for all the scenarios using MATLAB 6.5 Software. Using these figures the most vulnerable locations in the study area were identified. The model output file, containing the extent of inundation along the study area, was converted into a data file using MATLAB 6.5 Software. This data file was subsequently converted into a shapefile in order to carry out the analysis of the results easily. After converting the output file to a shapefile, another shapefile with a polygon feature called extent of inundation was created. The run-up values were grouped separately in 0.5 m interval and each group was assigned with a different colour so as to easily identify the minimum and maximum run-up values. Subsequently, wherever the inundation was noticed that area was digitized and accordingly the run-up value has been assigned with the extent of inundation shapefile for an easy perusal. Similarly, the plotting and estimation of the run-up values and the extent of inundation for all the scenarios was carried out in order to generate the inundation maps.

4.4.6 Preparation of Inundation Maps

Lastly, the inundation maps of 1:10,000 scale for the entire study area were prepared in ArcMap 9.2 software. To do this, firstly the various assets like roads, place names, public places and infrastructures were digitized and brought onto the maps. Inundation maps were prepared subsequently using the above. In the final vulnerability map the inundation for 2004 Sumatra, 1945 Makran, and the Hypothetical Worst Case Scenario, has been incorporated for getting a glimpse of site specific vulnerability in terms of run-up and inundation. The state level /district level disaster management centres should have these

maps and in the event of a tsunami warning, information is disseminated to the general public by referring to such maps. A sample inundation map is shown in Fig. 4.7.

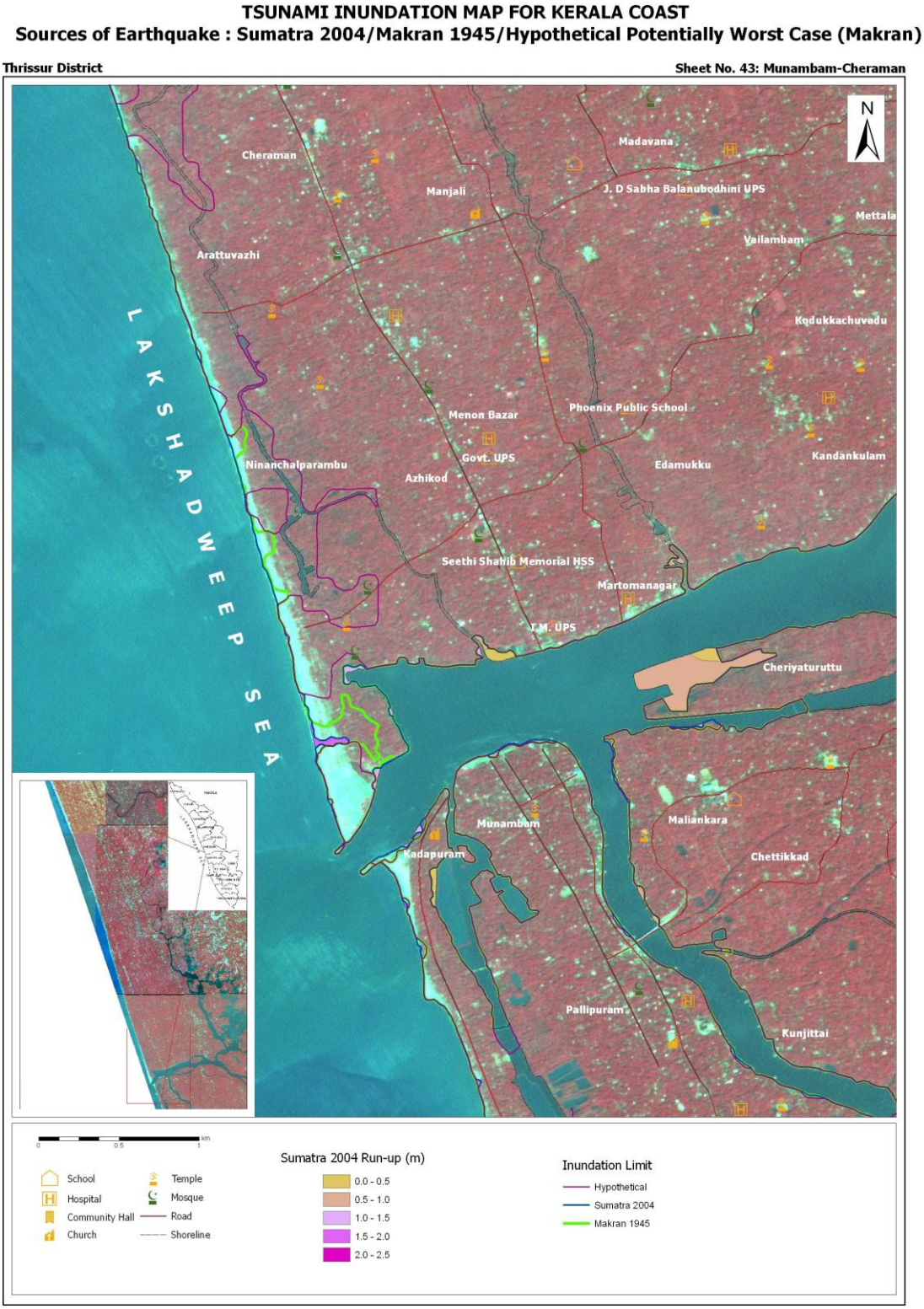

Fig. 4.7 A Typical Tsunami Inundation Map

4.5 MODEL CALIBRATION

A numerical model has to be calibrated prior to its application. The post tsunami field data pertaining to the 2004 Sumatra tsunami (Kurian et al., 2006) became very useful for the calibration exercise. The details relating to the calibration exercise are given in the following sections

4.5.1 Site Chosen for Model Calibration

The 34 km coastal stretch in the southern Kerala starting from Neendakara in the south of Kollam district to Trikkunnappuzha in the south of Alappuzha district was selected as the site for model calibration as it was one of the worst affected area during December 26, 2004 Tsunami. Besides a very good field database pertaining to run-up and inundation due to December 26, 2004 tsunami is available for this coast (Kurian et al., 2006 a-c). Apart from that Centre for Earth Science Studies have a very fine scale data set on bathymetry of this coast. Figure 4.8 shows the Neendakara-Trikkunnapuzha sector of the coast of Kerala that was selected to calibrate the TUNAMI N2 model.

4.5.2 The Calibration Process

The Model was run for the Neendakara-Trikkunnapuzha coast of southern Kerala by providing different Manning numbers which represent the bottom friction. The seismic parameters relevant for the 2004 Sumatra earthquake were given as input. The run-ups for different locations of the coast were noted from the simulation. The field data for calibration and comparison were taken from Kurian et al. (2006 b).

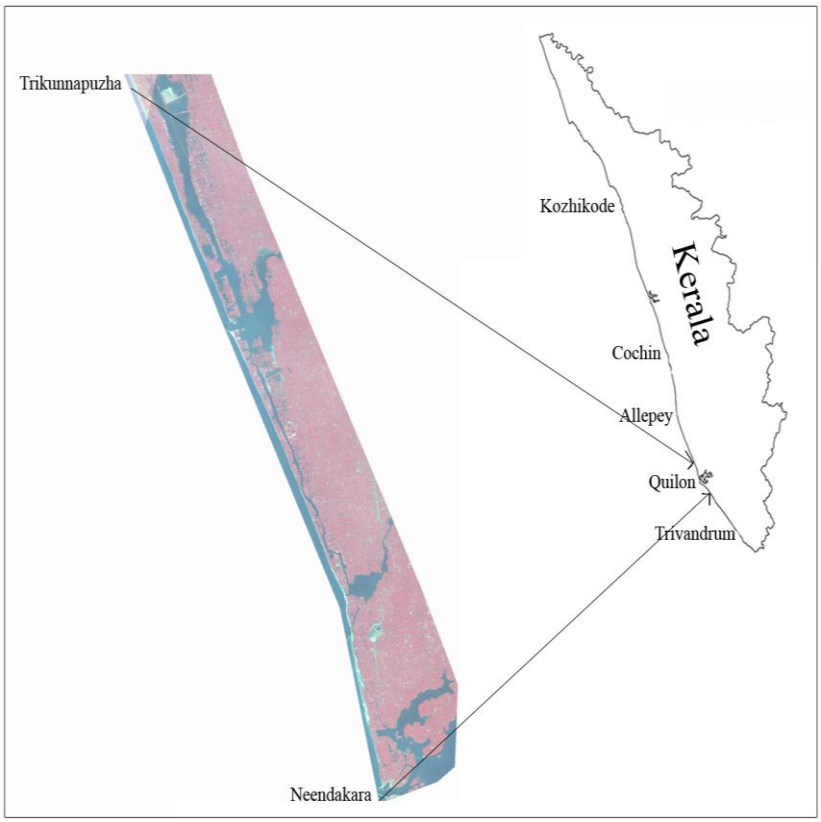

Fig. 4.8 Site chosen for model calibration

It was found that the simulations with a friction coefficient of 0.01 gave best comparisons with the field data (Table 4.2) with an average error estimate of around 9.22 %. Fig. 4.9 shows the tsunami run-up for the Neendakara-Trikkunnapuzha. A maximum run-up of 4.7 m is obtained at Valiyazhekkal and Azhekkal (north and south of Kayamkulam inlet respectively) with values further decreasing towards either side of the inlet. Run-up in the rest of this coast is in the range of 2-3 m. From the results it can be seen that the model has nearly reproduced what was observed in the field for December 26, 2004 Tsunami. Hence it can be concluded that the model with a friction co-efficient of 0.01 is calibrated and can be used for simulation of run-up and inundation in the rest of the study area.

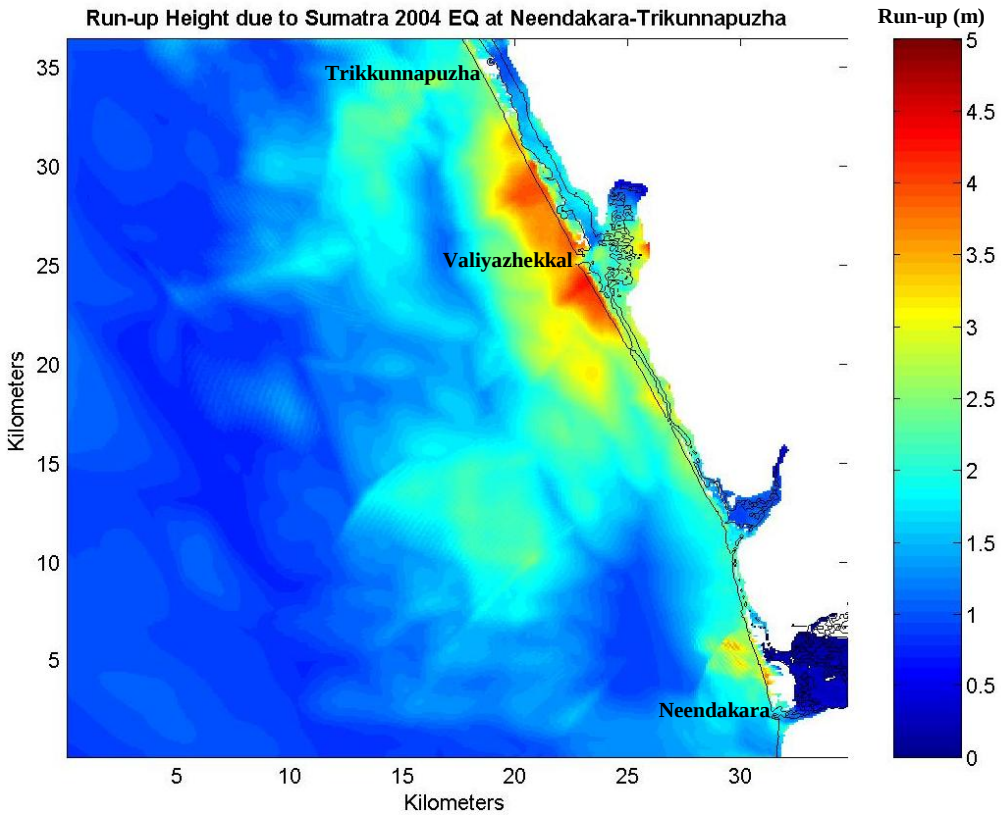

Fig. 4.9 Simulation result of the model calibration for the Neendakara-Trikkunnapuzha coastal stretch of Southern Kerala

Table 4.2 Comparison of observed and computed tsunami run-up (m) at selected locations on the coast of Kerala (Source: Praveen et al., 2011)

Sl. No.	Location	Latitude	Longitude	Run-up (m)	
				Simulated	Observed
1	Neendakara	8° 56' 09.77"	76° 32' 09.77"	2.3	2.75
2	Kovilthottam	8° 59' 44.23"	76° 31' 23.34"	2.3	2.75
3	Tharayilkadavu	9° 09' 18.44"	76° 27' 18.10"	2.3	3.25
4	Pandarathuruthu	9° 02' 12.84"	76° 30' 30.92"	3.0	3.25
5	Srayikadu	9° 05' 56.97"	76° 28' 50.36"	4.0	4.25
6	Cheriyazhekkal	9° 07' 52.57"	76° 28' 02.07"	4.5	4.25
7	Azhekkal	9° 08' 06.64"	76° 27' 50.09"	4.7	4.75
8	Valiyazhekkal	9° 08' 23.79"	76° 27' 43.54"	4.7	4.75
9	Kallikkadu	9° 12' 13.69"	76° 25' 59.18"	4.7	4.75
10	Arattuppuzha	9° 12' 55.08"	76° 25' 38.79"	4.5	4.25
11	Trikkunnapuzha	9° 15' 30.14"	76° 24' 26.34"	3.0	3.25

4.6 SUMMARY

The methodology followed for the study involved the set up of the TUNAMI N2 model, its calibration and finally simulations using the model for various studies. As accuracy of the model output is directly linked to the accuracy and resolution of the topographic/bathymetric data used for the coastal area (Grid D), every effort was made to prepare accurate fine grid topographic/bathymetric grid. As fine grid topographic data were not available for the coastal areas, extensive topographic measurements in the 4 km zone adjoining the shoreline were carried out using dumpy level and DGPS. The detailed methodology involved in the preparation of the topographic grid is given in the chapter. Bathymetric data was taken from CMAP and NHO charts, and coupled with measured data available at CESS. Open source bathymetry and topography data viz. General Bathymetric Chart of the Oceans (GEBCO), SRTM, C-Map, NHO chart are used for the outer grids A, B and C. The TUNAMI N2 model was calibrated using post-tsunami field survey data available at CESS for Sumatra 2004, for the 34 km long Neendakara-Trikkunnapuzha sector which was the worst affected during that tsunami. The run-up values of the calibrated model gives good correspondence with the field data with an error estimate of only 9.22 %.

CHAPTER 5

PROPAGATION OF TSUNAMI IN THE SOUTH EAST ARABIAN SEA (SEAS)

5.0 INTRODUCTION

The South East Arabian Sea (SEAS) is a very crucial zone as far as the tsunami wave propagation is concerned. It is here that the tsunami waves undergo transformation processes such as refraction, diffraction, reflection etc. leading to spatial variation in their amplitude, arrival times, etc. Hence a study of tsunami wave propagation in the SEAS is very important in understanding the run-up and inundation characteristics along the coast and is thus undertaken in this chapter. The role of Lakshadweep Maldive Ridge (LMR) in shaping the inundation along the coast has been critically analysed by carrying out numerical simulations with and without the LMR. The phenomenon of Helmholtz resonance occurring in harbours also has been studied for two representative sectors.

5.1 ROLE OF PHYSICAL OCEANOGRAPHIC PROCESSES IN THE PROPAGATION OF TSUNAMI

The nature of the 2004 Sumatra tsunami wave that devastated many parts of the Kerala coast was complex. The observed non-uniform pattern of wave run-up, inundation and site specific onslaught underscores the complexity of the tsunami wave. Striking differences or discrepancies in the characteristics of tsunami wave like initial withdrawal, number of waves and arrival times were noticed. Several physical oceanographic processes contributed individually or collectively for the observed characteristics of tsunami wave propagation. The identified processes as per (Kowalik et al., 2005 a, b; Murty et al., 2005 a-c, 2006 a-c; Nirupama et al., 2005 a, b, 2006) are:

1) Focussing and defocussing of tsunami energy due to ocean bathymetric features
2) Boundary reflections
3) Quarter wave resonance amplification in bays and gulfs
4) Helmholtz resonance in harbours
5) Constructive interference
6) Interaction with astronomical tides
7) Coupling with internal waves due to ocean density gradients

8) Trapping of long gravity energy on continental shelves through Oscillations of First Class (OFC) and Oscillations of the Second Class (OSC) via. the mechanism of trapped and partially leaky modes
9) Interaction with the strong tidal current gradients near regular and degenerate semidiurnal and diurnal tidal amphidromic points
10) Extraction of energy from opposing ocean currents through Reynolds eddy stresses
11) Interaction with the wind wave setup
12) Phase or frequency dispersion and amplitude dispersion
13) Breaks in the continental shelves through which tsunami waves travelling through the deeper water interact with tsunamis in the shallow water

5.2 SIMULATION RESULTS ON THE PROPAGATION CHARACTERISTICS OF TSUNAMI IN THE SOUTH EAST ARABIAN SEA

In order to understand the prominent physical processes during the propagation of tsunami in the SEAS the TUNAMI N2 model was run for a total time period of 10 hours for the 2004 December Sumatra tsunami. The output time series was enabled at every 15 seconds to understand the propagation characteristics. Each output file was further correlated to generate animation frames at an interval of one minute starting from the initial time of propagation. The each one minute files were plotted in Matlab for identifying the characteristics. The salient features of the transformation as noticed from the snapshots (Fig. 5.1) are described below.

The tsunami propagating from the Sumatra source region undergoes different transformation processes on reaching Sri Lanka. A portion of direct wave after hitting the eastern coast of Sri Lanka gets reflected back. This can be particularly attributed to the steep continental shelf and margin of this sector standing out from the deep sea basin of 3000 m depth. But the part of the direct wave towards north undergoes refraction and reaches the north north-east (NNE) portion of Sri Lanka. At the southern sector of Sri Lanka the waves diffract and propagate westward and northward. Part of this northward propagating wave close to the coast gets refracted due to the varying bathymetry and arrives at the west coast of Sri Lanka which includes the Palk bay. Consequently there is some delay in the arrival time of the tsunami waves in this Bay while comparing with the rest of Sri Lanka. It can be noted that a focusing of tsunami wave is visible in and around

the coast of Kanyakumari and Kolachel. Refraction is the main factor leading to the focusing of tsunami waves at Kanyakumari and Kolachel. The diffracted waves will propagate further north towards the Kerala coast.

Now coming to the tsunami propagation in the LMR region (Fig. 5.2), the direct wave coming from Sumatra reaches the eastern side of LMR by around 190 minutes. There is practically very less shoaling and the wave gets partially reflected.

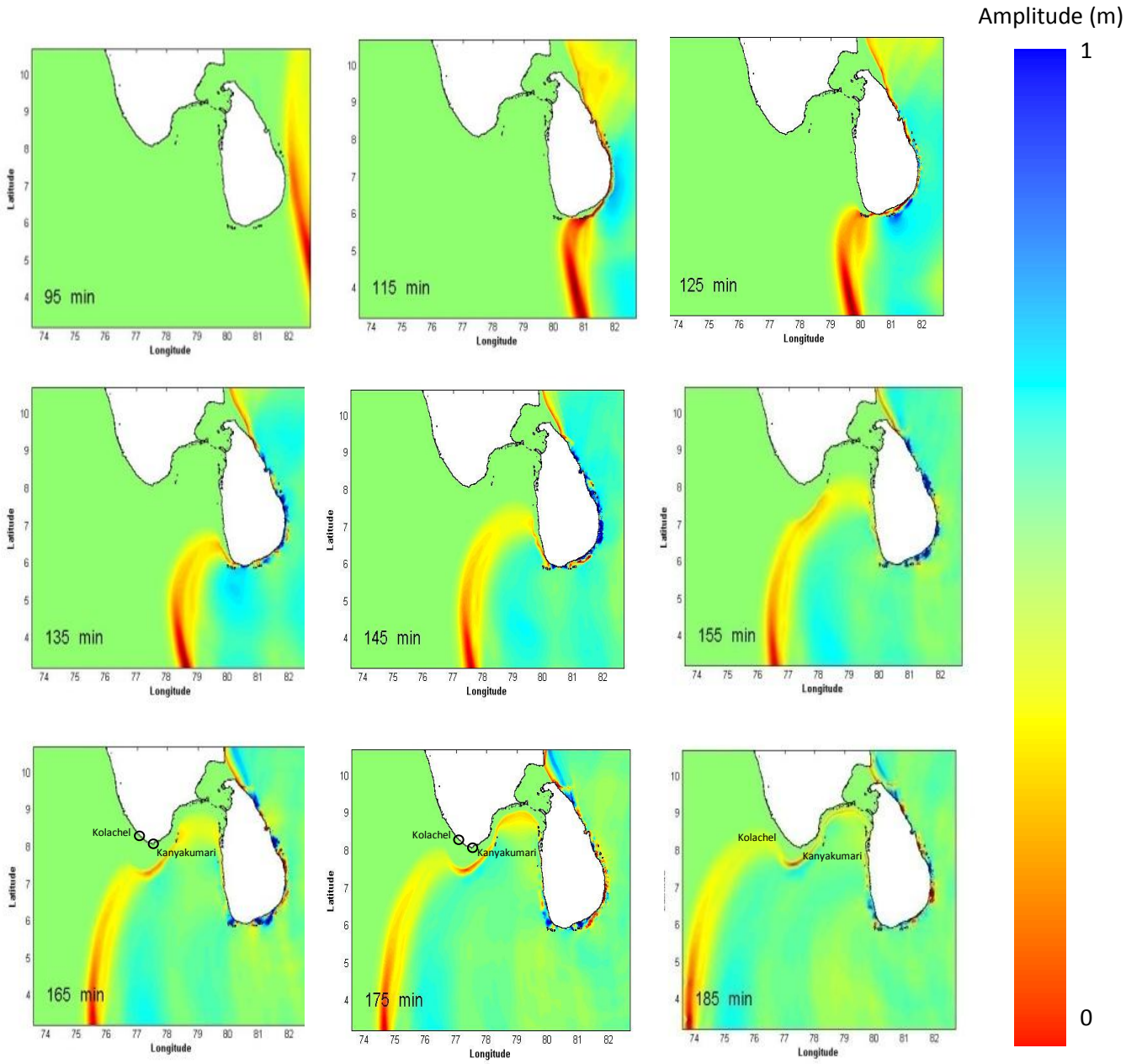

Fig. 5.1 Simulation result showing salient features of transformation around Sri Lanka

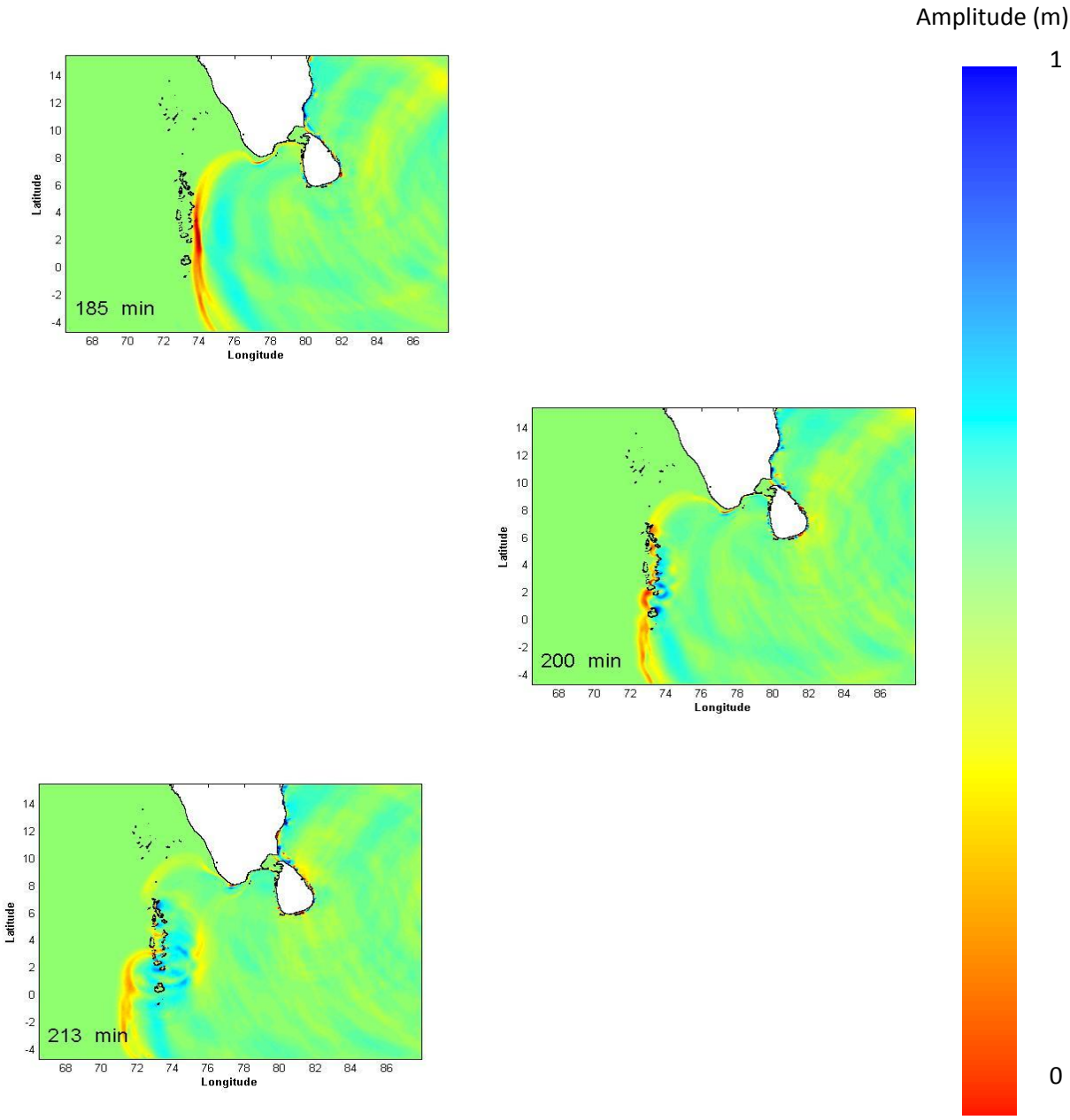

Fig. 5.2 Propagation snapshots of reflection happening in the eastern side of LMR

A part of this reflected wave proceeds towards the south west coast of Sri Lanka and another part move towards the Kerala coast. This is the second wave arriving at the coast which has generated higher run-up values than the initial wave due to the interference with the reflected waves from LMR. The combined effect of reflected waves with the normal waves contributed to the higher values at the coast. A portion of the non-reflected waves passes through LMR and reaches on the western side of the ridge. The western portion of the LMR is a shallow region when compared to the eastern side. So there is a scope for amplification of tsunami in this area due to increased shoaling. The westward moving wave undergoes Total Internal Reflection (TIR) (Murty et al., 2008) due to its propagation from shallow to deep water and can reach the west coast of Sri Lanka as well

as the south west coast of India. Some of the late arrivals observed along the Kerala coast could be attributed to the reflection and total internal reflection due to the LMR. Any late arrival beyond this time could be attributed to the boundary reflections from the east coasts of Somalia and Africa. So, to summarize the direct waves coming from Sumatra, the direct waves which had undergone refraction, reflection, diffraction and TIR due to the complex coastal configuration and bathymetry of the SEAS contribute individually or collectively towards the observed inundation and run-up along the shores of the SEAS.

5.3 RESONANCE OF TSUNAMI WAVES IN HARBOURS

Out of the various physical oceanographic processes that affect the propagation of tsunami, resonance plays a pivotal role in raising the tsunami amplitudes in harbours. Two types of resonances, Quarter Wave Resonance (QWR) and Helmholtz resonance are observed. As tsunami approaches the shore the wavelength gets compressed and if the linear dimension of the bay or gulf matches with ¼th wavelength of the incoming tsunami, the tsunami amplitude will increase gradually. This process is called Quarter Wave Resonance. When the long gravity wave energy of a tsunami enters the wide harbour through a narrow channel it cannot easily get out of the harbour because of reflection at various locations in the harbour boundary. This phenomenon is called Helmholtz resonance (Murty et al., 2006 a-c). During the tsunami of 26th December 2004 there were high water levels in certain harbours for several days after the tsunami which can be accounted to the credit of Helmholtz resonance.

Numerical modeling was conducted in two representative harbours along the south west coast of India for understanding the resonance phenomenon. They are:

1) Mangalore Port
2) Cochin Port

5.3.1 Mangalore Port

The New Mangalore Port located near Mangalore in the Karnataka state is one of the major ports of India and is currently the ninth largest port in India, situated in the city of Mangalore in the Karnataka state. This port is an artificial harbour constructed using the

latest technology to provide the best port facilities. The port has been established in such a way that it can bear all kinds of climatic hazards. It is the only major port of Karnataka and hence a number of industries depend on the Mangalore port, making it also a major establishment of socio-economic importance and thereby exposing the urgent need for studying the tsunami vulnerability.

A total of six points (Fig. 5.3) were selected for the resonance computations in the Mangalore port. The point number 1 was selected in the nearshore area of depth around 10 m. The point numbers 2, 3 and 4 were selected in the central channel while point numbers 5 and 6 are at the northern and southern arm of the harbour.

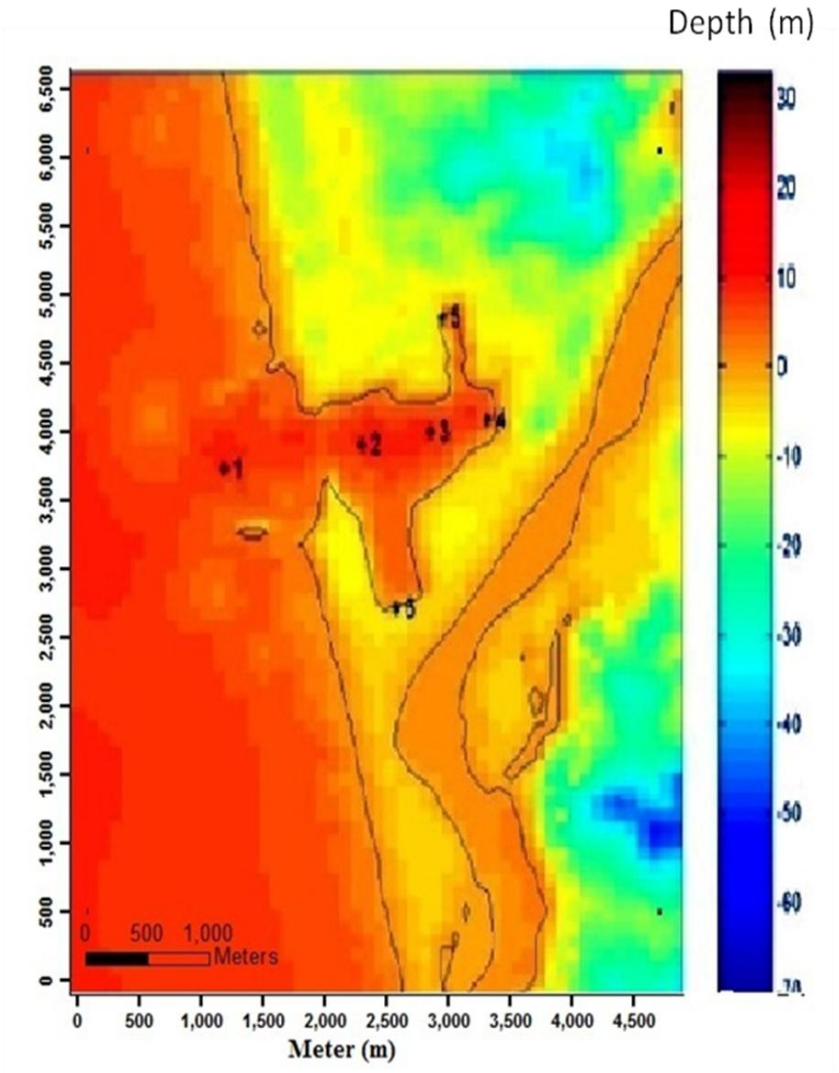

Fig. 5.3 Points selected in the Mangalore port for studying resonance

The simulation was carried out for the Sumatra 2004, Makran 1945 and Hypothetical Scenario (*Ref. Section 4.3.3 Page 63*). Table 5.1 gives the maximum water levels at all six points for the three sources. The simulation result for 2004 Sumatra source is given in the Figure 5.4. The tsunami amplitude at point no: 1 is around 1m at the time of the arrival of the first wave. The points 2 and 4 show an increase in amplitude exceeding greater than 1m which gradually increases with time and finally at the point no: 5 at the northern tip the amplitude comes to a maximum. All the points inside the inlet show high values of amplitude while comparing with that of the nearshore point.

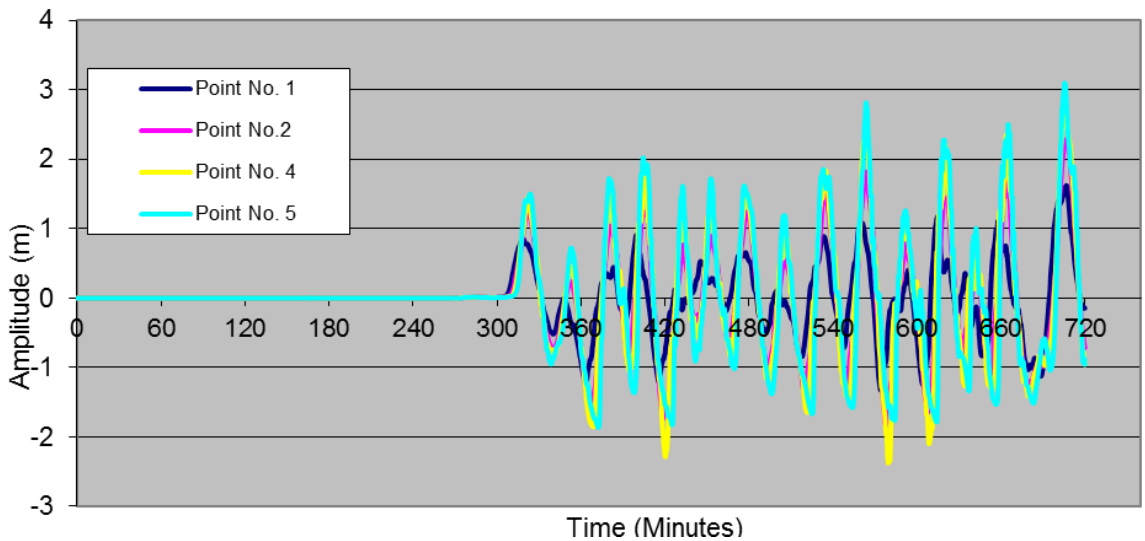

Fig. 5.4 Simulation result of resonance in the Mangalore port for Sumatra 2004

There is a small delay in the arrival time of initial waves of tsunami in all the points inside the inlet on comparison with the nearshore point which can be attributed towards the time taken for propagating towards the interior of the inlet. The very first wave arriving at point no. 5 itself shows an amplitude of 1.5 m which gradually increases and finally reaches a maximum value greater than 3 m after 10 hours. This is a clear epitome of Helmoltz resonance. The simulation results for all the three sources indicate the pattern of resonance in Mangalore port. The only variation is in the amplitudes. The hypothetical source dominates in terms of amplitude followed by Makran 1945 and Sumatra 2004. The initial wave at the nearshore point showed an amplitude in the order of less than 1 m for Sumatra, around 1.5 m for Makran and 2 m for hypothetical case.

Table 5.1 Maximum water levels at Mangalore port due to resonance

Sl. No.	Location	Maximum water level (m) : Sumatra	Maximum water level (m) : Makran	Maximum water level (m) : Hypothetical
1	Point 1	1.6	1.8	2
2	Point 2	2.1	2.2	2.5
3	Point 3	2.25	2.45	2.6
4	Point 4	2.5	2.8	2.7
5	Point 5	3.1	3.2	3.5
6	Point 6	2.5	2.7	2.9

5.3.2 Cochin Inlet

The Cochin Port (Fig. 5.5) is one of the largest ports in India. It is a natural harbour built on Vembanad Lake viz. Willingdon Island and Vallarpadam with the entrance to the harbour through the Cochin inlet bordered by Puthuvype in the northern side and Fort Kochi in the south. The modern port was established in 1926 and has completed 86 years of active service. The shipping channel is maintained with depths greater than 13 m through maintenance dredging. The points selected for the study are shown in the Figure 5.5. A total of 18 points were selected for the study. While point No. 1 lies in the offshore at the beginning of the shipping channel, point No. 2 is further inside the shipping channel, in the nearshore zone. Points 3 and 4 are located in the inlet region while rest of the points are inside the harbour in the shipping channel except for points 12, 13, 17 and 18 which are in the shallower portions of the lake.

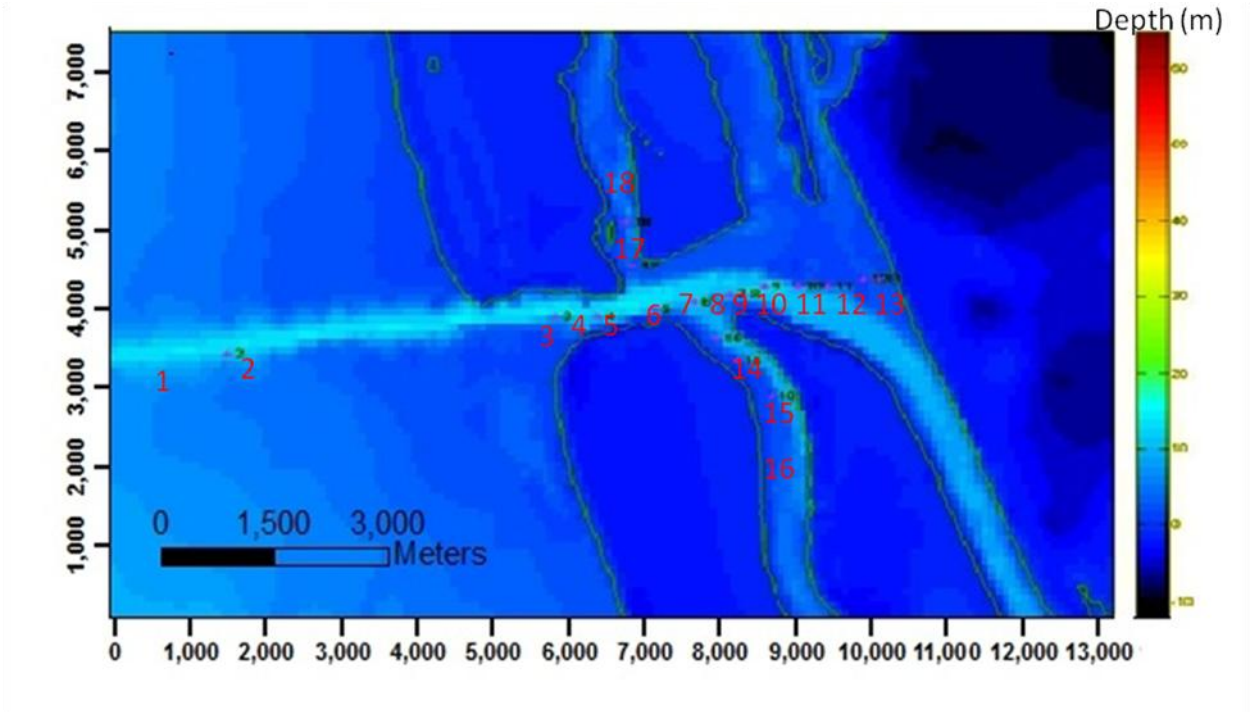

Fig. 5.5 Points selected in the Cochin harbour for studying resonance

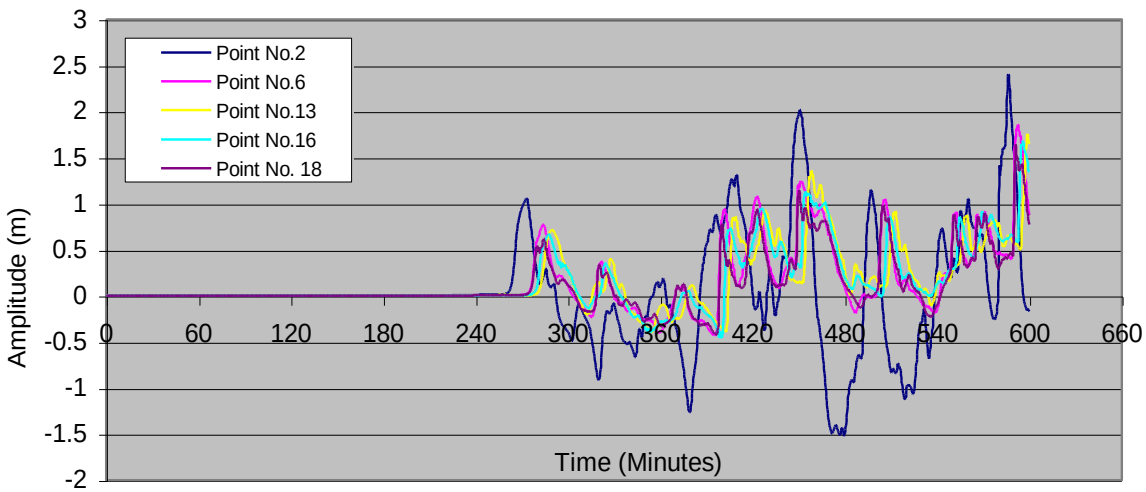

Fig. 5.6 Simulation result of resonance in the Cochin estuary for 2004

In Cochin Harbour the amplitude pattern is almost same for both nearshore point and the points inside the inlet (Fig. 5.6). The first wave arriving at the nearshore point (Point 2) shows an amplitude of 1 m. The first wave arriving at the interior points (Points 6, 13, 16 and 18) show considerably less values while comparing with the nearshore point i,e point 2. The final wave at the nearshore recorded an amplitude in the range of 2.0-2.5 m. But the values are less for points inside the inlet. This is applicable for other waves also, starting with first wave. From the results it is obvious that no resonance is visible inside this inlet. This can be attributed to the presence of good natural channels, reducing the

chances for the amplification caused in closed harbours like Mangalore inlets due to back and forth constrained oscillations.

5.4 ROLE OF LAKSHADWEEP MALDIVE RIDGE (LMR) IN TSUNAMI PROPAGATION IN THE SOUTH EAST ARABIAN SEA (SEAS)

The 2004 Sumatra tsunami appears to be the first of its kind to have devastated some locations of the Kerala coast. The nature of tsunami wave propagation in the SEAS as seen in section 5.2 was really complex. Murty et al. (2008) gave a schematic account of the prominent role played by LMR in the propagation of tsunami waves. According to them, the LMR in addition to reflecting tsunami wave in its eastern face also had caused total internal reflection of waves as evidenced by the solitary wave noticed at Neendakara near Kollam. The impact of the LMR in the run-up and inundation along the Kerala coast was closely examined by carrying out the numerical simulation in two cases, one with LMR and the other without LMR. With LMR is the situation as is prevalent now with the presence of Lakshadweep Maldive Ridge encompassing a chain of islands oriented in the north south direction (Fig. 5.7 a). Without LMR is a hypothetical case formulated for understanding the impact and role of LMR.

For the numerical simulation in the second case, the chain of islands or the land mass was totally excluded by providing bathymetric characteristics adjacent to the area. The depth values were incorporated into that area in accordance with the near most neighbourhood points prevailing in the coarse grid namely grid A (Fig. 5.7 b). Numerical simulation for the above two cases is done for two sectors of Kerala coast viz. the Neendakara Thottapally sector covering a total 44 km in the southern Kerala and Mogral-Talappadi sector of 25 km length in the northern Kerala.

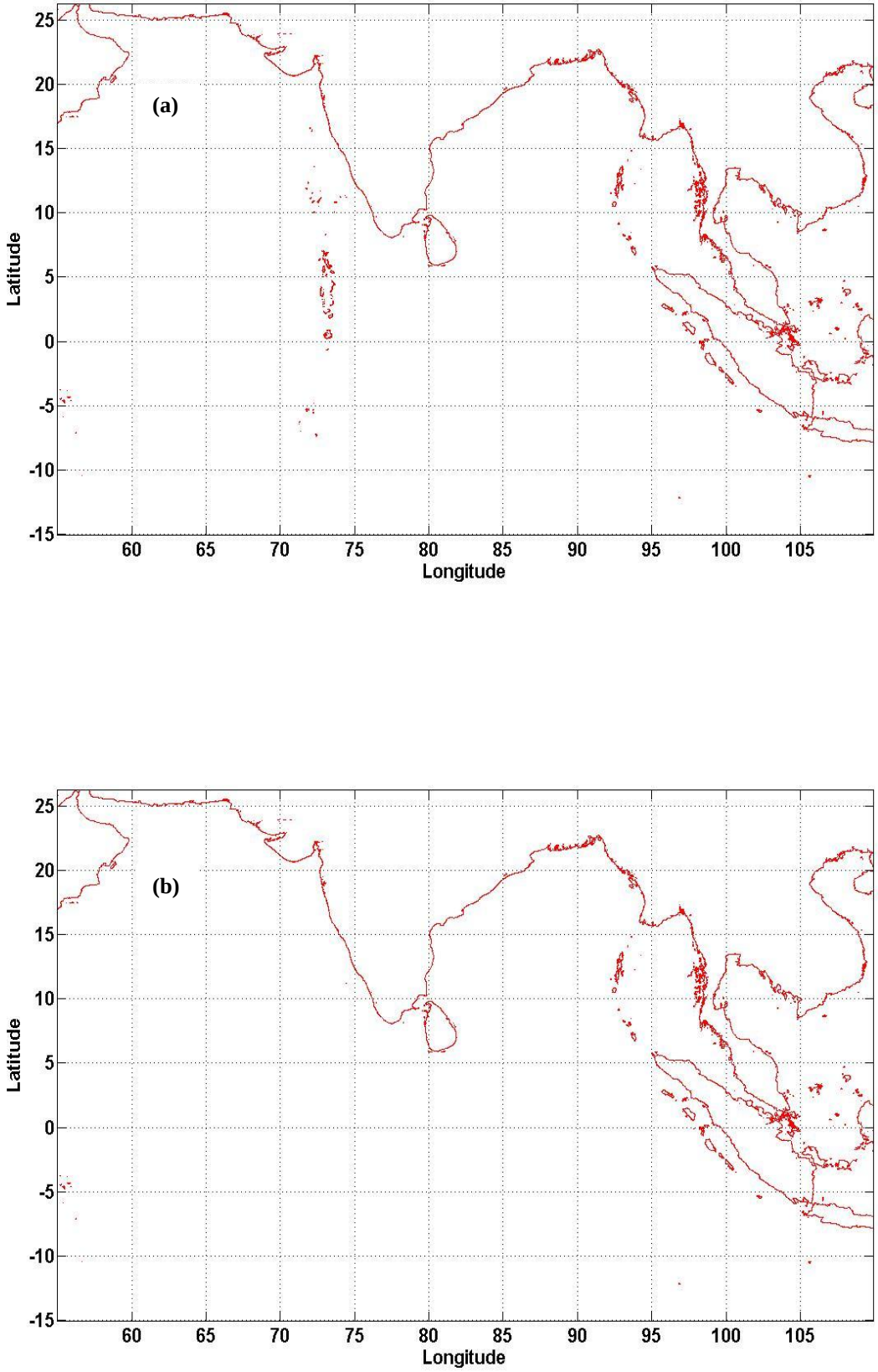

Fig. 5.7 Layout of 'A' grid used in modelling: a) With LMR, b) Without LMR

5.4.1 The Impact of LMR for 2004 Sumatra Tsunami

The tsunami amplitudes were derived for one representative location each at a depth of 1-2 m in the southern and northern sectors (Figures 5.8 and 5.9). Besides run-up at different locations of the southern and northern sectors were also derived for the two cases (Table 5.2). In the southern sector the arrival time of the initial wave is almost same for both LMR and Without LMR (Fig. 5.8). The initial wave arrives 283 minutes after the generation of tsunami, in the southern coast. Further the waves from Sumatra which are propagating towards the west encounters the LMR. The waves directly hit the LMR and get reflected back. The reflected waves undergo interaction with the direct wave coming from Sumatra leading to the constructive interference and resulting in higher amplitude values. The reflected waves in turn undergo refraction and arrive at the southern coast about 60 minutes after the arrival of initial wave. This is the second set of waves that arrived at the coast after the initial diffracted waves. Apart from that a section of waves that pass through the gaps in the LMR propagate westward. This leads to total internal reflection (Murty et al., 2008) due to the propagation of the wave from shallow to deep waters. This component reached some locations of the southern sector about 120 minutes after the first wave. The arrival of tsunami waves beyond this time is mainly due to the reflections from the East coast of Africa and Somalia. In the non-LMR case no reflection occurs from the LMR and the waves proceed towards the East coast of Africa and Somalia. Besides the direct diffracted and refracted waves, there will only be the reflected waves from Somalia and Africa for the non-LMR case.

In the northern sector also the initial waves are the diffracted and refracted waves from Sri Lanka which arrive at around 308 minutes after tsunami generation (Fig. 5.9). The most important thing to be noted is that if the tsunami were propagating through the western side of LMR there would have been a time delay in the case of LMR due to the blockade imposed by the LMR leading to the late arrival of the initial wave at northern Kerala. The values of initial wave in the northern sector is very less while comparing with that of the southern sector and this can be mainly attributed to the reduction in the wave energy due to dispersion and loss due to bottom dissipation processes.

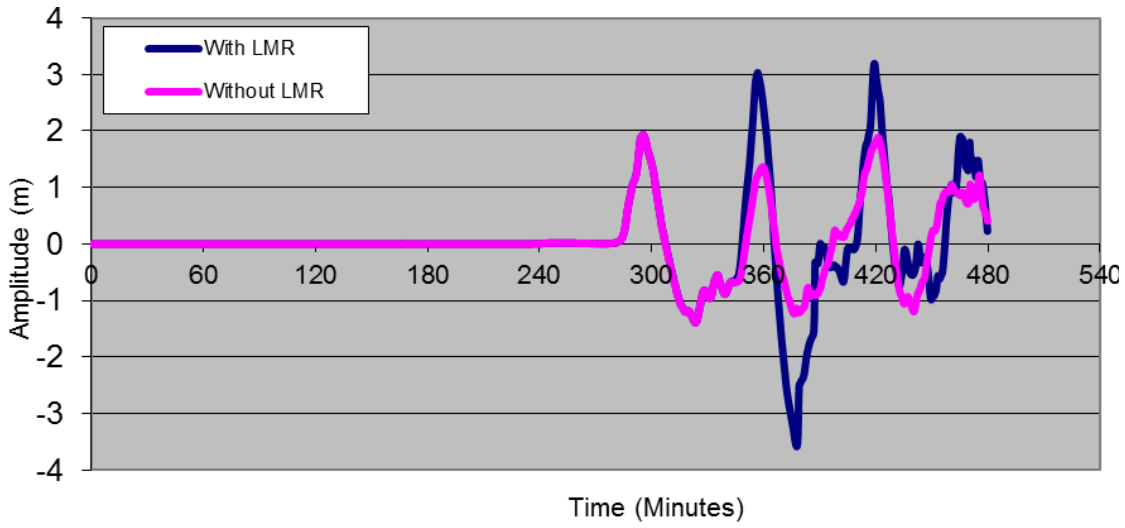

Fig. 5.8 Comparison of amplitudes with and without LMR for the Southern Kerala coast for 2004 Sumatra tsunami for studying the effect of LMR at Perumpally (76.450223 Long., 9.168448 Lat.)

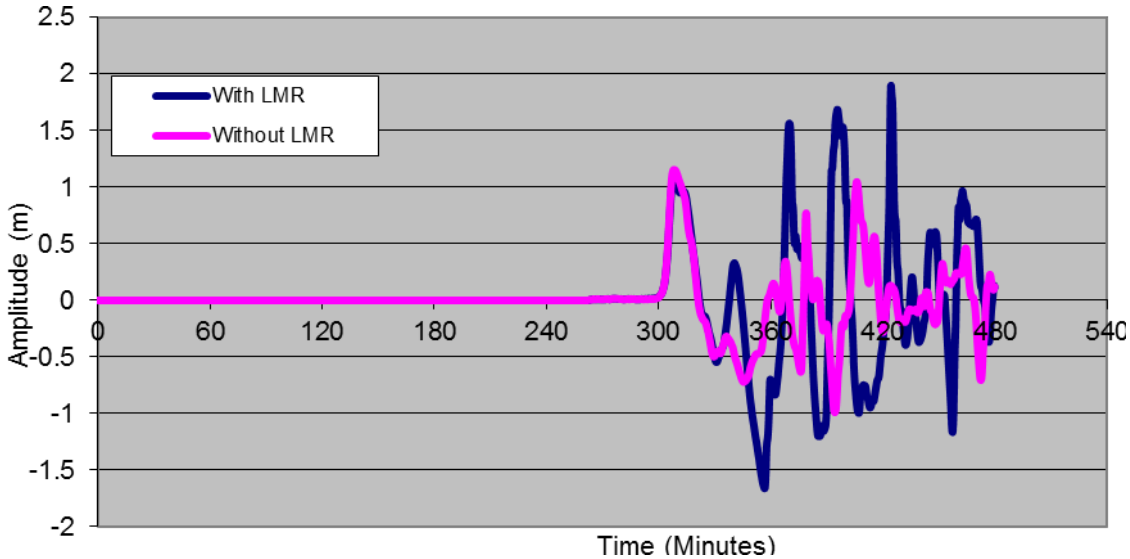

Fig. 5.9 Comparison of amplitudes with and without LMR for the Northern Kerala coast for Sumatra 2004 tsunami for studying the effect of LMR at Shiriya (74.927584 Long., 12.623148 Lat.)

In northern Kerala too we can see pattern of reflection after the arrival of initial wave. At around 370 minutes the reflected waves from the northeastern tip of LMR reaches this coast. The waves arriving beyond this time are also the reflected waves. In the non-LMR case, here also the amplitudes are considerably less implying that the subsequent waves are the diffracted and refracted waves. The difference between the direct wave and reflected wave comes in the range of 1.0-1.5 m (Table 5.3). Here also total internal reflection and reflection from east coast of Africa and Somalia played a significant role.

So both southern Kerala and northern Kerala show higher run-up values for the LMR case and is attributed to the interference of reflected waves from LMR with the direct waves. So to conclude it can be said that there is an increase in tsunami amplitudes due to the presence of LMR. The increase in run-up due to the presence of LMR is considerably high in the case of southern Kerala when compared to Northern Kerala. The average percentage variation in the run-up characteristics with and without LMR Sumatra case is 87.1% for southern Kerala and 91.25% for northern Kerala respectively (Table 5.2 & 5.3).

Table 5.2 Comparison of run-up in the cases with and without LMR for the Southern Kerala for the 2004 Sumatra tsunami

Sl. No.	Co-ordinates		Location	Run-up (m)		Percentage Variation (%)
	Longitude (Dec. Deg)	Latitude (Dec. Deg)		With LMR	Without LMR	
1	76.535719	8.942928	Neendakara North	2.5-3.0	1.5-2.0	57
2	76.523109	8.995798	Chavara	2.5-3.0	2.0-2.5	22
3	76.519408	9.017033	Pandarathuruthu	3.0-3.5	1.5-2.0	85
4	76.517031	9.021382	Pannickarkadavu	3.0-3.5	1.5-2.0	85
5	76.484287	9.092066	Alappad	4.0-4.5	2.0-2.5	88
6	76.472078	9.121339	Azhekkal	4.5-5.0	2.0-2.5	111
7	76.461804	9.141252	Valiyazhekkal	4.5-5.0	1.5-2.0	171
8	76.447579	9.171030	Arattuppuzha	4.0-4.5	1.5-2.0	142
9	76.409015	9.255039	Trikkunnapuzha	4.0-4.5	2.0-2.5	88
10	76.383861	9.310030	Thotappally	2.5-3.0	2.0-2.5	22

Table 5.3 Comparison of run-up in the cases with and without LMR for the Northern Kerala for the 2004 Sumatra tsunami

Sl. No.	Co-ordinates		Location	Run-up (m)		Percentage Variation (%)
	Longitude (Dec. Deg)	Latitude (Dec. Deg)		With LMR	Without LMR	
1	74.948067	12.567307	Mogral	1.5-2.0	0.5-1.0	133
2	74.938827	12.590811	Kumbla North	1.0-1.5	0.5-1.0	66
3	74.928751	12.612744	Ankadi	1.5-2.0	0.5-1.0	133
4	74.923380	12.625870	Kukkaru	1.0-1.5	0.5-1.0	66
5	74.902407	12.676011	Uppala North	1.5-2.0	0.5-1.0	133
6	74.890106	12.703345	Hosangadi	1.0-1.5	0.5-1.0	66
7	74.882435	12.715257	Manjeswaram	0.5-1.0	0.5-1.0	0
8	74.869511	12.746436	Talappadi South	1.5-2.0	0.5-1.0	133

5.4.2 Impact of LMR for Makran Tsunami

For understanding the role of LMR for a tsunami propagating from the west simulations were carried out for the cases both with and without LMR for the Makran 1945 source. Figures 5.10 and 5.11 show the comparison of tsunami amplitudes at nearshore locations of the southern and northern sectors of the Kerala coast for the two cases.

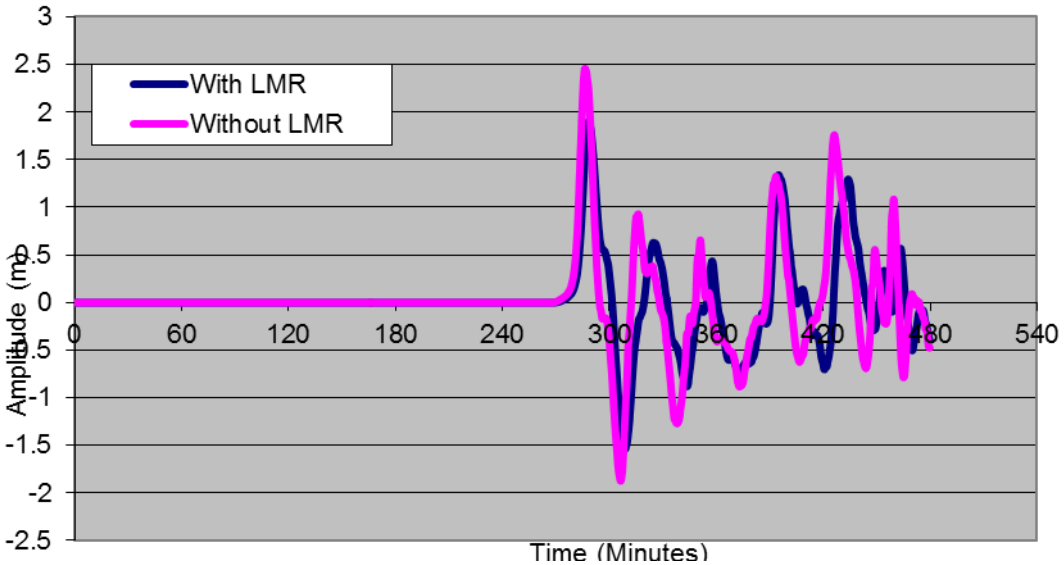

Fig. 5.10 Comparison of amplitudes with and without LMR for the Southern Kerala coast for Makran 1945 tsunami at Perumpally (76.450223 Long., 9.168448 Lat.)

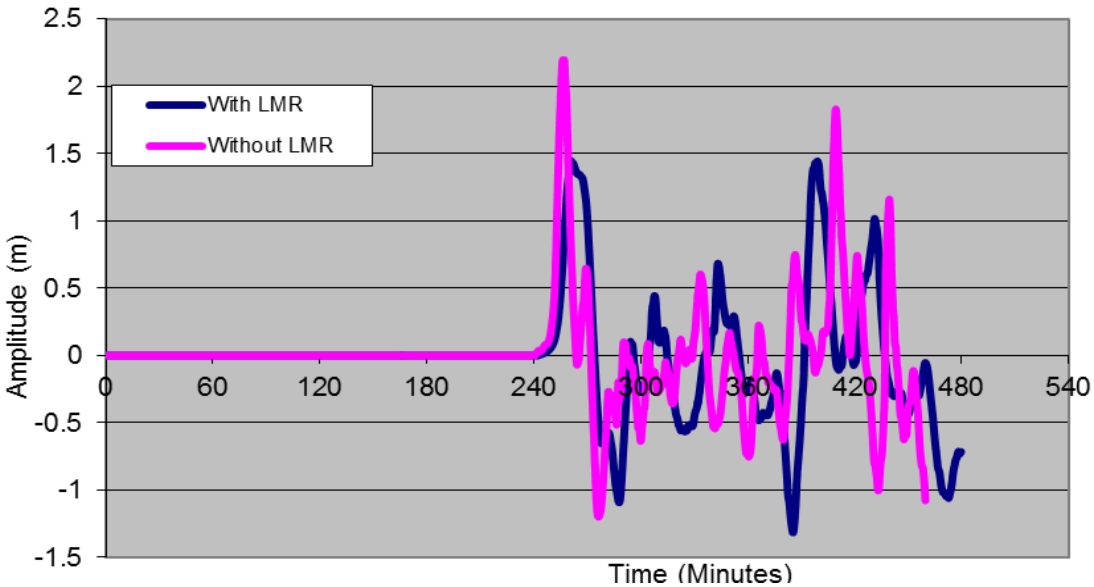

Fig. 5.11 Comparison of amplitudes with and without LMR for the Northern Kerala coast for Makran 1945 tsunami at Shiriya (74.927584 Long., 12.623148 Lat.)

The results show that, unlike Sumatra, the without LMR case really dominates in terms of increased run-up values along southern and northern Kerala coasts. It points to the fact that there is no reflection by LMR for a tsunami propagating from the west unlike the Sumatra**.** This has contributed to the loss of energy flux leading to lesser values for the with LMR scenario as indicated in Tables 5.4 & 5.5.

Table 5.4 Comparison of run-up in the cases with and without LMR for the Southern Kerala for the Makran 1945 tsunami

Sl. No.	Co-ordinates		Location	Run-up (m)		Percentage Variation (%)
	Longitude (Dec. Deg)	Latitude (Dec. Deg)		With LMR	Without LMR	
1	76.537261	8.938565	Neendakra	1.5-2.0	2.0-2.5	29
2	76.525720	8.983369	Kovilthottam	1.0-1.5	1.5-2.0	40
3	76.464467	9.133057	Cheriyazhekkal	0.5-1.0	1.0-1.5	66
4	76.461804	9.141252	Valiyazhekkal	0.5-1.0	1.0-1.5	66

Table 5.5 Comparison of run-up in the cases with and without LMR for the Northern Kerala for the Makran 1945 tsunami

Sl. No.	Co-ordinates		Location	Run-up (m)		Percentage Variation (%)
	Longitude (Dec. Deg)	Latitude (Dec. Deg)		With LMR	Without LMR	
1	74.941190	12.585185	Kumbla	1.5-2.0	2.0-2.5	29
2	74.904990	12.668329	Uppala	1.5-2.0	2.0-2.5	29
3	74.882435	12.715257	Manjeswaram	1.5-2.0	2.0-2.5	29
4	74.868263	12.751863	Talappadi	1.5-2.0	2.0-2.5	29

The absence of reflection can be mainly attributed to the orientation of the fault of Makran and the directivity of the tsunami. Due to the east-west orientation of the fault, the tsunami is propagated in the north-south direction and no effective reflection takes place in the LMR which is also oriented in the north-south direction. To conclude for a tsunami from Sumatra, LMR induces significantly higher run-up and inundation along the Kerala coast while the LMR impedes the run-up and inundation to a certain extent for a tsunami propagating from a source like Makran. The average percentage variation in the run-up characteristics with and without LMR Makran case is 50.25% for southern Kerala and 29% for northern Kerala respectively (Table 5.4 & 5.5).

5.5 SUMMARY

This chapter discusses about the propagation characteristics of tsunami in the South East Arabian Arabian Sea. Numerical Modelling was carried out for understanding the effect of LMR and the role played by it in contributing towards the vulnerability of Kerala coast leading to site specific run-up. From the result it was obvious that LMR has a significant role to play in initiating reflection of tsunami waves for a tsunami propagating from the east like the Sumatra 2004. The modeling studies revealed that the reflected waves from LMR were the highest that arrived in the southern and northern Kerala coast other than the initial diffracted waves from Srilanka, reflection from east coast of Africa and Somalia and the normal refracted waves due to varying bathymetric features. Simulations were also carried out excluding LMR and that too unraveled the importance of LMR. But LMR does not have a prominent role for a tsunami propagating from the west like the Makran and hence there is no scope for reflection. The effect would emerge much more higher for the Kerala coast if no LMR persist. The model has successfully reproduced the resonance pattern that happened in the Mangalore port and Cochin Port during December 26, 2004 Sumatra tsunami.

CHAPTER 6

NUMERICAL SIMULATION OF RUN-UP AND INUNDATION ALONG THE KERALA AND LAKSHADWEEP COASTS

6.0 INTRODUCTION

An essential requirement of a tsunami warning system is the availability of tsunami inundation maps for different scenarios of tsunami generation which can only be accomplished through the process of numerical modelling. Review of literatures show that the west coast of India is vulnerable to tsunami from tsunamigenic sources located in the Indian Ocean *(See. Pages 18-42)*. So to assess the tsunami vulnerability of Kerala and Lakshadweep coasts simulations were carried out for three different sources viz. Sumatra 2004, Makran 1945 and a hypothetical potentially worst case source from Makran. The results of tsunami vulnerability analysis in terms of run-up and inundation for the entire Kerala coast and four selected Islands of Lakshadweep viz. Androth, Chetlat, Kadmat and Kavaratti are presented in this chapter.

6.1 RUN-UP AND INUNDATION ALONG THE KERALA COAST

The run-up and inundation characteristics as obtained from the simulations for the different sectors of Kerala coast are given district wise from south to north below.

6.1.1 Thiruvananthapuram District

The coastal area pertaining to the Thiruvananthapuram district is spread over three sectors viz. 1) Pozhiyur-Thiruvallam, 2) Thiruvallam-Kazhakuttom and 3) Kazhakuttom-Varkala (Fig. 6.1). The results of numerical modelling for the above sectors are presented in Table 6.1 with a typical simulation output for a sector in Fig. 6.2. The run-up and inundation characteristics along the sectors are described below.

6.1.1.1 Pozhiyur - Thiruvallom

The simulation results for Sumatra 2004 projected a maximum run-up in the range 2.0-2.5 m at Pachalloor and Adimalathura. The regions south of this location showed a run-up in

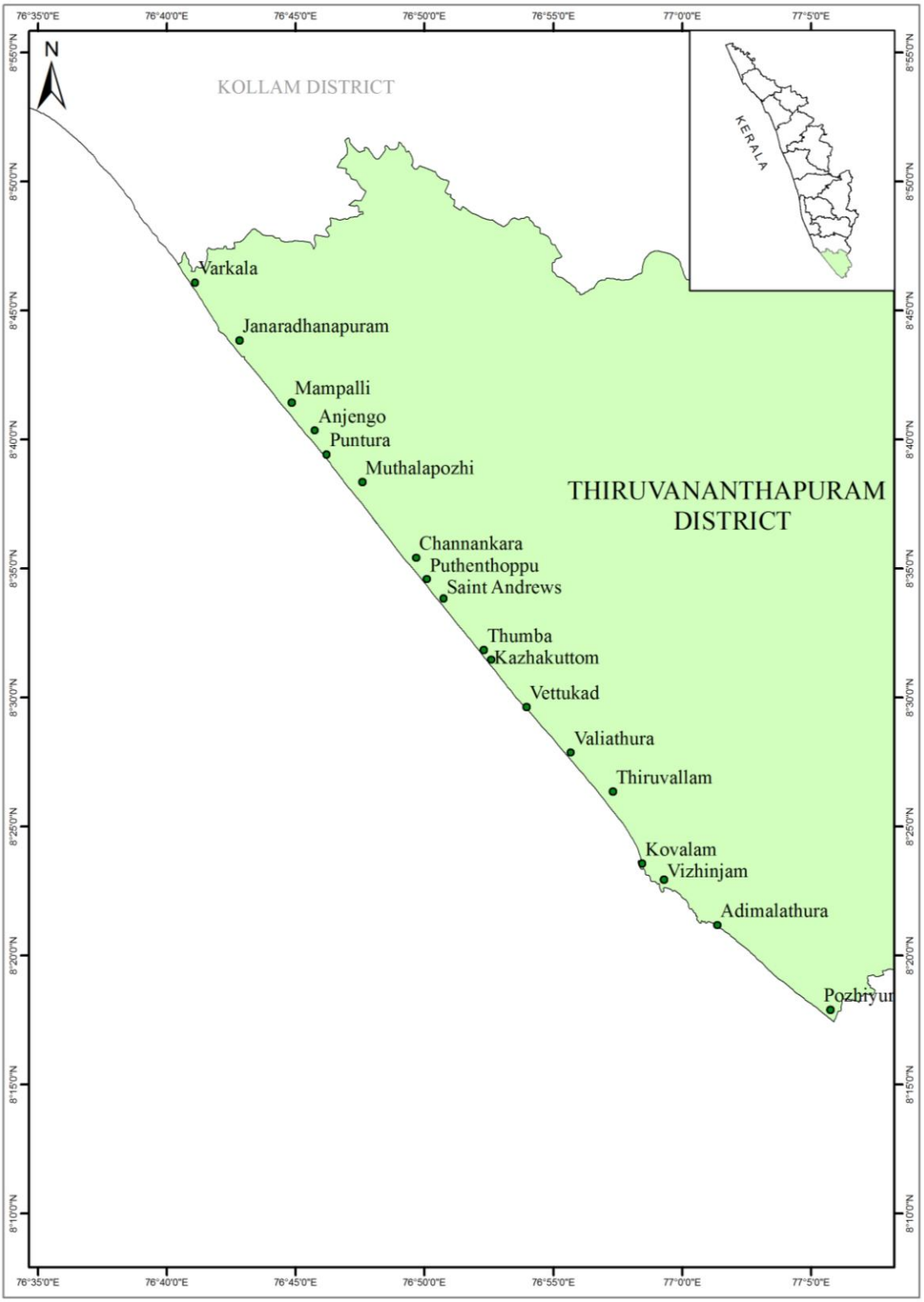

Fig. 6.1 Location map of Thiruvananthapuram district

the range1.5-2.0 m at Pozhiyur and Chowara. The regions north of this sector namely Vizhinjam and Kovalam showed run-up values in the range of 1.0-2.0 m. The simulation

predicted a maximum inundation of only 326 m which includes backwaters also. The Makran 1945 showed a lesser run-up while comparing with that of Sumatra 2004. Run-up in the range of 0.5-1.0 m was observed at Pozhiyur, Adimalathura, Chowara, Vizhinjam, Kovalam and Pachalloor. Here also the inundation was negligible. The simulation for the hypothetical potentially worst case showed a higher run-up value while comparing with that of Makran and lesser value on comparing with that of Sumatra 2004. A maximum run-up of around 1.3 m was predicted in this case at Pozhiyur while the run-up values at Adimalathura, Chowara and Kovalam were 1.17 m, 1.11 m and 1.25 m respectively.

6.1.1.2 Thiruvallom - Kazhakuttom

The simulation results for Sumatra 2004 showed a maximum run-up in the range of 3.0-3.5 m at the south of Puthenthoppu. The southern locations in this stretch showed a run-up value of 2.79 m and 2.48 m at Thiruvallam and Valiathura respectively. Shangumukham, one of the hot spots of tourism, showed a run-up value of 2.66 m. The other locations like Thumba and St. Andrews in the north showed a run-up value of 1.41 m and 2.18 m respectively. A maximum inundation of 416 m was observed at the north of Thiruvallam. The other locations like the south of Kochuveli and the north of Shangumukham showed lesser inundation of 327 m and 289 m repectively. All other locations showed practically very little of inundation. The simulation for the Makran 1945 case showed very small run-up in the range of 0.5-1.0 m without any inundation. The simulation for the potentially worst case from Makran showed a run-up value of 1.5 m at Vettukad and south of Kochuveli. The other places showed run-up values in the range of 1.0-1.5 m with negligible inundation

6.1.1.3 Kazhakuttom - Varkala

The simulation output for this sector is given in Figure 6.2. The Sumatra 2004 predicted a maximum run-up in the range of 3.0-3.5 m at Anjengo towards north of this sector. The other regions Mampalli and Janardhanapuram showed run-up values in the range of 2.5-3.0 m respectively. The regions in the south like Vadakevila and Muthalapozhi also showed 2.5-3.0 m run-up range. However, a maximum inundation of 611 m was noticed at Anjengo. The other noticeable inundations were 559 m at the south of Mundanchira, 308 m at Vadakevila and 280 m at Mampalli. The effect of the inlet and the waterbody resulted in inundation of 587 m at Muthalapozhi. The simulation for Makran 1945

showed a maximum run-up value of 1.25 m at Mampalli. Muthalapozhi and Janardhanapuram showed run-up in the range of 0.5-1.0 m. The simulation results showed no significant inundation. The simulation for the hypothetical worst case showed maximum run-up of 1.21 m at Mampalli and Anjengo and lesser values of 0.96 m and 0.84 m at Muthalapozhi and Puthenthura respectively. Here also no inundation was noticed.

Table 6.1 Run-up and inundation along the coastal stretch of Thiruvananthapuram district for three different cases of tsunami generation

Location	**Sumatra 2004**		**Makran 1945**		**Hypothetical**	
	Run-up (m)	**Inundation (m)**	**Run-up (m)**	**Inundation (m)**	**Run-up (m)**	**Inundation (m)**
Pozhiyur	1.5-2.0	Nil	0.5-1.0	Nil	1.0-1.5	Nil
Adimalathura	2.0-2.5	Nil	0.5-1.0	Nil	1.0-1.5	Nil
Chowara	1.5-2.0	Nil	0.5-1.0	Nil	1.0-1.5	Nil
Vizhinjam North	1.0-1.5	Nil	0.5-1.0	Nil	1.0-1.5	Nil
Kovalam	1.5-2.0	Nil	0.5-1.0	Nil	1.0-1.5	Nil
Pachalloor	2.0-2.5	326	0.5-1.0	216	1.0-1.5	243
Thiruvallam North	2.5-3.0	416	0.5-1.0	Nil	1.0-1.5	27
Beemappalli	2.5-3.0	301	0.5-1.0	Nil	1.0-1.5	30
Valiathura	2.0-2.5	73	0.5-1.0	Nil	1.0-1.5	Nil
Sangumukham North	2.5-3.0	289	0.5-1.0	Nil	1.0-1.5	Nil
Vettukad	2.5-3.0	35	0.5-1.0	Nil	1.5-2.0	Nil
Kochuveli south	2.5-3.0	327	0.5-1.0	Nil	1.5-2.0	Nil
Thumba	1.0-1.5	Nil	0.5-1.0	Nil	1.0-1.5	Nil
Saint Andrews	2.0-2.5	35	0.5-1.0	Nil	1.0-1.5	Nil
Puthenthoppu South	3.0-3.5	291	0.5-1.0	Nil	1.0-1.5	Nil
Channankara	2.5-3.0	Nil	0.5-1.0	Nil	1.0-1.5	Nil
Puthenthura	1.5-2.0	Nil	0.5-1.0	Nil	0.5-1.0	Nil
Mundanchira South	3.0-3.5	559	1.0-1.5	Nil	1.0-1.5	Nil
Vadakkevila	3.0-3.5	308	0.5-1.0	Nil	0.5-1.0	Nil
Muthalapozhi	2.5-3.0	587	0.5-1.0	Nil	0.5-1.0	Nil
Punthura	3.0-3.5	415	0.5-1.0	Nil	1.0-1.5	Nil
Anjengo	3.0-3.5	611	1.0-1.5	Nil	1.0-1.5	Nil
Mampalli	2.5-3.0	280	1.0-1.5	Nil	1.0-1.5	Nil
Janardhanapuram	2.5-3.0	Nil	0.5-1.0	Nil	0.5-1.0	Nil

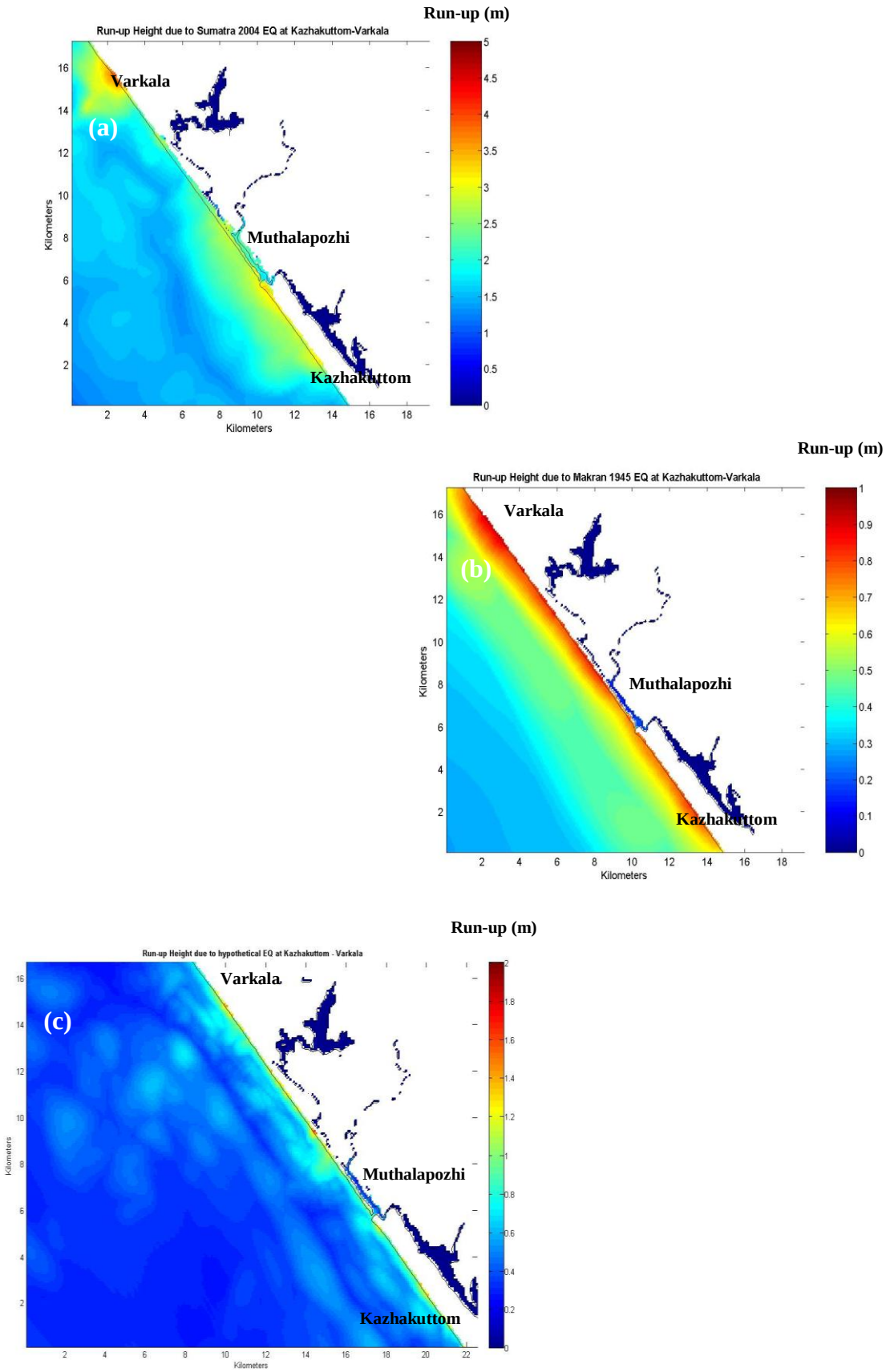

Fig. 6.2 Model simulation output for the Kazhakuttom-Varkala coast of Thiruvananthapuram district: (a) Sumatra 2004, (b) Makran 1945 & (c) Hypothetical worst case

6.1.2 Kollam District

The coastal area of Kollam district comprises of two sectors 1) Varkala-Neendakara, 2) Neendakara-Thotappally (Fig. 6.3). The Neendakara-Thottapally region contains a portion of Alappuzha district starting from the Valiyazheekal, the north of Kayamkulam Inlet. The Neendakara-Thotappally area is the area taken for the calibration which has already been discussed in Chapter 4. The results of numerical modelling are presented in Table 6.2 and the salient run-up and inundation characteristics are discussed below.

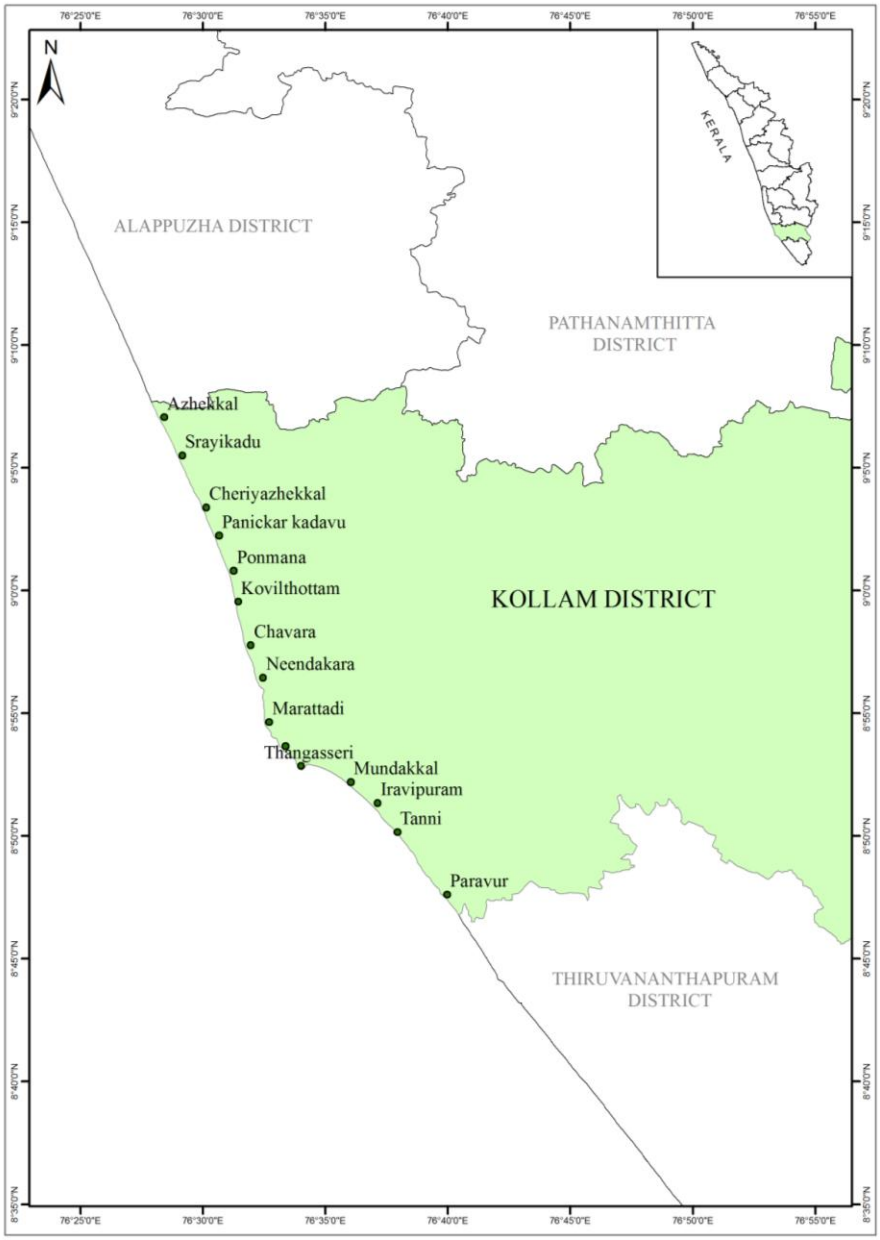

Fig. 6.3 Location map of Kollam district

6.1.2.1 Varkala - Neendakara

The simulation results for Sumatra 2004 showed a maximum run-up of 2.94 m at Varkala Papanasam beach and Kappil. The other areas like Paravur Thekkumbhagam, Tanni, Iravipuram and Thirumullavaram showed a run-up of 2.46 m, 2.09 m, 1.9 m and 2.62 m respectively. The simulation showed only negligible inundation in this sector (Fig. 6.4). This can mainly be attributed the presence of cliffs prevailing in this sector. The modelling results for the Makran 1945 show a maximum value of 1.03 m at Thirumullavaram with values further decreasing towards the south in the range of 0.5-1.0 m at Thangasseri, Iravipuram, Paravur Thekkkumbhagom and Varkala Papanasam beach. The simulation for the hypothetical worst case from Makran showed a maximum run-up of 1.89 m at Thirumullavaram whereas the other places in the sector like Thangasseri, Iravipuram and Papanasam beach shows 1.63 m, 1.76 m and 1.36 m respectively. An inundation of 107 m was noticed at Kappil and 90 m at Iravipuram.

6.1.2.2 Neendakara - Thottapally

This was the sector which was taken for the model calibration discussed in Chapter 3. This was the sector where the maximum inundation and casualties took place due to the 2004 tsunami. The simulation results for the 2004 Sumatra tsunami showed a maximum run-up of around 5 m in Valiyazhekkal, the north of the Kayamkulam inlet with values decreasing towards both south and north of inlet. A maximum inundation of around 3 km was predicted at Valiyazhekkal with the contribution from the T-S canal, a water body adjoining the coast in the north south direction. The run-up values of Makran 1945 were very much less while comparing with that of Sumatra 2004 with maximum values occurring in the range of 1.5-2.0 m. No significant inundation was projected by the model for this source. The hypothetical potentially worst case showed a marginal increase in run-up and inundation when compared to the Makran 1945 case along the entire stretch, but the values were much less than the Sumatra 2004 case.

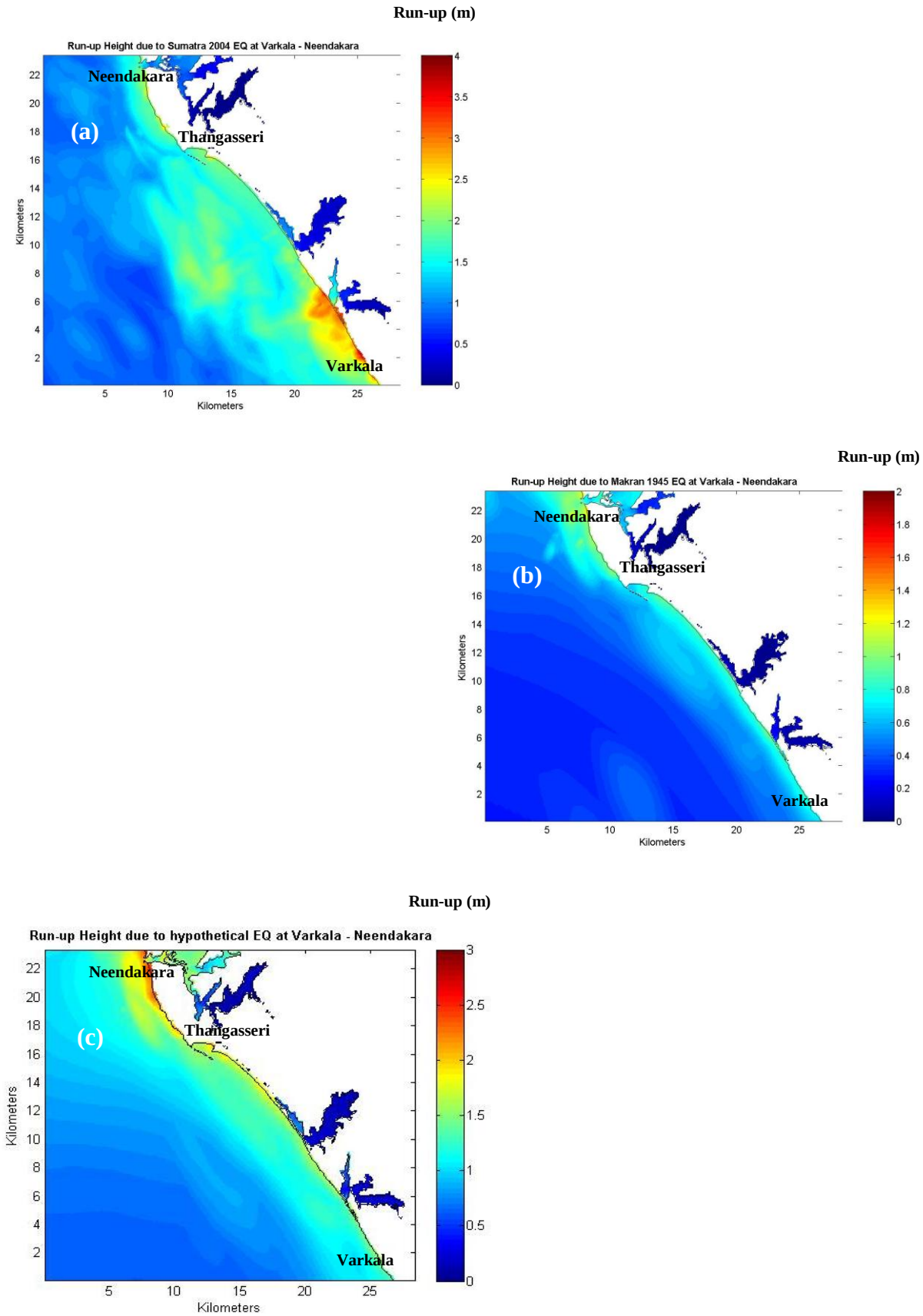

Fig. 6.4 Model simulation output for the Varkala-Neendakara coast of Kollam district: (a) Sumatra 2004, (b) Makran 1945 & (c) Hypothetical worst case

Table 6.2 Run-up and inundation along the coastal stretch of Kollam district for three different cases of tsunami generation

Location	Sumatra 2004		Makran 1945		Hypothetical	
	Run-up (m)	Inundation (m)	Run-up (m)	Inundation (m)	Run-up (m)	Inundation (m)
Papanasam Beach	2.5-3.0	Nil	0.5-1.0	Nil	1.0-1.5	Nil
Kappil	2.5-3.0	107	0.5-1.0	107	1.0-1.5	107
Paravur Tekkumbhagam	2.0-2.5	Nil	0.5-1.0	Nil	1.5-2.0	Nil
Tanni	2.0-2.5	169	0.5-1.0	Nil	1.5-2.0	Nil
Iravipuram	1.5-2.0	90	0.5-1.0	Nil	1.5-2.0	90
Thangasseri	1.5-2.0	Nil	0.5-1.0	Nil	1.5-2.0	Nil
Thirumullavaram	2.5-3.0	259	1.0-1.5	Nil	1.5-2.0	Nil
Neendakara	2.0-2.5	150	1.5-2.0	Nil	2.0-2.5	492
Kovilthottam	2.0-2.5	315	1.0-1.5	Nil	1.5-2.0	209
Panmana	4.0-4.5	757	1.0-1.5	190	1.5-2.0	664
Srayikadu	4.0-4.5	569	0.5-1.0	35	1.5-2.0	318
Alappad	4.0-4.5	558	0.5-1.0	60	1.5-2.0	415
Cheriyazhekkal	4.5-5.0	2500	0.5-1.0	Nil	1.5-2.0	537
Valiyazhekkal	4.5-5.0	3087	0.5-1.0	Nil	1.5-2.0	590

6.1.3 Alappuzha District

The simulation covered two sectors of the Alappuzha district viz. 1) Thottapally-Alappuzha and 2) Alappuzha-Vayalar as shown in Figure 6.5 and the results are summarized in the Table 6.3.

6.1.3.1 Thottapally - Alappuzha

The simulation for the 2004 Sumatra showed Vadakkal as a place of high run-up. The simulated run-up value at this place was in the range of 3.0-3.5 m. This point also showed an inundation of 211 m. The other places in this sector like Thottapaly, Purakkad and Ambalappuzha showed values of 2.81 m, 2.75 m and 2.71 m. These places showed negligible inundation in the range 60-80 m.

The simulation results for Makran 1945 showed low values with Vadakkal having the highest run-up in the range of 1.5-2.0 m. The other sectors like Ambalappuzha, Purakkad

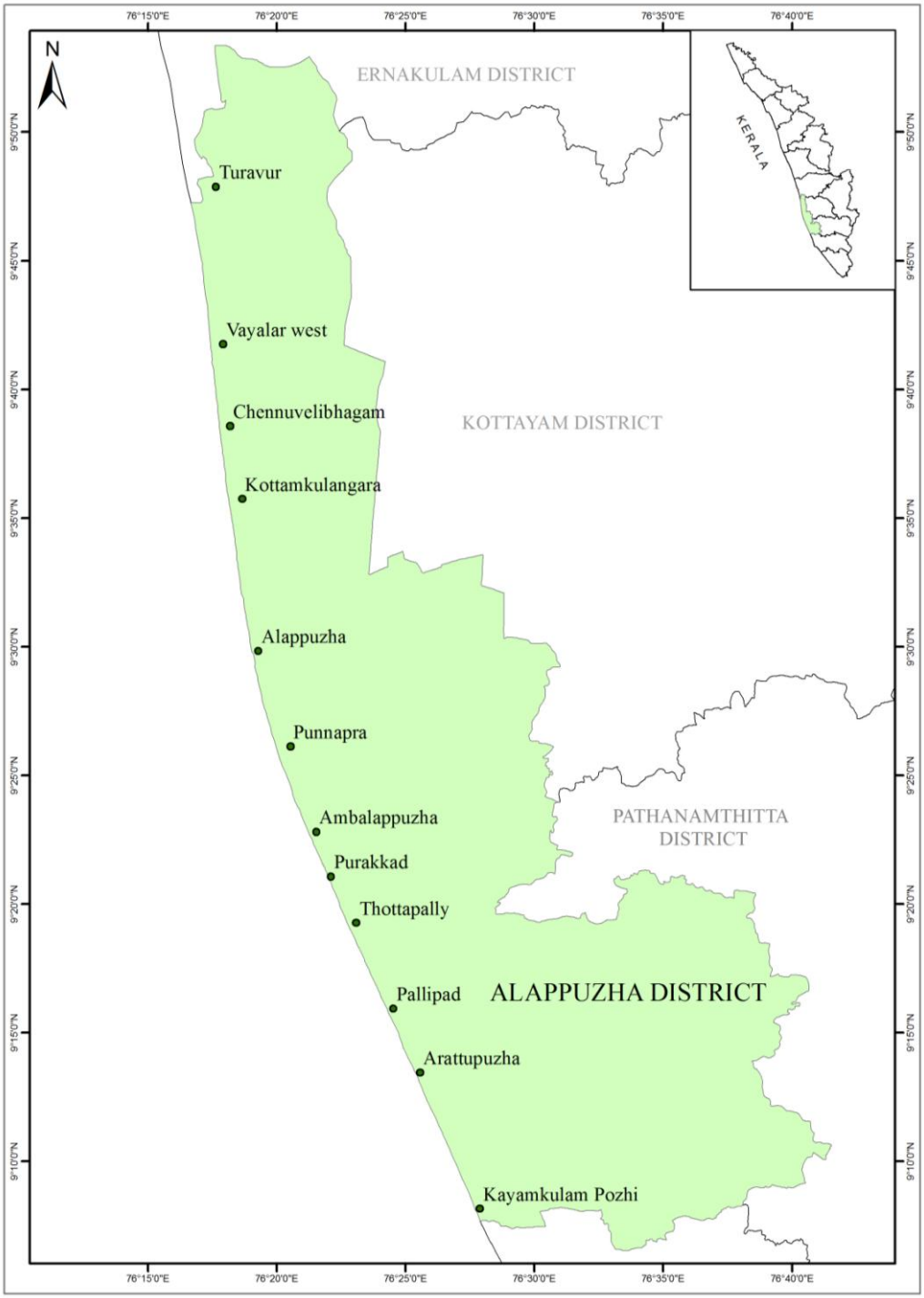

Fig. 6.5 Location map of Alappuzha district

and Thottapally showed run-up values of 1.60 m, 1.52 m and 1.41 m respectively. No significant inundation was predicted in this case.

The simulation for the hypothetically potentially worst case showed significant increase in the run-up while comparing with that of the simulation for Makran 1945. A run-up in

the range of 2.0-2.5 m was predicted at Thottapally which is the maximum in this sector. The places like Purakkad and Ambalappuzha where inundations of 43 m and 48 m were simulated, showed run-up values of 2.3 m and 2.27 m respectively.

6.1.3.2 Alappuzha -Vayalar

The simulation for Sumatra 2004 identified the south of Alisseri as the region of high run-up which was in the range of 3.5-4.0 m. Figure 6.6 shows the results of simulation for this sector. At locations like Alappuzha, Tondankulangara and Tumboli beach the run-up was in the range of 3.0-3.5m. A run-up of 2.0-2.5 m was obtained at Chennuvelibhagam and Vayalar. The model predicted high inundation along this sector for the Sumatra source. Tondankulangara, Chennuvelibhagam and Vayalar showed high inundation of 2500 m, 2000 m and 1140 m respectively. The simulation for Makran 1945 predicted a lesser run-up while comparing with that of Sumatra. The run-up was in the range of 1.5-2.0 m through the coast except at Vayalar where the run-up was in the range of 2.0-2.5 m and at Alisseri south where the run-up was in the range of 1.0-1.5 m. Inundation was almost insignificant except at Vayalar where a 600 m inundation was predicted by the model. The hypothetical case predicted an inundation of 1450 m and 1270 m at Chennuvelibhagam and Vayalar respectively. The run-up was almost uniform in the range of 2.0-2.5 m except at Kutirapanti where it showed a run-up in the range of 1.5-2.0. The maximum run-up in the range of 2.5-3.0 was predicted at Vayalar for the hypothetical source.

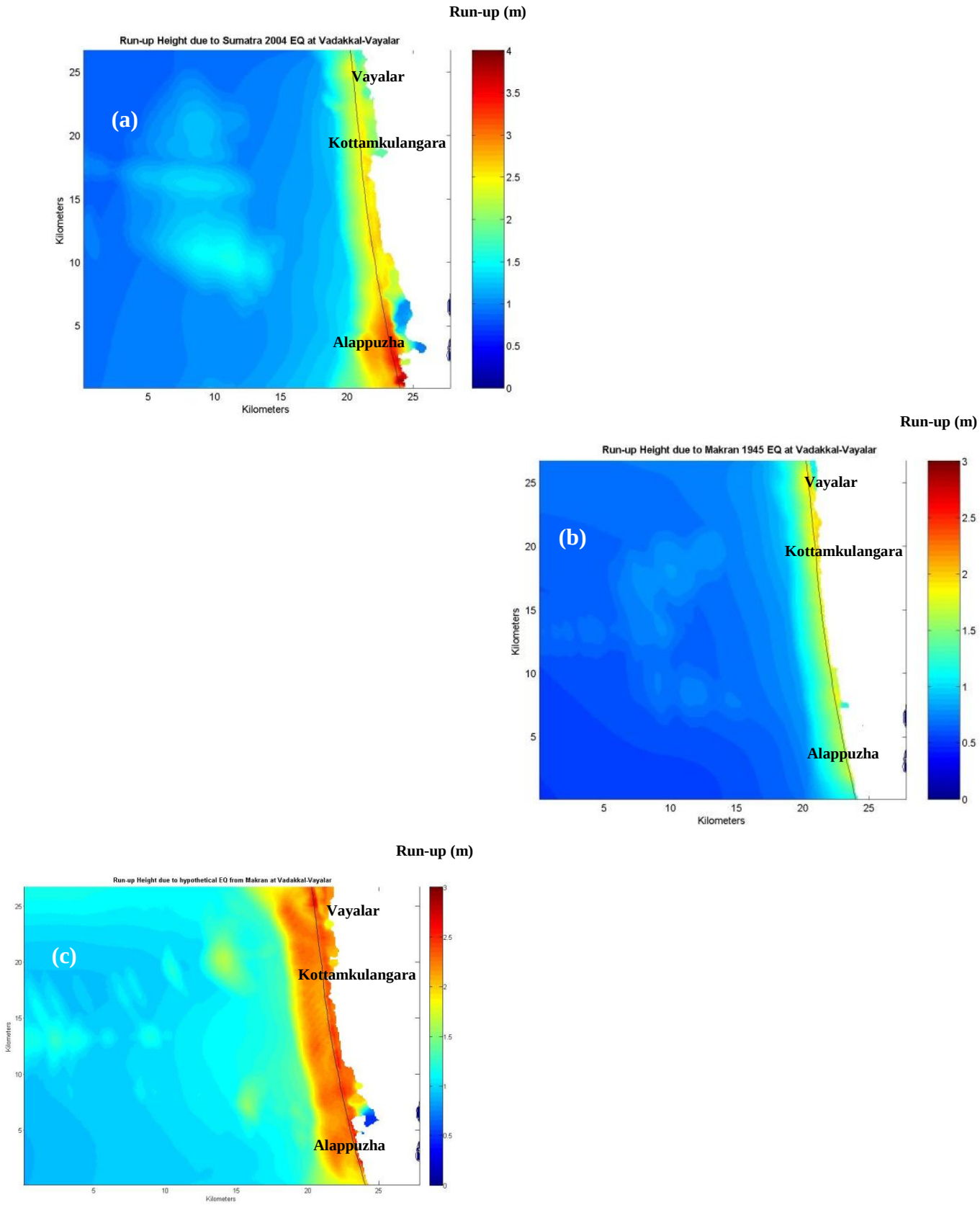

Fig. 6.6 Model simulation output for the Alappuzha-Vayalar coast of Alappuzha district: (a) Sumatra 2004, (b) Makran 1945 & (c) Hypothetical worst case

Table 6.3 Run-up and inundation along the coastal stretch of Alappuzha district for three different cases of tsunami generation

Location	Sumatra 2004		Makran 1945		Hypothetical	
	Run-up (m)	**Inundation (m)**	**Run-up (m)**	**Inundation (m)**	**Run-up (m)**	**Inundation (m)**
Thottapally	2.5-3.0	68	1.0-1.5	Nil	2.0-2.5	Nil
Purakkad	2.5-3.0	77	1.5-2.0	Nil	2.0-2.5	43
Ambalappuzha	2.5-3.0	76	1.5-2.0	Nil	2.0-2.5	48
Vadakkal	3.0-3.5	211	1.5-2.0	Nil	2.0-2.5	Nil
Kutirapanti	2.5-3.0	Nil	1.0-1.5	Nil	1.5-2.0	Nil
Alisseri South	3.5-4.0	670	1.0-1.5	Nil	2.0-2.5	90
Alappuzha	3.0-3.5	591	1.5-2.0	Nil	2.0-2.5	100
Tondankulangara	3.0-3.5	2500	1.5-2.0	60	2.0-2.5	180
Tumboli	3.0-3.5	1200	1.5-2.0	Nil	2.0-2.5	178
Kottamkulangara	2.5-3.0	917	1.5-2.0	197	2.0-2.5	546
Chennuvelibhagam	2.0-2.5	2000	1.5-2.0	84	2.0-2.5	1450
Vayalar	2.0-2.5	1140	2.0-2.5	600	2.5-3.0	1270

6.1.4 Ernakulam District

The coastal zone of Ernakulam district falls in two sectors: 1) Vayalar-Manasseri and 2) Manasseri-Munambam (Fig. 6.7). The results of numerical modelling for the above sectors are presented in Table 6.4.

6.1.4.1 Vayalar - Manasseri

In the Vayalar-Manasseri sector, the simulation for Sumatra 2004 showed run-up in the range of 2.5-3.0 m at Anthakarnazhi. The other locations like Chellanam and Maravukkad showed run in the range of 2.0-2.5 m. The effect of inlet and the backwaters has resulted in a 2 km inundation at Anthakarnazhi. The other places showed negligible inundation Fig. (6.8).

The simulation for Makran 1945 predicted relatively lower values. Manasseri showed a higher run-up with a value of 2.12 m. The model also showed a run-up of 1.68 m at Anthakarnazhi with an inundation of 1.15 km which can be attributed to the effect of the inlet and backwater.

The hypothetical case showed an increase in run-up value while comparing with not only Makran 1945 but also Sumatra 2004. Anthakarnazhi showed run-up of 2.44 m that is

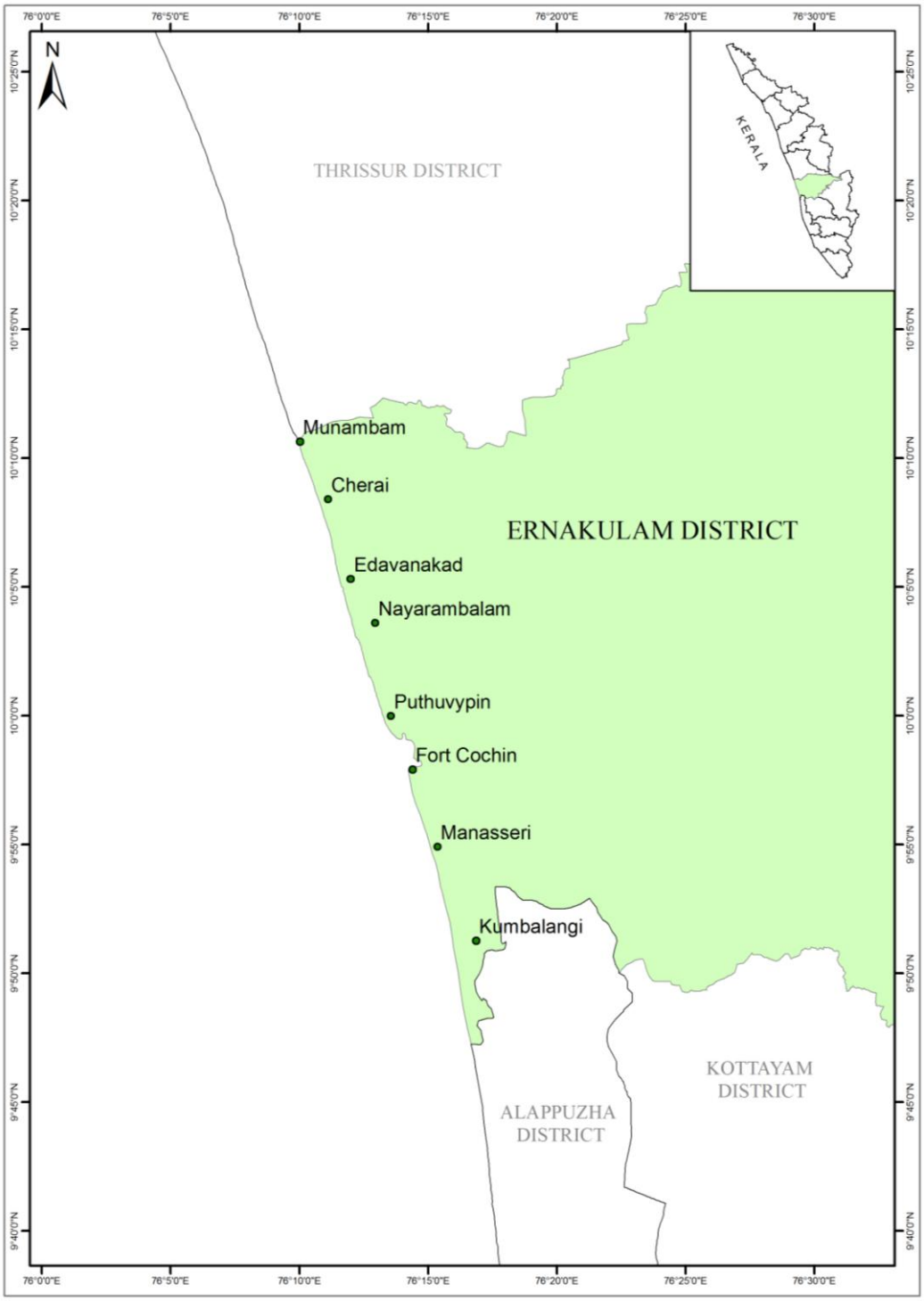

Fig. 6.7 Location map of Ernakulam district

much higher than the Makran 1945 resulting in an inundation of 2.4 km. The other places like Chellanam, Maravukad and Kannamali showed run-up values in the range of 2.0-3.0 m. The increased inundation in this sector for all the three sources is mainly due to the presence of inlet and backwaters.

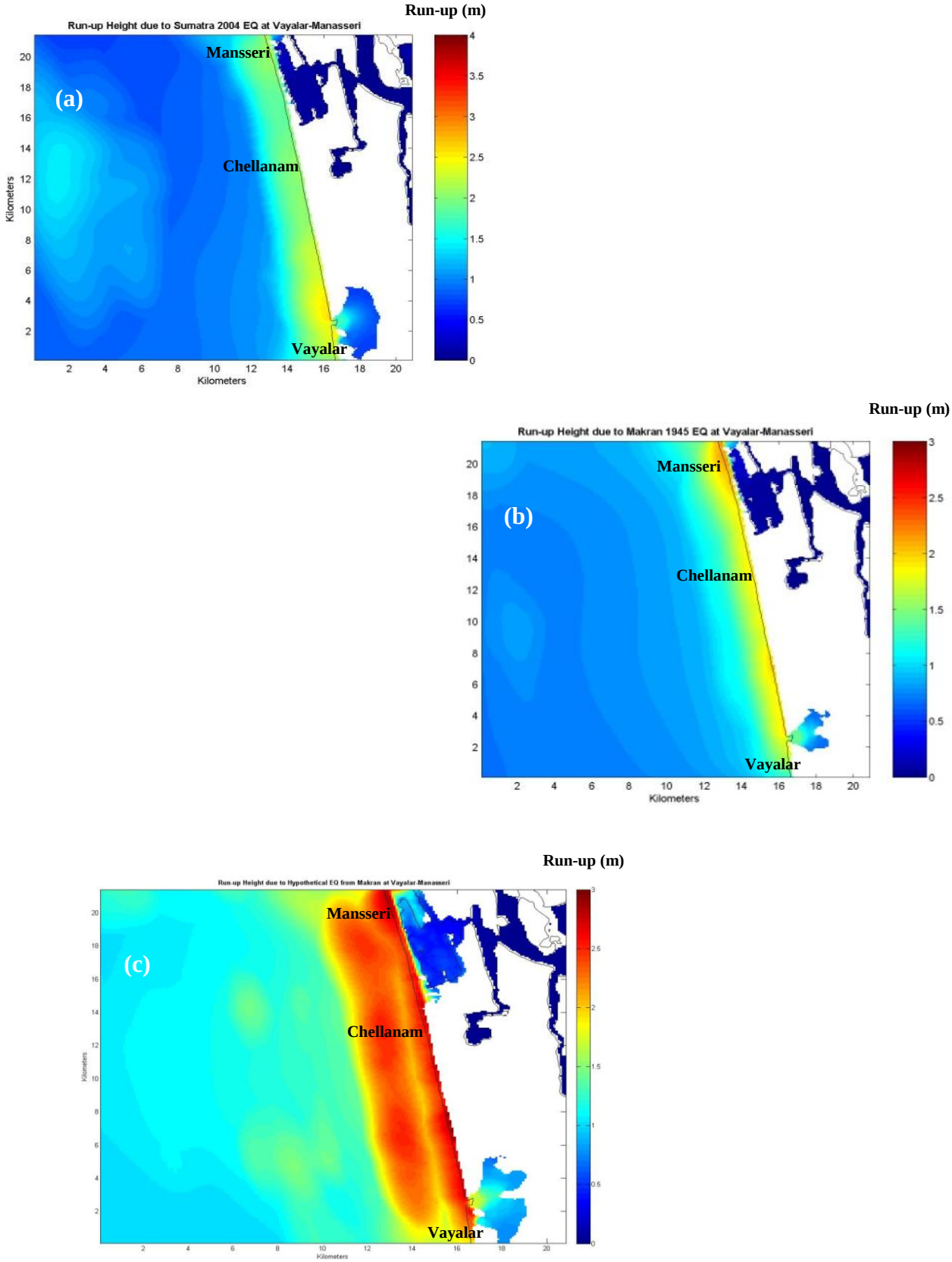

Fig. 6.8 Model simulation output for the Vayalar-Manasseri coast of Ernakulam district: (a) Sumatra 2004, (b) Makran 1945 & (c) Hypothetical worst case

Table 6.4 Run-up and inundation along the coastal stretch of Ernakulam district for three different cases of tsunami generation

Location	Sumatra 2004		Makran 1945		Hypothetical	
	Run-up	**Inundation**	**Run-up**	**Inundation**	**Run-up**	**Inundation**
Kadapuram	2.0-2.5	Nil	1.0-1.5	Nil	2.0-2.5	Nil
Anthakarnazhi	2.5-3.0	2000	1.5-2.0	1150	2.0-2.5	2400
Chellanam	2.0-2.5	Nil	1.5-2.0	Nil	2.5-3.0	45
Maravukad	2.0-2.5	30	1.5-2.0	32	2.0-2.5	47
Kannamali	1.5-2.0	186	1.5-2.0	94	2.0-2.5	2370
Manasseri	2.0-2.5	1102	2.0-2.5	1102	2.5-3.0	1500
Fort Cochin	1.5-2.0	Nil	2.0-2.5	Nil	2.0-2.5	80
Vypin	1.5-2.0	345	1.5-2.0	722	2.0-2.5	722
Puthuvypin	1.5-2.0	853	2.0-2.5	1060	2.0-2.5	1060
Njarackal	1.5-2.0	670	1.5-2.0	925	2.0-2.5	925
Edvanakkad	1.5-2.0	Nil	1.5-2.0	Nil	1.5-2.0	Nil

6.1.4.2 Manasseri - Munambam

The simulation results for Sumatra 2004 for Manasseri-Munambam sector showed Manasseri as the area of high run-up. The run-up was in the range of 2.0-2.5 m at Manasseri whereas the other regions like Vypin and Puthuvypin showed run-up in the range of 1.5-2.0 m. The simulated inundation was 345 m at Vypin, 853 m at Puthuvypin and 670 m at Njarackal.

The simulation for Makran 1945 showed in general an increase in run-up when compared to the previous sector in the range of 2.0-2.5 m throughout the coast. Here also high inundation was at Manasseri, roughly around 1102 m. Vypin and Puthuvypin showed 722 m and 1060 m inundation respectively. The simulation for the hypothetical case showed an increase in run-up and inundation along the entire stretch while comparing with that of Makran 1945 and even Sumatra 2004. The highest value of 2.76 m was at Manasseri which is considerably higher than the Sumatra 2004 case.

6.1.5 Thrissur District

The simulation is carried out under two sectors for this coastal district. They are 1) Munambam-Valappad and 2) Valappad-Palppetti (Fig. 6.9). The salient results of numerical modelling for the above sectors are presented in Table 6.5.

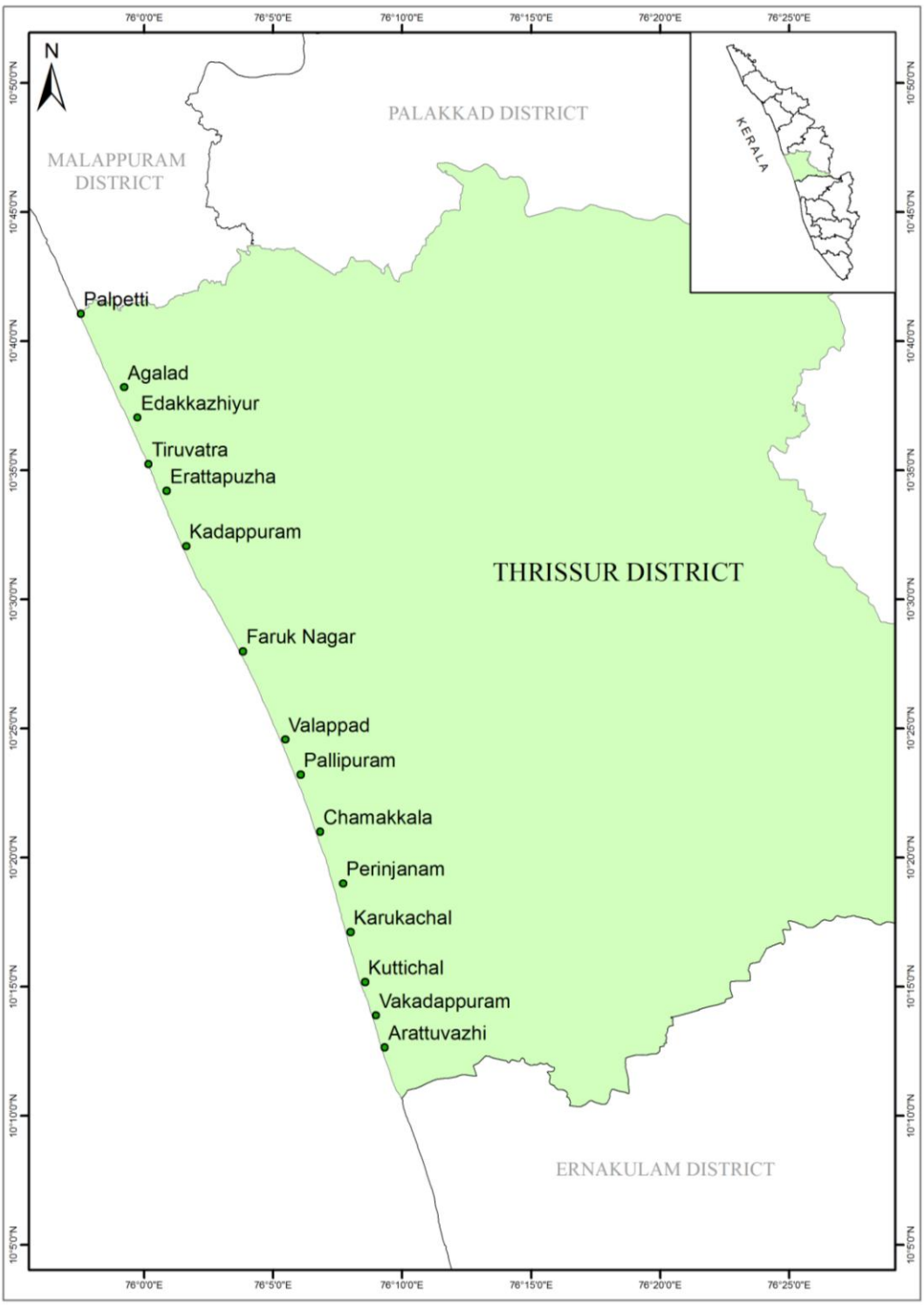

Fig. 6.9 Location map of Thrissur district

6.1.5.1 Munambam - Valappad

Munambam-Valappad is the southern most tip of the Thrissur coast. Here the simulation for Sumatra 2004 showed a run-up of 1.5-2.0 m in the Munambam area and the value got

reduced to 1.0-1.5 m as it approached the Valappad region in the north. A maximum inundation of 565 m was simulated at Peinjanam. Except for an inundation of 208 m at the north of Munambam inlet, other areas showed no inundation.

The simulation for Makran showed run-ups higher than Sumatra 2004 with maximum run-up of 2.0-2.5 m and inundation of about 412 m in the southern Munambam region. Towards the northern part namely Perinjanam, Pallipuram and Valappad area this run-up reduced to 1.5-2.0 m with no noticeable inundation. The simulation for the hypothetical case predicted a considerably higher run-up of 1.5-2.5 m along the stretch with a 500 m and 600 m inundation at the north of the Munambam inlet and Perinjanam respectively.

Table 6.5 Run-up and inundation along the coastal stretch of Thrissur district for three different cases of tsunami generation

Location	**Sumatra**		**Makran**		**Hypothetical**	
	Run-up (m)	**Inundation (m)**	**Run-up (m)**	**Inundation (m)**	**Run-up (m)**	**Inundation (m)**
Munnambam	1.5-2.0	208	2.0-2.5	412	2.0-2.5	510
Arattuvazhi	15-20	Nil	1.5-2.0	Nil	2.0-2.5	Nil
Kuttichal	1.0-1.5	Nil	1.5-2.0	Nil	2.0-2.5	Nil
Perinjanam	1.0-1.5	565	1.5-2.0	37	2.0-2.5	600
Kazhimbram	1.0-1.5	Nil	1.0-1.5	Nil	1.5-2.0	Nil
Pallipuram	1.0-1.5	Nil	1.5-2.0	Nil	1.5-2.0	Nil
Valappad	1.0-1.5	Nil	1.5-2.0	Nil	1.5-2.0	Nil
Nattika Beach	0.5-1.0	Nil	1.0-1.5	Nil	1.5-2.0	20
Putiyangadi	1.0-1.5	Nil	1.0-1.5	Nil	1.5-2.0	Nil
Faruk Nagar	1.0-1.5	Nil	1.0-1.5	Nil	1.5-2.0	Nil
Erattapuzha	1.0-1.5	Nil	1.5-2.0	Nil	2.0-2.5	Nil
Tiruvatra	1.0-1.5	Nil	1.5-2.0	Nil	2.0-2.5	Nil
Edakkazhiyur (south)	1.0-1.5	37	1.5-2.0	37	2.0-2.5	898
Agalad	1.0-1.5	Nil	1.5-2.0	Nil	2.0-2.5	Nil
Palpetti	1.0-1.5	Nil	1.5-2.0	Nil	2.0-2.5	Nil
Vadanapalli Beach	1.0-1.5	Nil	1.0-1.5	Nil	1.5-2.0	Nil

6.1.5.2 Valappad - Palpetti

This sector showed the relatively lower run-up in the range 0.5-1.5 m with no significant inundation for Sumatra 2004 (Fig. 6.10). The simulation for Makran 1945 showed higher

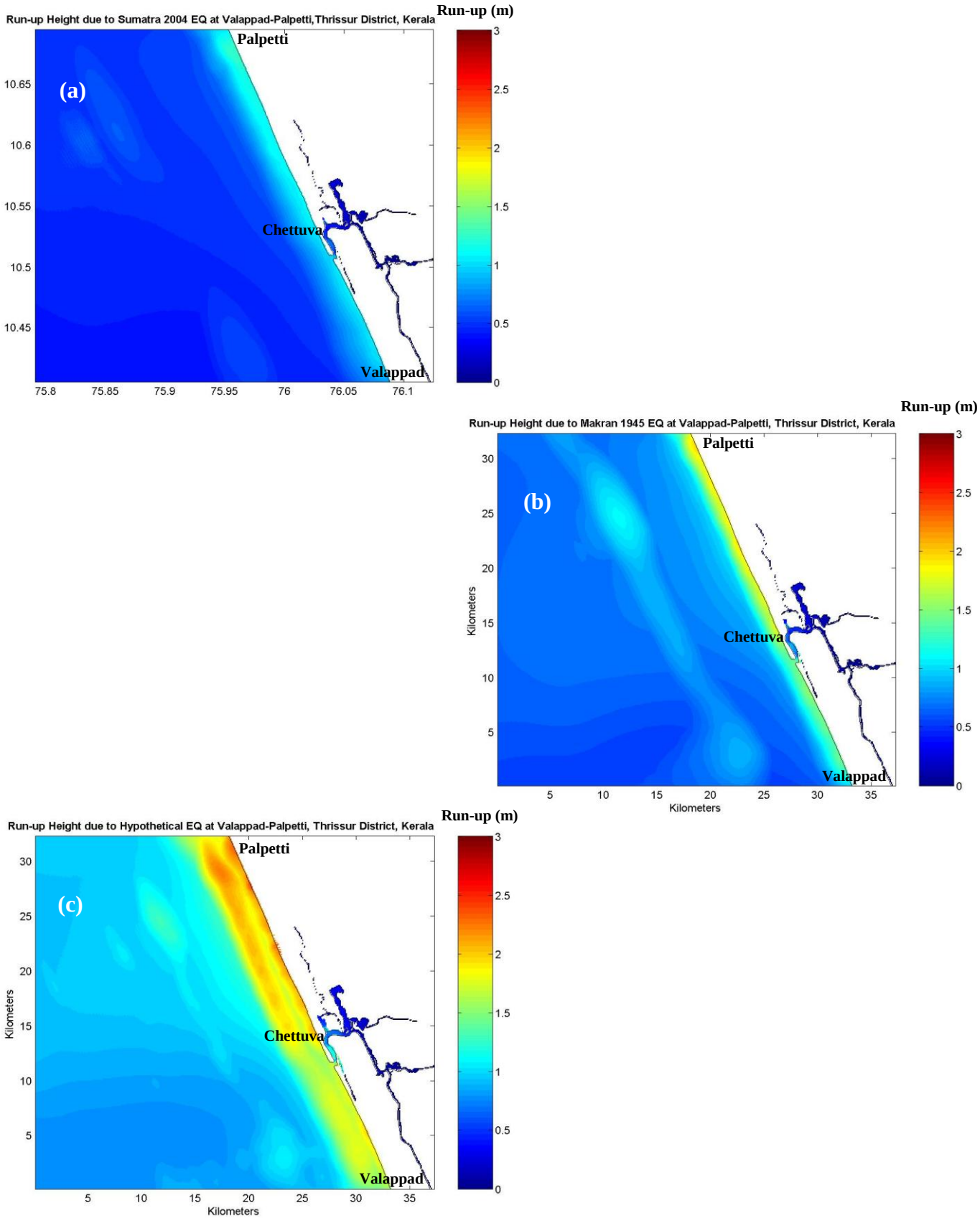

Fig. 6.10 Model simulation output for the Valappad-Palpetti coast of Thrissur district: (a) Sumatra 2004, (b) Makran 1945 & (c) Hypothetical worst case

run-ups with a maximum run-up of 1.5–2.0 m in the northern areas namely Tiruvatra, Agalad and Palpetti and the inundation was insignificant. A still higher run-up of 2.0–2.5 m resulted due to the hypothetical case and an inundation of about 900 m was seen at the south of Edakazhiyur.

6.1.6 Malappuram District

The simulation falls under two sectors for Malappuram district (Fig. 6.11). They are 1) Palpetti-Kuttayi and 2) Kuttayi-Parappanangadi.

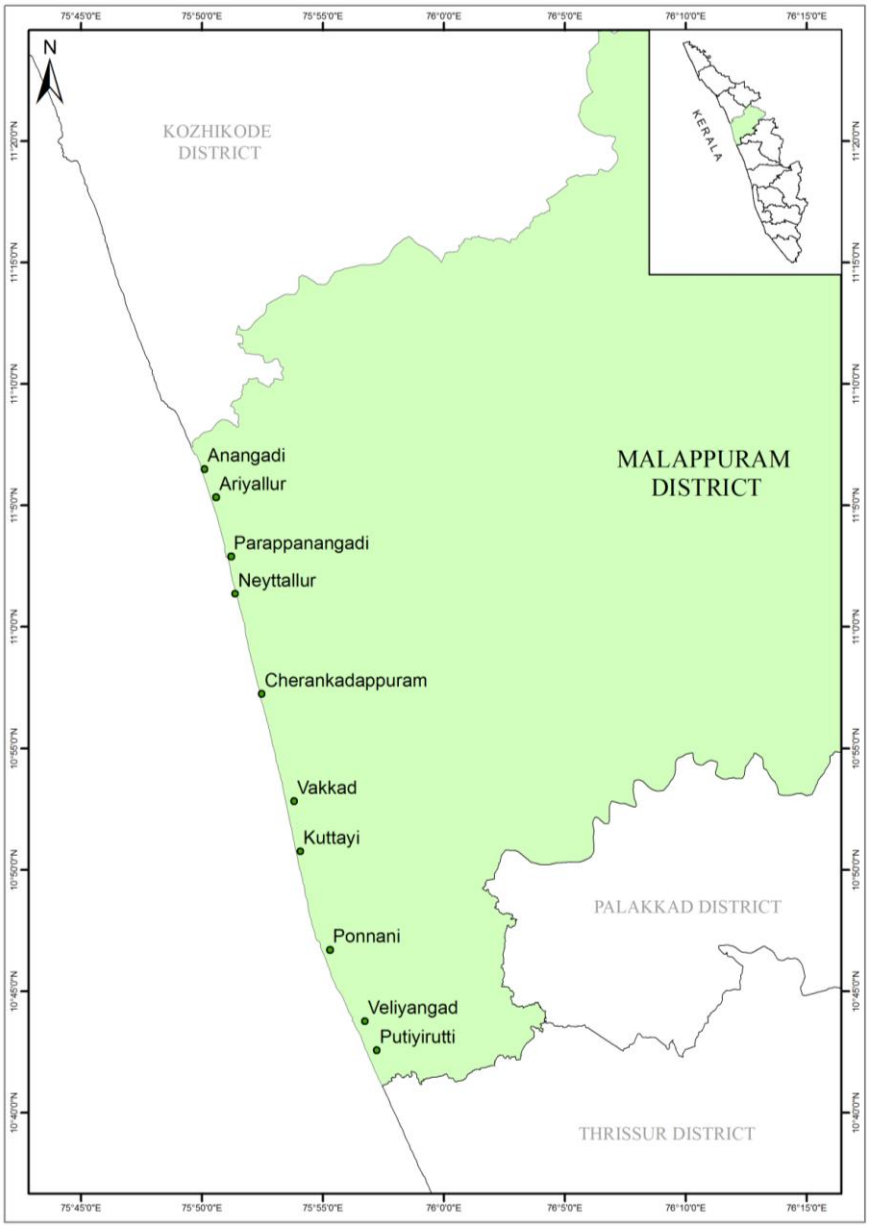

Fig. 6.11 Location map of Malappuram district

6.1.6.1 Palppetti - Kuttayi

Along this sector the simulation for Sumatra 2004 showed a run-up of 1.0-1.5 m. The simulation for Makran 1945 showed a higher run-up of 1.5-2.0 m throughout with a maximum inundation of 396 m at Veliyangad, north of Palpetti. Inundation was negligible at all other areas. A uniform run-up of 2.0-2.5 m was observed along the entire sector for the hypothetical simulation with a maximum inundation of about 550 m at Veliyangad.

Table 6.6 Run-up and inundation along the coastal stretch of Malappuram district for three different cases of tsunami generation

Location	Sumatra 2004		Makran 1945		Hypothetical	
	Run-up (m)	Inundation (m)	Run-up (m)	Inundation (m)	Run-up (m)	Inundation (m)
Kuttayi	1.0-1.5	Nil	1.5-2.0	Nil	2.0-2.5	Nil
Vakkad	1.0-1.5	Nil	1.5-2.0	Nil	2.0-2.5	Nil
Korangattu	1.0-1.5	Nil	1.5-2.0	Nil	2.0-2.5	185
Kalat Kadappuram	1.0-1.5	Nil	1.5-2.0	Nil	2.0-2.5	130
Pariyapuram	1.0-1.5	Nil	1.5-2.0	Nil	2.0-2.5	32
Puthen Kadappuram	1.5-2.0	Nil	1.5-2.0	Nil	2.0-2.5	Nil
Ayodhyanagar	1.0-1.5	Nil	1.5-2.0	Nil	2.0-2.5	176
Parappanangadi	1.5-2.0	Nil	1.5-2.0	Nil	2.0-2.5	Nil
Putiyirutty	1.0-1.5	Nil	2.0-2.5	26	2.0-2.5	Nil
Veliyangad	1.0-1.5	57	1.5-2.0	396	2.0-2.5	552
Putiyaponnani	1.0-1.5	Nil	1.5-2.0	Nil	2.0-2.5	31
Moonnangadi	1.0-1.5	Nil	1.5-2.0	Nil	2.0-2.5	65
Mukkola	1.0-1.5	Nil	1.5-2.0	Nil	2.0-2.5	59
Ponnani	1.0-1.5	Nil	1.5-2.0	Nil	2.0-2.5	Nil

6.1.6.2 Kuttayi - Parappanangadi

This coastal sector showed a run-up of 1.0-1.5 m from Kuttayi to Pariyapuram and a run-up of 1.5-2.0 m in the Parappanangadi area for Sumatra tsunami. There was no inundation (Fig. 6.12). The simulation for Makran showed a uniform run-up of 1.5-2.5 m in the entire sector except at Korangathu, north of Kuttayi, where a run-up of 2.0-2.5 m was obtained. The hypothetical case projected a uniform run-up of 2.0-2.5 m along the entire sector with a maximum inundation of 185 m at Korangattu.

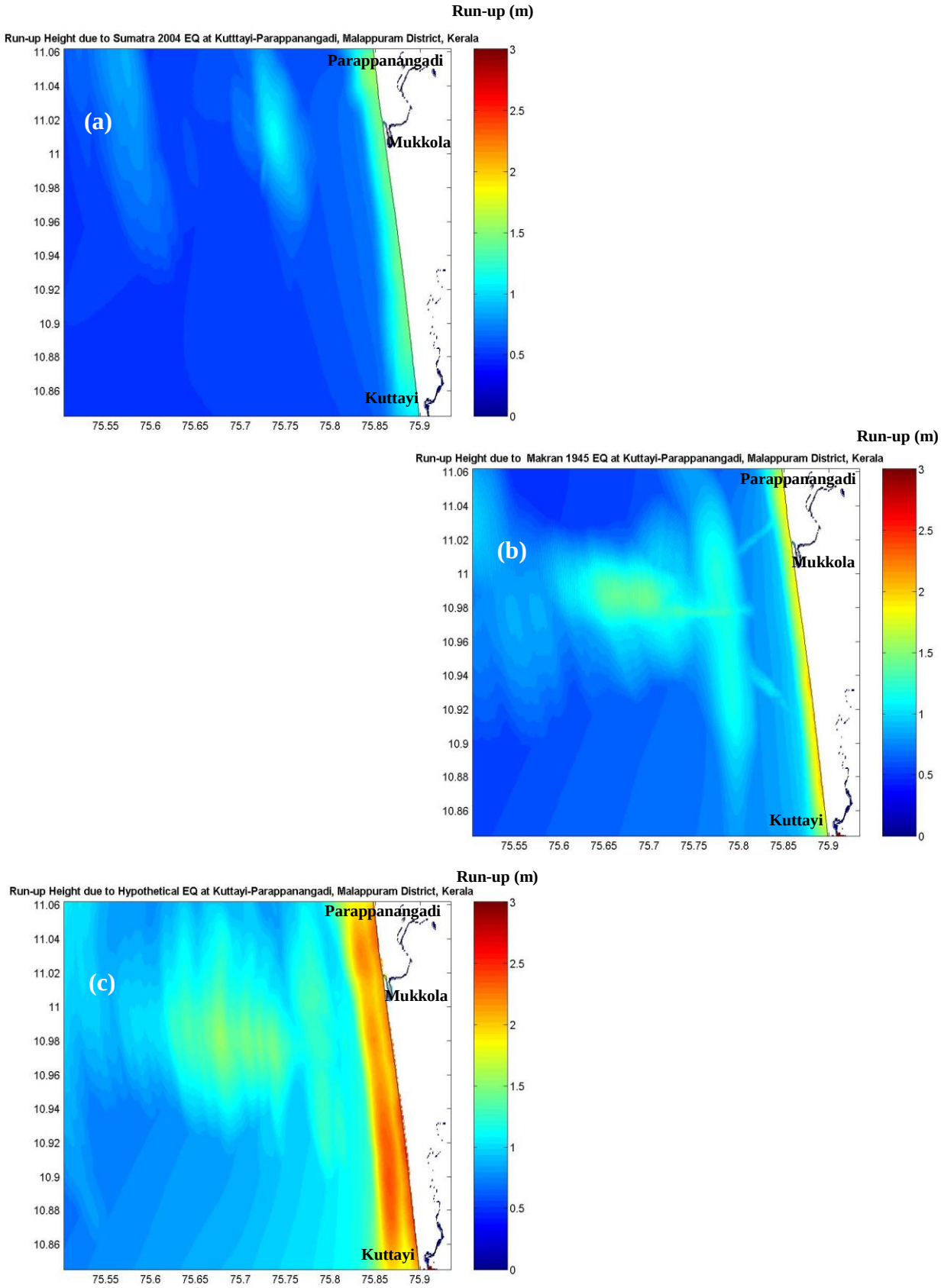

Fig. 6.12 Model simulation output for the Kuttayi-Parappanangadi coast of Malappuram district: (a) Sumatra 2004, (b) Makran 1945 & (c) Hypothetical worst case

6.1.7 Kozhikode District

Two sectors of simulation viz. Parappanangadi-Kappad and Kappad-Payyoli comes under Kozhikode district (Figure 6.13).

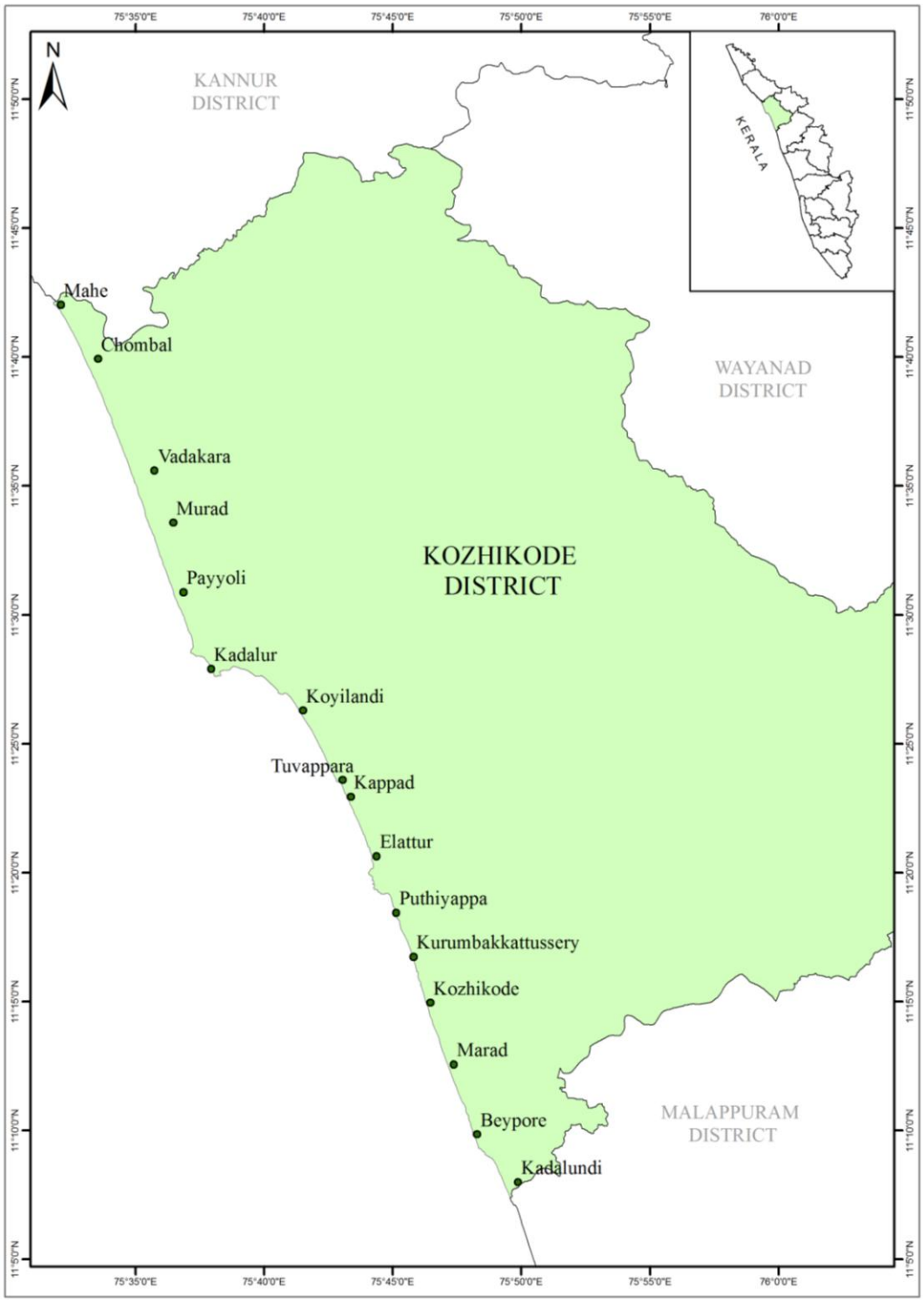

Fig. 6.13 Location map of Kozhikode district

6.1.7.1 Parappanangadi - Kappad

The simulation for Sumatra 2004 showed a run-up in the range 1.5-2.0 m at most of the places like Ariyallur, Kadalundi, Chaliyam, Beypore, Marad, Kozhikode Nagaram, Puthiyappa, Vengeli and Kappad of this sector. Except for an inundation of 150 m at Kadalundi, no other area showed any inundation. The simulation for Makran 1945 also showed a run-up in the range of 1.5-2.0 m at Alungal, Kadalundi, Marad, Kozhikode Nagaram and Vengeli with no inundation. The hypothetical case showed a higher run-up of 2.0-2.5 m along most of the locations with a maximum inundation of 654 m at Kadalundi.

6.1.7.2 Kappad - Payyoli

The simulation results for this sector are shown in Figure 6.14. The simulation for Sumatra 2004 for this sector showed a run-up of 1.0-1.5 m at Koyilandi, Tikkodi and

Table 6.7 Run-up and inundation along the coastal stretch of Kozhikode district for three different cases of tsunami generation

Location	Sumatra		Makran		Hypothetical	
	Run-up (m)	Inundation (m)	Run-up (m)	Inundation (m)	Run-up (m)	Inundation (m)
Alunkal	1.0-1.5	Nil	1.5-2.0	Nil	1.5-2.0	Nil
Ariyallur	1.5-2.0	Nil	1.5-2.0	Nil	2.0-2.5	Nil
Kadalundi	1.5-2.0	150	1.5-2.0	Nil	2.0-2.5	654
Chaliyam	1.5-2.0	Nil	1.0-1.5	Nil	2.0-2.5	Nil
Beypore	1.5-2.0	Nil	1.0-1.5	Nil	1.5-2.0	Nil
Marad	1.5-2.0	Nil	1.5-2.0	Nil	2.0-2.5	Nil
Kozhikode Nagaram	1.5-2.0	Nil	1.5-2.0	Nil	2.0-2.5	Nil
Vellayi	1.0-1.5	Nil	1.0-1.5	Nil	2.0-2.5	Nil
Putiyappa	1.5-2.0	Nil	1.5-2.0	Nil	2.0-2.5	Nil
Elattur	1.0-1.5	Nil	1.0-1.5	Nil	2.0-2.5	140
Vengali	1.5-2.0	Nil	1.5-2.0	Nil	2.0-2.5	Nil
Kappad	1.5-2.0	Nil	1.5-2.0	Nil	2.0-2.5	290
Tuvappara	1.0-1.5	Nil	1.0-1.5	Nil	1.0-1.5	Nil
Cheriya Mangad	1.5-2.0	Nil	1.0-1.5	Nil	1.5-2.0	Nil
Koyilandi	1.0-1.5	Nil	1.0-1.5	Nil	2.0-2.5	Nil
Kadalur	1.5-2.0	169	2.0-2.5	200	2.0-2.5	290
Tikkodi	1.0-1.5	50	1.5-2.0	134	1.5-2.0	165
Payyoli	1.0-1.5	Nil	1.0-1.5	Nil	1.5-2.0	Nil

Payyoli whereas Kadalur and Cheriyamangad showed a higher run-up of 1.5-2.0 m. The Makran 1945 simulation predicted a maximum run-up of 2.0-2.5 m at Kadalur whereas a value of only 1.0-1.5 m was predicted for the other locations like Payyoli, Koyilandi and Cheriyamangad. The simulation for the hypothetical case showed a run-up of 2.0-2.5 m for a few locations like Kadalur. At other locations the run-ups were in the range 1.5-2.0 m. Inundation was seen only at Kadalur with values of 290 m, 200 m, and 169 m for hypothetical, Makran 1945 and Sumatra 2004 respectively.

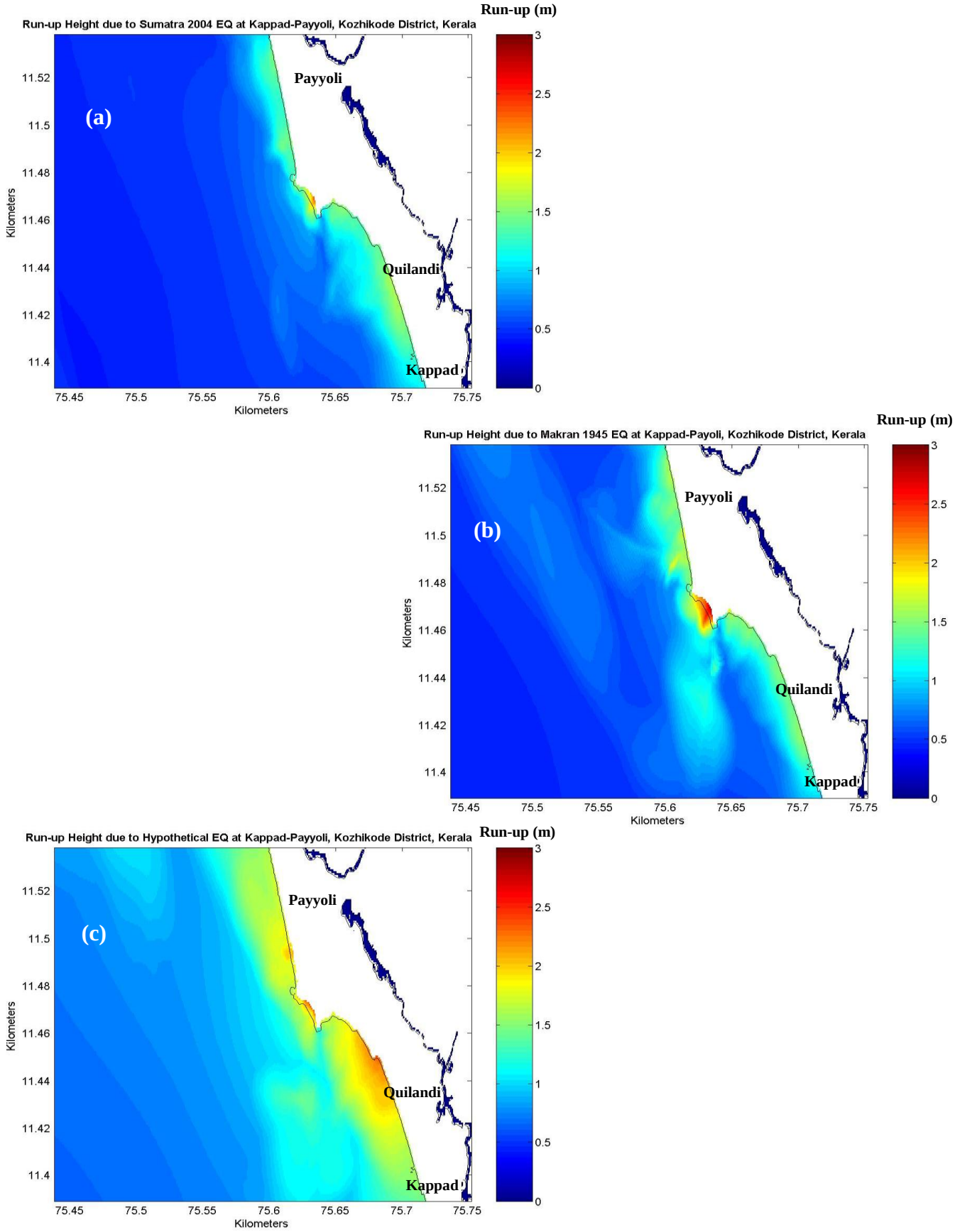

Fig. 6.14 Model simulation output for the Kappad-Payyoli coast of Kozhikode district: (a) Sumatra 2004, (b) Makran 1945 & (c) Hypothetical worst case

6.1.8 Kannur District

Three sectors of simulation come under this district. They are Murad- Kannur, Kannur-Mattul and Mattul-Trikkaripur (Fig. 6.15).

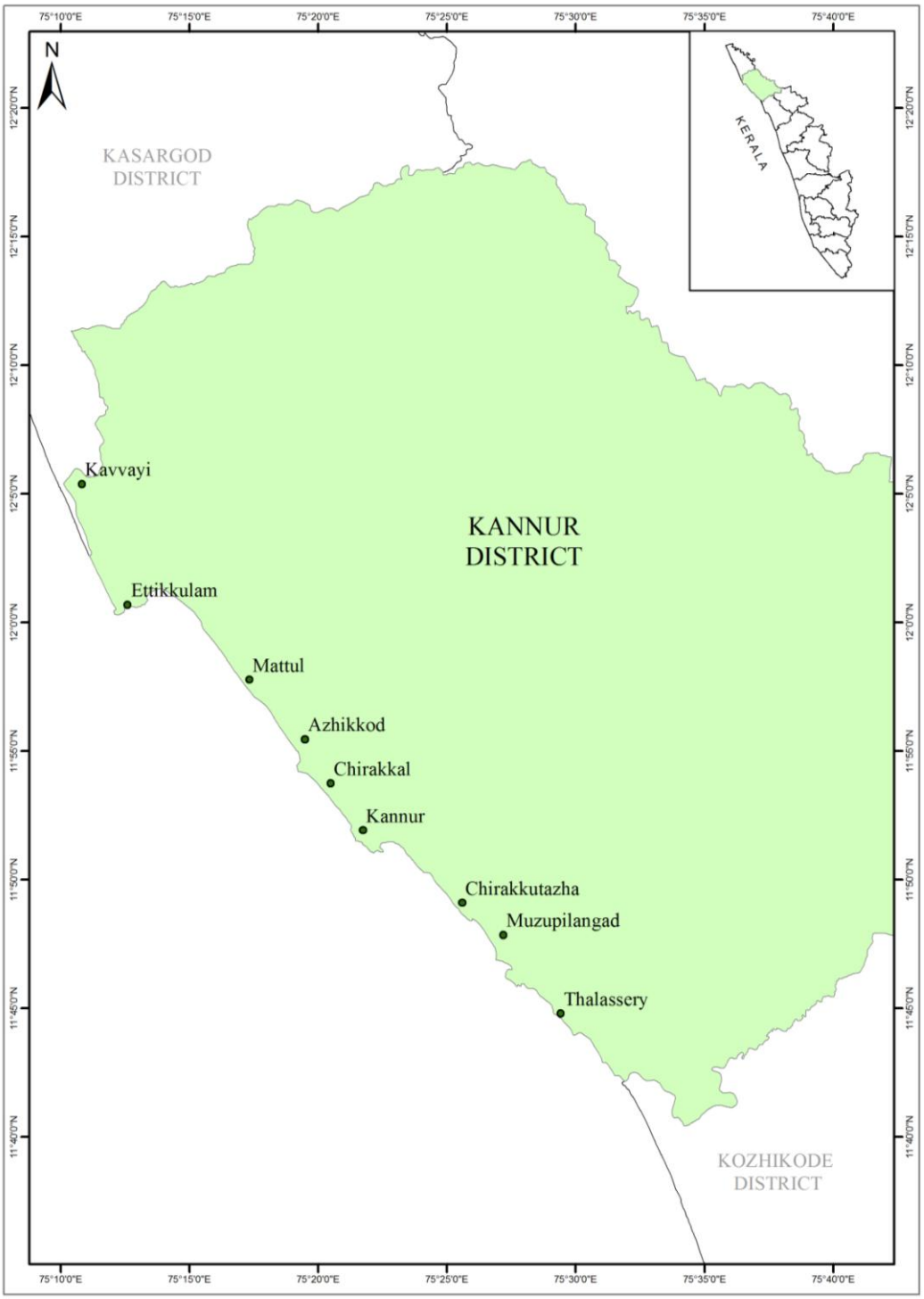

Fig. 6.15 Location map of Kannur district

6.1.8.1 Murad - Kannur

This coastal stretch showed a maximum run-up of 1.0-1.5 m at Chombal and Avikara whereas the other locations like Mahe, Thalassery, Dharmadam, Muzhapilangad and Kadalayi showed a run-up in the range of only 0.5-1.0 m for Sumatra 2004. The simulation for Makran 1945 showed a run-up of 1.0-1.5 m at Ayanikkad, Kuttakkal, Chombal, Avikara and Irikil whereas a run-up of 1.5-2.0 m was predicted by the model at a few locations like Muzhupilangad, Kadalayi, Mahe and Thalassery.

The simulation for the hypothetical case predicted a run-up of around 2.0-2.5 m along Dharmadam and Muzhapilangad. The places like Mahe, Thalassery and Kadalayi showed 2.5-3.0 m run-up. The hypothetical case predicted a 1.5-2.0 m run-up with a maximum inundation of 530 m at Ayanikkad, the southern location of this coastal stretch.

6.1.8.2 Kannur - Mattul

The simulation for the Sumatra 2004 for the Kannur-Mattul region showed a wide range in the run-up (Fig. 6.16). A maximum run-up of 3.0-3.5 m was observed at Tayyil, the southern tip of the sector whereas for the other locations like Ayikkara, Payyambalam, and Mattul north the run-up was in the range of only 1.5-2.0 m. The simulation for 1945 Makran predicted a maximum run-up of only 2.0 m. Some of the locations showed the same run-up as in the case of Sumatra, eg. Mattul north and south.

The hypothetical case predicted a run-up of 2.0-2.5 m in most of the places like Tayyil, Barnassery, Payyambalam and Mattul north. The model predicted some inundation in this stretch for all the three cases. Mattul South showed the highest inundation of 669 m for the hypothetical case.

6.1.8.3 Mattul -Trikkaripur

The simulation for Sumatra 2004 for the Mattul-Trikkaripur sector showed a highly pattern of varying run-up along the coastal stretch. The maximum value of 3.5-4.0 m was simulated at the north of Tai Kadappuram. The other locations Ettikulam and Puthiyangadi showed a run-up of 2.0-2.5 m and 2.5-3.0 m respectively, whereas Ezhimala showed only 1.0-1.5 m run-up.

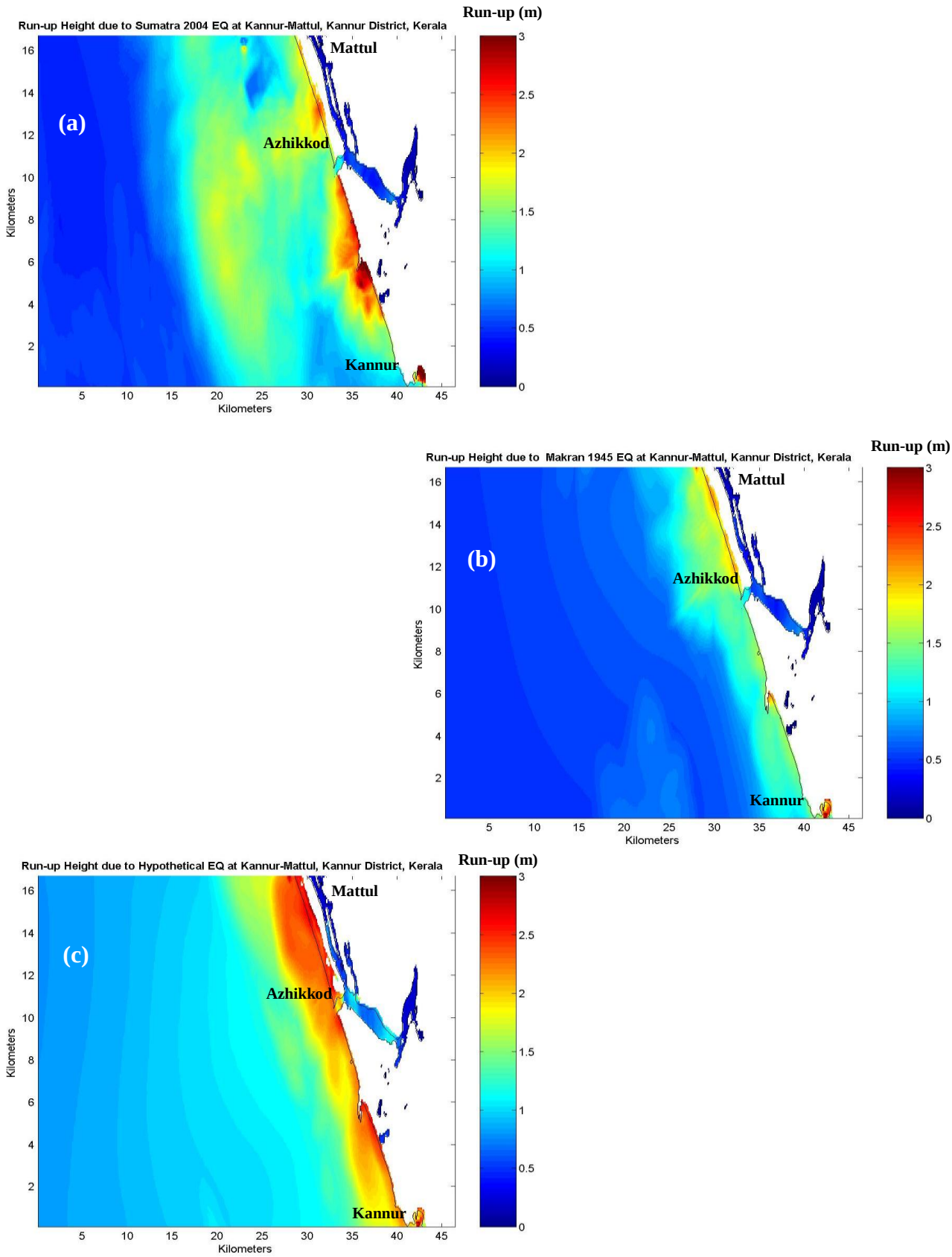

Fig. 6.16 Model simulation output for the Kannur-Mattul coast of Kannur district: (a) Sumatra 2004, (b) Makran 1945 & (c) Hypothetical worst case

Table 6.8 Run-up and inundation along the coastal stretch of Kannur district for three different cases of tsunami generation

Location	Sumatra		Makran		Hypothetical	
	Run-up (m)	Inundation (m)	Run-up (m)	Inundation (m)	Run-up (m)	Inundation (m)
Ayanikkad	0.5-1.0	40	1.0-1.5	402	1.5-2.0	530
Kuttakkal	0.5-1.0	230	1.0-1.5	224	2.0-2.5	264
Puvakara	1.0-1.5	196	1.5-2.0	344	2.5-3.0	480
Karuvachal	0.5-1.0	34	1.5-2.0	48	2.5-3.0	98
Chombal	1.0-1.5	41	1.0-1.5	90	2.5-3.0	90
Avikara	1.0-1.5	Nil	1.0-1.5	Nil	2.5-3.0	Nil
Irikil	0.5-1.0	Nil	1.0-1.5	Nil	2.5-3.0	Nil
Mahe	0.5-1.0	Nil	1.5-2.0	Nil	2.5-3.0	Nil
Thalassery	0.5-1.0	Nil	1.5-2.0	88	2.5-3.0	153
Dharmadam	0.5-1.0	Nil	1.0-1.5	53	2.0-2.5	66
Chalil	0.5-1.0	67	1.0-1.5	105	2.5-3.0	316
Kannokkara	0.5-1.0	370	1.0-1.5	370	2.0-2.5	460
Muzhupilangad	0.5-1.0	Nil	1.5-2.0	Nil	2.0-2.5	511
Kadalayi	0.5-1.0	Nil	1.5-2.0	Nil	2.5-3.0	Nil
Tayyil	3.0-3.5	100	2.0-2.5	Nil	2.0-2.5	Nil
Ayikara	1.5-2.0	Nil	1.5-2.0	Nil	1.5-2.0	Nil
Barnasseri	1.5-2.0	Nil	1.0-1.5	Nil	2.0-2.5	Nil
Payyambalam	1.5-2.0	Nil	1.0-1.5	Nil	2.0-2.5	Nil
Mattul south	1.5-2.0	264	1.5-2.0	343	2.0-2.5	669
Mattul north	1.5-2.0	308	1.5-2.0	257	2.5-3.0	539
Mattul	1.5-2.0	78	1.0-1.5	78	2.0-2.5	283
Puthiyangadi	2.5-3.0	262	1.5-2.0	81	3.0-3.5	262
Ettikulam	2.0-2.5	49	1.0-1.5	30	1.5-2.0	72
Ezhimala	1.0-1.5	Nil	1.0-1.5	Nil	1.5-2.0	Nil
North of Taikadappuram	3.5-4.0	515	2.5-3.0	219	3.0-3.5	380

In contrast the simulation for Makran 1945 showed a narrow range of run-up of 1.0-2.0 m except in the north of Tai Kadappuram where a higher run-up in the range 2.5-3.0 m was obtained. The simulations showed a higher run-up value in hypothetical case with 2.0-2.5 m at Mattul, whereas Puthiyangadi and Tai Kadappuram showed a run-up of 3.0-3.5 m. Ettikulam and Ezhimala recorded a 1.5-2.0 m run-up. The simulation predicted a maximum inundation of 515 m at the north of Tai Kadappuram for the Sumatra 2004 source coinciding with the highest run-up of 3.0-3.5 m. The same location showed an inundation of 380 m and 219 m for the hypothetical and Makran source respectively.

Higher run-up values were observed at the north of Tai Kadappuram in the range of 3.5-4.0 m, 2.5-3.0 m, 3.0-3.5 m for Sumatra 2004, Makran 1945 and hypothetical case respectively. It is also to be noted that unlike the other sectors of the central and northern Kerala coast, this sector showed the high value of run-up for the Sumatra 2004 simulation much in the same way as the southern Kerala coast.

6.1.9 Kasargod District

The coastal zone of Kasargod district falls under the following three sectors in the numerical simulation (Fig. 6.17).

1) Trikkaripur - Bekal
2) Bekal - Mogral
3) Mogral - Talappadi

6.1.9.1 Trikkaripur - Bekal

Trikkaripur to Bekal is the southern sector of Kasargod district. The simulation for Sumatra 2004 showed a maximum run-up of around 2.0-2.5 m at Padanna Kadappuram, whereas the simulation for Makran 1945 showed a maximum run-up of around 1.5-2.0 m at a few locations. The hypothetical case predicted a run-up of 2.0-2.5 m continuously along the coastal stretch except at Trikkaripur. The inundation was a maximum of 445 m at Trikkaripur for Sumatra 2004, Makran 1945 and hypothetical cases. Lesser inundations were observed at Mavila Kadappuram and Hosdurg for all the three cases.

6.1.9.2 Bekal - Mogral

Figure 6.18 show the simulation results for this sector for the three cases. In the Bekal-Mogral sector, which is the middle portion of Kasargod district, a maximum of 2.0-2.5 m run-up was observed at Kudlu and Kalmadi for the Sumatra 2004. For the Makran 1945 simulation, the maximum run-up of 2.0-2.5 m was observed only at Nellikunnu. The hypothetical case showed a maximum run-up of 2.5-3.0 m at Kalmadi and Kudlu. Nellikunnu showed maximum inundation for all the three cases of 390 m for the hypothetical worst case.

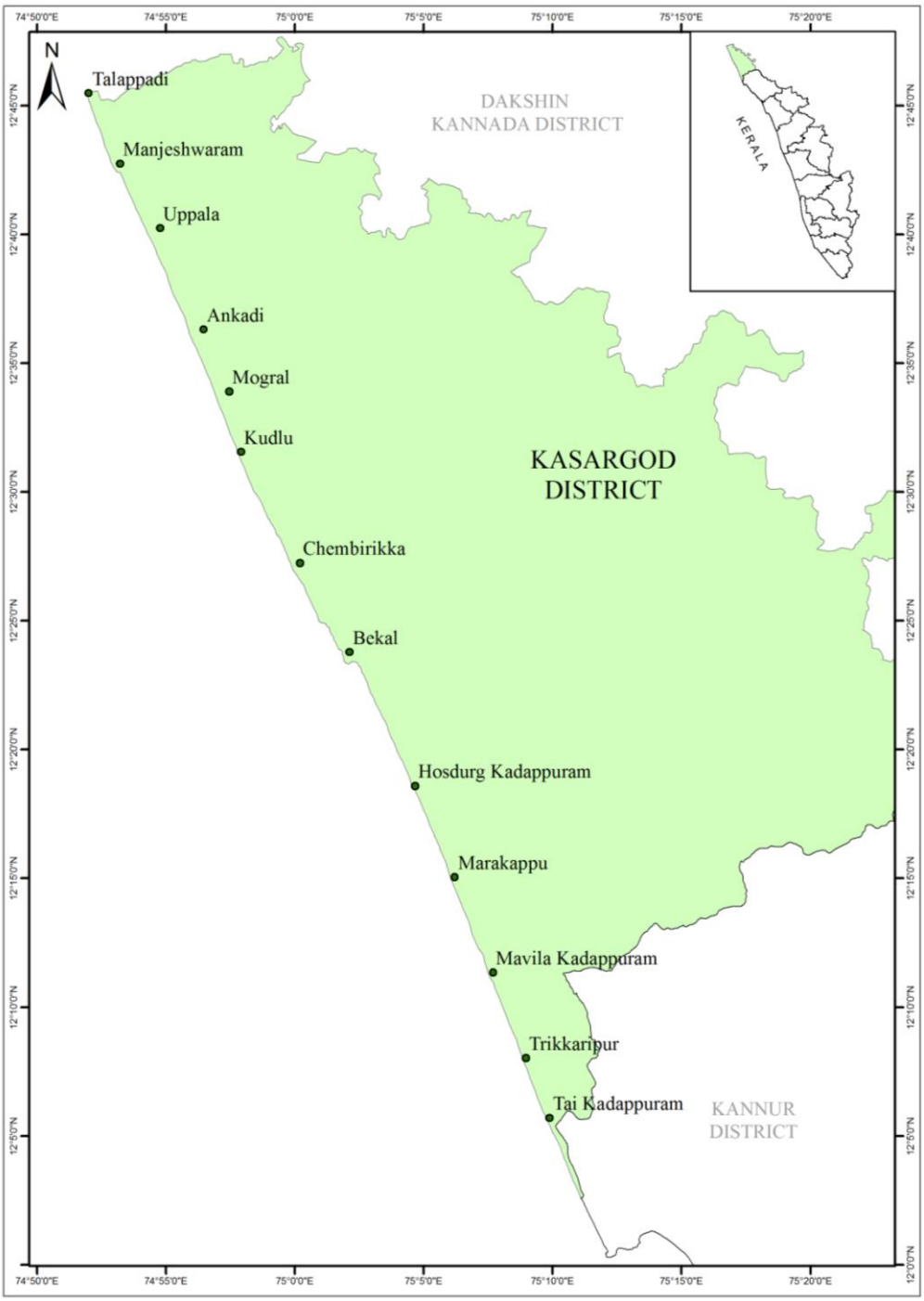

Fig. 6.17 Location map of Kasargod district

6.1.9.3 Mogral -Talappadi

This sector is the northernmost one of the Kasargod District and Kerala. The Sumatra 2004 simulated low run-ups in the range of 0.5-1.5 m in this sector. There was no significant inundation along this sector for Sumatra 2004.

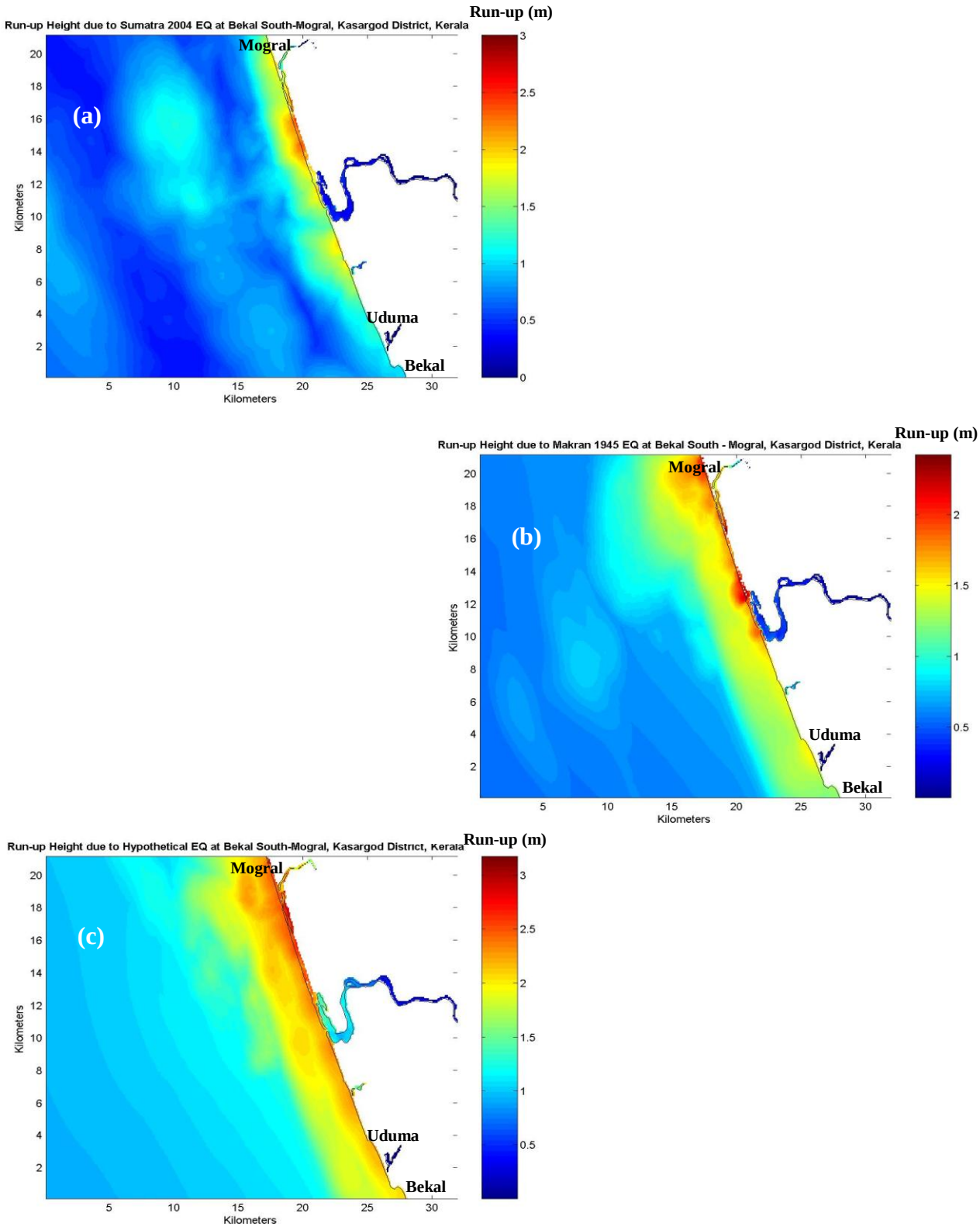

Fig. 6.18 Model simulation output for the Bekal-Mogral coast of Kasargod district: (a) Sumatra 2004, (b) Makran 1945 & (c) Hypothetical worst case

Table 6.9 Run-up and inundation along the coastal stretch of Kasargod district for three different cases of tsunami generation

Location	Sumatra		Makran		Hypothetical	
	Run-up (m)	Inundation (m)	Run-up (m)	Inundation (m)	Run-up (m)	Inundation (m)
Trikkaripur	1.0-1.5	445	1.0-1.5	445	1.5-2.0	445
Padanna kadappuram	2.0-2.5	Nil	1.5-2.0	Nil	2.0-2.5	Nil
North of Mavila Kadappuram	1.5-2.0	209	1.5-2.0	174	2.0-2.5	360
Hosdurg	1.5-2.0	250	1.0-1.5	246	2.0-2.5	286
Pallikara	1.0-1.5	Nil	1.0-1.5	Nil	2.0-2.5	Nil
Kanjahad	1.5-2.0	Nil	1.0-1.5	Nil	2.0-2.5	Nil
Bekal south	1.0-1.5	Nil	1.5-2.0	Nil	2.0-2.5	Nil
Bekal	1.0-1.5	Nil	1.0-1.5	Nil	2.0-2.5	Nil
Kudlu	2.0-2.5	161	1.5-2.0	145	2.5-3.0	207
Nellikunnu	1.5-2.0	330	2.0-2.5	390	2.0-2.5	390
Kalmadi	2.0-2.5	179	1.5-2.0	104	2.5-3.0	224
Mogral	1.5-2.0	50	1.5-2.0	50	2.0-2.5	220
Mogral north	0.5-1.0	Nil	1.0-1.5	Nil	2.0-2.5	86
Kumbla	0.5-1.0	98	1.5-2.0	206	2.0-2.5	208
Mutta	1.0-1.5	Nil	2.0-2.5	100	2.0-2.5	100
Uppala	1.0-1.5	Nil	1.5-2.0	Nil	2.0-2.5	110
Manjeswaram	0.5-1.0	Nil	1.5-2.0	Nil	2.0-2.5	70
Hosangadi	1.0-1.5	Nil	1.5-2.0	57	2.5-3.0	341
Thalappadi	0.5-1.0	180	1.5-2.0	Nil	2.0-2.5	157

The simulation for Makran 1945 showed higher run-up of 1.5-2.0 m at most of the locations in the sector with a maximum of 2.0-2.5 m at Mutta. However there was no noticeable inundation. The hypothetical case showed a maximum run-up of 2.5-3.0 m at Hosangadi and 2.0-2.5 m at all the other locations. However, there was no significant inundation in this case too except for a 341 m inundation at Hosangadi.

6. 2 TSUNAMI INUNDATION CHARACTERISTICS ALONG THE LAKSHADWEEP ISLAND COASTS

6.2.1 Characteristics of the Islands

Lakshadweep is an archipelago consisting of 12 atolls, 3 reefs, and 5 submerged banks. It is located between 8º - 12 º 13’ North latitude and 71º - 74º East longitudes, 220-440 Km

away from Kerala. Lakshadweep is a uni-district Union Territory with an area of 32 sq. km and has 11 inhabited islands including Bangaram. The inhabited islands are Kavaratti, Agatti, Amini, Androth, Kiltan, Kalpeni, Kadamat, Chetlet, Bitra and Minicoy (Fig. 6.19 & 6.20). Androth has the largest land area and Bitra is the smallest. The details regarding the Lakshadweep Islands are mentioned in Table 6.10.

Table 6.10 Details of 11 inhabited islands in Lakshadweep

Sl. No.	Island	Area (sq. km)	Length of coastline (km)
1	Kavaratti	3.63	11.46
2	Agatti	2.71	16.14
3	Amini	2.59	6.67
4	Androth	4.84	10.59
5	Bangaram	0.58	3.52
6	Kalpeni	2.28	11.86
7	Minicoy	4.37	23.07
8	Kiltan	1.63	7.81
9	Chetlat	1.04	5.82
10	Kadamat	3.12	18.38
11	Bitra	0.10	1.56

The islands are ring-shaped atolls lying along a north-south axis (except Androth) with a lagoon on the west and open sea on the east. The islands have a lagoon area of 4,200 km^2, Territorial waters of 20,000 km^2 and Exclusive Economic Zone (EEZ) of 4,00,000 km^2.

The four islands selected for this study are Chetlat, Kadmat, Androth and Kavarati (Fig. 6.20). Chetlat is the northernmost inhabited island of the group with an approximate area of 1sq. km. Kadmat is the longest island next to Agatti in the Lakshadweep group of islands with a large lagoon and abundant coral growth. Androth is the nearest island in the group to the main land and is the only island oriented in the east-west direction with no lagoon**.** Kavaratti is the third largest island in the north south direction with a shallow lagoon enclosed by coral reef on the west.

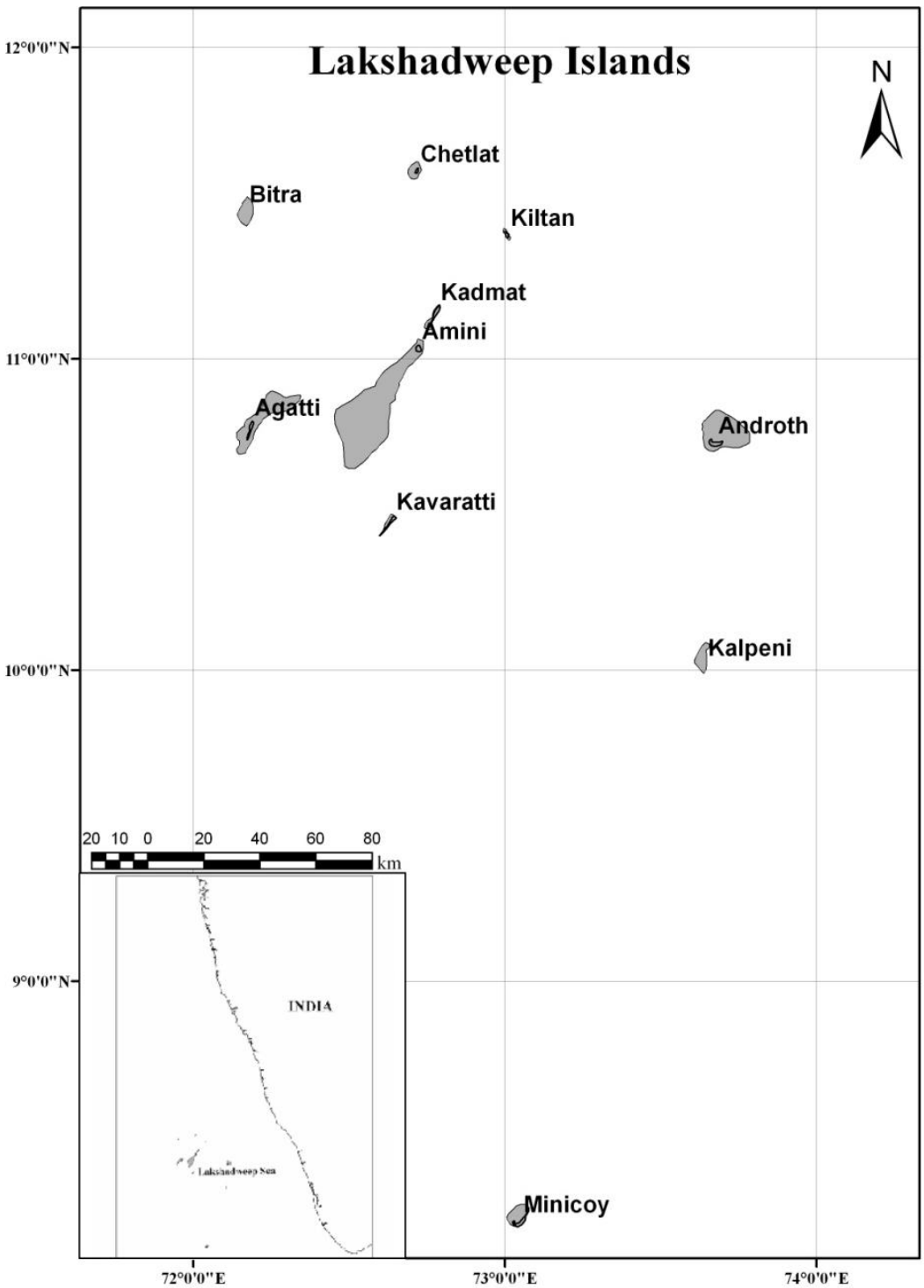

Fig. 6.19 Lakshadweep Islands

6.2.2 Results of Numerical Modelling

The run-up obtained at the four islands for the three different sources as in the case of Kerala coast are shown in Figures 6.21-6.24 and Table 6.11.

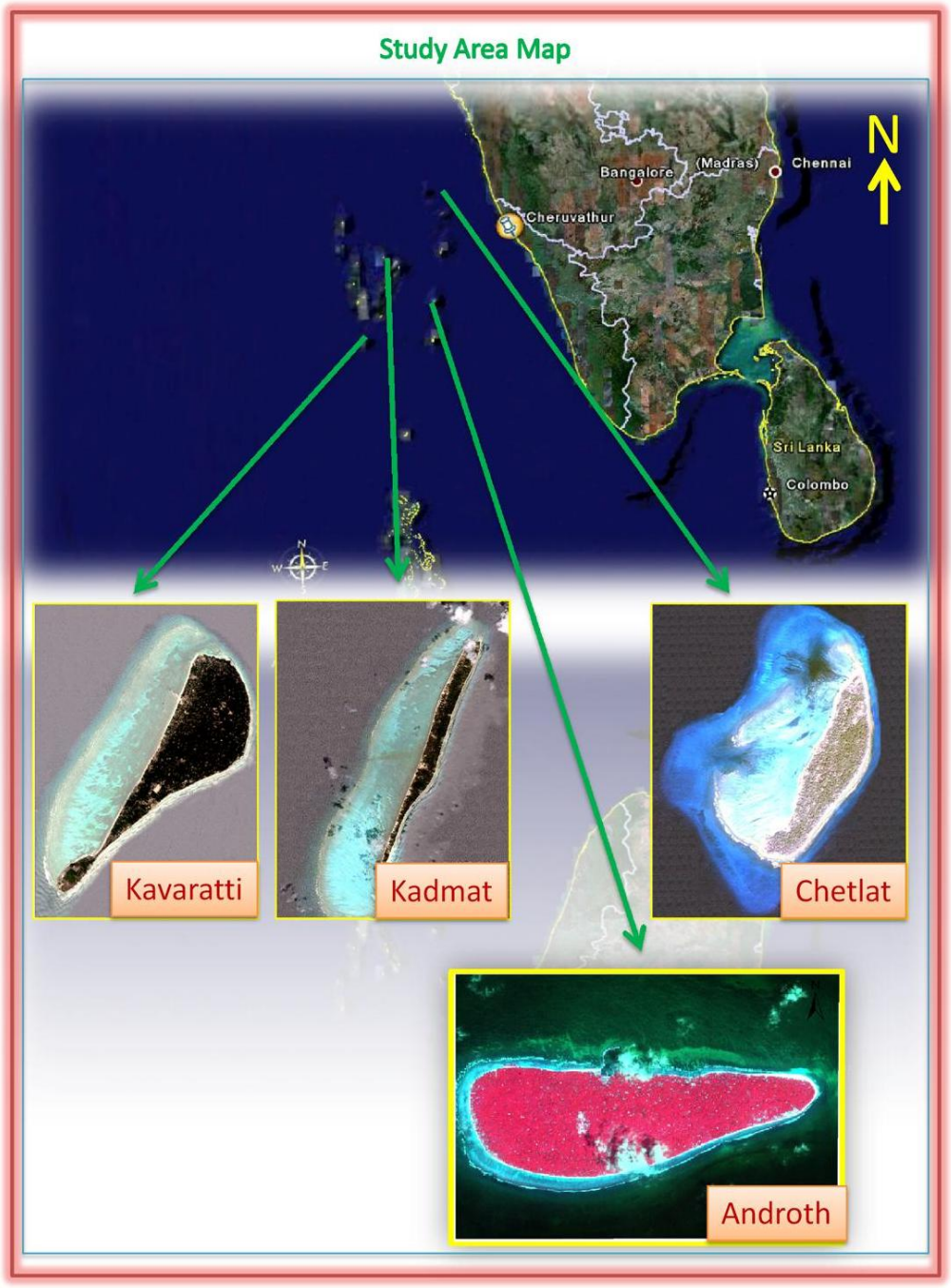

Fig. 6.20 Four representative Islands of Lakshadweep selected for studying the run-up / inundation characteristics

6.2.2.1 Androth Island

Out of the four islands a maximum run-up in the range of 1-2 m was obtained in the North East (NE) and North West (NW) coast of Androth. All other portions of the island

Table 6.11 Run-up and inundation along the four selected islands of Lakshadweep for three different cases of tsunami generation

Island	Sector of the Coast	Sumatra 2004		Makran 1945		Hypothetical	
		Run-up (m)	Inundation (m)	Run-up (m)	Inundation (m)	Run-up (m)	Inundation (m)
Androth	NE	1-2	91	0-1	91	1-2	163
	SE	0-1	84	0-1	86	0-1	117
	SW	0-1	NIL	0-1	NIL	1-2	NIL
	NW	1-2	NIL	1-2	NIL	3-4	388
Chetlat	NE	0-1	NIL	0-1	NIL	0-1	NIL
	SE	0-1	NIL	0-1	NIL	0-1	NIL
	SW	0-1	NIL	0-1	NIL	0-1	NIL
	NW	0-1	NIL	0-1	NIL	0-1	NIL
Kadmat	NE	0-1	NIL	0-1	NIL	0-1	NIL
	SE	0-1	NIL	0-1	NIL	0-1	NIL
	SW	0-1	NIL	0-1	NIL	1-2	38
	NW	0-1	NIL	0-1	NIL	0-1	NIL
Kavaratti	NE	0-1	NIL	0-1	NIL	0-1	NIL
	SE	0-1	NIL	0-1	NIL	0-1	NIL
	SW	0-1	NIL	0-1	NIL	0-1	NIL
	NW	0-1	NIL	0-1	NIL	0-1	NIL

showed run-up in the range of 0-1 m. The simulation for the hypothetical case showed a huge increase in run-up values on comparison with Makran 1945 and Sumatra 2004. The NW coast of the islands showed run-up in the range of 3-4 m, whereas the NE and SW sectors of the island showed run-up in the range of 1-2 m. Run-up in the range of 0-1 m was showed in the SE coast. Inundation was high for the hypothetical case. A maximum inundation of 388 m was observed at the NW portion of the island. The NE and SE portion showed an inundation of 163 m and 117 m respectively. The huge inundation for the hypothetical case can be attributed to the proximity of the source and the orientation in the east-west direction. The inundation for Sumatra 2004 and Makran 1945 was less while comparing with that of the hypothetical source. An inundation of less than 100 m was predicted by the model at the NE and SE sectors of the island for the two sources.

6.2.2.2 Chetlat Island

The simulations results for all the three sources for the Chetlat Island showed a uniform run-up in the range of 0-1 m along the NE, SE, SW and NW portions of the island. There was no inundation in any of the three sources.

6.2.2.3 Kadmat Island

Run-up pattern in the range of 0-1 m was predicted for the Kadmat Island for the Sumatra 2004 and Makran 1945 cases. In the hypothetical case also the same run-up was observed except for a maximum run-up in the range of 1-2 m observed in the SW sector of the island with an inundation of 38 m. The other sectors showed no inundation.

6.2.2.4 Kavaratti Island

The Kavaratti Island also showed a similar run-up and inundation pattern like the Chetalt and Kadmat Island. The predicted run-up was in the range of 0-1 m for the Sumatra 2004 and Makran 1945 simulations for all sectors. Even the simulation for the hypothetically worst case did not generate more than 1 m run-up. No inundation was predicted by the model for all the three sources.

6.3 DISCUSSION

The results of numerical simulation for the Sumatra 2004, Makran 1945 and the hypothetical case present very interesting characteristics of tsunami run-up and inundation along the Kerala and Lakshadweep coasts. The run-up and inundation characteristics are strikingly different for the Kerala and Lakshadweep coasts. While the Kerala coast appear to be vulnerable for inundation due to tsunami from different sources, the Lakshadweep coasts do not appear to be vulnerable to tsunami inundation.

As far as Kerala coast is concerned, the Sumatra 2004 tsunami generated run-ups as high as 5 m. However the Makran 1945, in spite of the source being in the Arabian Sea itself and proximate to the Kerala coast, did not produce any significant impact along the Kerala coast. Even the hypothetical scenario of Sumatra like rupture intensity of Makran does not produce the type of run-up along the Kerala coast as seen for Sumatra 2004. This can be attributed to the directivity of the tsunami generated.

Though the hypothetical Makran source does not generate run-up as high as the Sumatra 2004 along the Kerala coast, it indeed appears to be more hazardous for a major part of the Kerala coast in terms of inundation. This anomalous behavior in inundation in spite of lower run-up can be attributed to the beach elevation. In general the beach elevation is

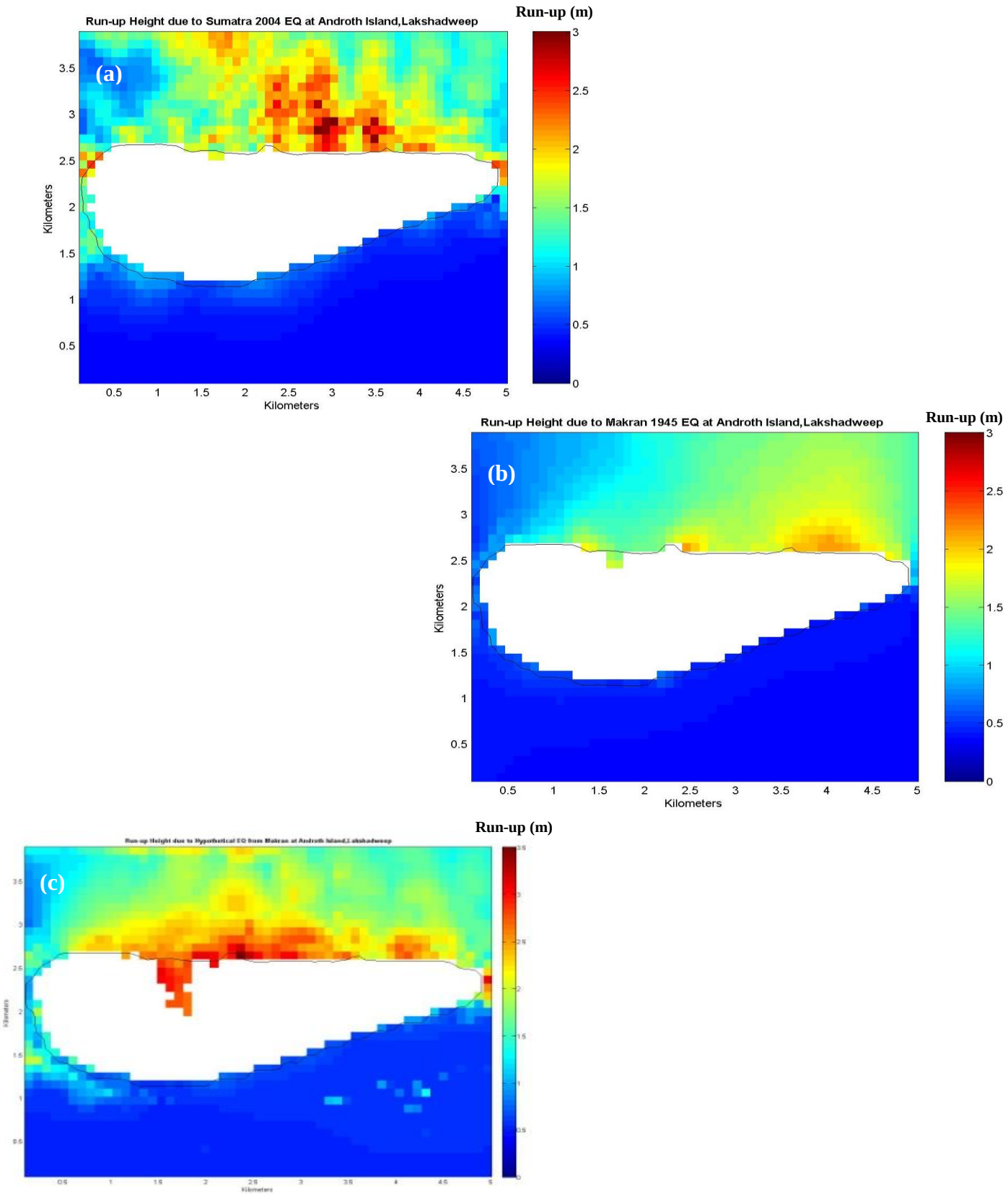

Fig. 6.21 Model simulation output for the Androth Island of Lakshadweep: (a) Sumatra 2004, (b) Makran 1945 & (c) Hypothetical worst case

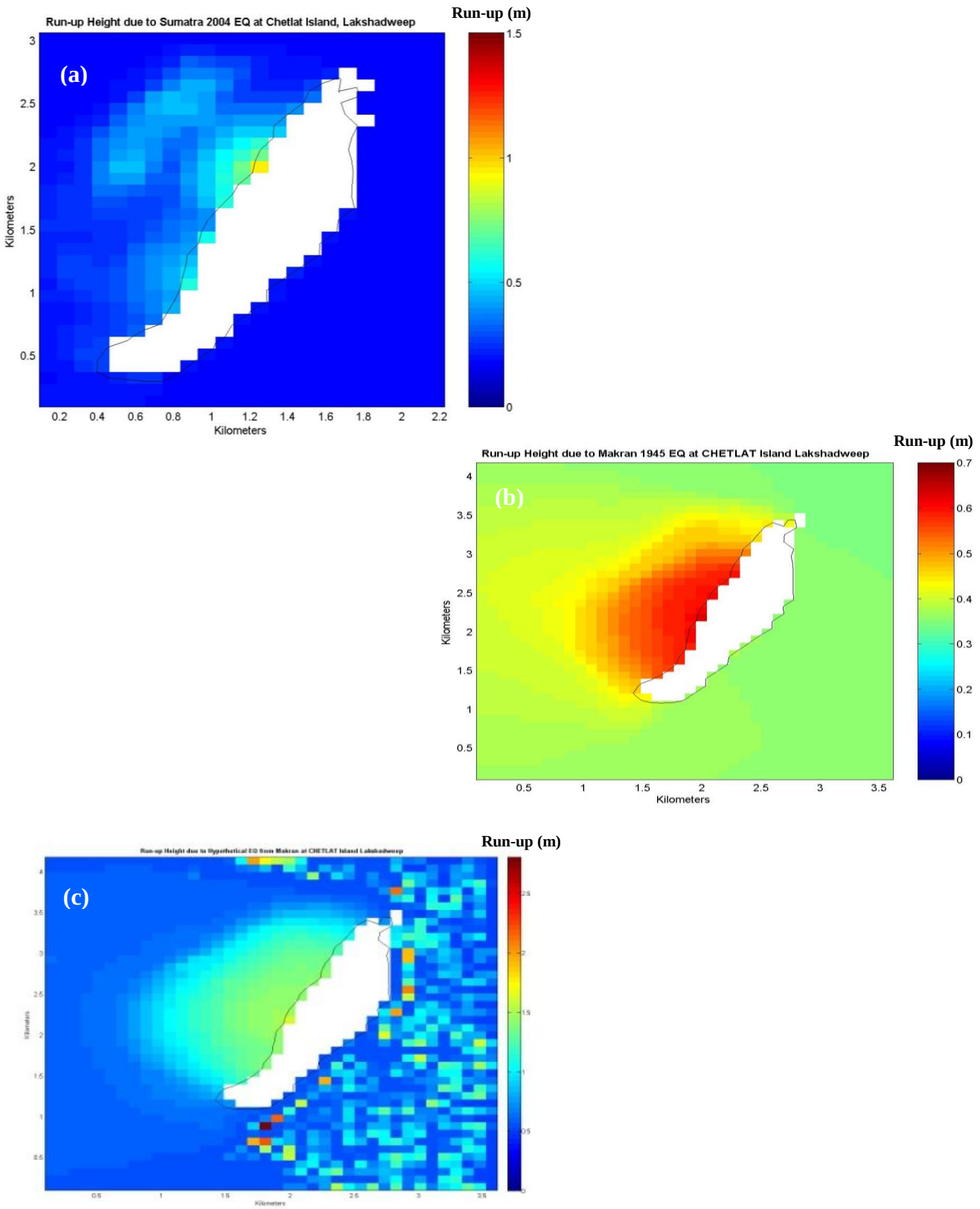

Fig. 6.22 Model simulation output for the Chetlat Island of Lakshadweep: (a) Sumatra 2004, (b) Makran 1945 & (c) Hypothetical worst case

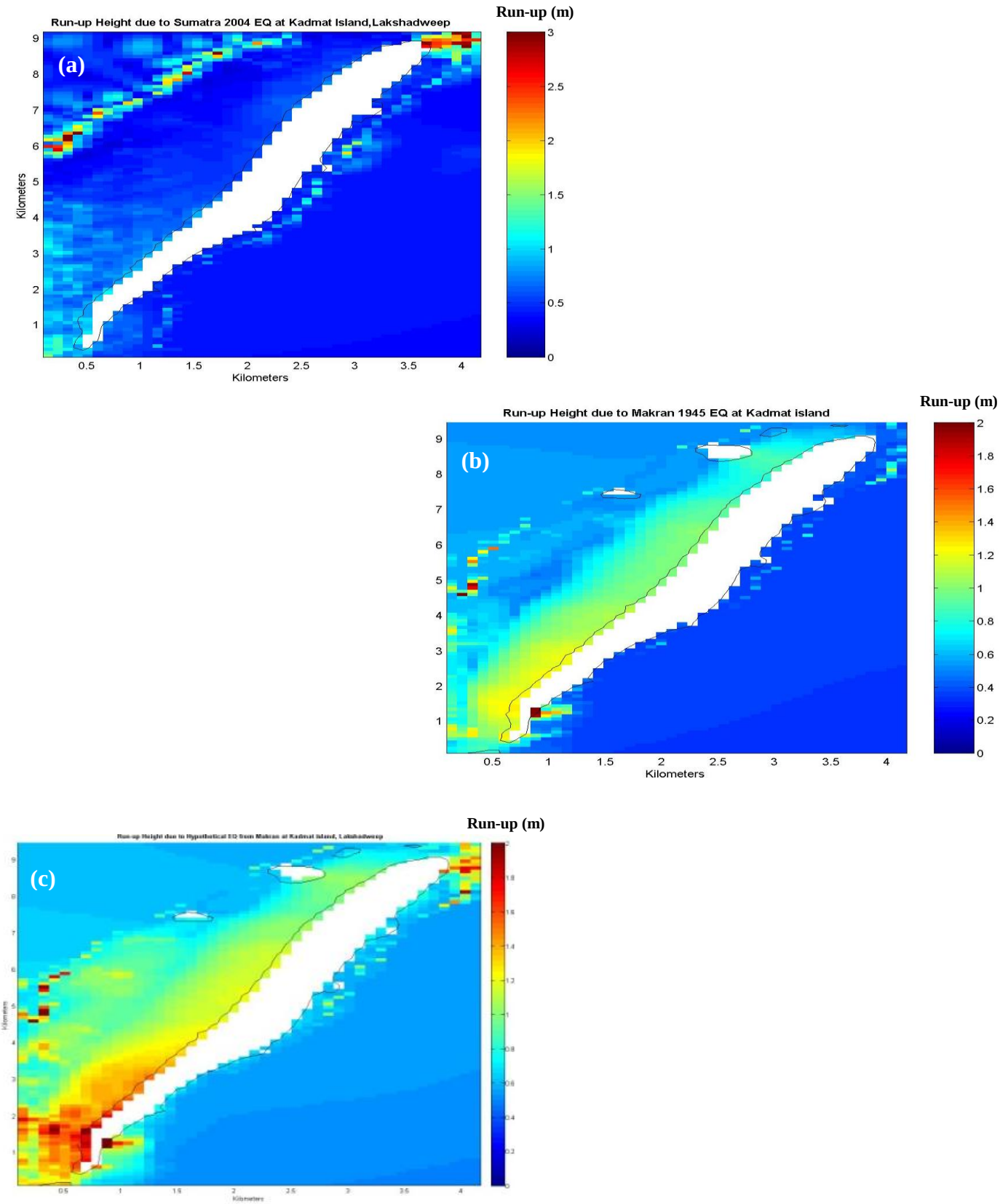

Fig. 6.23 Model simulation output for the Kadmat Island of Lakshadweep: (a) Sumatra 2004, (b) Makran 1945 & (c) Hypothetical worst case

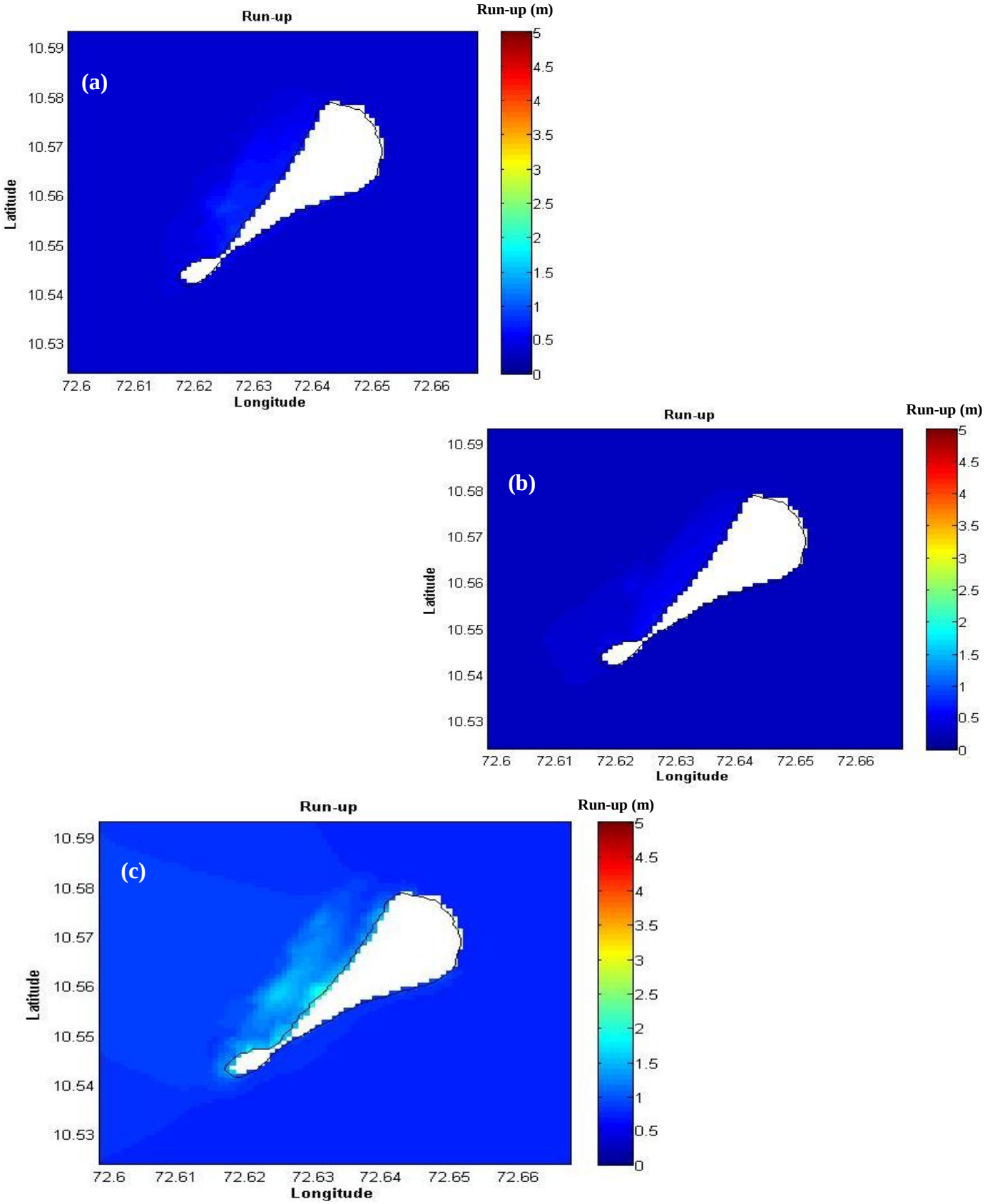

Fig. 6.24 Model simulation output for the Kavaratti Island of Lakshadweep: (a) Sumatra 2004, (b) Makran 1945 & (c) Hypothetical worst case

relatively less for the central and northern Kerala coast when compared to the higher energy southern Kerala coast (Baba and Kurian, 1988). Thus the same run-up can generally cause more inundation in the central and northern Kerala coast than the southern coast. The possibility of higher inundation along the northern Kerala coast is an important aspect from the point of view of tsunami hazard mitigation as Makran is considered to be the other potential tsunamigenic source (Chadha, 2007 and Rastogi, 2007).

The lesser run-up and inundation along the Islands of Lakshadweep when compared to the mainland can appear to be bit surprising but can be explained as follows. The Lakshadweep Islands are atolls, part of the Lakshadweep Maldive Ridge (LMR). Thus the islands stand out in the deep sea with practically no shallow seas around. The absence of shallow seas causes practically very less of shoaling and cause direct reflection of the waves after hitting the island. Though shallow lagoons are present in the western side of most of the islands, the reef crest on the seaward side bordering these lagoons dissipate a major part of the tsunami wave and thus restrict the energy input into the lagoon. When compared to the mainland, the tsunamis from Sumatra and Makran have produced only low run-up in the islands. No noticeable inundation is seen since the backshore is higher than the run-up level. It can finally be concluded that the Lakshadweep Islands are least vulnerable when compared to the mainland coast.

6.4 SUMMARY

In order to assess the tsunami vulnerability of Kerala and Lakshadweep coasts numerical simulations using the TUNAMI N2 model were carried out for three different sources viz. Sumatra 2004, Makran 1945 and a hypothetical potentially worst case from Makran. The results of tsunami vulnerability analysis in terms of run-up and inundation for the entire Kerala coast and four selected Islands of Lakshadweep viz. Androth, Chetlat, Kadmat and Kavaratti are presented. The results show strikingly different run-up and inundation characteristics for the Kerala and Lakshadweep coasts. While the Kerala coast appear to be vulnerable for inundation due to tsunami from different sources, the Lakshadweep coasts do not appear to be vulnerable to tsunami inundation.

As regards Kerala coast, the Sumatra 2004 tsunami generated run-ups as high as 5 m. However the Makran 1945, in spite of the source being in the Arabian Sea itself and proximate to the Kerala coast did not produce any significant inundation along the Kerala coast. Even the hypothetical worst case does not produce the kind of run-up along the southern Kerala coast as seen for Sumatra 2004. This can be attributed to the directivity of the tsunami generated. Though the hypothetical Makran source does not generate run-up as high as the Sumatra 2004 along the Kerala coast, it indeed appears to be more hazardous for a major part of the Kerala coast in terms of inundation. The run-up and inundation is high for major part of the Kerala coast starting from Chellanam (Ernakulam District) till Talappadi (Kasargod District) in the north for the hypothetical case.

CHAPTER 7

FUTURE SCENARIOS OF TSUNAMI INUNDATION IN VIEW OF SEA LEVEL RISE

7.0 INTRODUCTION

It is well recognized today that climate change is one of the most complex challenges that the human kind has ever faced in its history. All over the world concerted efforts are being undertaken to understand, analyse and combat the effects of climate change. The Intergovernmental Panel on Climate Change (IPCC) in its fourth synthesis report observed that “warming of the climate system is unequivocal as is now evident from observations of increases in global average air and ocean temperatures, widespread melting of snow and ice and rising global average sea level". The Sea Level Rise (SLR) emanating from climate change is expected to increase significantly the inundation and consequent damage due to any future tsunami. In this chapter an assessment of the tsunami inundation scenario is carried out for different sectors of the Kerala coast for the projected levels of SLR.

7.1 CAUSES OF SEA LEVEL RISE

The rise and the fall of sea level is influenced by both geological and climate factors. Changes in the mid ocean ridge systems may have been responsible for a drop in the sea level of 300 m over the last 80 million years (Hays and Pitman, 1973). Even today emergence and subsidence of land can have a noticeable effect on the local sea level (Boesch, 1982). The geological events affecting sea level are however generally slow and unlikely to accelerate, whereas climate influences sea level in two ways: i) by moving the earth’s water between glaciers resting on land the ocean and ii) by changing the temperature of the ocean water and thus its volume. If we think of a hypothetical situation in which all the glaciers in Antarctica and Greenland melts, sea level would definitely rise to more than 70 m. In the past lowering of sea level by around 150 m has occurred due to the accumulation of ocean waters in glaciers. Although the complete melting of land based glaciers would take thousands of years, partial melting could raise sea level by as much as a meter in the next century, whereas glaciers grounded under water could disintegrate more quickly. Hughes et al. (1979) and Bentley (1983) estimated that the

entire West Antarctic ice sheet, where the largest marine based glacier exists could enter the ocean in 200 years whereas a complete disintegration of the land based glacier will not occur in the near future. But parts of it coupled with other ice fields as well as mountain glaciers could be vulnerable in the next century. They also reported that a warmer climate could cause the SLR even without any contribution from glaciers. While the warming of the entire ocean would take several centuries, the upper layers could warm and cause SLR by as much as a meter by 2100.

The past trends in climate and sea level have indicated that for the last two million years and probably longer sea level and climate have fluctuated together in cycles of 100,000 years. During the last glacial period (12,000- 20,000 years ago), sea level was approximately 100 m lower than today (Donn et al., 1962). During the warm interglacial period temperatures and the sea have risen to approximately the levels of today, even though there is no evidence to prove that the land based glaciers in Greenland and Antarctica have completely melted in the last two million years. It is said that from the end of the last glacial until about 6000 years ago sea level rose approximately about 1 m per century (Mercer, 1972)

7.2 CONSEQUENCES OF SEA LEVEL RISE

Sea level rise has several physical consequences. They are

1) Inundation or permanent flooding
2) Enhanced flooding by coastal hazards
3) Shoreline retreat
4) Salt intrusion

A sea level rise of a few meters would inundate major portion of backshore, marshes and lowlying flood plain, besides rivers and bays. The rising sea will increase coastal erosion, pollution, storm damage and flooding. They would pose threats at a greater extent to coastal roads, bridges, breakwaters, docks, piers and water front property. As sea level rises and water depth increases near the shore, the shoreline advances shoreward facilitating erosion. Erosion will therefore accelerate on the coasts that were already retreating and may be initiated on coasts that were previously stable. The analysis of the physical impacts of a sea level rise has now become more complex by the dense human

occupation of many coastal areas, by their often high economic value and by the continuous interaction between human activities and natural processes. Submergence of coastal areas at risk will not occur gradually, but by steps, after severe storms which open breaches in natural or artificial coastal defences. Climatic changes may also modify force and direction, altering the sedimentary budgets of longshore drifts, increasing storm-surge frequencies and levels and accelerating shoreline displacements. Another cause of beach erosion from sea level rise is over wash and the resulting landward migration of coastal barriers (Massachusetts, 1981).

Sea level rise also causes the salt content of aquifers and estuaries to migrate landward. In coastal aquifers a layer of fresh water floats on top of the heavier salt water. The salt water generally focuses a wedge such that the farther inland (the higher the water table), the farther below ground is the boundary between fresh and saltwater. When sea level rise occurs, the shoreline moves landward and the boundary too move inland as well. Since the level of water table itself is determined by sea level, a rise in the sea level causes the fresh water/ salt water boundary to rise. A rise in sea level would also increase the salinity of rivers and estuaries. A decrease in the flow or an increase in the volume of water allows salt to migrate upstream. With higher sea level salt water would intrude farther into the estuary thus increasing salinity and moving the salt front farther upstream.

The advancement of the shoreline landward and deepening of the sea due to SLR will lead to significant increase in the inundated area in the event of the occurrences of a coastal hazard. The coastal hazards of particular relevance are storm surges and tsunami. A one metre increase in sea level can increase the inundated area many fold in some of the low terrain coastal sectors. So to conclude we can say that a global sea level rise would indeed make most lowlying coastal areas more vulnerable to submergence and erosion. However for an actively submerging coast where sea level problem already exists these problems will probably worsen during the next century even in the absence of an additional global sea level rise.

7.3 RATE OF SEA LEVEL RISE

The measurement of sea level was started in the early 1870s. Initially tide gauges which were installed in harbours were used for this purpose. By analyzing the past data, predictions of tides were done which were used for navigational purposes. For studying

global and regional sea level rise many modelers and oceanographers used the website (www.pol.ac.uk) of the Permanent Service for Mean Sea Level (PSMSL), of the Proud Man Oceanographic Laboratory (PMOL) UK, for getting the monthly sea level data for all the tide gauge stations over the globe (Douglas, 1991; Woodworth and Player, 2003). Church et al. (2001) in the Third Assessment Report of the IPCC reported the sea level rise in the past century to be between 1 and 2 mm/year. Bindoff et al. (2007) reported the estimated values of global sea level rise close to 1.8 mm/year for the period from 1961 to 2003.

The sea level rise studies along the Indian coasts were made by Emery and Aubrey (1989), Douglas (1991), Unnikrishnan et al. (2006), Unnikrishnan and Shankar (2007). Studies were also carried out by Clarke and Liu, (1994), Shankar (1998) and Shankar and Shetye (2001). Unnikrishnan and Shankar (2007) analyzed all the records in North Indian Ocean and estimated SLR trends for Aden, Karachi, Mumbai, Kochi, Vishakhapatnam. Their estimate of 1-2 mm/year closely matches with the findings of Church et al. (2001). The regional average SLR trends obtained from the estimates for the above stations are 1.29 mm/year. Unnikrishnan et al. (2006) estimated SLR trends for different locations of peninsular India. The SLR trends estimated by them for different periods are reproduced in Table 7.1. While Kochi records the highest rate of 1.14 mm/year, Chennai records a reverse trend with a fall in sea level of 0.65 mm/year.

Table 7.1 Rate of Sea Level Rise along selected locations of Indian Peninsula (Source: Unnikrishnan et al., 2006)

Sl.No.	Station	Period of Analysis	Rise in Sea Level (mm/year)
1	Mumbai	1878- 1994	0.78
2	Kochi	1939- 1997	1.14
3	Chennai	1955- 1994	-0.65
4	Vishakhapatnam	1939- 1994	0.75

7.4 SEA LEVEL PROJECTIONS FOR SIMULATIONS

The intergovernmental panel on climate change (IPCC) in its Third Assessment Report (TAR) predicted that by 2100 AD, global warming would rise sea level anywhere between 10 and 80 cm. The IPCC- TAR considered all the relevant factors of thermal expansion, mountain glaciers, glacial ice of Greenland and Antarctica, ground water and

soil moisture to arrive at their result. The IPCC has given future predictions of sea level in three different bands divided into low, moderate and extreme level (Fig.7.1). The lowest level predicts a rise of 0.10 m, moderate level 0.45 m and the extreme level 0.80 m over this century. The numerical model simulation for the estimation of tsunami inundation in the SLR scenario was carried out for all the three bands.

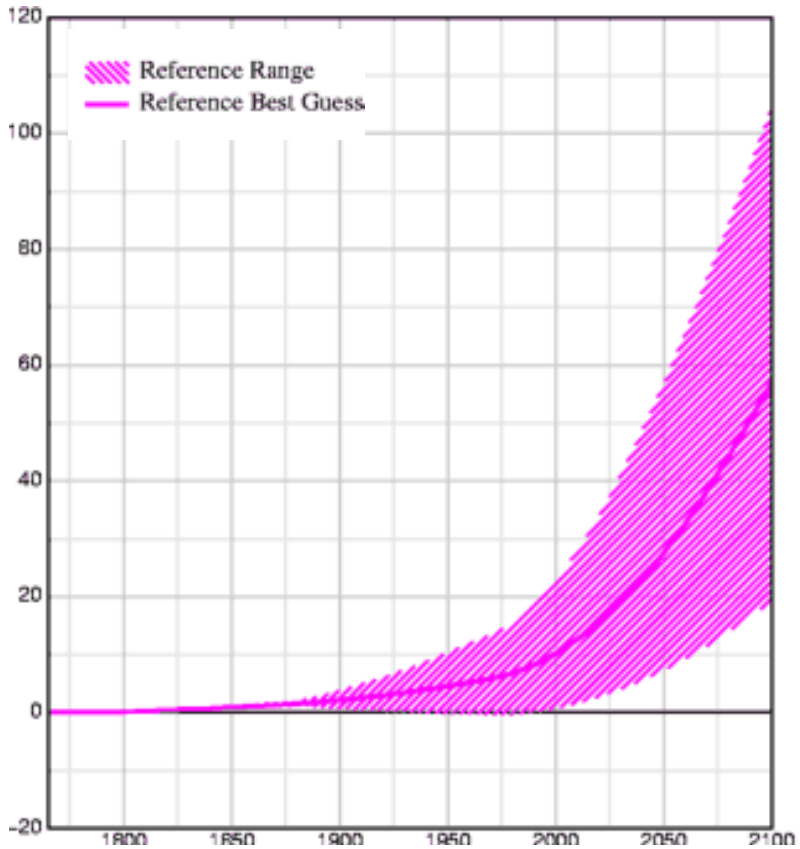

Fig. 7.1 Projections of sea level rise for the next century (IPCC, 2001)

7.5 SIMULATION RESULTS FOR SEA LEVEL RISE SCENARIOS

The simulations were carried out for three different scenarios of sea level rise with 0.10 m for the lowest level, 0.45 m for the moderate level and 0.80 m for the extreme level. In addition to the Sumatra 2004 and Makran 1945 sources the hypothetical worst case was selected for model computations taking into account the impact this case has on the Kerala coast. The simulations were carried out for three representative coastal sectors viz. Neendakara-Thottapally (Fig. 7.2, southern sector), Munambam-Valappad (Fig. 7.3, central sector) and Murad-Kannur (Fig. 7.4, northern sector). The results for the different

sectors of the coast are presented in Tables 7.2-7.4. Typical examples of simulations of worst case scenarios are presented in Figures 7.5-7.7.

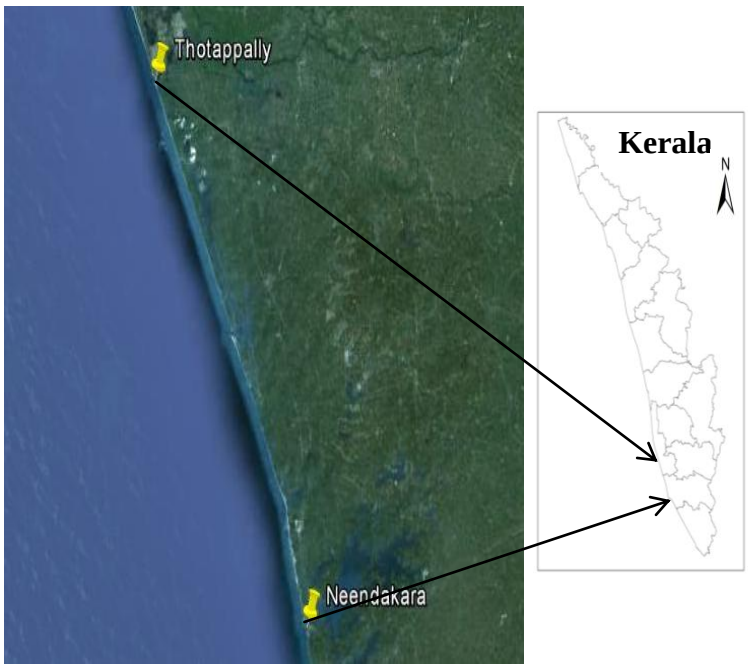

Fig. 7.2 The representative sector in the Southern Kerala for the simulation of SLR scenarios

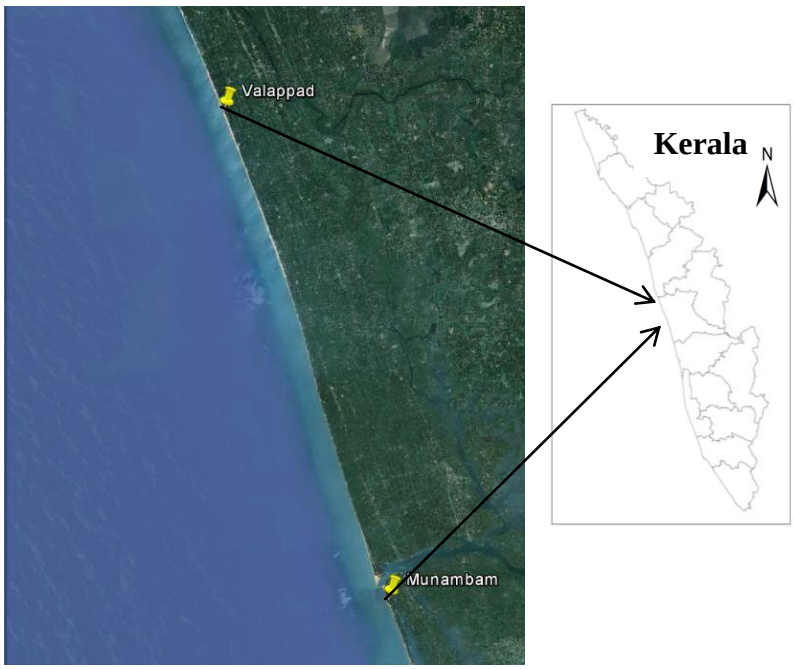

Fig. 7.3 The representative sector in the Central Kerala for the simulation of SLR scenarios

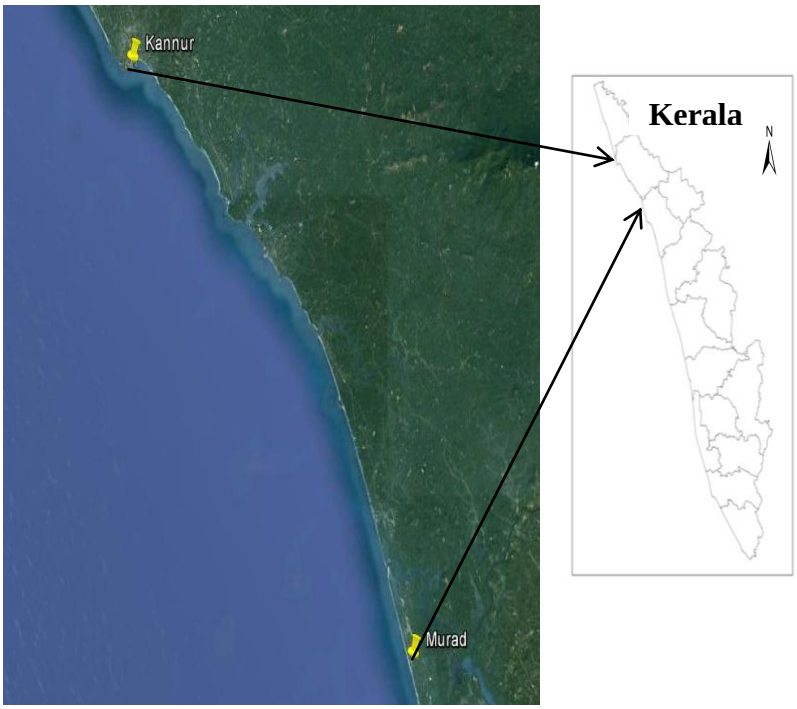

Fig. 7.4 The representative sector in the Northern Kerala for the simulation of SLR scenarios

7.5.1 Neendakara -Thottapally

The simulated inundation for the 2004 Sumatra tsunami for the Neendakara, Kovilthottam and Alappad are relatively low at 150 m, 315 m and 558 m respectively. When the extreme SLR was coupled with that, the inundation of the above mentioned locations increased to 250 m, 470 m and 645 m respectively. The extent of inundation at the above locations increased for the hypothetical case with extreme SLR. The increase in inundation value at Neendakara was phenomenal while the other two locations did not show that kind of an increase. Cheriyazhekkal, which is close to the Kayamkulam inlet, and which showed a high inundation of 2500 m for 2004 Sumatra does not show a proportionate increase even in the extreme SLR case.

The other locations north of this sector viz. Valiyazhekkal, Trikkunnapuzha and Thottapally simulated an inundation of 3087 m, 966 m and 913 m respectively for Sumatra 2004 which got increased to 3183 m, 1148 m and 2593 m for the hypothetical case with extreme SLR. Barring a few locations like Neendakara and Trikkunnapuzha, where the inundation multiplied a few times, the inundation did not show a pronounced increase for the other locations of the sector for the hypothetical case with extreme SLR.

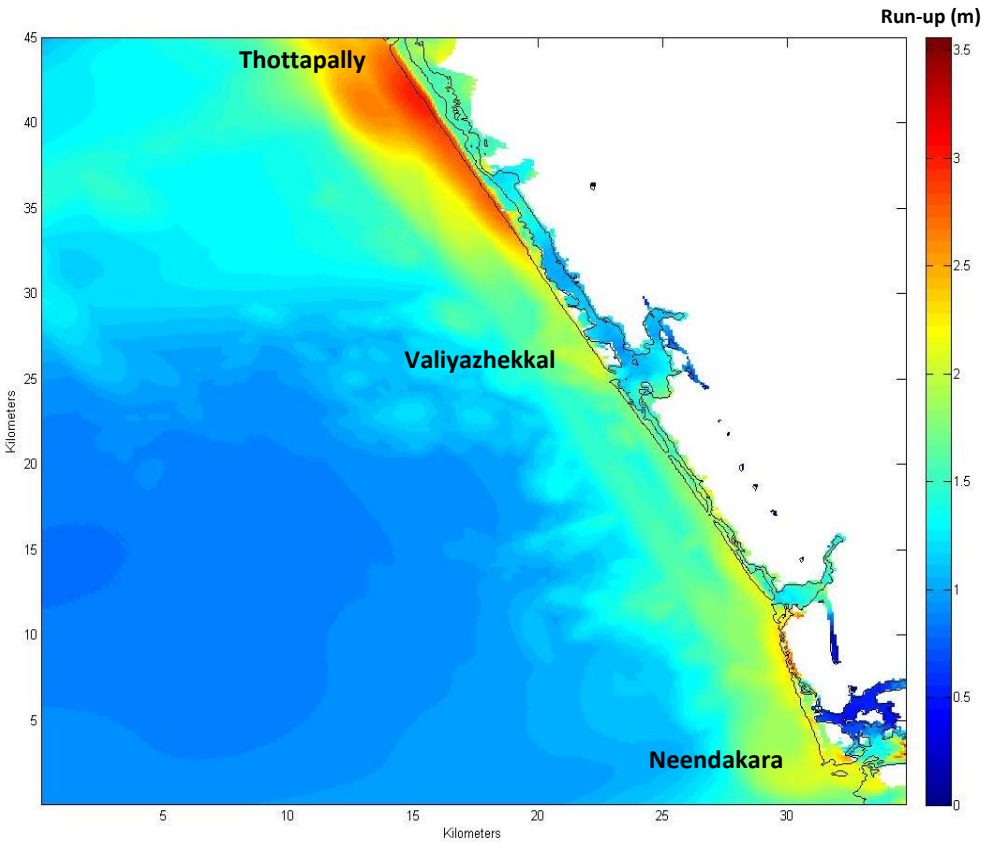

Fig. 7.5 Simulation result of the worst case SLR scenario of the Neendakara-Thottapally coastal stretch

Table 7.2 Comparison of tsunami inundation at different coastal locations of Neendakara-Thottapally sector for different sources and SLR scenario (Source: Praveen et al., 2012)

Districts	**Location**	**Inundation (m)**		
		Sumatra 2004 at present sea level	**Sumatra 2004 with Extreme Sea Level Rise**	**Hypothetical Worst Case Tsunami with Extreme Sea Level Rise**
Kollam	Neendakara	150	250	1051
	North Neendakara	541	627	1468
	Kovilthottam	315	470	430
	Alappad	558	645	774
	Cheriyazhekkal	2500	2720	2893
Alappuzha	Valiyazhekkal	3087	3250	3183
	Trikkunnapuzha	966	1050	1148
	Thottapally	913	1175	2593

7.5.2 Munambam - Valappad

The Munambam-Valappad sector of Central Kerala has very less inundation for the Sumatra 2004 with a maximum of 565 m at Perinjanam North. However, when simulation with the extreme SLR is done for both Sumatra 2004 and hypothetical case, the inundations increased to some extent. The maximum inundation is still observed at Perinjanam with values of 595 m and 764 m respectively for the extreme sea level rise scenarios of Sumatra 2004 and hypothetical case.

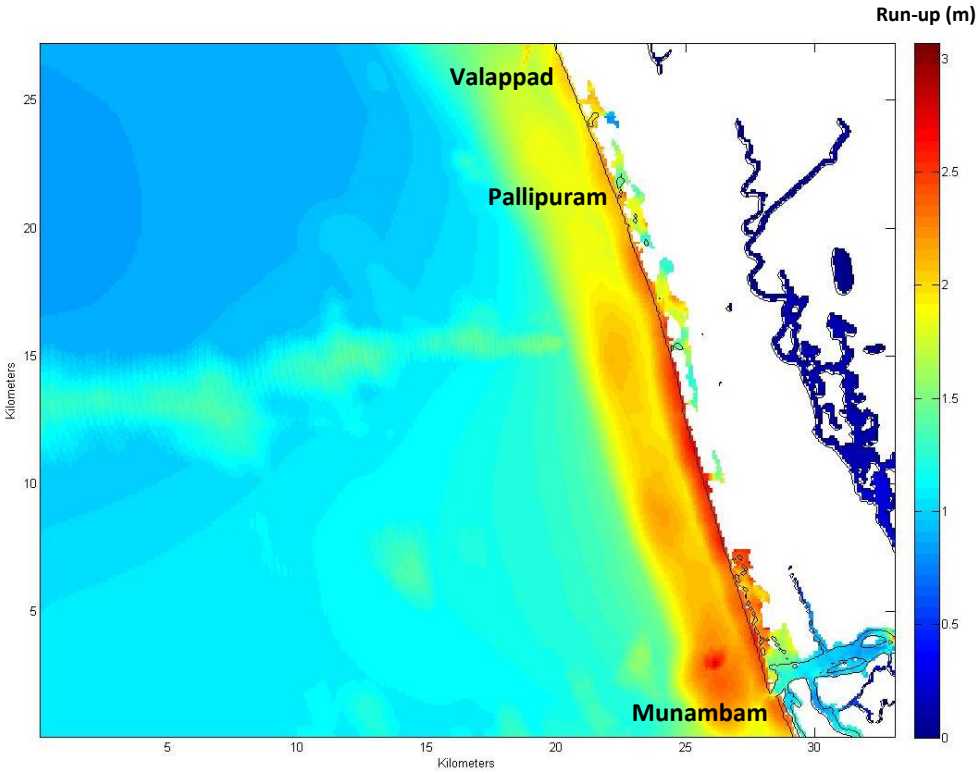

Fig. 7.6 Simulation result for the worst case SLR scenario of the Munnambam-Valappad coastal stretch

The extent of inundation at Munambam where it was 208 m and 225 m for Sumatra 2004 and Sumatra with extreme SLR respectively increased to 511 m when the hypothetical source was coupled with extreme SLR. The other locations like Palippuram, Cheraman and Valappad where no inundation was visible for the Sumatra 2004, showed an inundation in the range of 90-120 m for the Sumatra 2004 with extreme SLR and 341 m, 747 m and 400 m respectively when the extreme SLR was coupled with the hypothetical source.

Table 7.3 Comparison of tsunami inundation at different coastal locations of Munambam-Valappad sector for different sources and SLR scenario (Source: Praveen et al., 2012)

District	Location	Inundation (m)		
		Sumatra 2004 at present sea level	**Sumatra 2004 with Extreme Sea Level Rise**	**Hypothetical Worst Case Tsunami with Extreme Sea Level Rise**
Thrissur	Pallippuram	Nil	120	341
	Munambam	208	225	511
	Cheraman	Nil	90	747
	Perinjanam	565	595	764
	Valappad	Nil	90	400

7.5.3 Murad - Kannur

In the Murad-Kannur sector of northern Kerala the inundation was almost negligible for most of the locations for the Sumatra 2004 source. However, when the extreme sea level case for Sumatra 2004 is simulated, it shows some inundation at most of the locations. The hypothetical scenario with extreme SLR showed inundation at almost all the locations and Muzhappilangad showed highest inundation of 607 m.

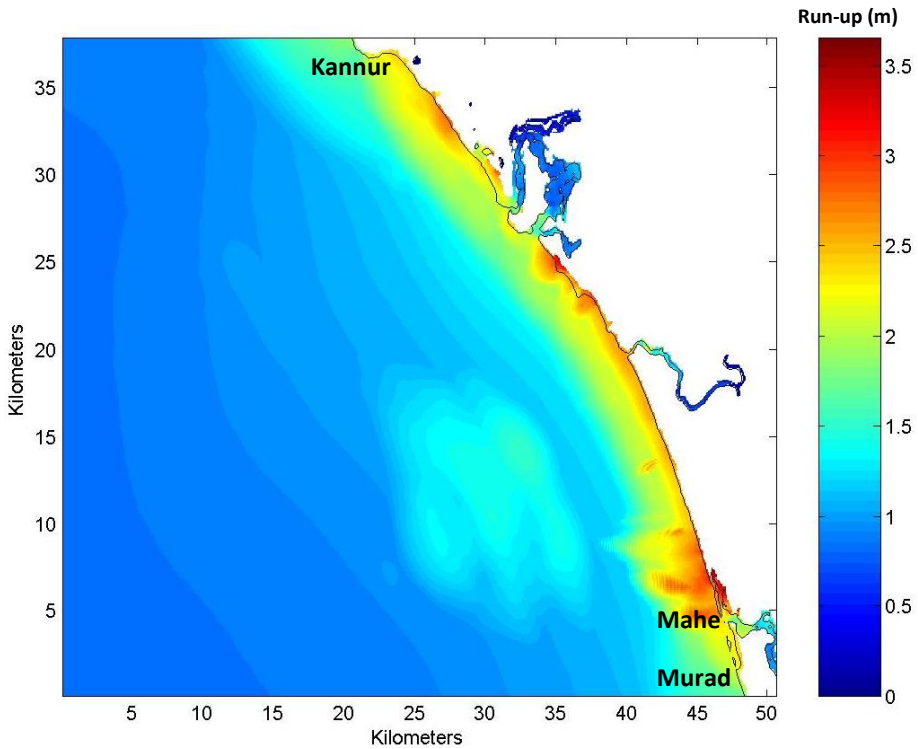

Fig. 7.7 Simulation result of the worst case SLR scenario of the Murad-Kannur coastal stretch

Table 7.4 Comparison of tsunami inundation at different coastal locations of Murad-Kannur sector for different sources and SLR scenario (Source: Praveen et al., 2012)

District	Location	Inundation (m)		
		Sumatra 2004 at present sea level	**Sumatra 2004 with Extreme Sea Level Rise**	**Hypothetical Worst Case Tsunami with Extreme Sea Level Rise**
Kannur	Ayanikkad	40	90	320
	Purakara	196	215	589
	Kuriyadi	Nil	Nil	30
	Karuvachal	Nil	30	153
	Mahe	Nil	Nil	47
	Chalil	67	90	187
	Muzhappilangad	Nil	120	607

7.6 DISCUSSION

The IPCC's projection of SLR for the next century (IPCC, 2001) gives the scenarios of sea level changes. Tsunami mitigation measures taking care of the prospects of enhanced inundation on account of SLR have to be taken up. The numerical simulations of tsunami inundation carried out for different bands of projected SLR give valuable information to facilitate mitigation measures. The simulation results show that there is no significant increase in inundation for the lower and moderate bands of sea level rise. However the potentially worst case scenario of tsunami generation compiled with extreme sea level rise can generate inundation many times higher than the normal one at locations like Neendakara and Thottapally, while the Kayamkulam inlet area continue to be a high risk zone with inundation greater than 3 km irrespective of the SLR scenario. The central and northern Kerala coasts studied are not highly vulnerable for inundation even in the extreme case of sea level rise. It is essential to carry out numerical model studies for the whole coast using accurate fine grid topographic data of the coast in order to prepare tsunami mitigation plans for climate change scenario.

7.7 SUMMARY

Climate change and associated Sea level Rise (SLR) is a reality. All over the world concerted efforts are being taken to understand, analyse and combat the effects of climate change. In this background, an analysis of the tsunami inundation scenario in the SLR

scenario is felt very important and relevant, and is undertaken. Based on the IPCC predictions of sea level, numerical modelling of tsunami inundation was carried out for three representative sectors of the Kerala coast for three scenarios of SLR viz. low, moderate and extreme. The simulations were carried out for three cases of tsunami generation viz. Sumatra 2004 at present sea level, Sumatra 2004 with extreme SLR and hypothetical worst case with extreme SLR. From the modelling results, it can be summarized that sea level rise can definitely cause manyfold increase in inundation in some of the stretches like Neendakara and Thottapally where the backshore elevation is comparatively low. It would be highly essential to carry out the numerical simulations for the extreme SLR scenarios for the whole coast by providing high resolution topographic grid for the coastal zone.

CHAPTER 8

SUMMARY AND CONCLUSIONS

8.1 SUMMARY

Tsunami is one of the most devastating natural coastal disasters. Most of the tsunamis are generated by submarine earthquakes occurring in subduction zones. Tsunamis can also be triggered by volcanic eruptions and large landslides. Although the skill for predicting earthquake is still in its infancy, tsunami warning is possible if the tsunami can be detected in the open ocean. Tsunami warning system has been operational in the Pacific Ocean for several decades and has proven its effectiveness and trustworthiness. If a similar early warning system had been available in the Indian Ocean in 2004, the devastation due to the 2004 Indian Ocean tsunami would have been much less. So the establishment of a Tsunami Warning System in the Indian Ocean was the immediate task undertaken by the Government of India in the aftermath of the 2004 Tsunami. The tsunami warning system has different components, one important component being the numerical models for prediction of tsunami inundation in the event of a tsunami. This can be accomplished by the set up of tsunami inundation models and by preparing inundation maps for vulnerable locations of the coasts for different scenarios of earthquakes. These models have to be set up for each coast and calibrated using past tsunami field data.

The set up of these models enables us to analyse the generation, propagation and inundation characteristics of tsunami and identify the different physical processes involved. It also helps us in simulating future scenarios which ultimately will pave way for planning of mitigation measures.

In the light of the above, the set up and calibration of a tsunami inundation model and an investigation on the tsunami propagation in the South East Arabian Sea (SEAS) and the scenarios of inundation characteristics along the Kerala and Lakshadweep coasts was felt very important and hence the present investigation was taken up.

The investigation which was the first of its kind for the SEAS was launched with the following objectives:

- Set up of Tsunami Inundation Model for the Kerala coast
- Study of tsunami propagation characteristics in the South East Arabian Sea (SEAS)
- Study of tsunami vulnerability along the Kerala coast for different sources
- Tsunami Vulnerability analysis for selected Islands of Lakshadweep
- Study of resonance in harbours during tsunami
- Assessment of scenarios of tsunami inundation in the context of Sea Level Rise (SLR) in the climate change scenario

An extensive review of literature pertaining to historical tsunami events in the global and Indian scenario, modelling / field investigation results on tsunami vulnerability, numerical modelling of tsunami, etc. was carried out. The literature reviews played a pivotal role in the selection of numerical model and identification of historical tsunamigenic sources used in this investigation. In the global scenario, records of tsunami are available since 1650 BC. The Pacific Ocean, being a zone of several convergent tectonic plate boundaries, is frequented by tsunamis. In Atlantic Ocean, the plate boundaries being divergent, tsunamigenic earthquakes are infrequent. Unlike the Pacific Ocean, tsunamis are not common in the Indian Ocean. Pacific Ocean reports at an average of about eight tsunamis per year, whereas Indian Ocean has one in three years or so. Out of the total 90 plus tsunamis that is reported so far for the Indian Ocean, 70 are from Sunda. Though rare, tsunamis have hit India earlier. Literature on run-up and inundation characteristics of some of the historic tsunamis is available. Being very recent, post-tsunami field survey data corresponding to the 2004 Sumatra tsunami is available for most of the Indian Ocean rim countries which were affected by the tsunami. The tsunami run-up and inundation characteristics along the Kerala coast pertaining to the 2004 Sumatra tsunami are well documented. There are several tsunami inundation models reported in the literature. TUNAMI N2 and MOST are the most widely used tsunami inundation models that are capable of modelling the entire range of tsunami wave propagation starting from its source till its inundation of the coast.

TUNAMI N2 and MOST differ in two ways. MOST uses a variable computational grid, no friction factors, and its run-up prediction is based on the elevation of the last wet grid point the wave encounters as it propagates up on the beach whereas TUNAMI N2 uses a fixed computational grid, involves a friction factor and it lets the wave advance past the initial shoreline and its maximum run-up prediction is based on the maximum wave

height at the shoreline. TUNAMI N2 gives more prominence to fine grid data which is of utmost importance while dealing with the run-up and inundation characteristics of the coast. Considering the above, as well as the fact that the Indian Tsunami Warning Centre is also relying upon this model for providing early warning, the TUNAMI N2 model was chosen for the studies under this investigation. The TUNAMI N2 numerical model uses four nested grids where the code has the option of switching to either a linear or a non-linear mode. The initial displacement is generated in the exterior domain (A), and it is interpolated into the higher resolution grids B, C and D, providing an initial sea surface profile that extends smoothly from the exterior, lower resolution, domain into the higher resolution domains.

The methodology followed involved the set up of the TUNAMI N2 model, its calibration and finally simulations using the model for various studies. As accuracy of the model output is directly linked to the accuracy and resolution of the topographic/bathymetric data used for the coastal area (Grid D), every effort was made to prepare accurate fine grid topographic/bathymetric grid. As fine grid topographic data were not available for the coastal areas, extensive topographic measurements in the 4 km zone adjoining the shoreline were carried out using dumpy level and DGPS. Bathymetric data was taken from CMAP and NHO charts, in addition to measured data available at CESS. Open source bathymetry and topography data viz. General Bathymetric Chart of the Oceans (GEBCO), SRTM, C-Map, NHO chart are used for the outer grids A, B and C. The algorithm of Mansinha and Smylie (1971) based on the seismic parameters strike, dip, slip, rake, dimensions of the rupture area and the earthquake depth was used to calculate the seafloor deformation. The TUNAMI N2 model was calibrated using post-tsunami field survey data available at CESS for Sumatra 2004, for the 34 km long Neendakara-Trikkunnapuzha sector which was the worst affected area during that tsunami. The run-up values of the calibrated model gives good correspondence with the field data with an error estimate of only 9.22 %.

In order to understand the run-up and inundation characteristics along the Kerala coast, a study of tsunami wave propagation in the SEAS was undertaken. Based on the simulations, the role of different wave transformation processes like diffraction, refraction, reflection, and total internal reflection in bringing out the observed run-up and inundation characteristics along the Kerala coast are elucidated. Simulation using the

model has successfully shown the phenomenon of Helmholtz resonance at Mangalore whereas no resonance is visible at Cochin Harbour. The lack of resonance at Cochin, unlike Mangalore, is attributed to the presence of good natural channels, eliminating the chances for the amplification caused in closed harbours like Mangalore. The role of Lakshadweep Maldive Ridge (LMR) in shaping the wave propagation and bringing out the observed inundation characteristics along the Kerala coast are specifically analysed by carrying out numerical simulations for two cases, one with LMR (present situation) and the other without LMR. It is seen that for a Sumatra 2004-like tsunami originating from the east, there is an increase in tsunami amplitudes due to the presence of LMR. The increase in run-up due to the presence of LMR is considerably high in the case of southern Kerala when compared to northern Kerala. In contrast, simulations carried out for the Makran 1945 shows that there is no reflection by LMR and the LMR impedes the run-up and inundation to a certain extent.

In order to assess the tsunami vulnerability of Kerala and Lakshadweep coasts numerical simulations using the TUNAMI N2 model were carried out for three different sources viz. Sumatra 2004, Makran 1945 and a hypothetical potentially worst case from Makran. The results of tsunami vulnerability analysis in terms of run-up and inundation for the entire Kerala coast and four selected Islands of Lakshadweep viz. Androth, Chetlat, Kadmat and Kavaratti are presented. The results show strikingly different run-up and inundation characteristics for the Kerala and Lakshadweep coasts. While the Kerala coast appear to be vulnerable for inundation due to tsunami from different sources, the Lakshadweep coasts do not appear to be vulnerable to tsunami inundation.

As regards Kerala coast, the Sumatra 2004 tsunami generated run-ups as high as 5 m. However the Makran 1945, in spite of the source being in the Arabian Sea itself and proximate to the Kerala coast, did not produce any significant inundation along the Kerala coast. Even the hypothetical worst case does not produce the kind of run-up along the southern Kerala coast as seen for Sumatra 2004. This can be attributed to the directivity of the tsunami generated. Though the hypothetical Makran source does not generate run-up as high as the Sumatra 2004 along the Kerala coast, it indeed appears to be more hazardous for a major part of the Kerala coast in terms of inundation. This anomalous behavior in inundation in spite of lower run-up can be attributed to the beach elevation.

In view of the climate change, concerted efforts are being made all over the world to understand, analyse and combat the effects of climate change. In this background, an analysis of the tsunami inundation scenario in the SLR scenario is felt very important and relevant, and is undertaken. Based on the IPCC predictions of sea level numerical modelling of tsunami inundation was carried out for three representative sectors of the Kerala coast for three scenarios of SLR viz. low, moderate and extreme. The simulation was carried out for three cases of tsunami generation viz. Sumatra 2004 at present sea level, Sumatra 2004 with extreme SLR and Hypothetical worst case with extreme SLR. From the modelling results it can be summarized that sea level rise can definitely make many fold increase in inundation in some of the stretches like Neendakara and Thottapally where the backshore elevation is comparatively low whereas the impact may not be significant in the central and northern sectors of Kerala coast. It would be highly essential to carry out numerical simulations for the extreme SLR scenarios for the whole coast by providing high resolution topographic grid for the coastal zone.

Thus the investigation has achieved all its objectives. For the first time, a calibrated model was set up for the Kerala coast for simulation of tsunami inundation. Using the model simulations, the salient aspects of tsunami wave transformation in the SEAS and its role in the observed tsunami wave characteristics along the Kerala coast, were brought out. The study has, for the first time, presented an objective analysis of the tsunami vulnerability along the Kerala and Lakshadweep coasts in terms of run-up and inundation. The study was innovative in bringing out the future scenarios of tsunami vulnerability along the Kerala coast in the context of the climate change.

8.2 RECOMMENDATIONS FOR FUTURE WORK

There is tremendous scope for further R & D efforts in this field. The following areas of work are proposed for the future.

8.2.1 Effect of Tides

Tide is an important hydrodynamic force which can definitely influence the propagation and inundation due to tsunamis. Non-linear interactions due to tide can significantly increase tsunami amplitude. In the present model tide is not incorporated. Incorporation

of tides will certainly give more accurate run-up and inundation values. So the model has to be suitably modified to include tides.

8.2.2 Initial Withdrawal of Ocean (IWO)

The Initial Withdrawal of Ocean (IWO) prior to a tsunami is usually referred as a harbinger of an upcoming tsunami wave. Kurian et al. (2006 c) analysed the initial withdrawal of ocean along the Kerala coast for the tsunami of December 26, 2004 and arrived at the conclusion that the sites which witnessed IWO and the sites which did not witness IWO do not highlight any peculiarities to differentiate them. There have been some efforts in this direction, but the IWO as observed in the field is yet to be fully explained. The post-tsunami survey data available for different coastal zones including Kerala, pertaining to the December 2004 tsunami, offers an opportunity for further research in this direction.

8.2.3 Energy Trapping

Murty et al. (2005 a-c, 2006 a-c) has discussed the trapping of long gravity energy on continental shelves through Oscillations of First Class (OFC) and Oscillations of Second Class (OSC) through the mechanism of trapped and partially leaked modes. This is one of the major processes that need to be simulated. The capability of the model in simulating the same must have to be tested out.

8.2.4 Seismic Parameters

Apart from bathymetry, seismic parameters are the most important input parameters in the numerical modelling of tsunami inundation. R & D efforts are required in formulating reliable algorithms to provide seismological parameters as model inputs.

8.2.5 Role of Other Physical Oceanographic Processes

There are several physical oceanographic processes such as swells, internal waves, currents, infra-gravity waves which can influence the run-up and inundation locally. The availability of post-tsunami survey data offers a wonderful opportunity for taking up studies in understanding the role of each and every process in the observed tsunami characteristics.

It is hoped that future research in the above lines will unravel many of the unknown characteristics of tsunami and will ultimately lead to accurate prediction of tsunami which is essential for tsunami hazard mitigation efforts.

REFERENCES

Aida, I., 1977. Tsunamis accompanied by land slides, Kaiyo-Kagaku. *J. Mar. Sci. Japan*, 9: 103-110.

Agarwal, V.K., Agarwal, N. and Rajkumar, 2005. Was there active tsunami generation during 28 March 2005 Sumatra earthquake? *Curr. Sci*., 89: 32-3.

Ambraseys, N.N. and Melville, C.P., 1982. *A History of Persian earthquakes*. Cambridge, Cambirdge University Press, 219p.

Annunziato, A. and Best, C., 2005. The tsunami event analyses and models. Institute for the protection and security of the citizen. *Joint Res. Centre, European Commission*.

Arjun, S., Kalarani., Dhanya, P., Praveen, S.S., Reshmi, A.K., Kurian, N.P., Ramanamurthy, M.V., Shahul Hameed, T.S. and Prakash, T.N., 2011. Numerical simulation of the Makran 1945 tsunami on the southwest coast and Lakshadweep Islands of India. *Mar. Geod. Spec. Tsunamis*, 34: 68-76.

Babeyko, A. and Sobolev, S., 2005. A Numerical simulation of the Indian Ocean Tsunami 26 December 2004. http://www.gfzpotsdam.de/news/recent/archive /20041226/ Tsunami Modelling/content.html.

Baba, M. and Kurian, N.P., 1988. *Ocean waves and beach processes of south west coast of India and their prediction*. Centre for Earth Science Studies, Trivandrum, 249p.

Baba, M., Kurian, N.P., Murali Krishnan, B.T., Nirupama, N. and Murty, T.S., 2006. Analysis of the tsunami of 26 December 2004 on the Kerala coast of India - Part II: Arrival times. *Mar. Geod.*, 29: 271-276.

Bapat, A., 2007. Tsunamigenic vulnerability of west coast of India. *Proc. Fourth Indian Nat. Conf. Harb. Ocean Engg*., National Institute of Technology, Karanataka, Surathkal, 426-431.

Bendick, R. and Bilham, R., 1999. A search for buckling of the south west Indian coast related to Himalayan collision. In: A. Macfarlame, R.B. Sorkhabi and J. Quade

(Eds.) Himalayan and Tibet: mountain roots to mountain tops. *Geol. Soc. America Spec*., 328: 313-322.

Bentley, C.R., 1983. West Antarctic ice sheet: Diagnosis and prognosis In; *Proc. Carbon Dioxide Res. Conference:* Carbon dioxide Science and Consensus. Conference 820970. Washington, D.C., Department of Energy IV.3-IV. 50.

Berninghausen, W.H., 1966. Tsunamis and seismic Seiches reported from regions adjacent to the Indian Ocean. *Bull. Seism. Soc. America*, 56: 69-74.

Biham, R., Engdahl, R., Feld, N. and Sayabala, S.P., 2005. Partial and complete rupture of the Indo-Andaman plate boundary from 1847-2004. *Seism. Res. Lett*., 76: 299-311.

Bindoff, N.L., Willebrand, J., Artale, V., Cazenave, A., Gregory, J., Gulev, S., Hanawa, K., Le Quere, C., Levitus, S., Nojiri, Y., Shum, C.K., Talley, L.D. and Unnikrishnan, A., 2007. Observations: Oceanic climate change and sea Level. In: S. Solomon, D. Qin, M. Manning, Z. Chen, M. Marquis, K.B. Averyt, M. Tignor and H.L. Miller (Eds.) *Climate Change 2007: The Physical science basin*, Cambridge University Press, 385-432.

Boesch, D.F., 1982 (Ed.). *Proc. Conf. on Coastal Erosion and Wetland Modification in Louisiana*: Causes, consequences and options. FWS-OBS-82/59. Washington, D.C., Fish and Wildlife service, Biological services program.

Borah, R., Rajapaksha, J., Hazarika, M.K. and Samarkoon, L., 2007. Report on tsunami risk assessment of Galle city, SriLanka integrating numerical model with remote sensing and GIS data. *Proc. Asian Conf. Remote Sensing*, TW 2.1.

Borrero, J.C., 2005. Field survey of northern Sumatra and Banda Aceh, Indonesia after the tsunami and earthquake of 26 December 2004. *Seism. Res. Lett*., 75: 312-320.

Byrne, D.E., Sykes, L.R. and Davis, D.M., 1992. Great thrust earthquakes and aseismic slip along the plate boundary of the Makran subduction zone, *J. Geophys. Res*., *97*: 449-478.

Chadha, R.K., 2007. Tsunamigenic sources in the Indian Ocean: Factors and impact on the Indian landmass, In: T.S. Murty, U. Aswathanarayana and N. Nirupama (Eds.) *The Indian Ocean Tsunami*, Taylor and Francis/ Balkema, Netherlands, 33-48.

Chittibabu, P. and Murty, T.S., 2006. Numerical models for the Indian Ocean tsunami of 26 December 2004: A Brief Review, In: T.S. Murty, U. Aswathanarayana and N. Nirupama (Eds.) *The Indian Ocean Tsunami*, Taylor & Francis, 159-173.

Chlieh, M., Avouac, J.P., Hjorleifsdottir, V., Song, T.R.A., Ji, C., Sieh, K., Sladen, A., Hebert, H., Prawirodirdjo, L., Bock, Y. and Galetska, J., 2007. Coseismic slip and afterslip of the great Mw 9.15 Sumatra-Andaman earthquake of 2004. *Bull. Seism. Soc. America*, 97: S152-S173.

Church, J.A., Gregory, J.M., Huybrechts, P., Kuhn, M., Lambeck, K., Nhuan, M.T., Qin, D. and Woodworth, P.L., 2001. Changes in sea level. In: M. Noguer, P. Van der Linden, X. Dai, K. Maskell, C.I. Johnson, J.T.Y. Ding and D.J. Griggs (Eds.) *Climate change 2001: The scientific basis*. Contribution of Working Group 1 to the Third Assessment Report of the Intergovernmental Panel on Climate Change. Houghton, Cambridge University Press, 639-694.

Clarke, A.J. and Liu, X., 1994. Interannual sea level in the northern and eastern Indian Ocean. *J. Geophys. Res*., 99: 1224-1235.

Divyalakshmi, K.S., Rammohan, V. and Ramana Murthy, M.V., 2011. Modification of tsunami wave by submarine canyon: Case study of multiple canyons at south east coast of India. *Mar. Geod. Spec. Tsunamis*, 34: 2-15.

Donn, W.L., Farand, W.R. and Ewing, M., 1962. Pleistocene ice volumes and sea level lowering. *J. Geol*., 70: 206-214.

Douglas, B.C., 1991. Global sea level rise. *J. Geophys. Res*., 96: 6981-6992.

Emery, K.O. and Aubrey, D.G., 1989. Tide guage of India. *J. Coast. Res*., 5: 489-501.

Fujima, K., Masamura, K. and Goto, C., 2002. Theoretical examinations of long-wave damping by sea bottom friction. *Coast. Engg. J*., 44: 217-245.

Goto, C. and Ogawa, Y., 1992. Numerical method of tsunami simulation with the leap-frog scheme. Translated for the TIME Project by N. Shuto, Disaster Control Res. Cent., Faculty of Engg. Tohoku Univ. Japan.

Goto, C., Ogawa, Y., Shuto, N. and Imamura F., 1997. Numerical method of tsunami simulation with the leap-frog scheme (IUGG/IOC Time Project), IOC Manual, UNESCO, No. 35.

Goto, C. and Shuto, N., 1983. Effects of large obstacles on tsunami inundations. In: K. Iida and T. Iwasaki (Eds.) *Tsunamis: Their science and engineering*, Tokyo, 521-525.

Gupta, H., 2005. Mega-Tsunami of 26 December 2004: Indian initiative for early warning system and mitigation of oceanogenic hazards. *Episode*, 28: 1-5.

Gusiakov, V.K., 1978. Static displacement on the surface of an elastic space. Ill-posed problems of mathematical physics and interpretation of geophysical data, Novosibirsk, *VC SOAN SSSR*, 23-51.

Hays, J.D. and Pitman, W.C., 1973. Listhospheric plate motion, sea level changes and climatic and ecological consequences. *Nature*, 246: 18-22.

Heck, N.H., 1947. List of seismic sea waves. *Bull. Seism. Soc. America*, 37: 269-286.

Heidarzadeh, M., Pirooz, M.D., Zaker, N.H., Yalciner, A.C., Mokhtari, M. and Esmaeily, A., 2008. Historical tsunami in the Makran subduction zone off the southern coasts of Iran and Paksitan and results of numerical modelling. *Ocean Engg*., 35: 774-786.

Heidarzadeh, M., Pirooz, M.D., Zaker, N.H. and Synolakis, C.E., 2008. Evaluating tsunami hazard in the northwestern Indian Ocean. *Pure Appl. Geophys*., 165: 2045-2058.

Heidarzadeh, M., Pirooz, M.D., Zaker, N.H. and Yalciner, A.C., 2009. Preliminary estimation of the tsunami hazards associated with the Makran subduction zone at the northwestern Indian Ocean. *Natural Hazards*, 48: 229-243.

Heidarzadeh, M. and Kijko, M., 2010. A probabilistic tsunami hazard assessment for the Makran subduction zone at the northwestern Indian Ocean. *Natural Hazards*, 56: 577-593.

Hettiarachchi, S.S.L. and Samarawickrama, S.P., 2005. Experience of the Indian Ocean tsunami on the Sri Lankan coast. *Int. Conf. on Coastlines Structures and Breakwaters, Institution of Civil Engineers*, United Kingdom, 20-22.

Hibbard, S. and Peregrine, Y., 1979. Surf and run-up on a beach: A uniform bore. *J. Fluid Mech*., 95: 323-345.

Hirata, K., Satake, K., Tanioka, Y., Kuragano, T., Hasegawa, T., Hayashi, Y. and Hamada, N., 2005. The Indian Ocean Tsunami: Tsunami source model from satellite altimetery. G.A. Papadopoulos and K. Satake (Eds.) *Proc. Int. Tsunami Symp*., Chania, Greece, 72-76.

Houston, J.R. and Butler, H.L., 1979. A numerical model for tsunami inundation. U.S. Army Corps of Engineers, Hydraulic Laboratory, Waterways Experiment Station, Viksburg, Mississippi, *Tech. Rep*. HL-79-2.

Hughes, T., Fastook, J.L. and Denton, G.H., 1979. *Climatic warming and the collapse of the west Antarctic ice sheet*. Orano, Marine, University of Maine.

Ilayaraja, K., Ioualaleln, M., Chileh, M., Krishnamurthy, R.R. and Ramana Murthy, M.V., 2008. Numerical modelling of the 26 December 2004 Indian Ocean tsunami at Andaman and Nicobar Islands, *J. Coast. Conserv*., 12: 115-124.

Imamura, F., 1996. Review of tsunami simulation with a finite difference method. In: H. Yeh, P. Liu, C. Synolakis and N.J. Hackensack (Eds.) L*ong wave run-up models*, World Scientific Publishing Co., 25-42.

Imamura, F., 2006. TUNAMI-N2 (Tohoku University's numerical analysis model for investigation of near field tsunamis version 2 Manual draft, http://www.tsunami. civil .tohoku.ac.jp/hokusai3/J/projects/manual-ver-3.1.pdf.

Ioualalen, M., Migeon, S. and Sardou, O., 2010. Landslide tsunami vulnerability in the Ligurian Sea: Case study of the 1979 nice airport submarine landslide and of identified geological mass failure, *Int. J. Geophys*., 181: 724-740.

IPCC., 2001. Intergovernmental Panel on Climate Change. IPCC Third Assessment Report - The Scientific Basis. The IPCC Secretariat, Switzerland.

Jackson, J.A. and McKenzie, D., 1984. Active tectonics of the Alpine-Himalayan belt between western Turkey and Pakistan. *Geophys. J.R. Astr. Soc*., 77, 185-264.

Jaiswal, R.K., Singh, A.P. and Rastogi, B.K., 2008. Simulation of the Arabian Sea tsunami propagation generated due to 1945 Makran earthquake and its effect on western parts of Gujarat, India. *Natural Hazards*, 48: 245-248.

Jayakumar, S., Ilangovan, D., Naik, K.A., Gowthaman, R., Tirodkar, G., Naik, G.N., Ganesan, P., Mani Murali, R., Michael, G.S., Ramana Murthy, M.V. and Bhattacharya, G.C., 2005. Run-up and inundation limits along southeast coast of India during the 26 December 2004 Indian Ocean tsunami. *Curr. Sci*., 88: 1741-1743.

Kajiura, K., 1963. The leading wave of a tsunami. *Bull. Earthq. Res. Inst*., 41: 535-571.

Kajiura, K., 1970. Tsunami source, energy and the directivity of wave radiation. *Bull. Earthq. Res. Inst*., 48: 835-869.

Kervella, Y., Denys, D. and Frederic, D., 2007. Comparison between three dimensional linear and non linear tsunami generation models. *Theor. Comput. Fluid Dyn*., 21: 245-269.

Koh, H.L., Teh, S.Y., Liu, P.L.F., Izani, A.M.I. and Lee, H.L., 2009. Simulation of Andaman 2004 tsunami for assessing impact on Malaysia. *J. Asian Earth Sci*., 36: 74-83.

Kopp, C., Fruehnb, J., Flueha, E.R., Reichert, C., Kukowski, N., Bialas, J. and Klaeschena, D., 2000. Structure of the Makran subduction zone from wide-angle and reflection seismic data. *Tectonophys*., 329: 171-191.

Kowalik, Z., Knight, W., Logan, T. and Whitmore, P., 2005a. Numerical modelling of the global tsunami: Indonesian tsunami of 26 December 2004. *Sci. Tsunami Haz*ards 23: 40-56.

Kowalik, Z., Knight, W., Logan, T. and Whitmore, P., 2005b. The tsunami of 26 December 2004: Numerical modelling and energy considerations, *Proc. Int. Tsunami Sym*., Eds. G.A. Papadopoulos and K. Satake, Chania, Greece, 140-150.

Kurian, N.P., Rajith, K., Murali Krishnan, B.T., Kalaiarasan, P. and Abilash, P.P., 2005. December 2004 Tsunami: Run up level and impact along the Kerala coast, In: S.M. Ramaswamy and C.J. Kumanan (Eds.) *Tsunami: The Indian Context*, Allied Publishers, Chennai, 111-127.

Kurian, N.P., Abilash, P.P., Rajith, K., Murali Krishnan, B.T. and Kalaiarasan, P., 2006. Inundation characteristics and geomorphological impacts of December 2004 tsunami on Kerala coast. *Curr. Sci*., 90: 240-249.

Kurian, N.P., Prakash, T.N., Baba, M. and Nirupama, N. 2006a. Observations of tsunami impact on the coast of Kerala, India. *Mar. Geod*., 29: 135-145.

Kurian, N.P., Baba, M., Rajith, K., Nirupama, N. and Murty, T.S., 2006b. Analysis of the tsunami of 26 December 2004 on the Kerala coast of India - Part I: Amplitudes. *Mar. Geod.*, 29: 265-270.

Kurian, N.P., Rajith, K., Murali Krishnan, B.T., Nirupama, N. and Murty, T.S., 2006c. Analysis of the Tsunami of 26 December 2004 on the Kerala coast of India - Part III: Inundation and Initial Withdrawal. Marine Geodesy, 29, 277-281.

Kurian, N.P., Prakash, T.N. and Baba, M., 2007. Field observations on the tsunami impact along the Kerala coast, southwest India, In: T.S. Murty, U. Aswathanarayana, and N. Nirupama (Eds.) *The Indian Ocean Tsunami*, Taylor & Francis/Balkema, Netherlands, Ch. 27, 323-338.

Lay, T., Kanamori, H., Ammon, C., Nettles, M., Ward, S., Aster, R., Beck, S., Bilek, S., Brudzinski, M., Bulter, R., DeShon, H., Ekstrom, G., Satake, K. and Sipkin, S.,

2005. The great Sumatra-Andaman earthquake of 26 December 2004. *Science*, 308: 1127-1133.

Lisitzin, E., 1974. *Sea-level changes*, Elsevier Oceanographic series, No. 8, Elsevier Sci, Publ. Co., Amsterdam, Oxford, New York, 286p.

Macmurdo, C., 1821. Account of the Earthquake which occured in India in June 1819. *Edinburgh Phil. J.*, 4: 106-109.

Mansinha, L. and Smylie, D.E., 1971. The displacement field of inclined faults. *Bull. Seism. Soc. America*, 61: 1433-1440.

Massachusetts, State of., 1981. Barrier Beaches: A few questions answered, Boston: *Massachusetts Office of Coast. Zone Management*.

Mathur, S.M., 1998. *Physical Geology of India*. National Book Trust of India, New Delhi 180p.

Mercado, A. and McCann, W., 1998. Numerical simulation of the 1918 Puerto Rico tsunami. *Natural Hazards*, 18: 57-76.

Merrifield, M.A., Firing, Y.L., Aarup, T., Agricole, W., Brundrit, G., Chang-Seng, D., Farre, R., Kilonsky, B., Knight, W., Kong, L., Magori, C., Manurung, P., McCreery, C., Mitchell, W., Pillay, S., Schindele, F., Shillington, F., Testut, L.,Wijeratne, E.M.S., Caldwell, P., Jardin, J., Nakahara, S., Porter, F.Y. and Turetsky, N., 2005. Tide gauge observations of the Indian Ocean tsunami, December 26, 2004. *Geophys. Res. Lett*., 32: L09603, doi: 10.1029/ 2005GL022610.

Mercer, J.H., 1972. The lower boundary of the Holocene. *Quat. Res*., 2: 15-24.

Mohan, R.V. and Krishnamurthy, R.R., 2007 Early warning system development for tsunami and storm surges in Indian Ocean. http: // sitesources.worldbank.org / CMUDLP / Resources / Day4-3 ram_mohan_kris.pdf.

Muraleedharan, G., Sinha, M., Rao, A.D. and Murty T.S., 2006. Statistical simulation of the boxing day tsunami of the Indian Ocean and a predictive equation for beach run up heights based on work energy theorem. *Mar. Geod.*, 29: 223-231.

Murty, T.S., 1984. Storm surges-meterological ocean tides. *Bull. 212. Fish. Res. Board*, Canada, Ottawa, 897p.

Murty, T.S., Bapat, A. and Prasad, V., 1999. Tsunamis on the coastlines of India. *Sci. Tsunami Haz*ards, 17: 167-172.

Murty, T.S., Nirupama, N., Nistor, I. and Rao, A.D., 2005. Leakage of the Indian Ocean tsunami energy into the Atlantic and Pacific Oceans, *Can. Assoc. Explor. Geophys*., *CSEG Recorder*, 33-36.

Murty, T.S., Rao, A.D. and Nirupama, N., 2005a. Inconsistencies in travel times and amplitudes of the 26 December 2004 Tsunami. *J. Mar. Med*., 7: 4-11.

Murty, T.S., Nirupama, N., Nistor, I. and Rao, A.D., 2005b. Conceptual differences between the Pacific, Atlantic and Arctic tsunami warning systems for Canada. *Sci. Tsunami Hazards*, 23: 39-51.

Murty, T.S., Nirupama, N. and Rao, A.D., 2005c. Why the earthquakes of 26 December 2004 and the 27 March 2005 differed so drastically in their tsunami-genic potential. *Newslett., Voice of the Pacific*, 21: 2-4.

Murty, T.S., Nirupama, N., Nistor, I. and Hamdi, S., 2006a. Far field characteristics of the tsunami of 26 December 2004. *ISET J. Earthq. Technol*., 42: 213-217.

Murty, T.S., Nirupama, N., Nistor, I. and Hamdi, S., 2006b. Why the Atlantic generally cannot generate trans-oceanic tsunamis. *ISET J. Earthq. Technol*., 42: 227-236.

Murty, T.S., Rao, A.D., Nirupama, N. and Nistor, I., 2006c. Numerical modelling concepts for the tsunami warning systems. *Curr. Sci*., 90: 1073-1081.

Murty, T.S., Kurian, N.P. and Baba, M., 2008. Roles of reflection, energy trapping and secondary undulations in the tsunami on Kerala coast. *Int. J. Ecol. Dev*., 10: 100-114.

Narayana, A.C., Tatavarti, R. and Shakdwipe, M., 2005. Tsunami of 26 December 2004: Observation on Kerala coast. *J. Geol. Soc. India*, 265: 239-246.

Nelson, C., 1846. Notice of an earthquake and a probable subsidence of the land in the district of Cutch near the mouth of Koree, on the eastern branch of the Indus in June 1845. *Quart. J. Geol. Soc. London*, 2: 103-107.

Nirupama, N., Murty, T.S., Rao, A.D. and Nistor, I. 2005a. The Role of gravoid and elastoid modes in oscillations around Andaman and Nicobar Islands. In: V. Sundar (Ed.) *Indian Ocean Tsunami*, Indian Institute of Technology, Madras, India, 41-52.

Nirupama, N., Murty, T.S., Rao, A.D. and Nistor, I., 2005b. Numerical tsunami models for the Indian Ocean countries and states. *Indian Ocean Surv*., 2: 1-14.

Nirupama, N., Murty, T.S., Nistor, I. and Rao, A.D., 2006. The energetics of the tsunami of 26 December 2004 in the Indian Ocean: A brief review. *Mar. Geod*., 29, 39-48.

Okada, Y., 1985. Surface deformation due to shear and tensile faults in a half-space. *Bull. Seism. Soc. America*, 75: 1135-1154.

Ortiz, M. and Bilham, R., 2003. Source area and rupture parameters of the 31 December 1881 Mw = 7.9 Car Nicobar earthquake estimated from tsunamis recorded in the Bay of Bengal. *J. Geophys. Res. Solid Earth*, 108: 1-16.

Page, W.D., Alt, J.N., Cluff, L.S. and Plafker, G., 1979. Evidence for the recurrence of large magnitude earthquakes along the Makran coast of Iran and Pakistan. *Tectonophys*., 52: 533-547.

Papazachos, B.C., Scordilis, E.M., Panagiotopoulos, D.G., Papazachos, C.B. and Karakaisis, G.F., 2004. Global relations between seismic fault parameters and moment magnitude of earthquakes. *Bull. Geol. Soc. Greece*, 36: 1482-1489.

Papadopoulos, G.A., Caputo, R., McAdoo, B., Pavlides, S., Karastathis, V., Fokaefs, A., Orfanogiannaki, K. and Valkaniotis, S., 2006. The large tsunami of 26 December

2004: Field observations and eyewitnesses accounts from Sri Lanka, Maldives Isand and Thailand. *Earth Planets and Space*, 58: 233-241.

Pararas-Carayannis, G. 2006b. The Earthquake and tsunami of 28 November 1945 in southern Pakistan. http://drgeorgepc.com/Tsunami1945Pakistan.html.

Pendse, C.G., 1946. The Mekran earthquake of the 28 November, 1945. *India Meteorological Depart. Scientific Notes* 10: 141-145.

Prakash, T.N., Kurian, N.P., Rajith K., Abilash, P.P., Murali Krishnan, B.T., Kalaiarasan, P. and Tiju Varghese., 2005. December 2004 Tsunami: Some results of field surveys along the Kerala coast, *Proc. Nat. Workshop on Tsunami and Mitigation Measures*, Dept. of Ocean Engineering, IIT Madras, 307-320.

Prakash, T.N., Chattopadhyay, S. and Nair, A.S.K., 2006. Impact of Tsunami on the Kerala coast and rehabilitation plan for the worst affected stretch at Alappad. In: G.V. Rajamanickam (Ed.) *26th December 2004 Tsunami: Causes, effects, remedial measures, pre and post tsunami disaster management- A geoscientific perspective*. New Academic Publishers, New Delhi, 150-174.

Praveen, S.S., Reshmi, A.K., Dhanya, P., Arjun, S., Kalarani, Kurian, N.P., Ramana Murthy, M.V., Shahul Hameed, T.S. and Prakash, T.N., 2011. Numerical simulation of 26 December 2004 Tsunami on the southwest coast and Lakshadweep Islands of India. *Mar. Geod. Spec. Issue on Tsunamis*, 34: 59-67.

Praveen, S.S., Kurian N.P. and Shahul Hameed, T.S., 2012. Tsunami inundation modelling for the coast of Kerala, India. *Mar. Geod*. in press.

Rabinovich, A.B. and Thomson, R.E., The 26 December 2004 Sumatra tsunami: Analysis of tide gauge data from the World Ocean. Part-1. Indian Ocean and South Africa, *Pure Appl. Geophys*., 164: 261-308.

Rajakumari, S. and Subramaniyan, B.R., 2011. Behaviour of tsunami waves along the coasts of Kancheepuram and Villupuram districts in Tamil Nadu, India. *Natural Hazards* 60: 101-114.

Rajendran, C.P., Ramana Murthy, M.V., Reddy, N.T. and Kusala Rajendran, 2008. Hazard implication of the late arrival of the 1995 Makran tsunami. Curr. Sci., 95: 1739-1743.

Ramana Murthy, M.V., Sundaramoorthy, S., Pari, Y., Ranga Rao, V., Mishra, P., Bhat, M., Usha, T., Venkatesan, R. and Subramanian, B.R., 2005. Inundation of seawater in Andaman and Nicobar Islands and parts of Tamil Nadu coast during 2004 Sumatra tsunami. *Curr. Sci*., 88: 1736-1740.

Ramana Murthy, M.V., Tune U., Pari, Y. and Reddy, N.T., 2011. Tsunami vulnerability assesment of Cuddalore using numerical modelling and GIS. *Mar. Geod. Spec. Issue on Tsunamis*, 34: 16-28.

Ramana Murthy M.V., Reddy, N.T., Pari, Y., Usha, T. and Mishra, P., 2012. Mapping of seawater inundation along Nagapattinam based on field observations. *Natural Hazards*, 60: 161-179.

Ranga Rao, V., Reddy, N.T., Sriganesh, J., Ramana Murthy, M.V. and Murty, T.S., 2011. Tsunami hazard evaluation at selected locations along the south Andhra coast: Numerical modelling and field observations. *Mar. Geod. Spec. Issue on Tsunamis*, 34: 29-47.

Rasheed, K.A.A., Das, V.K., Revichandran, C., Vijayan, P.R. and Thottam, T.J., 2006. Tsunami impacts on morphology of beaches along south Kerala coast, west coast of India. *Sci. Tsunami Hazards*, 24: 24-34.

Rastogi, B.K. and Jaiswal, R.K., 2006. A catalogue of historical tsunamis in Indian Ocean. *Sci. Tsunami Hazards*, 25: 128-143.

Rastogi, B.K., 2007. A Historical Account of the earthquakes and tsunamis in the Indian Ocean, In: T.S. Murty, U. Aswathanarayana and N. Nirupama (Eds.) *The Indian Ocean Tsunami*, Taylor and Francis/Balkema, The Netherlands, 3-18.

Schluter, H.U., Prexl, A., Gaedicke, C.H., Roeser, H., Reichert, C.H., Meyer, H. and Daniels, C.V., 2002. The Makran accretionary wedge: Sediment thicknesses and ages and the origin of mud volcanoes. *Mar. Geol*., 185: 219-232.

Shankar, D., 1998. Low-frequency variability of sea level along the coast of India. *Unpubl. Ph. D., Thesis, Goa University*, India, 199p.

Shankar, D. and Shetye, S.R., 2001. Why is mean sea level along the Indian coast higher in the Bay of Bengal than in the Arabian Sea? *Geophys. Res. Lett*., 28: 563-565.

Sharma, P.K., Ghosh, B., Singh, R.K., Ghosh, A.K. and Kushwaha, H.S., 2005. *Numerical simulation of tsunami*: A case study, International Workshop on External Flooding Hazards at Nuclear Power Plant Sites, Jointly Organized by: Atomic Energy Regulatory Board of India, Nuclear Power Corporation of India Ltd., and International Atomic Energy Agency, Kalpakkam, Tamil Nadu, India.

Shuto, N. and Goto, C., 1978. Numerical simulation of tsunami run-up. *Coast. Engg. Japan*, 21: 13-20.

Smylie, D.E. and Mansinha, L., 1971. The elasticity theory of dislocations in real earth models and changes in the rotation of the earth. *Geophys. J. R. Astr. Soc*., 23: 329-354.

Snead, R.E., 1966. Recent morphological changes along the coast of west Pakistan. *Annals Assoc. Am. Geogra*., 57: 550-565.

Somporn, Chuai-Aree. and Wattana, K., 2007. Fast and real-time simulation of tsunami propagation. *Proc. First Asia Int. Conf. Modelling and Simulation*, 490-495.

Stoneley, R., 1974. Evolution of the continental margins bounding a former Tethys, In: C.A. Burk and C.L. Drake (Eds.) *The Geology of Continental Margins*, Springer, New York, 889-903.

Subramanian, B.R. et al., 2006. Inundation of seawater due to the Indian Ocean tsunami along the Indian coast. 26 December 2004 Tsunami: Causes, effects, remedial measures, pre and post tsunami Disaster Management- A Geoscientific perspective. (Ed.) G.V.Rajamanickam, New Academic Publishers, New Delhi, 10-44.

Swaroopa, R.V., Kirti, S. and Dimri, V.P., 2011. Tsunami propagation and inundation due to tsunamigenic earthquakes in the Sumatra-Andaman subduction zone: Impact at Vishakapatnam. *Mar. Geod. Spec. Issue on Tsunamis*, 34: 48-58.

Synolakis, C.E., 2003. Tsunami and Seiche. In: W.F. Chen and C. Scawthorn (Eds.) *Earthquake Engineering handbook*, Washington 9.1-9.79.

Takeda, H., 1984. Numerical simulation of run-up by variable transformation. *Oceanogra. J.* Japan, 40: 271-278.

Titov, V.V. and Synolakis, C.E., 1995. Modelling of breaking and nonbreaking long wave evolution and runup using VTCS-2. *J. Waterways Ports Coast. Ocean Engg*., 121: 308-316.

Titov, V.V. and Synolakis, C.E., 1996. Numerical modelling of 3-D long wave runup using VTCS-3. In: P. Liu, H. Yeh and C. Synolakis (Eds.) *Long-wave runup models*, World Scientific Publishing Co. Pte. Ltd., Singapore, 242-248.

Titov, V.V. and Gonzalez, F., 1997. Implementation and testing of the method of splitting tsunami (MOST) model. *NOAA Technical Memorandum ERL, PMEL*- 112: 1-11.

Uda, T., 1988. Numerical simulation and experiment on tsunami run-up. *Coast. Engg. Japan* 31: 87-104.

Unnikrishnan, A.S., Rupakumar, K., Fernander, S.E., Michael, G.S. and Patwardhan, S.K., 2006. Sea-level changes along the Indian coast: Observations and projections, *Curr. Sci*., 90: 362-368.

Unnikrishnan, A.S. and Shankar, D., 2007. Are sea-level rise trends along the coasts of north Indian Ocean coasts consistent with global estimates? *Global and Planetary Change*, 57: 301-307.

USGS, 2004. Preliminary Earthquake Report, USGS National Earthquake Information Center, http://neic.usgs.gov/neis/bulletin/mag7.html.

Usha, T., Ramana Murthy, M.V., Reddy, N.T. and Murty, T.S., 2009. Vulnerability assessment of Car Nicobar to tsunami hazard using numerical model. *Sci. Tsunami Hazards*, 28: 15-34.

Usha, T., Ramana Murthy, M.V., Reddy, N.T. and Mishra, P. 2012. Tsunami vulnerability assessment in urban areas using numerical model and GIS. *Natural Hazards*, 60: 135-147.

Varma, K.K. and Sakheer, H., 2007. Refraction of tsunami waves of 26 December 2004 along southwest coast of India, *Sci. Tsunami Hazards*, 26: 42-58.

Vernant, P.H., Nilforoushan, F., Hatzfeld, D., Abbasi, M.R., Vigny, C., Masson, F., Nankali, H., Martinod, J., Ashtiani, A., Bayer, R., Tavakoli, F. and Chery, J., 2004. Present-day crustal deformation and plate kinematics in the Middle East constrained by GPS measurements in Iran and northern Oman. *Geophys. J. Int*., 157: 381-398.

Watts, P., Grilli, S.T., Kirbi, J.T., Fryer, G.J. and Tappin, D.R., 2003. Landslide tsunami case studies using a Boussinesq model and a fully non linear tsunami generation model. *Nat. Haz. Earth Syst. Sci.*, 3: 391-402.

Website of Dart locations - conceptual plan, http://nctr.pmel.noaa.gov / Dart / dart _ home. html.

Webiste of Disaster Pages of Dr. George Pararas - Carayannis, http: // www. drgeorgepc.com.

Wiedicke, M., Neben, S. and Spiess, V., 2001. Mud volcanoes at the front of the Makran accretionary complex, Pakistan. *Mar. Geol*., 172: 57-73.

Woodworth, P.L. and Player, R., 2003. The permanent service for mean sea-level. An update to the 21st Century. *J. Coast. Res*., 19: 287-295.

Yalciner, A.C., Alpar, B., Altinok, Y., Ozbay, I. and Imamura, F., 2002. Tsunamis in the sea of Marmara: Historical documents for the past, models for future. *Mar. Geol*., 190: 445-463.

Yalciner, A.C., Pelinovsky, E., Talipova, T., Kurkin, A., Kozelkov, A. and Zaitsev, A., 2004. Tsunamis in the Black Sea: Comparison of the historical, instrumental and numerical data. *J. Geophys. Res*., 109: 2003-2113.

Yalciner, A.C., Dogan, P., Sukru, E., Gegar, S., Presteya, G.S., Hidayat, R. and McAdoo, B., 2005. December 26 2004, Indian Ocean tsunami field survey, north of Sumatra Island, UNESCO, http://ioc.unseco.org/iosurveys/Indonesia/yalciner/yalciner.htm.

Yeh, H., Francis, M., Peterson, C., Katada, T., Latha, G., Chadha, R.K., Singh, J.P. and Raghuraman, G., 2007. Effects of the 2004 great Sumatra tsunami, southeast Indian Coast. *J. Waterways Port Coast. Ocean Engg*., 133: 382-400.

Zahibo, N., Pelinovsky, E., Yalc¸ A., Kurkin, A., Koselkov, A. and Zaitsev, A., 2003. The 1867 Virgin Island tsunami: Observations and modelling. *Oceanologica Acta* 26: 609-621.

PUBLICATIONS

Praveen, S.S., Kurian, N.P and Shahul Hameed, T.S. 2012. Tsunami inundation modelling for the coast of Kerala, India. *Marine Geodesy* (in press).

Praveen, S.S., Reshmi, A.K., Dhanya, P., Arjun, S., Kalarani, Kurian, N.P., Ramana Murthy, M.V., Shahul Hameed, T.S. and Prakash, T.N., 2011. Numerical simulation of 26 December 2004 tsunami on the southwest coast and Lakshadweep Islands of India. *Marine Geodesy Special Issue on Tsunamis*, 34: 59-67.

Arjun, S., Kalarani, Dhanya, P., **Praveen, S.S.,** Reshmi, A.K., Kurian, N.P., Ramanamurthy, M.V., Shahul Hameed, T.S. and Prakash, T.N., 2011. Numerical simulation of the Makran 1945 tsunami on the southwest coast and Lakshadweep Islands of India. *Marine Geodesy Special Issue on Tsunamis*, 34: 68-76.

Kurian, N.P. and **Praveen, S.S.,** 2010. Tsunami wave propagation in the Arabian Sea and its implications on run-up/inundation characteristics along the Kerala coast. *Indian Journal of Geo-Marine Sciences*, 39: 531-540.

Murty, T.S., Kurian, N.P., Vittal Hegde, A., Subba Rao, Kiran, G.S., **Praveen, S.S.,** Santhosh, V.H., Numerical modelling of tsunami run-up and inundation along the central Kerala coast, India. *Science of Tsunami Hazards* (Accepted for Publication).

Papers Ready for Communication

Praveen, S.S., Shafeer, K.B., Kurian, N.P. and Shahul Hameed, T.S., Numerical modelling of the propagation Characteristics of tsunami in the South East Arabian Sea (SEAS).

Praveen, S.S., Kurian, N.P. and Shahul Hameed, T.S. and Prakash, T.N., Numerical modelling studies on tsunami inundation along the Lakshadweep Islands.

Praveen, S.S., Kurian, N.P. and Shahul Hameed, T.S., Numerical simulation of resonance of tsunami waves in gulfs and ports along the south west coast of India.

Praveen, S.S., Numerical Modelling of Tsunami Inundation along the Southwest Coast of India, Invited chapter in the book “Tsunami” ISBN-979-953-307-835-8.

List of Conference Proceedings / Presentations

Praveen, S.S., Kurian, N.P. and Shahul Hameed, T.S., 2011. Tsunami inundation along the Kerala coast for different sources and scenarios of sea level rise. Extended Abstract, *Kerala Science Congress* (KSC-2011), Thiruvananthapuram.

Kurian, N.P. and **Praveen, S.S.**, 2010. Tsunami wave propagation in the Arabian Sea and its effect on run-up/inundation characteristics along the south west coast of India. Extended Abstarct, *National Conference on Coastal Processes, Resources and Management* (NCPRM–2010), Thiruvananthapuram.

Mithun, V.K., Shanawaz, C.P., **Praveen, S.S.,** Kurian, N.P. and Shahul Hameed¸ T.S., 2010, Validation of ALTM and Cartosat derived topographic data. 13th INCA International Congress, Dehradun.

Praveen, S.S., Kalarani, Shanavaz, C.P., Arjun, S., Kurian, N.P., Shahul Hameed, T.S. and Prakash, T.N., 2010. Numerical modelling studies on tsunami inundation along the Lakshadweep Islands. *Extended Abstract, Ninth International Conference on Hydroscience and Engineering* (ICHE - 2010), Chennai.

Praveen, S.S., Dhanya, P., Kalarani, Arjun, S., Kurian, N.P., Shahul Hameed and T.S. Prakash, T.N., 2009. Numerical modelling of tsunami inundation for the southern Kerala coast. *Extended Abstract National Conference of Ocean Society of India on Recent developments in Ocean Science, Engineering and Technology* (OSICON-'09).

Praveen, S.S., Kalarani, Dhanya, P., Arjun, S. Kurian, N.P. and Shahul Hameed, T.S., 2009. Numerical modeling of tsunami inundation and run-up along the Kerala coast for tsunami disaster mitigation. *Extended Abstract National Workshop on Natural Hazards Disaster Mitigation and Management*, Thiruvananthapuram.

Praveen, S.S., Arjun, S. Kalarani, Dhanya, P., Reshmi, A.K., Kurian, N.P. and Shahul Hameed, T.S., 2007. Simulation of tsunami amplitudes along the Trivandrum coast for 1945 Makran and 2004 Sumatra Earthquake. *Extended Abstarct Swadesi Science Congress* (SSC-2007*)*, Thiruvananthapuram.

Praveen, S.S., Kalarani, Reshmi, A.K., Arjun, S., Shanavaz, C.P., Dhanya, P., Kurian, N.P. and Shahul Hameed, T.S., 2007. Numerical Modelling of Tsunami inundation along the Kerala coast. *Extended Abstract Kerala Science Congress* (*KSC*-2007), Thiruvananthapuram.